Study of the roles of autophagy in human follicular and diffuse large B-cell lymphoma

Áine Claire McCarthy

Submitted in partial fulfilment of the requirements of the Degree of Doctor of Philosophy

June 2014

Centre for Haemato-Oncology,
Barts Cancer Institute,
Queen Mary School of Medicine and Dentistry,
Queen Mary University of London

Statement of originality

I, Áine Claire McCarthy, confirm that the research included within this thesis is my own work or that where it has been carried out in collaboration with, or supported by others, that this is duly acknowledged below and my contribution indicated. Previously published material is also acknowledged below.

I attest that I have exercised reasonable care to ensure that the work is original, and does not to the best of my knowledge break any UK law, infringe any third party's copyright or other Intellectual Property Right, or contain any confidential material.

I accept that the College has the right to use plagiarism detection software to check the electronic version of the thesis.

I confirm that this thesis has not been previously submitted for the award of a degree by this or any other university.

The copyright of this thesis rests with the author and no quotation from it or information derived from it may be published without the prior written consent of the author.

Details of collaboration:

Data presented in Chapter III and Chapter IV was done in collaboration and shared with Vincent Yeung during his time as a masters student in our department

Flow sorting was performed by William Day and Guglielmo Rosignoli

Hierarchical clustering of gene expression data was performed by Jacek Marzec

Tissue microarrays were previously constructed by Andrew Clear and Andrew Owen

CD68 Immunohistochemistry staining was performed by Rita Coutinho

Details of publications:

"Aberrant expression of autophagy-related genes in human follicular and diffuse large B-cell lymphomas" – Aine McCarthy, Jacek Marzec, Andrew Clear, Robert D Petty, Rita Coutinho, Janet Matthews, Andrew Wilson, Sameena Iqbal, Maria Calaminici, John G Gribben and Li Jia - submitted to the journal Blood, June 2014.

Signature:  Date: 4/6/2014

Abstract

Autophagy, a cellular self-degradation process, plays important roles in cancer development and progression. Autophagy can be inhibited by the anti-apoptotic protein BCL-2 which binds and sequesters the autophagy essential protein Beclin-1, therefore preventing autophagy induction. It is currently unclear whether BCL-2 inhibits autophagy as well as apoptosis in follicular lymphoma (FL) and diffuse large B-cell lymphoma (DLBCL) which frequently express BCL-2 at high levels. This study aimed to determine (1) the role of BCL-2 in the basal level autophagy status and autophagy flux in primary FL and DLBCL samples, and lymphoma cell lines at both the gene and protein levels; (2) whether aberrant autophagy activity in these lymphoma patients is associated with clinical outcome.

We initially found that the BCL-2 inhibitor ABT-737 concurrently induced autophagy and apoptosis in BCL-2^{HIGH} DLBCL cell lines. Blocking autophagy degradation with chloroquine sensitised BCL-2^{HIGH} cells to ABT-737-induced cell death, indicating that acquired autophagy acts as a cytoprotective mechanism in these cells. Expression levels of autophagy-related genes were analyzed by qRT-PCR. The BCL-2^{HIGH} cell line Su-DHL4 showed up-regulation of more autophagy machinery genes at both the basal level and following starvation-induced autophagy compared with the BCL-2^{LOW} cell line. These results suggest that inhibition of BCL-2 can induce cytoprotective autophagy, but overexpression of BCL-2 alone may increase basal level autophagy by inhibiting apoptosis.

The expression levels of autophagy-related genes were examined in purified primary FL and DLBCL B cells or un-purified whole FL and DLBCL tumour tissue biopsies and compared with non-malignant reactive lymph nodes. A number of autophagy machinery genes were significantly up-regulated in malignant samples. In particular, more autophagy machinery genes showed significantly increased expression in both purified and un-purified FL samples, indicating that despite frequently overexpressing BCL-2, FL appears to have increased basal level autophagy activity.

Expression of the key autophagy proteins p62, Beclin-1, LC3 and BCL-2 were determined in FL and DLBCL using tissue microarrays and immunohistochemistry. Both p62 and LC3, substrates of autophagic degradation, served as markers for autophagy activity. Significantly decreased expression of p62 and LC3, indicating active autophagy, was observed in FL samples (n=117). DLBCL samples (n=109) showed a heterogeneous expression pattern of these four proteins. We identified p62 as an independent prognostic biomarker in DLBCL with decreased expression predicting shorter overall, disease specific and progression-free survival. DLBCL patients with lower p62 or LC3 expression and higher levels of BCL-2, i.e. active autophagy and inhibited apoptosis, had the worst prognosis. Beclin-1 expression was significantly reduced in both FL and DLBCL, where lower levels were significantly associated with shorter overall and disease-specific survival.

In summary, this study demonstrates that FL, characterised by overexpression of BCL-2, shows increased autophagy activity, indicating that BCL-2 may not inhibit basal level autophagy in this indolent lymphoma. High levels of BCL-2 and active autophagy did not affect the clinical outcome of FL, but significantly shortened the survival rates of DLBCL patients. Our data propose that active autophagy could be used as a biomarker for DLBCL prognosis, but not FL.

Dedication

To Mom and Dad – thank you for your never ending support and encouragement.

Acknowledgments

The work presented in this thesis was possible due to funding provided by Cancer Research UK.

I would sincerely like to thank my primary supervisor, Dr. Li Jia, for providing the conceptual framework for this project and for her ongoing guidance, support, patience and encouragement over the last four years - I am truly grateful. I would also like to thank my second supervisor Professor John Gribben for his continued support and for giving me the opportunity to attend several conferences during the course of my PhD.

I would like to thank the tissue bank staff Sameena Iqbal, Catherine Durance and Tom Dowe for gathering and retrieving patient samples, and Dave Williamson for knowing where everything is, chasing up orders and offering encouragement. I am extremely grateful to Janet Matthews and Andrew Wilson who supplied the patient information and offered guidance on how to navigate my way through it. Thank you to Eleni Kotsiou, Timothy Farren, Farideh Miraki-Moud and Jeff Davies for their expertise and advice regarding flow cytometry, and to William Day and Guglielmo Rosignoli for advising me regarding B cell purification experiments and for performing the flow sorting. I would also like to thank Fenting Liu for his help and advice with cell culture techniques.

To Robert Petty, who provided unparalleled advice, guidance and wisdom for all gene expression profiling experiments, for teaching me how to analyse and scrutinize data, and for being a true, genius friend, I am beyond grateful. Thank you also to Jacek Marzec who performed the hierarchical clustering analysis for his willingness to help.

I am particularly grateful to Andrew Clear and Rita Coutinho for their expertise, help and guidance regarding all things tissue microarray and immunohistochemistry related, and for their continued friendship, support and encouragement. I would also like to thank Andrew Owen who constructed the tissue microarrays used in this study and Abi Lee and Maria Calaminici for offering their histopathology expertise.

Thank you to everyone in Haemato-Oncology and Barts Cancer Institute, past and present, for their advice, support and camaraderie – it’s been a great four years. In particular I want to thank Lauren Wallis and Lenushka Maharaj for taking me under their wing when I

started, Kiran Tawana, Tracy Chaplin-Perkins, Paul Greaves and Tom Butler for being so willing to help at all times and everyone in room 326 for their friendship.

Finally, to my family and friends for their never ending words of encouragement and continued understanding, for their unfaltering support and belief in me and for all the care packages sent and trips over made – thank you.

Table of contents

Statement of originality 2
Abstract 3
Dedication 5
Acknowledgments 6
Table of contents 8
List of figures 14
List of tables 17
List of abbreviations 18
Chapter I Introduction 23
1.1 Autophagy 24
1.1.1 The distinct types of autophagy 25
1.1.2 The autophagy genes and proteins 26
1.1.3 The autophagy flux 26
1.1.4 Measuring the autophagy flux 30
1.1.5 Autophagy inducers and inhibitors 35
1.1.6 Apoptotic and autophagic cell death 38
1.1.7 Autophagy in cancer 42
1.2 Beclin-1 47
1.2.1 Beclin-1 is essential to the autophagy pathway 47
1.2.2 Beclin-1 is a multi-domain protein 47
1.2.3 Beclin-1 localises to the mitochondria and the ER 48
1.2.4 Beclin-1 is a tumour suppressor protein 48
1.3 The BCL-2 family of proteins 51
1.3.1 The BCL-2 protein 52
1.3.2 BCL-2 - an inhibitor of apoptosis and autophagy 53
1.3.3 Overexpression of BCL-2 promotes tumourigenesis 53
1.4 Binding between BCL-2 and Beclin-1 can inhibit autophagy 56
1.4.1 BCL-2 and Beclin-1 can bind at the ER and mitochondria 56
1.4.2 Binding between BCL-2 and Beclin-1 can be disrupted in various ways 57
1.5 The adaptor / scaffold protein p62 59

1.5.1 p62 is a multi-domain protein involved in different cellular pathways 59
1.5.2 p62 delivers substrates to the autophagosome 61
1.5.3 p62 is involved in disease pathogenesis 62
1.6 Lymphomas 65
1.6.1 FL is an indolent, incurable malignancy of the germinal centre 65
1.6.2 FL is associated with multiple genetic abnormalities 66
1.6.3 FL can be divided into distinct clinical grades 67
1.6.4 FL treatment varies depending on disease stage 67
1.6.5 The tumour microenvironment in FL 69
1.6.6 Transformation of FL to DLBCL is associated with morphological changes and acquisition of genetic mutations 70
1.7 Diffuse Large B-Cell Lymphoma 71
1.7.1 DLBCL is an aggressive B-Cell lymphoma 71
1.7.2 DLBCL can be divided into two distinct subgroups 71
1.7.3 DLBCL is associated with a variety of genetic aberrations 72
1.7.4 Up-regulation of various signalling pathways is associated with a poor prognosis in DLBCL 73
1.7.5 Treatment of DLBCL 74
1.7.6 The tumour microenvironment of DLBCL 76
1.8 Aims 77
1.8.1 To evaluate the role of BCL-2 in autophagy in lymphoma cells 77
1.8.2 To determine the basal level autophagy status of primary lymphoma samples. 77
1.8.3 To establish if expression levels of key autophagy-related proteins can be used as prognostic biomarkers in NHL 78
Chapter II Materials and Methods 79
2.1 Cell line and cell culture 80
2.2 Patient Samples 80
2.2.1 Ethical considerations 80
2.2.2 Patient sample selection 80
2.3 Preparation of cell lysates for Western blotting 81
2.4 Determination of protein concentration – Bradford assay 81
2.5 Western blotting 82

2.6 Immunofluorescent microscopy 83
2.7 Tissue microarray construction 84
2.8 Immunohistochemistry 85
2.9 Measurement of caspase-3 activity 87
2.10 Flow cytometry 88
2.10.1 Evaluation of mitochondria membrane potential and cell death 89
2.10.2 Isolation of B cell populations by flow assisted cell sorting 90
2.11 RNA extraction 91
2.11.1 Phenol-chloroform based RNA extraction (TRIzol® Reagent) 91
2.11.2 RNA extraction using QIAGEN RNeasy® mini kit 92
2.12 RNA quantity and quality assessment 93
2.12.1 NanoDrop spectrophotometer 93
2.12.2 Agilent bioanalyser 93
2.13 Gene expression analysis by qRT- PCR 94
2.13.1 Complementary DNA synthesis 94
2.13.2 Quantitative real-time polymerase chain reaction 95
2.13.3 Validation of qRT-PCR 96
2.13.4 Endogenous control selection 97
2.13.5 Calculation of relative quantification values 98
2.13.6 Hierarchical clustering 100
2.14 Co-Immunoprecipitation 100
2.15 Statistical analysis 101
2.15.1 General statistical analysis 101
2.15.2 X-tile 102
2.15.3 Kaplan-Meier survival analysis 102
2.15.4 Continuous data analysis 103
2.15.5 Categorical (cut-point) data analysis 103
Chapter III Evaluation of the dual roles of BCL-2 in apoptosis and autophagy in DLBCL cell lines 104
3.1 Introduction 105
3.2 Results 106

3.2.1 BCL-2 family proteins are differentially expressed in DLBCL cell lines 106

3.2.2 DLBCL cell lines exhibit differential sensitivity to ABT-737-induced cell death 108

3.2.3 Association between expression of BCL-2 family of proteins and sensitivity to ABT-737-induced cell death 110

3.2.4 Evaluation of DLBCL cell lines sensitivity to ABT-737-induced Bax activation 112

3.2.5 Sensitivity of DLBCL cell lines to ABT-737-induced PARP cleavage 114

3.2.6 ABT-737 induces autophagy in BCL-2^{HIGH} DLBCL cell lines 115

3.2.7 BCL-2 and Beclin-1 co-localize, but do not bind in BCL-2^{HIGH} cells 118

3.3 Discussion 123

3.3.1 Conclusions 123

Chapter IV Evaluation of the role of autophagy in ABT-737-induced cell death 124

4.1 Introduction 125

4.2 Results 126

4.2.1 Inhibition of autophagy by chloroquine sensitises BCL-2^{HIGH} cells to ABT-737-induced cell death 126

4.2.2 Inhibition of autophagy by CQ sensitises BCL-2^{HIGH} cells to ABT-737-induced PARP cleavage 132

4.2.3 Inhibition of caspase activation blocks ABT-737 and ABT-737+CQ-induced apoptosis in BCL-2^{HIGH} DLBCL cell lines 134

4.2.4 Inhibition of caspase activation showed less inhibitory effect on ABT-737+CQ induced ΔΨm depolarization 138

4.3 Discussion 141

4.3.1 Conclusions 141

Chapter V Evaluation of the effect of increased BCL-2 expression on the autophagy status and autophagy flux in lymphoma cells 142

5.1 Introduction 143

5.2 Results 144

5.2.1 BCL-2^{HIGH} DLBCL cells have higher basal level autophagy activity compared to BCL-2^{LOW} DLBCL cells 144

5.2.2 Increased expression of BCL-2 does not inhibit the autophagy flux 150

5.2.3 Purification of B cells from primary FL, DLBCL and reactive control samples for gene expression analysis 155

5.2.4 FL samples displayed higher autophagy activity despite increased expression of BCL-2 157

5.2.5 Autophagy-related genes are up-regulated in cells of the tumour microenvironment 168

5.3 Discussion 172

5.3.1 Conclusions 174

Chapter VI Evaluation of the prognostic significance of autophagy-related proteins in non-Hodgkin's lymphomas 175

6.1 Introduction 176

6.2 Results 178

6.2.1 p62, LC3 and Beclin-1 proteins are expressed at lower levels in primary FL tissue biopsies 178

6.2.2 Expression levels of p62, LC3 and Beclin-1 were correlated in FL and DLBCL 183

6.2.3 Decreased expression of p62 is associated with a worse prognosis in DLBCL 185

6.2.4 Beclin-1 is an independent biomarker of clinical outcome in FL 192

6.2.5 LC3 or BCL-2 alone do not predict clinical outcome in patients with FL or DLBCL 193

6.2.6 Lower levels of autophagy-related proteins combined with high BCL-2 expression predicts a worse outcome in DLBCL 194

6.3 Discussion 198

6.3.1 Conclusions 199

Chapter VII Discussion 201

7.1 The main findings of this study 202

7.2 Autophagy plays paradoxical roles in cancer development 202

7.3 Do key autophagy markers reflect autophagy activity in lymphoma cells? 204

7.3.1 p62 is a marker of autophagy activity in lymphoma cells 204

7.3.2 Active autophagy results in decreased expression of LC3 in lymphoma cells 205

7.3.3 Beclin-1 is not a marker of the autophagy flux in lymphoma cells 208

7.4 The autophagy-related GEP of lymphoma cells reflects their autophagy status 209

7.4.1 p62 mRNA levels increase when autophagy is induced 210
7.4.2 LC3 and Beclin-1 mRNA levels can be used as a marker of autophagy activity 211
7.5 Does overexpression of BCL-2 inhibit autophagy in lymphoma cells? 212
7.5.1 BCL-2 inhibits apoptosis but not autophagy in lymphoma cells 212
7.5.2 ABT-737 induces cytoprotective autophagy in lymphoma cell lines 214
7.5.3 Overexpression of BCL-2 does not inhibit autophagy in primary FL samples 216
7.5.4 Inhibition of apoptosis by BCL-2 promotes autophagy in lymphoma cells 219
7.6 Autophagy activity is increased in cells of the tumour microenvironment 220
7.7 Can expression levels of key autophagy-related proteins predict outcome in FL and/or DLBCL? 221
7.7.1 Low levels of p62 predict a worse outcome in DLBCL 221
7.7.2 Low levels of Beclin-1 are associated with shorter survival rates in FL and DLBCL 223
7.7.3 LC3 does not predict outcome in NHL 224
7.7.4 BCL-2 expression alone does not predict outcome in FL or DLBCL 226
7.8 Conclusion 226
7.9 Future Work 227
References 229
Appendices 258
Appendix I 259
Appendix II 273

List of figures

Figure 1.1 The autophagy flux 27

Figure 1.2 The Atg12-Atg5-Atg16 and Atg8-PE Ubl conjugation systems involved in autophagosome expansion and elongation 29

Figure 1.3 Representative output images from various autophagy assays 34

Figure 1.4 Structural organisation of the autophagy essential protein Beclin1 48

Figure 1.5 The BCL-2 family of proteins 52

Figure 1.6 Disruption of BCL-2/Beclin-1 binding promotes autophagy 58

Figure 1.7 The adaptor protein p62 contains multiple binding domains 60

Figure 2.1 Absorption spectra of the Alexa Fluor® dyes 83

Figure 2.2 Dextran polymer indirect IHC staining method 86

Figure 2.3 Example of typical flow cytometer 89

Figure 2.4 Representative Electropherogram generated by the Agilent 2100 Bioanalyser 94

Figure 2.5 RT^2 Profiler PCR Array, 384-well plate, Format E Layout 96

Figure 2.6 Identification of the most stable endogenous control gene(s) using gNorm software 98

Figure 2.7 Diagrammatic representation of a co-IP experiment 101

Figure 3.1 Expression of BCL-2 family proteins in DLBCL cell lines 107

Figure 3.2 Comparison of the sensitivity of BCL-2^{HIGH} and BCL-2^{LOW} DLBCL cell lines to ABT-737 109

Figure 3.3 Association between expression of BCL-2 family proteins and the sensitivity of DLBCL cells to ABT-737-mediated ΔΨm reduction and cell death 111

Figure 3.4 ABT-737-induced Bax activation in BCL-2^{HIGH} and BCL-2^{LOW} DLBCL cells 113

Figure 3.5 ABT-737-induced PARP cleavage in BCL-2^{HIGH} and BCL-2^{LOW} DLBCL cells 114

Figure 3.6 Evaluation of ABT-737-induced autophagy in BCL-2^{HIGH} and BCL-2^{LOW} DLBCL cell lines 117

Figure 3.7 Determination of the cellular location of BCL-2 in Su-DHL4 cells 119

Figure 3.8 Determination of the cellular location of Beclin-1 in Su-DHL4 cells 120

Figure 3.9 Evaluation of BCL-2 and Beclin-1 co-localisation in Su-DHL4 cells 121

Figure 3.10 Determination of BCL-2 and Beclin-1 interaction by co-immunoprecipitation 122

Figure 4.1 Evaluation of the effect of the autophagy inhibitor CQ on ABT-737-induced cell death in BCL-2^{HIGH} cells 127

Figure 4.2 Evaluation of the effect of the autophagy inhibitor CQ on ABT-737-induced cell death in BCL-2^{HIGH} cells 128

Figure 4.3 Effect of the autophagy inhibitor CQ on ABT-737-induced ΔΨm depolarization in BCL-2^{HIGH} DLBCL cells 130

Figure 4.4 Effect of the autophagy inhibitor CQ on ABT-737-induced ΔΨm in BCL-2^{LOW} DLBCL cells 131

Figure 4.5 Evaluation of the effect of autophagy inhibition on ABT-737-induced PARP cleavage in BCL-2^{HIGH} and BCL-2^{LOW} DLBCL cell lines 133

Figure 4.6 Comparison of the effect of CQ and ABT-737 on caspase-3 activation in BCL-2^{HIGH} DLBCL cell lines 134

Figure 4.7 Inhibitory effect of Z-VAD.fmk on TRAIL-induced caspase-3 activation and PARP cleavage 135

Figure 4.8 Effect of Z-VAD.fmk on ABT-737+CQ-induced caspase-3 activation 136

Figure 4.9 Inhibition of caspase activation blocks ABT-737+CQ-induced PARP cleavage 137

Figure 4.10 Evaluation of the effect of caspase inhibition on ABT-737+CQ-induced cell death in Su-DHL4 and CRL cells 139

Figure 4.11 Evaluation of the effect of caspase inhibition on ABT-737+CQ-induced ΔΨm in Su-DHL4 and CRL cells 140

Figure 5.1 Evaluation of expression of key autophagy-related proteins in Su-DHL4 and Su-DHL8 DLBCL cell lines 144

Figure 5.2 Su-DHL4 and Su-DHL8 cells differ in their expression of autophagy-related genes 147

Figure 5.3 Incubation with HBSS induces autophagy in Su-DHL4 and Su-DHL8 cell lines 152

Figure 5.4 HBSS-induced starvation alters the autophagy-related GEP of Su-DHL4 and Su-DHL8 cell lines 154

Figure 5.5 Flow sorting strategy for purification of B cells from primary FL, DLBCL and RA single cell suspensions 156

Figure 5.6 Evaluation of the autophagy-related GEP of primary FL, DLBCL and RA B cells 159

Figure 5.7 Evaluation of the autophagy-related GEP of primary FL, DLBCL and RA whole tumour samples.....162

Figure 5.8 Analysis of expression levels of autophagy-related proteins in un-purified primary FL, DLBCL and RA tissues 167

Figure 5.9 Analysis of CTSD and TGM2 expression in primary lymphoma samples using IHC 169

Figure 5.10 Higher levels of CTSD are associated with a poor prognosis in FL and DLBCL.....171

Figure 6.1 Representative images of immunohistochemical staining of p62, LC3, Beclin-1 and CD10 in primary RA, FL and DLBCL tissue.....180

Figure 6.2 Comparison of p62, LC3 and Beclin-1 protein expression in primary RA, FL and DLBCL tissue samples.....181

Figure 6.3 Evaluation of BCL-2 expression in primary RA, FL and DLBCL tissue biopsies.....182

Figure 6.4 Decreased expression of key autophagy-related proteins in DLBCL predicts a worse clinical outcome.....188

Figure 6.5 Decreased expression of Beclin-1 predicts shorter overall and disease specific survival in FL.....189

Figure 6.6 Decreased expression of p62 combined with BCL-2 overexpression predicts a worse outcome in DLBCL 196

List of tables

Table 1.1 Genes and proteins involved in autophagy regulation 37

Table 1.2 Chemical Compounds involved in autophagy regulation 38

Table 1.3 Dual roles of autophagy and apoptosis genes 42

Table 1.4 Genetic abnormalities associated with FL 66

Table 1.5 Grading of FL 67

Table 1.6 Prognostic factors considered when determining an FLIPI scores 68

Table 1.7 Treatment response classifications 69

Table 1.8 Genes frequently altered in transformation from FL to DLBCL 70

Table 1.9 Genetic abnormalities observed in the GCB- and ABC-subtypes of DLBCL 73

Table 1.10 Prognostic factors considered when determining an individual's IPI/R-IPI score 75

Table 2.1 BSA Standard Curve for Bradford Assay 82

Table 2.2 AFC Standard Curve for Caspase-3 Assay 88

Table 2.3 Calculation of Survival Outcomes 102

Table 5.1 Autophagy-machinery genes 148

Table 5.2 Autophagy-regulatory genes 149

Table 5.3 Autophagy-machinery genes differentially regulated in primary lymphoma samples compared to RA controls 163

Table 5.4 Autophagy-regulatory genes differentially regulated in primary lymphoma samples compared to RA controls 164

Table 5.5 Validation of differential expression of autophagy-related genes in FL and DLBCL samples compared to RA controls 166

Table 6.1 Evaluation of correlation between autophagy-related proteins in primary RA (A), FL (B) and DLBCL (C) tissue samples 184

Table 6.2 Univariate Cox-regression analysis of autophagy-related proteins as continuous variables in DLBCL 186

Table 6.3 Univariate Cox-regression analysis of autophagy-related proteins as continuous variables in FL 187

Table 6.4 Categorical multivariate proportional hazard model analysis for IPI, p62, LC3, Beclin-1 and BCL-2 in DLBCL and for Beclin-1 in FL 191

Table 6.5 Categorical multivariate analysis of expression levels of autophagy-related proteins in combination with BCL-2 expression levels in primary DLBCL samples .. 197

List of abbreviations

3-MA	3-methyladenine
ABC	Activated B-cell like
AFC	7-amino-4-trifluoromethylcoumarin
aPKC	Atypical protein kinase C
Atg	Autophagy-related gene
BCL-2	B-cell lymphoma/leukaemia-2
BH	BCL-2 homology domain
BL	Burkitts lymphoma
CCD	Central coiled-coiled domain
cDNA	Complementary DNA
cIAPS	Cellular inhibitors of apoptosis protein
CLL	Chronic lymphocytic leukaemia
CMA	Chaperone mediated autophagy
CML	Chronic myeloid leukaemia
CQ	Chloroquine
CR	Complete remission
C_T	Cycle threshold
DAB	3,3’-diaminobenzidine
DAPI	4',6-Diamidino-2-Phenylindole, Dihydrochloride
dATP	Deoxyadenosine triphosphate
DEVD	Aspartic acid, glutamic acid, valine, aspartic acid
DISC	Death induced signalling complex
DLBCL	Diffuse large B-cell lymphoma
DNA	Deoxyribonucleic acid
DPX	Distrene 80, Dibutyl phthalate and Xylene

DS	Double stranded
DSS	Disease specific survival
DTT	Dithiothreitol
ECD	Evolutionarily conserved domain
ECOG	Eastern cooperative oncology group
EDTA	Ethylenediaminetetraacetic acid
ENDOG	Endonuclease G
ER	Endoplasmic reticulum
FACS	Flow assisted cell sorting
FAM	Carboxyfluorescein
FCS	Fetal calf serum
FDM	Factor-dependent myeloid
FL	Follicular lymphoma
FLIPI	Follicular lymphoma international prognostic index
FMO	Fluorescence minus one
GC	Germinal centre
GCB	Germinal centre B-cell-like
GDC	Genomic DNA control
GDE	Genomic DNA elimination
GEP	Gene expression profile / Gene expression profiling
GFP	Green-fluorescent protein
GPR	Good partial remission
H&E	Haematoxylin and eosin
HCQ	Hydroxychloroquine
HDAC	Histone-deacetylase
HKG	Housekeeping gene

HL	Hodgkin's lymphoma
HSC	Heat-shock cognate
iBMK	Immortalised baby mouse kidney
IC	Initiator complex
IFM	Immunofluorescent microscopy
IgH	Immunoglobulin heavy chain
IgM	Immunoglobulin heavy chain M
IHC	Immunohistochemistry
IPI	International prognostic index
KIR	KEAP1-interacting region
LC3	Light chain 3
LDH	Lactate dehydrogenase
LIR	LC3-interacting region
MCL	Mantle cell lymphoma
MEF	Mouse embryonic fibroblast
miRNA	Micro RNA
MOMP	Mitochondrial outer membrane permeabilisation
mRNA	Messenger RNA
mTOR	Mammalian target of rapamycin
mTORC1	Mammalian target of rapamycin complex 1
mTORC2	Mammalian target of rapamycin complex 2
NES	Nuclear export signal
NHL	Non-Hodgkin's lymphoma
NK	Natural killer
Nrf2	Nuclear factor, (erythroid-derived 2)-like 2
NTC	No-template control

OS	Overall survival
PARP	Poly(ADP-ribose) polymerase
PAS	Phagophore assembly site
PB1	Phox/Bem 1p
PBS	Phosphate buffered saline
PBST	Phosphate buffered saline with Tween-20
PCD	Programmed cell death
PCR	Polymerase chain reaction
PDAC	Pancreatic ductal adenocarcinoma
PE	Phosphatidylethanolamine
PFS	Progression free survival
PI3K	Phosphoinositide-3 kinase
PIC	Protease inhibitor cocktail
PMBL	Primary mediastinal B-cell lymphoma
PMSF	Phenylmethylsulfonyl fluoride
PPC	Positive PCR control
PVDF	Polyvinylidene difluoride
qRT-PCR	Quantitative real-time PCR
RA	Reactive lymph-nodes
RAPTOR	Regulatory-associated protein of mTOR
R-CHOP	Rituximab, cyclophosphamide, doxorubicin, vincristine, prednisone
ReTr	Reverse-transcription
RIN	RNA integrity number
R-IPI	Rituximab international prognostic index
RNA	Ribonucleic acid
ROS	Reactive oxygen species

RQ	Relative quantity
RT	Room temperature
RTC	Reverse transcription control
SD	Standard deviation
siRNA	Short-interfering RNA
SMI	Small molecule inhibitor
SQSTM1	Squestosome1
SS	Single stranded
Taq	*Thermus aquaticus* polymerase
TB	TRAF6-binding
TEM	Transmission electron microscopy
TGN	Trans-Golgi network
TMA	Tissue microarray
TMRM	Tetramethylrhodamine, methyl ester, perchlorate
UBA	Ubiquitin-associated
Ubl	Ubiquitin-like
Z-VAD.fmk	N-Benzyloxycarbonyl-Val-Ala-Asp(O-Me) fluromethyl ketone
ZZ	Zinc-finger
ΔC_T	Delta C_T
$\Delta\Delta C_T$	Delta Δ C_T
$\Delta\Psi m$	Mitochondrial membrane potential
κ	Kappa
λ	Lambda

Chapter I

Introduction

Autophagy is a cellular self-degradation process whose activity is increased in cells upon encountering stress such as starvation and hypoxia. Understanding the role of this adaptive process in cancer is important as it is now known that tumour cells utilise autophagy to prolong their survival. It is also becoming increasingly apparent that activity of this pathway can influence the efficacy of chemotherapy agents. While our knowledge and understanding of the role autophagy plays in cancer is expanding, it is still unclear if this pathway is modulated in the same way in all cancer types. It has been reported that autophagy can be inhibited by the anti-apoptotic protein BCL-2 (B-cell lymphoma/leukaemia-2) which binds and sequesters the pro-autophagy protein Beclin-1 and prevents autophagy induction. It is currently unclear if BCL-2 inhibits autophagy as well as apoptosis in human follicular lymphoma (FL) and diffuse large B-cell lymphoma (DLBCL) which frequently overexpress BCL-2, and if autophagy activity is associated with clinical outcome in these lymphomas.

1.1 Autophagy

Autophagy is a bulk degradation process involved in maintenance of cellular homeostasis. Typically considered a pro-survival mechanism, autophagy occurs at a basal level within the majority of cell types where it functions to remove and recycle old and damaged cellular organelles and protein aggregates (Choi et al., 2013a; Deter et al., 1967; Galluzzi et al., 2012; He and Klionsky, 2009). Autophagy activity increases under stressed conditions such as nutrient deprivation and hypoxia to allow cells to avoid such stresses and prolong their survival. Substrates of the autophagy pathway include long-lived proteins, large organelle/protein aggregates and intracellular pathogens (Korolchuk et al., 2010; Levine and Klionsky, 2004; Levine and Kroemer, 2008; Schmid and Munz, 2007).

This pathway is also involved in physiological processes such as development, immunity and aging (Dikic et al., 2010; Mizushima et al., 2008). As part of the innate and adaptive immunity, autophagy aids in maintenance of lymphocyte homeostasis and the removal of microorganisms while increased autophagy activity has been found to delay aging and improve longevity (Deretic et al., 2013; Rubinsztein et al., 2011). This degradation process also plays a role in the pathogenesis of various diseases including

neurodegenerative disorders, muscular diseases and cancer (Choi et al., 2013a; Lucin and Wyss-Coray, 2013).

1.1.1 The distinct types of autophagy

There are three types of autophagy – chaperone mediated autophagy (CMA), microautophagy and macroautophagy – which degrade cellular proteins by different mechanisms (Boya et al., 2013; Choi et al., 2013a; Schmid and Munz, 2007).

During CMA, proteins destined for degradation are recognised by the heat-shock cognate (HSC) chaperone protein HSC-70 which binds LAMP-2 and facilitates translocation of bound proteins to the lysosome where they are degraded. Conversely, in microautophagy, proteins targeted for degradation are engulfed by direct invagination of the lysosomal membrane. A small vesicle containing these proteins then buds off into the lysosomal lumen where the contents are degraded. Macroautophagy (referred to as autophagy), which is the best understood of these subtypes, involves formation of double layered-membrane vesicles called autophagosomes which sequester cytosolic components including protein aggregates and old cellular organelles destined for degradation. Autophagosomes fuse with lysosomes forming autophagolysosomes within which lysosomal hydrolases function to degrade the contents of the autophagosome (Section 1.1.3) (Boya et al., 2013; Choi et al., 2013a; Schmid and Munz, 2007).

Autophagy can be non-selective or selective with regards the substrates it degrades (He and Klionsky, 2009; Johansen and Lamark, 2011). Non-selective autophagy removes general, long-lived, damaged proteins/organelles from cells by sequestering a large bulk of the cytosol. Conversely, selective autophagy targets specific proteins and organelles to the autophagosome for degradation, with different terms used for selective degradation of specific cargo; for example mitophagy and ribophagy refer to autophagic degradation of mitochondria and ribosomes respectively (He and Klionsky, 2009; Johansen and Lamark, 2011).

1.1.2 The autophagy genes and proteins

Although we have known about autophagy since the 1950s through the visualisation of autophagosomes by electron microscopy, we have only begun to understand the molecular basis of this pathway in the last 20 years. A key turning point in our understanding of this pathway came when Ohsumis' group identified the autophagy-related gene (*Atg*) *Atg1* by screening for autophagy mutants in the yeast *Saccharomyces cerevisiae*, the sequence of which was published in 1997 (Matsuura et al., 1997; Tsukada and Ohsumi, 1993). More than a decade on a further 30 *Atg* genes have been identified, the majority of which are evolutionarily conserved from yeast to mammals (Kabeya et al., 2007; Klionsky, 2007). While some genes such as *Atg8* were first identified in yeast and their homologs (e.g. LC3) subsequently discovered in mammals, others, such as the *Atg12* and *Atg5*, were found first in mammals and later in yeast, again highlighting the conservation of these genes (Klionsky, 2007; Mizushima et al., 1998).

The *Atg* genes are essential to the autophagy process and are involved in all stages of the pathway. They are particularly prevalent in the early phases of autophagy where they aid in autophagosome membrane formation, elongation and expansion (Section 1.1.3) (He and Klionsky, 2009; Rubinsztein et al., 2012).

Other genes and proteins which are important in the autophagy pathway include LC3, p62, Beclin-1 and BCL-2 which can act as biomarkers, inducers and inhibitors of autophagy respectively, which will be discussed in later sections (Lee et al., 2012; Rubinsztein et al., 2012; Russell et al., 2013).

1.1.3 The autophagy flux

Autophagy is a dynamic process comprised of different stages including initiation, elongation, sequestration and fusion (Figure 1.1) (Rubinsztein et al., 2012).

1.1.3.1 Initiation / Formation

Autophagy begins with the generation of a single layered membrane termed the phagophore which forms at the phagophore assembly site (PAS) and requires an initiator complex (IC) for nucleation and assembly. The IC comprises multiple proteins including the class III PI3K Vps34, Vps15/p150, Beclin-1 (the mammalian homolog of Atg6), Atg14 or UVRAG and AMBRA1, which facilitate phagophore formation (Boya et al., 2013; Pyo et al., 2012; Rubinsztein et al., 2012). This complex is regulated by Atg13 as well as ULK1 and ULK2, the mammalian homologs of Atg1. For example ULK1 promotes IC activity by phosphorylating Beclin-1 leading to activation of Vps34 and induction of autophagy (Rubinsztein et al., 2012; Russell et al., 2013). Despite our increasing understanding of the autophagy pathway, there is still debate as to the origin of the phagophore which is thought to arise from cellular organelles such as the mitochondria, endoplasmic reticulum (ER), Golgi-apparatus or plasma membrane. (Pyo et al., 2012; Rubinsztein et al., 2012).

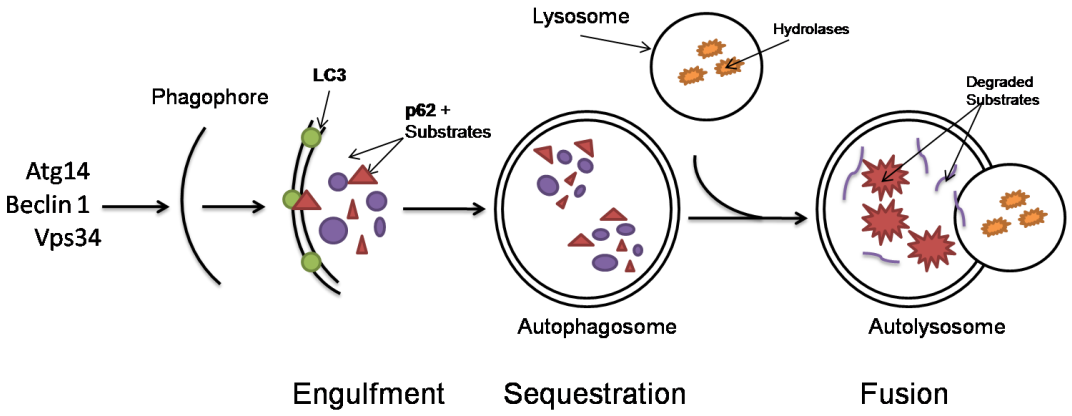

Figure 1.1 The autophagy flux

Autophagy begins with nucleation of a single layered membrane, the phagophore from an existing organelle such as the ER. Proteins including Beclin-1 and Vps34 form an initiator complex (IC) at the phagophore where they function to recruit autophagy genes (*Atg*) to the membrane. These genes promote elongation of the phagophore allowing it to surround and engulf portions of the cytoplasm destined for degradation. Upon closure the phagophore forms the autophagosome to which LC3-II is bound. The autophagosome then binds a lysosome forming the autophagolysosome in which the contents of the autophagosome are degraded by lysosomal hydrolases such as cathepsin B and cathepsin D. Adapted from Kang, Zeh *et al*. 2011.

1.1.3.2 Maturation and Elongation

Elongation and maturation of the phagophore from a single a layered membrane vesicle to a double layered autophagosome is facilitated by two ubiquitin-like (Ubl) conjugation systems - Atg12-Atg5-Atg16 and Atg8-phosphatidylethanolamine (PE) (He and Klionsky, 2009; Rubinsztein et al., 2012).

In the Atg12-Atg5-Atg16 system, Atg12 is activated by Atg7 which acts as an E1 ubiquitin-activating enzyme and transferred to Atg10, an E2 ubiquitin-conjugating enzyme. Atg12 is then covalently bound to Atg5 forming the Atg12-Atg5 conjugate which binds Atg16 non-covalently inducing self-oligomerisation and the formation of a tetramer which binds the phagophore (Figure 1.2) (He and Klionsky, 2009; Rubinsztein et al., 2012).

In the second Ubl system, Atg8 is cleaved by Atg4 resulting in exposure of a C-terminal glycine residue. Atg8 is then activated by Atg7, transferred to Atg3 which acts as an E2 enzyme and conjugated to PE by an amide bond via the Atg12-Atg5 conjugate which acts as an E3 enzyme (Figure 1.2) (He and Klionsky, 2009; Rubinsztein et al., 2012). There are three mammalian homologs of Atg8 – LC3, GATE-16 and GABARAP (Wang et al., 2011). Of these, LC3 is the best characterised and is commonly used as an autophagy marker. Upon receipt of an autophagy inducing stimulus LC3 is cleaved and bound to PE, altering its cellular distribution from a diffuse cytoplasmic form (LC3-I) to a membrane-bound punctate form, LC3-II. Conversion of LC3-I to LC3-II and an increase in LC3-II levels is typically considered a sign of active autophagy; however, this is not always the case and LC3-II levels should be interpreted carefully (section 1.1.4) (He and Klionsky, 2009).

Once bound to the phagophore, the Ubl conjugation systems aid in its expansion and elongation to a double layered membrane vesicle which surrounds and engulfs autophagy substrates and upon closure forms the autophagosome (Figure 1.1).

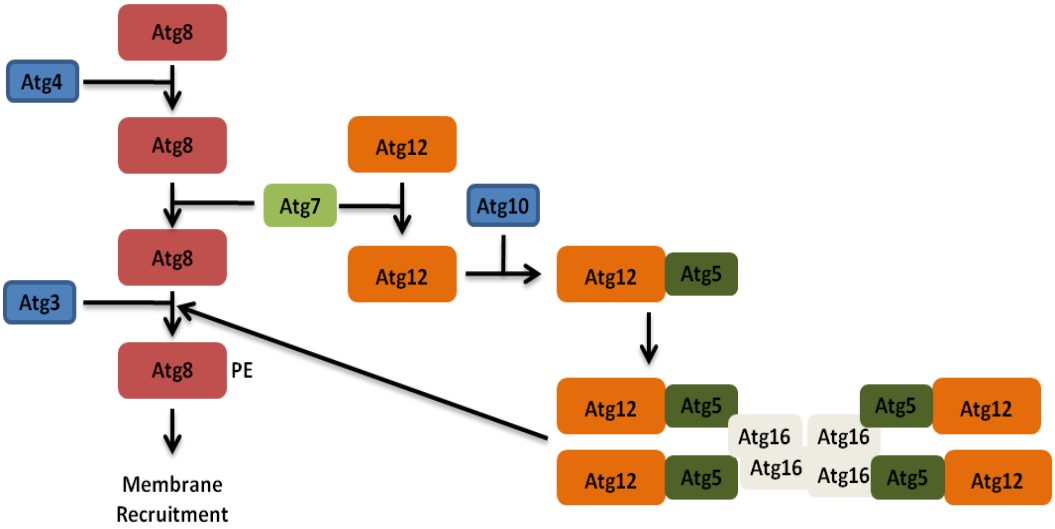

Figure 1.2 The Atg12-Atg5-Atg16 and Atg8-PE Ubl conjugation systems involved in autophagosome expansion and elongation

Two Ubl-conjugation systems aid in the elongation and maturation of the single-layered phagophore to a double-layered autophagosome. Atg12 is activated by Atg7, transferred to Atg10 and subsequently covalently conjugated to Atg5. This Atg12-Atg5 conjugate then interacts with Atg16 resulting in self-oligomerisation of the Atg12-Atg5-Atg16 complex and its incorporation into the phagophore whose elongation it promotes. Atg8 is cleaved by Atg4 exposing a C-terminal glycine residue. Atg7 transfers cleaved-Atg8 to Atg3 which promotes conjugation of Atg8 to PE via the Atg12-Atg5 conjugate. Atg8-PE is incorporated into the autophagosome membrane and also promotes its maturation. Lipidation and membrane incorporation of Atg8 and its mammalian homolog LC3 is widely used as a marker of active autophagy. Adapted from Levine, Klionsky, 2004.

1.1.3.3 Autophagosome / Lysosome fusion

The final step in the autophagy process involves fusion of the autophagosome with a cellular lysosome which is facilitated by LAMP-2 and the small GTPase Rab7 and results in formation of the autophagolysosome (He and Klionsky, 2009; Wang et al., 2011). Following fusion, resident lysosomal acid hydrolases including cathepsin B and cathepsin D break down and degrade the autophagy substrates, which include protein aggregates and old organelles, along with the inner autophagosome membrane (Figure 1.1). Degradation generates new macromolecules and amino acids which are released back into the cytosol and utilised in protein synthesis (Figure 1.1) (He and Klionsky, 2009; Wang et al., 2011).

1.1.4 Measuring the autophagy flux

Examination of the autophagy flux is not straight-forward. While a number of criteria and assays are routinely used to determine autophagy activity within a cell, our increased understanding and improved ability to study this pathway means these criteria are changing and expanding. The difficulty in studying the autophagy flux was summarised by Klionsky and colleagues who state that "there are no absolute criteria for determining autophagy status that are applicable in every biological or experimental context" (Klionsky et al., 2012a).

Not all assays report the dynamic flux through the entire autophagy pathway but rather reflect activity at a specific stage. The timing at which autophagy is evaluated following autophagy induction or inhibition is important as it is a dynamic process. Some reports suggest examination after 30min while others suggest up to 8hr or more (Amaravadi et al., 2007; Shi et al., 2013). Selection of an appropriate time is further complicated by the fact that degradation of substrates (e.g. p62) generally occurs after the appearance of induction markers (e.g. LC3-II) (Klionsky et al., 2012a).

1.1.4.1 Western blotting

Upon activation of autophagy, pro-LC3 is cleaved by *Atg4* to LC3-I which is present in cells in a diffuse cytoplasmic manner. LC3-I becomes conjugated to PE forming LC3-II, which integrates into the autophagosome membrane and is visible as puncta within cells (Pyo et al., 2012). Conversion of cytoplasmic LC3-I to membrane-bound LC3-II, resulting in a decrease in LC3-I levels and an increase in LC3-II, is commonly used as a marker of autophagosome formation and active autophagy when detected by Western blotting (Kabeya et al., 2000; Klionsky et al., 2012a; Mizushima and Yoshimori, 2007). However, care must be taken with this interpretation as LC3-II is itself an autophagy substrate which is degraded by active autophagy. Therefore, absence of an LC3-II band may indicate either impaired autophagy or increased autophagic degradation of LC3-II. It is also reported that LC3-II can be more amenable to detection by immunoblotting than LC3-I and that conversion of LC3-I to LC3-II can be cell-type specific (Klionsky et al., 2012a; Mizushima and Yoshimori, 2007). Treatment of cells with an autophagy inhibitor such as chloroquine (CQ) can be used to determine if increased LC3-II levels

represent increased autophagy flux or impaired substrate degradation. CQ is an autophagosome/lysosome inhibitor which prevents degradation of autophagy substrates including LC3-II, resulting in their accumulation (Amaravadi et al., 2007; Jia et al., 2012). An increase in LC3-II levels upon treatment with an autophagy inducer and CQ compared to induction-only treated cells indicates an increase in the autophagy flux and autophagy activity, while an increase in LC3-II levels by the same degree in induction-only and induction/inhibition treated cells suggests a block in autophagy degradation (Mizushima and Yoshimori, 2007).

p62 binds ubiquitinated proteins and delivers them to the autophagosome via interactions with LC3-II meaning this adaptor protein is itself an autophagy substrate whose cellular levels are commonly used as a marker of autophagy activity. Active and inhibited autophagy result in degradation and accumulation of p62 respectively (Bjorkoy et al., 2005; Klionsky et al., 2012a; Mathew et al., 2009). However care should be taken when correlating p62 levels with autophagy flux activity as this protein is involved in a variety of pathways which modulate and affect its cellular levels (section 1.5). In a similar manner to LC3-I/LC3-II, p62 levels should be examined in cells treated with an autophagy inhibitor (e.g. CQ). A decrease in p62 levels following autophagy stimulation which is inhibited by CQ resulting in p62 accumulation indicates an increase in the autophagy flux (Klionsky et al., 2012a; Mizushima and Yoshimori, 2007). A recent publication has demonstrated that prolonged starvation (~4-8hr) can promote sustained autophagy which is marked by reappearance of p62. Between 0.5 and 2hr post-starvation p62 levels decreased; however, starvation for >4hr resulted in re-emergence of p62 at the protein level (Sahani et al., 2014).

1.1.4.2 Immunofluorescent microscopy

Immunofluorescent microscopy (IFM) allows visualisation of the distribution pattern and cellular location of autophagy-related proteins, as well as examination of their binding partners. LC3-II puncta, which can be identified using IFM, are a widely used marker of autophagosomes and an active autophagy flux. Increased numbers of LC3-II puncta typically indicate increased numbers of autophagosomes and active autophagy, while larger puncta suggest inhibition of autophagic degradation and an accumulation of

this autophagy substrate (Figure 1.3 A) (Kabeya et al., 2000). The cellular distribution of p62 can also be visualised by IFM to assess autophagy activity. When autophagy is active, p62 binds ubiquitinated proteins and LC3-II to form clear cellular aggregates which accumulate and increase in size upon autophagy inhibition (Bjorkoy et al., 2005). Quantification of LC3-II and p62 by IFM should be done by counting the number of punctate/aggregates per cell rather than the number of positive cells (Klionsky et al., 2012a). The autophagy essential protein Beclin-1 can also be visualised by IFM and is typically present in either a diffuse cytoplasmic form or as puncta present in the perinuclear region of cells, the latter of which can be indicative of macro-aggregates and represent active autophagy (Nicotra et al., 2010b). Dual-fluorescent microscopy can be used to examine protein-protein interactions within cells at the basal level and under different experimental conditions and to evaluate the effects of treatments on protein bindings (Bjorkoy et al., 2005; Pattingre et al., 2005).

In cases where endogenous protein expression is low, green-fluorescent protein (GFP) tagged constructs, (e.g. GFP-LC3) can be transfected into cells and used as surrogate markers to monitor the autophagy flux. These assays are extremely useful for monitoring autophagy activity. However, transfection may not always be possible as not all cell types are amenable to this process and transfection efficiency may not always be sufficient or comparable within and between cells. Importantly, the transfection process itself may induce or increase autophagy activity (Klionsky et al., 2012a; Klionsky et al., 2012b). Thus adequate controls, including un-transfected, mock-transfected and autophagy-inhibited cells, should be included in these assays and if possible endogenous levels examined in parallel. Prior to evaluation of the autophagy flux by IFM, stringent criteria of what constitutes puncta/aggregates, the number of cells to be examined and selection of a consistent, standardised exposure time should be established (Klionsky et al., 2012a). Basal or low level autophagy should also be pre-determined to correctly identify/differentiate increased autophagy activity.

1.1.4.4 Transmission electron microscopy

Transmission electron microscopy (TEM) has been used to examine autophagy since the 1950s and still remains a widely used technique which can be used to study non-

selective and selective autophagy (Eskelinen et al., 2011; Jia et al., 1997; Novikoff and Essner, 1962). TEM allows visualisation and identification of autophagy vacuoles, from phagophores to autophagolysosomes, based on morphological features (Klionsky et al., 2012a; Yla-Anttila et al., 2009). For example, early autophagosomes are identifiable as double-layered membrane vesicles containing morphologically intact substrates not yet degraded (Jia et al., 1997), while late-stage autophagolysosomes are characterised by a single-layered membrane comprised of autophagy substrates in various states of degradation (Figure 1.3 B) (Eskelinen, 2008a, b; Yla-Anttila et al., 2009). Care must be taken when using TEM to identify these structures as every double-layered membrane vesicle within a cell is not necessarily an autophagy vacuole (Eskelinen, 2008b; Giammarioli et al., 2012). Goldlabeling immuno-TEM which uses antibodies bound to GFP which are directed against autophagy-related proteins allows more accurate identification of autophagy vacuoles compared to standard TEM.

1.1.4.5 Immunohistochemistry

Expression levels of various autophagy-related proteins have been examined in animal and human tissues using immunohistochemistry (IHC). Endogenous Atg4B, Atg9A and LC3 have been studied in rat and mouse tissues while Beclin-1, LC3, and to a lesser extent p62 have been evaluated in a number of human cancer tissues, where their expression was shown to be prognostically significant (Klionsky et al., 2012b; Klionsky et al., 2007; Lu et al., 2001). As IHC is not a technique which lends itself well to dynamic assays, it is more likely to provide a snapshot of autophagy activity within a cell than give information on the entire autophagy flux (Klionsky et al., 2012a). However, IHC is becoming increasingly employed as an autophagy assay. Staining by IHC can detect diffuse cytoplasmic proteins (e.g. LC3-I) and protein puncta (e.g. LC3-II), the latter of which can be difficult to interpret and so should be evaluated with caution (Figure 1.3 C).

Difficulties encountered when performing IHC include selection of an appropriate, high-quality antibody and identification of the most appropriate antigen-retrieval method which if optimised prior to staining can reduce background levels and false-negatives (Conway et al., 2008; Shi et al., 2001; Shi et al., 1991). Prior to analysis by

IHC a representative tissue area should be selected for examination and clear guidelines for quantification established which are maintained across all samples.

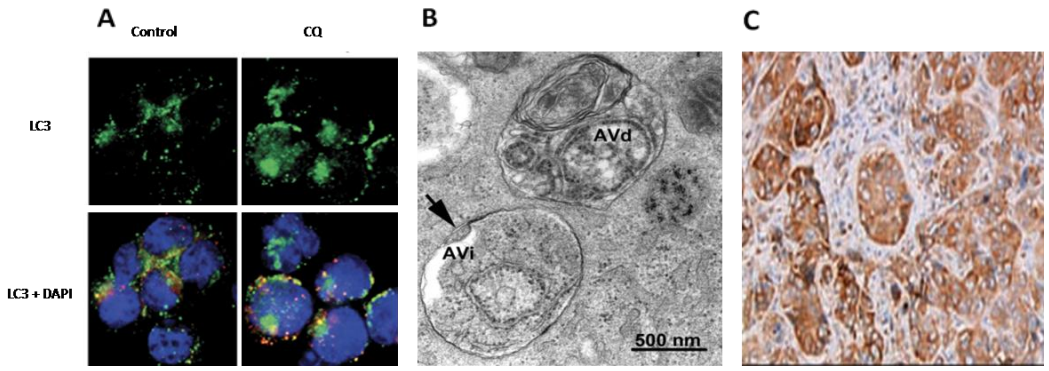

Figure 1.3 Representative output images from various autophagy assays
Late stage inhibition of autophagy by the lysosomal inhibitor chloroquine (CQ) results in accumulation of LC3-positive punctate indicative of LC3-II in Su-DHL8 cell lines stained with rabbit polyclonal anti-LC3B (A). Autophagy vacuoles visualised in isolated mouse hepatocytes by TEM. An early autophagosome (AVi) and late autophagolysosome (AVd) are shown. The AVi is identified by a double membrane separated by an electron-cleft (arrow) and intact cytoplasmic contents; the AVd is identified by its partially degraded contents and rough endoplasmic reticulum (B). Representative image of a Beclin-1^{+} hepatocellular carcinoma patient tissue sample stained by IHC using rabbit monoclonal anti-Beclin-1 antibody and visualised at 400x magnification (C). Adapted from Jia *et al* 2012, Klionsky *et al* 2012, and Ding *et al* 2008 respectively.

1.1.4.3 Gene expression analysis / quantitative real-time polymerase chain reaction

Examination of autophagy at the messenger RNA (mRNA) level using gene expression profiling (GEP) and quantitative real-time polymerase chain reaction (qRT-PCR) is becoming increasingly common. These assays allow simultaneous examination of expression levels of a plethora of genes involved in all stages of the autophagy flux and will undoubtedly provide more information and improve our understanding of this complex process.

While we are aware of what happens to key autophagy players such as LC3 and p62 at the protein level, it is still unclear what happens these and other proteins at the mRNA level when autophagy is active or inhibited. Some reports indicate LC3 mRNA levels remain unchanged while others have reported an increase in its synthesis following starvation-induced autophagy. It has been suggested that modulations in LC3 mRNA are cell-type specific and so should be examined on a case-by-case basis (Klionsky et al., 2012b; Mizushima and Yoshimori, 2007; Nara et al., 2002). It is also unclear what

happens to Squestosome1 (*SQSTM1*) levels during autophagy. Unaltered *SQSTM1* levels have been reported where as an increase in p62 mRNA levels following autophagy induction has also been observed (Komatsu et al., 2010; Nakaso et al., 2004; Sahani et al., 2014).

1.1.5 Autophagy inducers and inhibitors

As well as extracellular signals, intracellular genes and proteins (Table 1.1) and a variety of chemical compounds (Table 1.2) are involved in induction and inhibition of the autophagy pathway.

1.1.5.1 Inducers of the autophagy pathway

A well established inducer of the autophagy pathway is oxygen deprivation or hypoxia. Increased autophagy activity under hypoxic conditions, particularly in cancer cells, can promote cell survival, tumour progression and resistance to treatment (Brahimi-Horn et al., 2007). HIF-1 is a transcription factor which induces autophagy and a plethora of genes which allow cells to adapt to and survive hypoxia (Semenza, 2010). Hypoxia-induced autophagy can occur in a HIF-dependent or -independent manner. HIF-1-dependent autophagy involves HIF-1-mediated transcriptional activation of the BCL2-homolgy3 (BH3) only proteins BNIP3 and BNIP3α which disrupt binding between BCL-2 and Beclin-1, allowing autophagy to proceed (Bellot et al., 2009; Mazure and Pouyssegur, 2010). Conversely, HIF-independent autophagy involves increased activation of AMPK which functions to inhibit the mammalian target of rapamycin (mTOR) pathway and thus increase levels of autophagy activity (Papandreou et al., 2008).

Autophagy is also induced by nutrient deprivation or starvation through numerous mechanisms. Reactive oxygen species (ROS), particularly hydrogen peroxide (H_2O_2) and super oxide (O_2^-) which originate at the mitochondria, are highly involved in starvation-induced autophagy (Scherz-Shouval and Elazar, 2011). Accumulation of ROS induces activation of AMPK and the JAK/STAT3 pathway both of which induce autophagy activity (Li et al., 2013; Yoon et al., 2010). Starvation also induces autophagy by inhibiting mTOR and by inducing phosphorylation of BCL-2 which promotes its dissociation from Beclin-1 (Jung et al., 2010; Yang and Klionsky, 2010).

The tumour suppressor protein PTEN induces autophagy by acting as an upstream negative regulator of the AKT/mTOR pathway through its lipid phosphatase activity (Azad et al., 2009; Sarkar et al., 2009). AMPK also promotes autophagy via inhibition of mTOR. Direct mTOR inhibition by AMPK occurs following AMPK mediated phosphorylation and inhibition of RAPTOR (regulatory-associated protein of mTOR), a component of the mTORC1 complex (Alers et al., 2012; Kim et al., 2011). AMPK can also indirectly inhibit mTOR by phosphorylating and activating tuberous sclerosis complex-2 (TSC2) a member of the TSC1/2 complex which negatively regulates mTOR (Feng et al., 2005; Maiuri et al., 2010).

Rapamycin is a lipophilic secondary metabolite compound used as an immunosuppressive agent which induces autophagy by inhibiting the mTORC1 complex and facilitating activation of the ULK1-Atg13-FIP200 complex required for autophagosome formation (Benjamin et al., 2011; Renna et al., 2010; Sarkar et al., 2009; Wu et al., 2011). ABT-737 is a BH3-mimetic originally developed to bind the anti-apoptotic proteins BCL-2, BCL-xL and BCL-w via BH3 domain interactions resulting in their sequestration and the subsequent induction of apoptosis (Kang and Reynolds, 2009; van Delft et al., 2006; Vogler et al., 2009). Binding of ABT-737 to BCL-2 has also been shown to induce autophagy (Levine et al., 2008; Marquez and Xu, 2012). BCL-2 can bind and sequester the pro-autophagy protein Beclin-1 and inhibit autophagy. By binding BCL-2, ABT-737 prevents its interaction with Beclin-1 and thus inhibits the anti-autophagic action of BCL-2 (Section 1.4) (Levine et al., 2008; Malik et al., 2011; Marquez and Xu, 2012). ABT-737 has also been found to induce autophagy by phosphorylating and activating the previously discussed autophagy inducer AMPK as well as through inhibition of AKT and mTOR (Malik et al., 2011). The effect of ABT-737 on BCL-2 and the autophagy pathway and how this may affect tumour cell killing by this BH3-mimetic have yet to be determined in FL and DLBCL cells.

1.1.5.2 Inhibitors of the autophagy pathway

One of the key inhibitors of the autophagy pathway is the PI3K/AKT/mTOR pathway, with active mTOR signalling promoting cell growth and inhibition of autophagy. mTOR is comprised of two complexes – mTORC1 and mTORC2 - and is located

downstream in the class I PI3K pathway (Sarkar et al., 2009). It is positively regulated by the kinase AKT and the RHEB G-protein but is negatively regulated by TSC2 and the TSC1/TSC2 complex (Feng et al., 2007; Renna et al., 2010; Sarkar et al., 2009). Inhibition of autophagy by mTOR involves ULK1, Atg13 and FIP200, all of which are necessary for phagophore formation. Under nutrient rich conditions mTOR phosphorylates and inhibits ULK1 and Atg13 preventing development of the phagophore (Nazio et al., 2013; Renna et al., 2010; Sarkar et al., 2009).

Pharmacological inhibitors of autophagy include 3-methyladenine (3-MA) (Jia et al., 1997), Bafilomycin-A1 and CQ which exert their function at different stages in the pathway. 3-MA is a PI3K inhibitor which negatively regulates autophagy early in the pathway by inhibiting the class III PI3K Vps34 and preventing autophagosome formation (Liu et al., 2011; Seglen and Gordon, 1982). Conversely, Bafilomycin-A1 and CQ inhibit autophagy later in the pathway by interfering with autophagosome fusion and lysosomal degradation. The widely used anti-malaria drug CQ is a lysosomotropic agent which raises the lysosomal pH and prevents autophagosome/lysosome fusion and substrate degradation. Impairment of this final step in the autophagy pathway results in accumulation of substrate containing autophagosomes and prevents recycling of old proteins and organelles back into the cytoplasm (Amaravadi et al., 2007; Sasaki et al., 2010). Treatment with CQ therefore results in accumulation of LC3-II and p62 which are autophagy substrates sequestered by the autophagosome (Amaravadi et al., 2007; Bjorkoy et al., 2005; Jia et al., 2012).

Table 1.1 Genes and proteins involved in autophagy regulation

Gene/Protein	Inducer/Inhibitor	Reference
AMPK1	Inducer	(Alers et al., 2012)
PTEN	Inducer	(Azad et al., 2009)
DAPK1	Inducer	(Maiuri et al., 2010)
ROS (H_2O_2)	Inducer	(Scherz-Shouval et al., 2007)
Nuclear p53	Inducer	(Maiuri et al., 2010)
mTOR (PI3K/AKT//mTOR)	Inhibitor	(Nazio et al., 2013)
Cytoplasmic p53	Inhibitor	(Maiuri et al., 2010)
NF-κB	Inhibitor	(Djavaheri-Mergny et al., 2006)
BCL-2; BCL-xL	Inhibitor	(Kang et al., 2011)

Table 1.2 Chemical Compounds involved in autophagy regulation

Compound	Inducer/Inhibitor	Reference
TNF-α	Inducer	(Jia et al., 1997)
Rapamycin	Inducer	(Sarkar et al., 2009)
ABT-737	Inducer	(Marquez and Xu, 2012)
Metformin	Inducer	(Ben Sahra et al., 2010)
Lithium	Inducer	(Renna et al., 2010)
CQ/HCQ	Inhibitor	(Jia et al., 2012)
3-Methylamine (3-MA)	Inhibitor	(Jia et al., 1997; Liu et al., 2011)
Bafilomycin-A1	Inhibitor	(Klionsky et al., 2008b)

1.1.6 Apoptotic and autophagic cell death

It is becoming increasingly apparent that autophagy and apoptosis are not mutually exclusive pathways, but rather share common regulators and can act in synergy with or antagonistically toward one another (Denton et al., 2012; Eisenberg-Lerner et al., 2009; Maiuri et al., 2007c).

1.1.6.1 Apoptosis - type-I programmed cell death

Apoptosis, classified as a type-I form of programmed cell death (PCD), is the controlled killing of cells which are deemed superfluous or potentially dangerous and is involved in maintenance of homeostasis and developmental processes. It can be divided into two pathways – intrinsic and extrinsic – which differ with respect to initiation signals, mode of action and molecules involved. Morphological characteristics of apoptotic cells include nuclear fragmentation, membrane blebbing and chromatin condensation (Kerr et al., 1972; Maiuri et al., 2007c; Ola et al., 2011).

The intrinsic apoptotic pathway is stimulated upon receipt of intracellular signals such as oxidative stress and DNA damage and centres on the mitochondria. Triggering of the intrinsic pathway promotes translocation of BCL-2 family members Bim, Bid, Bax and Bak to the mitochondria. Once there, Bim and Bid, classified as BH3-only activator proteins stimulate a conformational change in Bax and Bak promoting their oligomerisation and inducing mitochondrial outer membrane permeabilisation (MOMP) (Deng et al., 2007; Maiuri et al., 2007c). MOMP decreases mitochondrial membrane potential ($\Delta\Psi m$) and facilitates the release of pro-death molecules such as cytochrome c, apoptosis-inducing factor (AIF) and endonuclease G (ENDOG). AIF and ENDOG migrate to the nucleus where they trigger large scale DNA fragmentation and the

caspase-independent apoptosis pathway, while cytochrome c binds deoxyadenosine triphosphate (dATP) and apoptotic protease-activating factor (APAF1) to form the apoptosome which induces caspase-dependent apoptosis. The caspase-cascade involves 'activator' caspases (e.g. caspase-8) inducing activation of 'executioner' caspases (e.g. caspase-3) which once activated facilitate apoptosis by promoting and inducing cellular proteolysis and marking cells destined for phagocytic engulfment and cell death (Deng et al., 2007; Galluzzi et al., 2012; Ola et al., 2011).

The extrinsic apoptosis pathway is induced upon receipt of an extracellular signal and involves binding of ligands such as FASL, TNF-α and TRAIL to their respective transmembrane receptors FAS, TNFR or TRAILR and inducing trimerisation. These trimers then recruit cellular inhibitors of apoptosis proteins (cIAPs) and death-domain containing adaptor molecules such as FADD to the cytoplasmic side of the mitochondrial membrane to form the death induced signalling complex (DISC). The DISC then stimulates caspase-8 or caspase-10 to induce the caspase-cascade and cell death (Galluzzi et al., 2012; Maiuri et al., 2007c; Ola et al., 2011).

1.1.6.2 Autophagy - type-II programmed cell death

Although predominantly considered a pro-survival mechanism, autophagy has also been classified as a form of cell death depending on the cell type and the nature of the stimulus (Galluzzi et al., 2012). Autophagy was classified as a type-II PCD based on morphological features when dying cells were shown to exhibit a different morphology to that typically seen in cells undergoing apoptosis. Cells dying by autophagy are characterised by the presence of large numbers of autophagosomes and large-scale cytoplasmic vacuolisation (Fulda, 2012; Jia et al., 1997; Sasi et al., 2009; Shen and Codogno, 2011). However, confirmation of autophagy as a *bona fide* form of cell death is ongoing.

Some reports suggest autophagy occurs and cell death ensues; however others state that cells die directly as a result of the autophagy pathway, with evidence emerging that the latter is true (Eisenberg-Lerner et al., 2009; Fulda, 2012; Gonzalez-Polo et al., 2005; Rosenfeldt and Ryan, 2011). It has been shown that in Bax^{-}/Bak^{-} cells defective for apoptosis, an increase in autophagy corresponds to an increase in cell death. Similarly,

inhibition of the autophagy pathway using pharmacological inhibitors such as CQ, or short-interfering RNA (siRNA) targeted against autophagy genes such as *Atg7*, results in decreased cell death in apoptosis-deficient cells (Fulda, 2012; Shen and Codogno, 2011; Shimizu et al., 2004). An increase in the entire autophagy flux, not only cellular levels of autophagy markers must be observed in order to classify cell death as autophagic. Shen and colleagues have proposed three criteria which must be met in order for autophagy to be classified as a genuine cell death mechanism: (i) cells must be defective for apoptosis, i.e. death occurs without activation of apoptosis; (ii) inhibition of autophagy genetically or pharmacologically attenuates cell death and increases cell survival; (iii) there is an increase in the autophagy flux (Shen and Codogno, 2011).

1.1.6.3 Cross-talk between autophagy and apoptosis

Autophagy and apoptosis are conflicting pathways – one typically promotes cell survival, the other cell death. Maintaining the appropriate balance between these pathways is therefore important when determining cell fate (Maiuri et al., 2007c; Mukhopadhyay et al., 2014). It is also important to consider the cross-talk between these pathways when considering the effects of anti-cancer treatments on either pathway.

Depending on the stimulus received and cellular conditions, autophagy and apoptosis may be induced in a combined or mutually exclusive manner. Upon receipt of a stress signal cells generally up-regulate autophagy in a bid to survive, where as death-receptor activation typically results in promotion of apoptosis and cell death (Eisenberg-Lerner et al., 2009). The sensitivity threshold of cells to different stimuli is also involved in deciding which pathway to induce. Low level mitochondrial damage may result in increased autophagy, while a high degree of injury to these essential organelles will induce apoptotic or necrotic cell death (Maiuri et al., 2007c). Cross-talk between these pathways can be divided into three broad categories – co-operative, antagonistic and enabling. Under the co-operative setting autophagy and apoptosis promote cell death and compensate for one another if needed. For example, in Bax^{-}/Bak^{-} apoptosis-deficient cells autophagy activity can increase and ultimately result in autophagic cell death (Maiuri et al., 2007c; Mukhopadhyay et al., 2014). In the antagonist setting,

induction of one pathway can prevent promotion of the other. Following administration of chemotherapeutic drugs for example, autophagy can be induced by cells as a cytoprotective mechanism to escape this stress, mitigate cellular damage and avoid apoptosis (Eisenberg-Lerner et al., 2009; Kimmelman, 2011). Finally, induction of autophagy can enable apoptosis without itself promoting cell death by responding to a stress but subsequently assisting in triggering the apoptotic cascade and cell death (Eisenberg-Lerner et al., 2009; Maiuri et al., 2007c).

Autophagy and apoptosis share many common triggers and regulators. Increased cellular levels of ROS which promote MOMP, a key step in induction of the intrinsic apoptosis pathway, can also promote autophagy by activating *Atg4*, an important step in autophagy induction (Maiuri et al., 2007c; Scherz-Shouval et al., 2007). Similarly, ER-stress, a well established trigger of apoptosis, also induces reticulophagy, the autophagy-mediated degradation and removal of damaged ER (Abida and Gu, 2008; Eisenberg-Lerner et al., 2009; Yorimitsu et al., 2006). BH3-only proteins also regulate induction of autophagy and apoptosis. These pro-survival proteins can induce autophagy by binding BCL-2 and promoting the release of Beclin-1. They also promote apoptosis via inhibitory-interactions with anti-apoptotic proteins such as BCL-2 or inducing-interactions with pro-apoptotic proteins, e.g. Bak (Maiuri et al., 2007c; Marquez and Xu, 2012; Mukhopadhyay et al., 2014). The cellular location of these BH3-only interactions is thought to play a role in determining autophagy/apoptosis induction. Binding of BH3-only proteins to Beclin-1 at the ER induces autophagy, while their binding to BCL-2 family members occurs at the mitochondria and promotes apoptosis (Maiuri et al., 2007b).

A number of key autophagy genes and proteins have been shown to regulate and be regulated by the intrinsic and extrinsic apoptosis pathway. For example the N-terminal cleavage product of the autophagy essential protein Atg5 has been shown to translocate to the mitochondria where it interacts with BCL-xL to promote cytochrome c release and the intrinsic apoptosis pathway, while cleavage of Atg3 by caspase-8 results in autophagy inhibition during the extrinsic apoptosis pathway (Mukhopadhyay et al.,

2014). Table 1.3 lists other autophagy genes and proteins involved in regulation of both pathways.

Table 1.3 Dual roles of autophagy and apoptosis genes

Protein	Function	Role in Autophagy	Role in Apoptosis
Beclin-1	Autophagy	Autophagosome nucleation	Cleaved C-fragment induces intrinsic apoptosis
AMBRA	Autophagy	Up-regulates interaction between Vps34 and Beclin-1	Cleaved by caspase and calpins; regulates intrinsic apoptosis
UVRAG	Autophagy	Up-regulates interaction between Vps34 and Beclin-1	Inhibits Bax translocation to the mitochondria; anti-apoptotic
ATG5	Autophagy	Conjugates to Atg12 and promotes membrane elongation	Promotes intrinsic apoptosis; inhibits extrinsic apoptosis via FADD interactions
ATG3	Autophagy	Conjugates with Atg12	Regulates intrinsic apoptosis
p62	Autophagy	Delivery of substrates to the autophagosome	Processing and activation of caspase-8
BCL-2/ BCL-xL	Apoptosis	Sequesters Beclin-1; inhibits autophagy	Anti-apoptotic
Bad/Bak	Apoptosis	Disrupts BCL-2/Beclin-1 binding; induces autophagy	Pro-apoptotic
Bim	Apoptosis	Sequesters Beclin-1; inhibits autophagy	Pro-apoptotic

1.1.7 Autophagy in cancer

The role of autophagy in cancer development is a paradoxical one. While on the one hand described as a tumour suppressing mechanism, autophagy has also been reported to promote and maintain tumour cell survival (Choi et al., 2013a; Eisenberg-Lerner and Kimchi, 2009; Mizushima et al., 2008). Autophagy activity, which is regulated by both tumour suppressors and oncogenic promoters, has been reported to be increased and decreased within tumour cells with both instances shown to be pro- and anti-tumourogenic (Guo et al., 2011; Liang et al., 1999; Mathew et al., 2009; Rosenfeldt et al., 2013; Yang et al., 2011). Levels of autophagy activity can modulate the response of tumour cells to chemotherapeutic agents by promoting or hindering their pro-apoptotic function, and correlate with clinical outcome in cancer patients (Bellodi et al., 2009; Verschooten et al., 2012).

1.1.7.1. The tumour suppressing role of autophagy

The principle role of autophagy is to degrade and remove old and damaged cellular organelles and proteins which if allowed accumulate in cells can promote instability and tumourigenesis. By removing accumulated intracellular aggregates, autophagy maintains genomic stability, prevents DNA damage, mitigates oxidative stress and suppresses tumourigenesis. Autophagy can also suppress tumour formation by degrading damaged cellular organelles and inducing autophagic cell death, therefore preventing necrotic cell death and the subsequent inflammatory response it induces (Eisenberg-Lerner et al., 2009; Helgason et al., 2013; Mathew et al., 2009; Pattingre and Levine, 2006; Rosenfeldt and Ryan, 2011).

Autophagy was considered a tumour suppressor mechanism when it was shown that ablation of key autophagy genes and proteins induces tumour formation. The observation that increased expression of the autophagy essential protein Beclin-1 suppresses tumourigenesis in nude mice identified it as a haploinsufficient tumour suppressor molecule (Liang et al., 1999) and demonstrated that active autophagy can act as a tumour suppressing pathway. Autophagy inhibition due to ablation of *Atg* genes can also promote tumour growth. For example, it has been reported that mice with liver-restricted deletion of *Atg7* develop hepatocarcinomas while frameshift mutations in *Atg2B*, *Atg5*, and *Atg12* are frequently observed in colorectal and gastric carcinomas. Active autophagy can therefore function to suppress the development of multiple different neoplasms (Helgason et al., 2013; Kang et al., 2009; Takamura et al., 2011).

1.1.7.2 The tumour promoting role of autophagy

Exploitation of the pro-survival role of autophagy is not restricted to healthy cells but is also employed by tumour cells which use this pathway to evade stress and maintain survival (Kimmelman, 2011; Kroemer et al., 2010). The main manner in which autophagy promotes tumour cell survival is by mitigating metabolic stresses encountered by malignant cells. It is well known that tumour cells deprived of nutrients and/or oxygen (hypoxic cells) induce autophagy to adapt to these stresses and stay alive (Degenhardt et al., 2006; Eisenberg-Lerner and Kimchi, 2009; Guo et al., 2011; Kimmelman, 2011). A cell autonomous role for autophagy in tumour cell maintenance

has also been suggested where neoplastic cells have developed a requirement for active autophagy in order to survive (Guo et al., 2011). Yang and co-workers reported that active autophagy is necessary for pancreatic tumour cell survival and that inhibition of autophagy resulted in attenuation of *in vitro* cell growth and improved response to cancer therapy (Kimmelman, 2011; Yang et al., 2011). It has also been reported that *in vivo* inhibition of autophagy through *Atg3* deletion results in decreased BCR-Abl-induced leukaemogenesis and increased cell death indicating a dependency on the autophagy pathway in these cells (Altman et al., 2011). Autophagy is also known to play a role in tumour maintenance by allowing malignant cells to escape cellular stress induced by anti-cancer therapies (Choi et al., 2013a).

The role of autophagy in tumour development appears to be cell type-dependent, implying that autophagy activity should be examined on a cancer by cancer basis (Eisenberg-Lerner and Kimchi, 2009). A possible model for the role of autophagy in malignancies is as follows: inhibition of autophagy results in an increase in genomic instability and DNA damage which can induce and promote malignant transformation. Once transformation of a normal cell to a cancerous cell has occurred, persistence of autophagy inhibition and its cellular effects (e.g. increase ROS production) are incompatible with survival. Thus, established tumours reactive or up-regulate the autophagy flux to avoid stress, maintain survival and promote growth (Kimmelman, 2011; Scherz-Shouval and Elazar, 2011).

1.1.7.3 The role of autophagy in cancer therapy

It is widely accepted that treatment of neoplastic cells with anti-cancer agents can induce autophagy activity. The influence of therapy-induced autophagy on the efficacy of chemotherapy drugs varies from a bystander effect to promoting cell death to functioning as a cytoprotective, pro-survival mechanism (Choi et al., 2013a; Wu et al., 2011).

Although not as commonly reported, therapy-induced autophagy can potentiate the pro-death function of chemotherapeutic agents. For example, induction of apoptosis and autophagy following treatment with ABT-737 and rapamycin respectively has been shown to increase sensitivity of non-small cell lung carcinoma *in vitro* and *in vivo* (Kim

et al., 2009; White, 2012). However, a more common observation is the induction of autophagy as a cytoprotective mechanism which allows cancer cells mitigate therapy induced stress and avoid apoptosis (Choi et al., 2013a; Helgason et al., 2013).

Amaravadi and colleagues have shown that in a *Myc*-induced lymphoma model, inhibition of autophagy can increase cell death. They reported that treatment of $p53^{-/-}$ mice with tamoxifen can restore apoptosis but also induces cytoprotective autophagy within these cells. Inhibition of therapy-induced autophagy via genetic knockdown of *Atg5* or pharmacological inhibition by CQ resulted in increased killing of tumour cells, indicating a rationale for the use of autophagy inhibitors in conjunction with standard alkylating and p53 activating cancer therapies (Amaravadi et al., 2007). It has also been shown that prostate cancer and chronic myeloid leukaemia (CML) cells induce cytoprotective autophagy following treatment with Tunicamycin and Imatinib, respectively, suggesting that combined treatment with autophagy-inhibiting agents may improve the efficacy of these therapeutic agents (Helgason et al., 2013). Treatment with BH3-mimetic compounds such as (-)-Gossypol induces apoptosis by inhibiting BCL-2/BCL-xL and also induces cytoprotective autophagy in breast cancer cell lines (Gao et al., 2010).

In contrast with these findings, a recent study by Rosenfeldt and colleagues has shown that inhibition of autophagy with CQ in Kras-positive, p53-null mice with pancreatic ductal adenocarcinoma (PDAC) results in increased, accelerated tumour formation *in vivo* (Rosenfeldt et al., 2013). They found that autophagy competent mice which expressed mutated, activated Kras developed PDAC while mice which were autophagy defective due to ablation of *Atg5* and *Atg7* developed pre-malignant pancreatic lesions which did not progress to PDAC. Inhibition of p53 in either setting resulted in development of PDAC, however tumour formation and progression was accelerated in autophagy-defective cells. They confirmed this finding by treating autophagy competent $p53^{-/-}$, Kras mutated mice with the late autophagy inhibitor CQ and found that PDAC formation occurred at an accelerated rate compared to non-treated cells (Rosenfeldt et al., 2013). These findings demonstrate that the effects of autophagy inhibition on

tumour progression should be tested on a case by case basis and again highlight the conflicting role of this pathway in different malignancies.

A number of clinical trials are currently underway which are investigating the use of autophagy inhibitors in various cancer settings (Helgason et al., 2013). For example the CHOICES (CHlOrquine and Imatinib(IM) Combination to Eliminate Stem Cells) phase I clinical trial is studying combination of Imatinib with hydroxychloroquine (HCQ) in CML patients, while a phase I/II trial investigating the effect of HCQ in combination with gemcitabine in pancreatic cancer is also underway (Bellodi et al., 2009; Helgason et al., 2013; Sinclair et al., 2013). While CQ and HCQ inhibit autophagy, they are not specific inhibitors of this pathway. Therefore, while administration of these drugs does potentiate the pro-apoptotic effects of multiple chemotherapy drugs, it cannot be definitively stated that this is due to targeted autophagy inhibition (Helgason et al., 2013; Sinclair et al., 2013).

New compounds are currently being developed which are more specific inhibitors of autophagy. Potential targets for such compounds include Vps34, ULK1/2 and *Atg* genes. Spautin-1, a small molecule inhibitor (SMI) directed against Vps34 has already been developed and is showing promise in the pre-clinical setting, while studies have also shown that ablation of *Atg7* or *Atg5* in combination with Imatinib results in decreased tumour cell colony formation and cell proliferation (Helgason et al., 2013; Sinclair et al., 2013). It therefore seems likely that autophagy inhibiting agents may soon be administered alongside standard chemotherapy agents in a bid to improve tumour cell killing by these drugs.

It is unknown if the chemotherapy regimens currently used to treat FL and DLBCL induce or inhibit autophagy activity within these tumours and if so, whether controlling autophagy modulation can improve the efficacy of these anti-cancer agents.

1.2 Beclin-1

1.2.1 Beclin-1 is essential to the autophagy pathway

Beclin-1 was discovered by Liang and co-workers in 1998 while searching for binding partners of BCL-2. They identified Beclin-1/Vps30, the mammalian homolog of the autophagy gene *Atg6*, a novel 60kDa coiled-coiled protein to be capable of binding this anti-apoptotic protein (Liang et al., 1998). Subsequent studies revealed Beclin-1 to be essential for autophagy initiation as it binds Vps34 and Vps15 at the PAS as part of the IC, recruits other proteins such as AMBRA and UVRAG and promotes phagophore formation (He and Levine, 2010; Kihara et al., 2001; Marquez and Xu, 2012; Pattingre et al., 2005).

1.2.2 Beclin-1 is a multi-domain protein

Beclin-1 is comprised of an N-terminal BH3 domain, a central coiled-coiled domain (CCD) and a C-terminal evolutionarily conserved domain (ECD) which allow Beclin-1 to interact with a wide variety of proteins and are important to its pro-autophagic and anti-tumour roles (Figure 1.4 A) (Kang et al., 2011). The autophagy promoters UVRAG, AMBRA and Atg14L bind to the CCD, Vps34 binds to the CCD and ECD domains, and the autophagy inhibitor BCL-2 binds Beclin-1 via BH3 domain interactions (Figure 1.4). Beclin-1s' ECD is essential for promotion of autophagy and inhibition of tumourigenesis, as is the nuclear export signal (NES) located in the CCD (Kang et al., 2011). Ubiquitination and phosphorylation of residues within the BH3 domain of Beclin-1 also induces autophagy (Figure 1.4 B; Section 1.4.2.2) (Kang et al., 2011; Marquez and Xu, 2012).

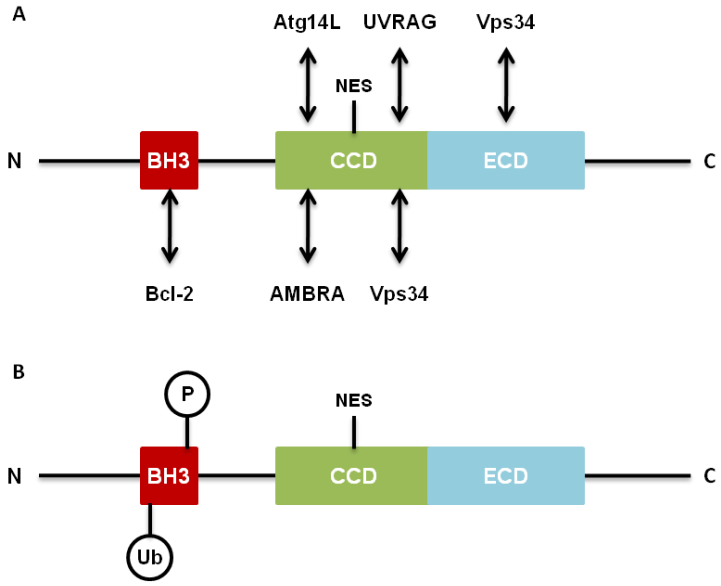

Figure 1.4 Structural organisation of the autophagy essential protein Beclin1
Beclin1 contains multiple binding domains which facilitate its self-oligomerisation and interaction with various proteins (A). The BH3 domain of Beclin-1 can be phosphorylated and ubiquitinated (B). BH3 - BCL-2 homology 3; CCD - coiled-coiled domain; ECD - evolutionarily conserved domain; NES - nuclear export signal; Ub - ubiquitination site; P - phosphorylation site; N - N-terminal; C -C-terminal. Adapted from Kang, Zeh *et al* 2011.

1.2.3 Beclin-1 localises to the mitochondria and the ER

This pro-autophagy protein is expressed by various mammalian cells and tissues where it interacts with multiple different proteins (Kang et al., 2011; Pattingre et al., 2005). Within cells, Beclin-1 was initially reported to locate primarily to the trans-Golgi network (TGN); however, further studies by Pattingre and colleagues using confocal microscopy revealed co-localisation of Beclin-1 with dyes targeted to the ER and the mitochondria (Pattingre et al., 2005). Beclin-1 interacts with Vps34 at the TGN and BCL-2 at the ER and mitochondria.

1.2.4 Beclin-1 is a tumour suppressor protein

Beclin-1 maps to chromosome 17q21, a tumour susceptibility locus which is mono-allelically deleted in 40-75% of human malignancies including spontaneous breast and ovarian cancers. This leads to classification of Beclin-1 as a haploinsufficient tumour suppressor protein which when overexpressed can inhibit tumourigenesis (Liang et al., 1999; Marquez and Xu, 2012; Qu et al., 2003; Yue et al., 2003).

The direct effect of heterozygous deletion of Beclin-1 on autophagy and tumour growth was demonstrated by Liang and co-workers in 1999. Using MCF-7 breast carcinoma cells which do not express Beclin-1 (MCF-7.control) and cells transfected with full-length *Beclin-1* (MCF-7.*beclin-1*) they identified a higher number of autophagosomes and increased autophagy activity within MCF-7.*beclin-1* cells under normal and starved conditions. Proliferation rates were found to be lower in cells expressing *Beclin-1* as were incidences of tumour formation in nude mice injected with MCF-7.*beclin-1* cells compared to MCF-7.control treated mice (Liang et al., 1999). Together, these results show autophagy activity is inhibited when Beclin-1 is absent and also demonstrate the tumour suppressing role of Beclin-1, in turn highlighting the anti-neoplastic role of autophagy.

Expression levels of Beclin-1 have also been shown to be associated with clinical outcome (Huang et al., 2010; Marquez and Xu, 2012). A recent study by Nicotra and colleagues found that in a cohort of 102 non-Hodgkin's lymphoma (NHL) patients, increased expression of Beclin-1 (≥20%) was associated with better overall survival (Nicotra et al., 2010b). Of the 59 NHL cases classified as having high Beclin-1 expression, 16 were diagnosed as FL and 15 as DLBCL. They reported an overall positive correlation between Beclin-1 expression and the presence of LC3-II puncta, and thus suggest that higher Beclin-1 expression reflects increased autophagy activity. Expression levels of BCL-2 and Beclin-1 were found to be negatively correlated, which they propose indicates that in the absence of BCL-2, levels of Beclin-1 and autophagy activity are increased (Nicotra et al., 2010b). However, while increased numbers of LC3-II puncta are often taken to reflect an active autophagy flux, it is also well established that inhibition of autophagy degradation results in accumulation of this autophagy substrate (Kabeya et al., 2000; Klionsky et al., 2012b; Maycotte et al., 2012; Pankiv et al., 2007). Similarly, while Beclin-1 is known to be an autophagy-essential protein, it is not firmly established that its expression levels directly reflect autophagy activity (Castino et al., 2011; Klionsky et al., 2012b). In their study, Nicotra and colleagues provide no evidence to confirm that increased Beclin-1 expression directly reflects increased autophagy activity, or that accumulation of LC3-II puncta is not as a

result of a block in degradation. Therefore, while the prognostic significance of Beclin-1 is clear from this study, it is not fully elucidated that the favourable prognosis associated with increased Beclin-1 expression is due to increased autophagy activity. Interestingly, p62 expression levels were not evaluated in this study.

1.2.4.1 Expression levels of Beclin-1 can predict clinical outcome

Cellular levels of Beclin-1 have previously been reported to predict clinical outcome in a variety of malignancies (Marquez and Xu, 2012). As it is described as a tumour suppressor protein, it is unsurprising that decreased Beclin-1 expression in particular is often associated with a poor prognosis. For example, Chen *et al* have described lower levels of Beclin-1 as being a marker of decreased survival rates among oesophageal squamous cell carcinoma patients (Chen et al., 2009), while Huang and colleagues reported a similar finding in patients with extranodal natural killer T-cell lymphoma (Huang et al., 2010). Decreased expression of Beclin-1 has also been shown to predict a poor outcome in NHL, as previously discussed (Nicotra et al., 2010b).

1.3 The BCL-2 family of proteins

The BCL-2 family of proteins contains over a dozen members which possess at least one of the four BCL-2 homology (BH) domains (BH1 - BH4). These proteins are categorised into three groups - anti-apoptotic, pro-apoptotic or 'BH3' only pro-apoptotic - based on the number of BH domains they contain and their cellular function (Figure 1.5) (Adams and Cory, 1998; Kelly and Strasser, 2011; Ola et al., 2011).

Anti-apoptotic BCL-2 family members which include BCL-2, BCL-xL and BCL-w for the most part contain all four BH domains and function to inhibit apoptosis. Pro-apoptotic proteins, of which Bax and Bak are the prototypes, are similar in structure to anti-apoptotic proteins but typically contain three BH domains and function to induce cell death. 'BH3-only' pro-apoptotic proteins, including Bim and Bad, only contain a BH3 domain and promote apoptosis (Figure 1.5) (Kelly and Strasser, 2011; Levine et al., 2008; Ola et al., 2011). 'BH3'-only proteins are further classified as activators which induce apoptosis by binding Bax/Bak directly or sensitizers which bind anti-apoptotic proteins, preventing them from binding and inhibiting activator 'BH3'-only proteins (Deng et al., 2007; Kuwana et al., 2005; Letai et al., 2002). Not all 'BH3'-only proteins bind all other BCL-2 proteins with the same affinity. For example, Noxa binds MCL-1 not BCL-2, while Bad binds BCL-2 but not MCL-1 (Chen et al., 2005; Kelly and Strasser, 2011).

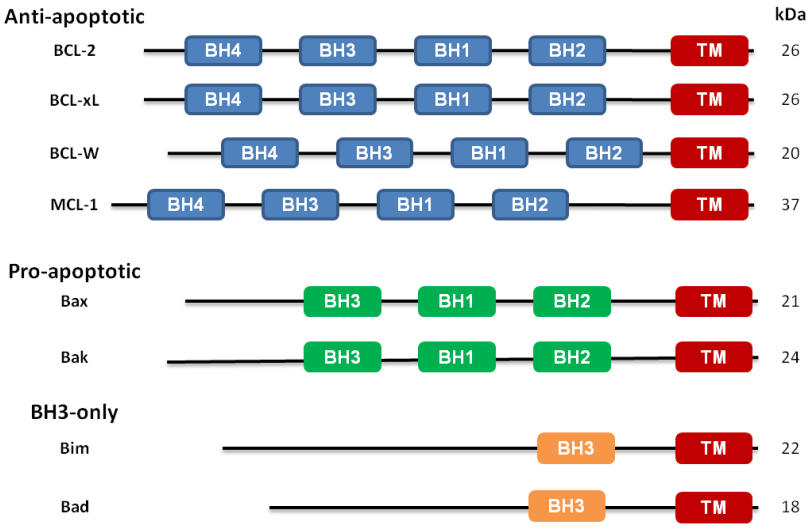

Figure 1.5 The BCL-2 family of proteins
Structural organisation of key members of the BCL-2 family of proteins. Members of the BCL-2 family are classified based on the number of BCL-2 homology (BH) domains they contain and their function within the cell. The anti-apoptotic members of the family contain all four BH domains (BH1-BH4). The pro-apoptotic members vary in the number of BH domains they contain. Some members contain three while others, termed 'BH3'-only proteins containing only one BH domain. TM – transmembrane domain. Adapted from Kelly and Strasser 2011.

1.3.1 The BCL-2 protein

BCL-2, the founding member of the BCL-2 family of proteins, is a 26kDa protein which contains all BH1-BH4 domains (BH1-BH4) (Figure 1.5). This pro-survival protein was first identified in a cell line derived from a leukaemic patient harbouring the t(14;18)(q32;q21) translocation and was predicted to be of importance in pathogenesis of B-cell malignancies carrying this translocation (Tsujimoto et al., 1984). The t(14;18) translocation places BCL-2 under the control of Eμ, the promoter of the immunoglobulin heavy chain (IgH) gene resulting in increased expression of BCL-2 which inhibits cell death (Kelly and Strasser, 2011; Tsujimoto et al., 1984; Vaux et al., 1988). BCL-2 localises to the ER, nuclear envelope and outer mitochondrial membrane via its hydrophobic carboxy-terminal domain where it interacts with various binding partners to inhibit apoptosis and/or autophagy (Ola et al., 2011; Rodriguez et al., 2011; Strappazzon et al., 2011).

1.3.2 BCL-2 - an inhibitor of apoptosis and autophagy

BCL-2 inhibits the intrinsic apoptosis pathway by binding and sequestering the multi-domain pro-apoptotic proteins Bax and Bak or the activator 'BH3'-only proteins Bim and Bid (Deng et al., 2007; Kelly and Strasser, 2011). By binding Bax/Bak at the mitochondria, BCL-2 prevents MOMP and inhibits the release of pro-apoptotic molecules such as cytochrome c and SMAC/DIABLO, thus preventing induction of the caspase cascade and inhibiting cell death (Llambi and Green, 2011; Ola et al., 2011). Binding of BCL-2 to Bim and Bid at the mitochondria prevents Bim and Bid from binding Bax/Bak and exerting their pro-apoptotic function (Letai et al., 2002; Llambi and Green, 2011).

BCL-2 can also act as an anti-autophagic protein by binding and sequestering Beclin-1. The mechanism of action by which BCL-2 does this will be discussed in detail in section 1.4. BCL-2 has also been shown to inhibit autophagy by binding and sequestering the Beclin-1 activator AMBRA1 at the mitochondria (Marquez and Xu, 2012; Strappazzon et al., 2011). However, it has recently been suggested that BCL-2 negatively regulates autophagy, not through direct interaction with key players in the autophagy pathway such as Beclin-1 and AMBRA1, but rather indirectly, through inhibition of the pro-apoptotic molecules Bax and Bak (Lindqvist et al., 2014).

1.3.3 Overexpression of BCL-2 promotes tumourigenesis

In 1989 Mc Donnell and colleagues demonstrated BCL-2 to be an oncogene by showing that transgenic mice carrying a minigene fusion which mimicked the t(14;18) translocation developed lymphoma and follicular hyperplasia (McDonnell et al., 1989). Classification of BCL-2 as an oncogene lead to establishment of a new category of oncogene which rather than promoting cell proliferation act to inhibit cell death; evasion of apoptosis is now considered a hallmark of cancer cells (Hanahan and Weinberg, 2011; Kelly and Strasser, 2011; Kerr et al., 1972; Pietras and Ostman, 2010).

While aberrant expression of BCL-2 due to this chromosomal rearrangement is frequently observed in FL and some DLBCL patients, increased expression of BCL-2 is not restricted to these lymphomas. High levels of BCL-2 are also observed in chronic lymphocytic leukaemia (CLL), mantle cell lymphoma (MCL) and certain solid tumours

due to homo- or hemizygous deletion of the BCL-2 inhibiting microRNAs miR-15a and miR-16, or as a result of hypo-methylation of the BCL-2 promoter (Castle et al., 1993; Cimmino et al., 2005; Hanada et al., 1993; Kelly and Strasser, 2011).

Neoplastic cells inhibit apoptosis by increasing expression of pro-survival proteins such as BCL-2 and MCL-1 or decreasing expression of pro-apoptotic proteins such as Bim, rendering tumour cells immortal (Kelly and Strasser, 2011; Llambi and Green, 2011; Vaux et al., 1988). In this way, increased expression of BCL-2 and mutations associated with this protein promote tumourigenesis by facilitating the survival of damaged, deregulated cells.

Increased expression of pro-survival BCL-2 family members in cancer cells makes them attractive targets for therapeutic intervention. Indeed a number of anti-cancer agents have been shown to modulate their anti-apoptotic effects at both the gene and protein level. For example, treatment with the cytotoxic retinoid fenretinide and depsipeptide a histone-deacetylase (HDAC) inhibitor results in decreased expression of BCL-2, BCL-xL and MCL-1 in leukaemia and multiple myeloma cells respectively and promotion of tumour cell death. Although these therapies do not specifically inhibit BCL-2 family proteins, their anti-neoplastic function has been proven, suggesting a role for them in combination therapy (Kang et al., 2008; Khan et al., 2004).

'BH3'-mimetic compounds have been developed which bind anti-apoptotic BCL-2 proteins via BH3 domain interactions, inhibit their pro-survival function and induce tumour cell death (Kang and Reynolds, 2009). ABT-737, ABT-263 and ABT-199 are synthetic 'BH3'-mimetics which bind BCL-2, BCL-w and BCL-xL or BCL-2 only, but not MCL-1 (Souers et al., 2013; Tse et al., 2008; Vogler et al., 2009). ABT-737 has shown anti-neoplastic activity in combination therapy and as a single agent in lymphoma and CLL, while ABT-263 has been effective in myeloma and lymphoma as well as relapsed/refractory lymphoid malignancies, again as a single agent or in combination therapy (Del Gaizo Moore et al., 2007; Tse et al., 2008; van Delft et al., 2006). Similarly, treatment with ABT-199 has proved effective in patients with refractory CLL (Souers et al., 2013). 'BH3'-mimetics therefore represent a new and promising form of cancer therapeutics.

The sensitivity of cancer cells to 'BH3'-mimetic compounds can potentially be determined by identifying a cells BH3 profile (Deng et al., 2007). Deng and colleagues have shown that tumour cells which inhibit apoptosis by expressing high levels of anti-apoptotic proteins such as BCL-2 and BCL-xL are 'primed for death' and are sensitive to therapeutic intervention by 'BH3'-mimetics. BH3-profiling has also been shown to predict sensitivity to standard chemotherapy agents such as vincristine and etoposide (Deng et al., 2007; Llambi and Green, 2011).

While established as an oncogene with regards its anti-apoptotic function, the role of BCL-2 in autophagy inhibition in cancer is unclear. In particular, it is unclear whether or not the aberrant expression of BCL-2 observed in FL cells affects autophagy in these malignant cells and/or plays a role in FL progression and transformation.

1.4 Binding between BCL-2 and Beclin-1 can inhibit autophagy

Binding between BCL-2 and Beclin-1 was initially discovered in a yeast-two-hybrid screen in 1998 by Liang and colleagues (Liang et al., 1998). Further work by Pattingre and co-workers revealed that this binding sequesters Beclin-1 away from the IC and results in autophagy inhibition. Generation of mutant forms of BCL-2 which were unable to bind Beclin-1 resulted in increased levels of autophagy activity, confirming that binding of BCL2 to Beclin-1 inhibits autophagy (Pattingre et al., 2005). Interestingly, this inhibition is unidirectional with BCL-2/Beclin-1 binding having no impact on the ability of BCL-2 to inhibit apoptosis (Marquez and Xu, 2012; Mukhopadhyay et al., 2014; Rodriguez et al., 2011).

1.4.1 BCL-2 and Beclin-1 can bind at the ER and mitochondria

Intracellular Beclin-1 and BCL-2 localise to the mitochondria and ER. Localisation of these two proteins within the cell is a determining factor in their interaction and in autophagy inhibition (Maiuri et al., 2007a; Marquez and Xu, 2012). Pattingre and colleagues have demonstrated that ER-restricted BCL-2 mutants, which maintained functional BH3 domains and the ability to bind Beclin-1, were able to inhibit autophagy to the same level as wild-type BCL-2. Conversely, mutants targeted to the mitochondria had no inhibitory effect on the autophagy pathway, suggesting that BCL-2/Beclin-1 binding at the ER inhibits autophagy (Kang et al., 2011; Maiuri et al., 2007a; Pattingre et al., 2005). This apparent dichotomy may explain why Beclin-1 binding does not affect the anti-apoptotic role of BCL-2 - BCL-2 inhibits apoptosis at the mitochondria by binding pro-death proteins, where as it inhibits autophagy by binding Beclin-1 at the ER (Maiuri et al., 2007a).

While it is well known that BCL-2 is over expressed in FL due to the t(14;18) translocation, it is currently unknown: (a) if this protein binds Beclin-1 in these cells at either the mitochondria or the ER and (b) if binding does occur at either site, does BCL-2 inhibit autophagy in FL?

1.4.2 Binding between BCL-2 and Beclin-1 can be disrupted in various ways

1.4.2.1 Competitive binding inhibits BCL-2/Beclin-1 interactions

High mobility group box 1 (HMGB1) is a pro-autophagy damage associated molecular pattern (DAMP) molecule involved in inflammation, apoptosis and autophagy. HMGB1 shuttles between the nucleus and the cytoplasm and can disrupt binding between BCL-2 and Beclin-1 (Tang et al., 2010). The positively charged 'A Box' and 'B Box' domains of HMGB1 contain three cysteines which are essential for its pro-autophagy role. Cysteines C23 and C45 facilitate interaction between HMGB1 and Beclin-1 by forming a disulfide bridge between the two. This interaction displaces Beclin-1 from BCL-2 and facilitates autophagy induction (Figure 1.6 A). Translocation of HMGB1 from the nucleus to the cytoplasm which is essential for its pro-autophagy role is promoted by C106 and can be induced by Rapamycin and starvation (Kang et al., 2010; Marquez and Xu, 2012; Tang et al., 2010).

BCL-2/Beclin-1 binding can also be disrupted by 'BH3'-only proteins. Pro-apoptotic proteins BNIP3, Bim and tBid and BH3-mimetic compounds such as ABT-737 and (-)-Gossypol bind BCL-2 via BH3 domain interactions, releasing Beclin-1 and allowing autophagy to proceed (Figure 1.6 A) (Bellot et al., 2009; Marquez and Xu, 2012). The amphipathic α-helix of the BH3 domain binds the hydrophobic cleft of BCL-2, dispelling Beclin-1 and allowing autophagy to proceed. Mutations in the BH3 domain of either BCL-2 or Beclin-1 can also inhibit their binding resulting in autophagy induction (Kang et al., 2011; Maiuri et al., 2007a).

1.4.2.2 Post-translational modifications of BCL-2 or Beclin-1 prevents their binding

Starvation-induced activation of c-Jun N-terminal protein kinase 1 (JNK1) induces phosphorylation of threonine (T69) and serine (S70, S87) residues within the unstructured loop of BCL-2 which disrupts its binding with Beclin-1 (Marquez and Xu, 2012; Wei et al., 2008). Similarly DAPK-1, a tumour suppressor regulatory protein can induce autophagy by phosphorylating the T119 residue of Beclin-1 and promoting its dissociation from BCL-2 (Kang et al., 2011; Zalckvar et al., 2009). HMGB1 also promotes phosphorylation of BCL-2 by extracellular signal-related kinase 1/2 (ERK1/2), promoting BCL-2/Beclin-1 dissociation (Kang et al., 2011; Tang et al.,

2010). Tumour necrosis factor receptor-associated factor 6 (TRAF6) promotes ubiquitination of Lysine^{63} residue of Beclin-1, which induces its self-oligomerisation and subsequent activation of the Beclin-1/Vps34/Vps15 complex (Figure 1.6 B). Conversely the de-ubiquitinating enzyme A20 removes ubiquitin from Lysine^{63}, promoting the autophagy-inhibiting interaction of Beclin-1 with BCL-2 (Kang et al., 2011; Shi and Kehrl, 2010).

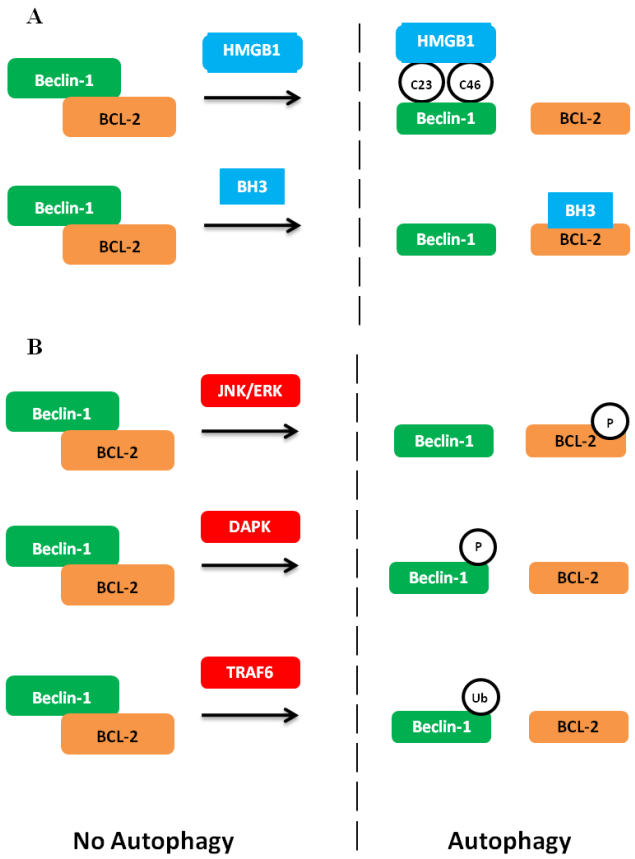

Figure 1.6 Disruption of BCL-2/Beclin-1 binding promotes autophagy
Binding between the anti-apoptotic protein BCL-2 and the pro-autophagy protein Beclin-1 can be inhibited by competitive binding (A) and post-translational modifications (B). The DAMP protein HMGB1 and BH3-only proteins can bind Beclin-1 and BCL-2 respectively, freeing Beclin-1 and allowing autophagy to proceed. JNK/ERK and DAPK promote BCL-2 and Beclin-1 phosphorylation respectively, while TRAF6 induced Beclin-1 ubiquitination, all of which endorse Beclin-1/BCL-2 dissociation and autophagy activation. P - phosphorylation; Ub- ubiquitination. Adapted from: Kang *et al*, 2011.

1.5 The adaptor / scaffold protein p62

p62 is a 62kDa adaptor/scaffold protein encoded for by *SQSTM1* which is ubiquitously expressed by all types of cells. It was initially identified as a binding partner of atypical protein kinase C (aPKC) (Moscat and Diaz-Meco, 2012; Puls et al., 1997; Sanchez et al., 1998). As a multi-domain protein, it binds a host of cellular proteins resulting in the formation of p62-positive cellular speckles or aggregates within the cytosol and nucleus of a cell (Bjorkoy et al., 2005; Moscat and Diaz-Meco, 2012; Nakamura et al., 2010; White, 2012). Modulation and accumulation of p62 is associated with the pathogenesis of different diseases including protein aggregate disorders and cancer (Bjorkoy et al., 2005; Komatsu et al., 2012; Mathew et al., 2009).

1.5.1 p62 is a multi-domain protein involved in different cellular pathways

p62 is comprised of various binding domains which facilitate its interaction with different proteins and promote its involvement in numerous cellular pathways (Figure 1.7) (Bjorkoy et al., 2005; Shi et al., 2013; White, 2012).

The centrally located ZZ-type Zinc-finger (ZZ) and TRAF6-binding (TB) domains facilitate interaction of p62 with RIP1 (receptor-interacting protein 1) and TRAF6 respectively, resulting in activation of the NF-κB pathway and osteoclastogenesis (Moscat and Diaz-Meco, 2012; White, 2012; Wooten et al., 2008). p62 also promotes NF-κB activation by binding aPKC via its N-terminally located Phox/Bem 1p (PB1) domain, where as its binding to ERK1/2 via the same domain inhibits ERK-mediated adipogenesis and prevents against the onset of obesity (Mathew et al., 2009; Nakamura et al., 2010; Rodriguez et al., 2006). PB1 domain mediated interactions also facilitates the role of p62 in autophagy via binding of neighbour of BRCA1 (NBR1) which promotes packaging and delivery of p62-positive aggregates to the autophagosome for degradation (Lamark et al., 2003; White, 2012). p62s PB1 domain also facilitates homodimerisation, resulting in incorporation of this adaptor protein into intracellular inclusion bodies (Komatsu et al., 2012; Nakamura et al., 2010; White, 2012). The KIR (KEAP1-interacting region) domain of p62 binds KEAP1 (Kelch-like ECH-associated protein 1) which results in activation of the transcription factor Nrf2 (nuclear factor,

(erythroid-derived 2)-like 2) and expression of numerous antioxidant and cytoprotective genes (Figure 1.7) (Komatsu et al., 2010; White, 2012).

p62 is well established as a key player in the autophagy pathway, a role which is facilitated by its ubiquitin-associated (UBA) domain and LC3-interacting region (LIR) (Johansen and Lamark, 2011). Ubiquitination was previously thought to only mark out proteins destined for degradation by the proteasome. However, we now understand that autophagy can selectively degrade larger ubiquitinated substrates by employing UBA domain-containing adaptor proteins such as p62 (Kirkin et al., 2009). Via its C-terminally located UBA domain, p62 acts as a cargo receptor which binds mono- and poly-ubiquitinated proteins/ organelles and packages them into p62-positive aggregates. It then facilitates delivery of these aggregates to the autophagosome (Kirkin et al., 2009; Komatsu et al., 2012; Pankiv et al., 2007). Via its LIR, p62 directly binds autophagosome-membrane bound LC3-II and delivers these protein aggregates to the autophagosome for degradation. As it is itself a component of the aggregates it forms, p62 is also delivered to the autophagosome for degradation and thus has been proven to be a substrate of the autophagy pathway (Bjorkoy et al., 2005; Johansen and Lamark, 2011; Pankiv et al., 2007).

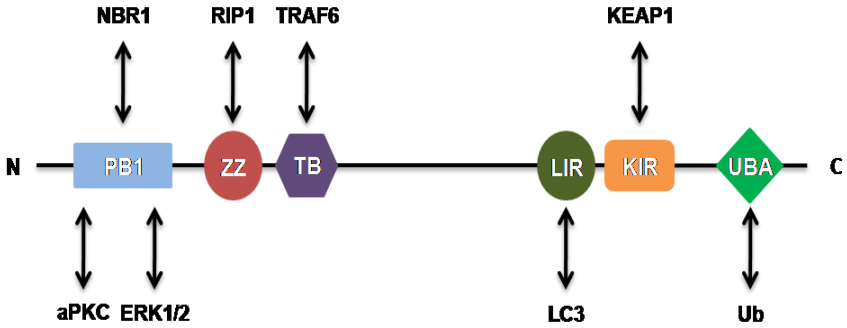

Figure 1.7 The adaptor protein p62 contains multiple binding domains
The binding domains of p62 facilitate its homodimerisation and heterodimerisation with various cellular proteins, thus promoting its participation in different signalling pathways. PB1- Phox/Bem 1p; ZZ-ZZ-type zinc finger; TB-TRAF6-binding; LIR-LC3-interacting region; KIR - KEAP1-interacting region; UBA-Ubiquitin-associated. Adapted from Moscat and Diaz-Meco, 2009.

1.5.2 p62 delivers substrates to the autophagosome

The role of p62 in autophagy was first described by Bjorkoy and colleagues in 2005 (Bjorkoy et al., 2005). Using confocal microscopy, they showed that p62 homodimerises and polymerises with ubiquitinated proteins via its PB1 and UBA domains respectively, to form inclusion bodies. These inclusions become embedded in double-layered membrane vesicles, indicative of autophagosomes. This lead Bjorkoy and colleagues to hypothesise that p62 may be involved in the autophagy pathway. To test their hypothesis, they studied p62 levels following treatment with Rapamycin or Bafilomycin-A1 which induce and inhibit autophagy respectively (Bjorkoy et al., 2005). Upon induction of autophagy, a decrease in p62 levels and the number of p62-containing aggregates was observed. On the other hand, inhibition of late stage autophagy by Bafilomycin-A1 resulted in an increase in both the number and size of p62-positive inclusion bodies. This data suggested that p62 may be involved in delivery of large, ubiquitinated protein aggregates to the autophagosome and that this adaptor protein is itself an autophagy substrate. p62 was also shown to co-localise with the autophagy essential protein LC3-II with depletion of p62 found to prevent incorporation of LC3-II into the autophagosome. This lead to the conclusion that p62 mediates delivery of autophagy substrates, including itself, to the autophagosome via interactions with the autophagosome-membrane bound protein LC3-II (Bjorkoy et al., 2005).

Bjorkoy and colleagues suggested that interaction between p62 and LC3 may not be direct but mediated by a third party. However, Pankiv and co-workers later demonstrated using co-immunoprecipitation and other assays that LC3-II/p62 bind directly via a 22-amino acid residue within p62 (the LIR) and that this binding is essential for degradation of p62-containing aggregates (Pankiv et al., 2007). Further work by Komatsu and colleagues confirmed that autophagy inhibition via *Atg7* knock-down results in p62 accumulation with no increase at the mRNA level, indicating that p62 is degraded by the autophagic process (Komatsu et al., 2007).

As p62 protein levels have been shown to decrease upon activation of autophagy due to its increased degradation, cellular levels of p62 have been frequently used as a marker of autophagy activity (White, 2012). However, a recent study by Sahani and colleagues

reports that care should be taken when interpreting p62 levels as an autophagy marker (Sahani et al., 2014). They observed that starvation induced autophagy in mouse embryonic fibroblast (MEF) and HepG2 cell lines resulted in an initial decrease in p62 levels but prolonged nutrient-withdrawal (≥4hrs) resulted in restoration of p62 protein levels to almost basal level. Restoration of p62 at the protein level was associated with and dependent on an increase in mRNA levels of *SQSTM1*. They therefore suggest that p62 protein levels may not always accurately reflect autophagy activity within a cell and so mRNA levels, which heretofore were thought to remain unchanged upon autophagy activation or inhibition, should also be examined (Sahani et al., 2014).

1.5.3 p62 is involved in disease pathogenesis

As p62 is involved in regulating multiple signalling pathways, it is unsurprising that perturbation of this gene can result in a number of disorders. For example, mutations in *SQSTM1* have been identified as the cause of Paget's disease of bone, a genetic disorder which results in aberrant osteoclastogenesis and disorganised bone formation, while loss of p62 is associated with increased activation of ERK and increased adipogenesis resulting in obesity (Duran et al., 2004; Moscat and Diaz-Meco, 2009; Rodriguez et al., 2006). Accumulation of p62 due to defective autophagy is associated with neurological disorders such as Parkinson's and Alzheimer's as well as liver failure, where toxic p62-containing aggregates build up in neuronal cells or hepatocytes, causing cell injury and death (Komatsu et al., 2012; Komatsu et al., 2007; Moscat and Diaz-Meco, 2009). p62 has also been shown to play a role in the development and promotion of cancer.

1.5.3.1 The role of p62 in cancer

In 2008, Duran and colleagues reported an essential role for p62 in the formation of RAS-induced lung adenocarcinomas (Duran et al., 2008). They demonstrated that the oncogene RAS promotes p62 activation and polyubiquitination of TRAF6, a positive regulator of IKK (IκB kinase). *In vivo* ablation of p62 ($p62^{-/-}$) resulted in decreased RAS-induced carcinogenesis, confirming that RAS-induced transformation is p62-dependent. A similar role has been described for p62 in the promotion of PDAC. (Ling et al., 2012). Thus, p62 can act as a tumour promoter by activating the pro-survival NF-κB pathway via the oncogene RAS (Duran et al., 2008; Moscat and Diaz-Meco, 2012).

This potential tumour promoting role of p62 was substantiated by Mathew and colleagues when they reported that accumulation of p62 in autophagy defective cells promoted tumourigenesis in immortalised baby mouse kidney (iBMK) cells (Mathew et al., 2009). They demonstrated that in response to a metabolic stress, autophagy incompetent iBMK cells showed accumulation of p62, damaged mitochondria, increased ROS production and DNA damage. Accumulation of p62 was attributed to impaired autophagic degradation as no change was observed in *SQSTM1* mRNA levels. *In vivo* experiments revealed that autophagy-defective cells, in which p62 was accumulated, had increased tumour growth compared to autophagy-competent cells. *Atg5*$^{-/-}$ tumour cells displayed large p62-positive aggregates, giant, heterochromatic nuclei indicative of aneuploidy and polyploidy and increased growth. They also found, contrary to Duran and colleagues, that accumulation of p62 resulted in decreased NF-κB activity and an increase in ROS levels, oxidative stress and genomic instability which promoted tumourigenesis (Mathew et al., 2009). A potential explanation for the discrepancy observed in NK-κB signalling is that iBMK cells may not facilitate polyubiquitination of p62 or TRAF6 which is necessary for NF-κB activation (Moscat and Diaz-Meco, 2009). Elimination of p62 aggregates from autophagy-defective iBMK cells was sufficient to suppress the cytotoxic, tumour promoting effects induced by autophagy inhibition. Similar results have been reported in hepatocarcinomas where it has been observed that elimination of accumulated p62 from *Atg7*$^{-/-}$ cells inhibits tumour formation (Komatsu et al., 2007; Mathew et al., 2009; Moscat and Diaz-Meco, 2012).

Thus, p62 appears to be able to promote tumour growth by altering expression of the NK-κB signalling pathway, promoting the oncogenic function of RAS, and inducing oxidative stress and genomic instability. This pro-tumour role of p62 appears to be reversible as elimination of p62 can prevent RAS-induced transformation and the induction of oxidative stress (Duran et al., 2008; Mathew et al., 2009; Moscat and Diaz-Meco, 2012).

1.5.3.2 p62 expression levels have been used as a prognostic biomarker

p62 has been shown to act as a biomarker for clinical outcome in a variety of malignancies. For example, accumulation of this autophagy-substrate was reported to predict a worse outcome and resistance to chemotherapy in oral carcinoma patients (Inui et al., 2013), where as in melanoma patients increased p62 expression was associated with a better prognosis (Ellis et al., 2014).

To date, the roles of p62 in autophagy, tumourigenesis or tumour promotion, and its association with clinical outcome in FL and/or DLBCL have not been reported.

1.6 Lymphomas

Lymphomas (cancers of the lymphatic system) can be broadly divided into two categories – Hodgkin's lymphoma (HL) and NHL. NHLs, which are more common than HLs, can arise from abnormal T or B cells, although the vast majority are B cell derived (Skibola et al., 2009).

1.6.1 FL is an indolent, incurable malignancy of the germinal centre

FL is the most common form of indolent NHL accounting for 20-40% of newly diagnosed cases each year in Western Europe and the United States (Freedman, 2012; Glass et al., 1997; Kridel et al., 2012). FL typically presents in middle-aged and elderly individuals (median age 60 years) with a slight predominance of occurrence in women (Armitage and Weisenburger, 1998; Freedman, 2012). Although an indolent disease with a median survival rate of >10 years, FL is still considered to be a fatal incurable malignancy associated with a high rate of relapse and/or transformation to the more aggressive DLBCL (Kridel et al., 2012; Lossos and Levy, 2003).

Morphologically, FL B cells resemble normal germinal centre B (GCB) cells and are organised into clearly discernible follicle centres (Lossos and Levy, 2003). Centrocytes and centroblasts are present in high numbers in FL samples with centroblasts tending to be present in greater numbers (Nathwani et al., 1999). FL cells express the pan-B cell markers CD19 and CD20, the well defined germinal centre B cell marker CD10 as well as BCL-6 and BCL-2 (Dogan et al., 2000; Kridel et al., 2012; Lenz and Staudt, 2010; Shaffer et al., 2012).

The FL cell of origin is not a normal GCB-cell but a more immature B cell. The oncogenic hit that gives rise to FL occurs during the early stages of haematopoiesis but does not hinder cellular differentiation. Therefore, FL B cells resemble mature GCB-cells rather than their actual cell of origin (Shaffer et al., 2012). In the case of FL the initial oncogenic event, typically the t(14;18) translocation, is acquired by pre-B cells in the bone marrow which migrate to lymphoid tissues where they undergo germinal centre reaction and remain. Acquisition of this translocation therefore increases BCL-2 expression but does not affect the differentiation potential of these cells (Kridel et al.,

2012; Lossos and Levy, 2003). Increased expression of BCL-2, which is not normally expressed in the GC, confers a survival advantage to FL cells and promotes treatment resistance (Kridel et al., 2012; Shaffer et al., 2012).

1.6.2 FL is associated with multiple genetic abnormalities

FL is characterised by the t(14;18)(q32;q21) translocation which is present in 80-90% of cases at diagnosis and results in aberrant expression of BCL-2 (Boonstra et al., 2003; Fukuhara et al., 1979; Lipford et al., 1987; Yunis et al., 1982). The t(14;18) translocation occurs following a double-strand break at the BCL-2 locus (chr18) and the IGH locus (chr14) which places the BCL-2 promoter region under the control of the heavy-chain locus, resulting in increased expression of the BCL-2 protein (Galteland et al., 2005; Kridel et al., 2012; Masir et al., 2009). Despite its near ubiquitous overexpression among FL patients, cellular levels of BCL-2 do not impact or predict clinical outcome in this indolent NHL (Llanos et al., 2001). While acquisition of this translocation is common in FL development, it is not necessary or sufficient to drive malignant progression as is evident by ~15% of t(14;18)-negative FL cases, meaning secondary mutations are required for full disease manifestation (Table 1.4) (Kridel et al., 2012; McDonnell and Korsmeyer, 1991; Shaffer et al., 2012). One of the most common secondary chromosomal aberrations in FL is heterozygous deletion of the *TNFSRF14* gene, a member of the tumour necrosis factor receptor (TNFR) superfamily (Cheung et al., 2010; Launay et al., 2012). Other genes mutated in FL include the histone3 lysine4 (H3K4), methyl transferase *MLL2* and *EZH2*, a member of the polycomb repression complex-2 (PRC2) (Table 1.4) (Bodor et al., 2013; Morin et al., 2011; Nogai et al., 2011; Pasqualucci et al., 2011; Shaffer et al., 2012).

Table 1.4 Genetic abnormalities associated with FL

Gene	Frequency (~%)	Function	LOF/GOF*
BCL-2 t(14;18)	85-95	Apoptosis regulator	GOF
TNFRSF14	18-46	Immune Regulator	LOF
MLL2	89	Epigenetic Modifier	LOF
EZH2	7-20	Epigenetic Modifier	GOF
CREBBP	33	Epigenetic Modifier	LOF
BCL-6	6-14	Transcription Factor	GOF

*LOF = loss-of-function; GOF = gain-of-function

1.6.3 FL can be divided into distinct clinical grades

FL is divided into clinical grades based on the proportion of centrocytes to centroblasts. According to the World Health Organisation (WHO) classification and the Revised European-American Classification of Lymphoid Neoplasms (REAL), there are three grades of FL – grades 1-3 – with grade 3 being further subdivided into grade 3A and 3B (Table 1.5) (Campo et al., 2011). Grades 1-2 are similar and contain low numbers of centroblasts while grade 3A contains a higher number of centroblasts with some centrocytes still visible. FL grade 3B contains only centroblasts and is considered to appear biologically more similar to *de novo* DLBCL and lacks CD10 expression (Campo et al., 2011; Kridel et al., 2012; Salaverria and Siebert, 2011).

Table 1.5 Grading of FL

Grade	Number of Centroblasts per High Power Field
1 (Low Grade)	**0 – 5**
2 (Low Grade)	**6 – 15**
3A (High Grade)	**>15**
3B (High Grade)	**Solid sheets of Centroblasts**

1.6.4 FL treatment varies depending on disease stage

Although treatment of FL has been improved in recent years, it is still considered a fatal malignancy plagued by frequent relapses and transformation (Glas et al., 2005; Goy et al., 2005). While initially relatively chemosensitive, FL patients become increasingly refractory to treatment with each relapse (Glas et al., 2005; Montoto et al., 2007). Despite the multiple regimens available for treatment of FL, to date there is no consensus on how to treat this clinically variable incurable malignancy (Dave et al., 2004; Marcus et al., 2008; Solal-Celigny et al., 2004). The most appropriate treatment choice for FL is often guided by an individual's FLIPI (Follicular Lymphoma International Prognostic Index) score, a prognostic index which stratifies patients into risk groups based on the number of adverse clinical factors they present with at diagnosis (Table 1.6) (Marcus et al., 2008; Solal-Celigny et al., 2004). Patients receive a mark per adverse variable – age >60 years; Ann Arbor stage III/IV; LDH (lactate dehydrogenase) level >480U/L; serum haemoglobin levels <120g/L and >4 affected nodal areas – giving them their FLIPI score, which ranges from 0 to 5. Based on this

score, patients are stratified into one of three risk groups - low (0-1), intermediate (2) or high (3-5) (Buske et al., 2006; Solal-Celigny et al., 2004).

Table 1.6 Prognostic factors considered when determining an FLIPI scores

Prognostic Factor	Good Prognosis	Poor Prognosis
Age (years)	≤ 60	> 60
Ann Arbor Stage	I/II	III/IV
Serum LDH Level	≤ Normal	> Normal
Haemoglobin (g/L)	>120	≤ 120
Number of Affected Nodal Areas	≤ 4	> 4

Asymptomatic, low-grade FL patients are often not treated with chemotherapeutic agents but rather observed under a "watch and wait" regimen where they are monitored regularly for disease progression, at which point treatment is administered (Ardeshna et al., 2003). This regimen is advantageous as it avoids unpleasant side-effects of therapy including myeloablative suppression and sicca syndrome (Dreyling et al., 2011). Low-grade FL patients with limited non-bulky disease are typically treated with radiotherapy or radio-immunotherapy, a combination of radiotherapy and radio-labelled monoclonal antibodies, which is highly affective (Dreyling et al., 2011; Kaminski et al., 2005; Morschhauser et al., 2008). Although considered an incurable malignancy, first-line treatment for low-grade FL patients is often administered with curative intent (Dreyling et al., 2011; Montoto et al., 2007).

More advanced stages of FL are typically treated with the standard chemotherapy drugs CHOP (cyclophosphamide, doxorubicin, vincristine, prednisone) or CVP (cyclophosphamide, vincristine, prednisone) in combination with the monoclonal anti-CD20 antibody Rituximab (Fisher et al., 1993; Hiddemann et al., 2005; Marcus et al., 2008). Addition of Rituximab to CHOP/CVP has greatly improved progression free survival and partial remission rates in FL. However, patients still frequently relapse, becoming less chemosensitive with each relapse (Friedberg, 2011; Glennie et al., 2007; Vidal et al., 2011). Administration of Rituximab as maintenance therapy has also improved PFS and PR rates, with no clear indications as to its effect on overall survival (Dreyling et al., 2011; Friedberg, 2011; Salles et al., 2011; Vidal et al., 2011). The proteasome inhibitor bortezomib combined with R-CHOP/R-CVP has also been

reported to prolong PFS in FL (Goy et al., 2005; Salles, 2011). Relapsed patients are treated in a similar way to *de novo* FL cases with modifications made based on previous treatment (Dreyling et al., 2011). Stem-cell transplantation may be offered as a form of treatment for more advanced stage or relapsed FL patients who have a good outlook (Dreyling et al., 2011; Kridel et al., 2012). Patient responses are listed in table 1.7.

Table 1.7 Treatment response classifications

Classification	Outcome	Abbreviation
1	Complete Remission	CR
2	Good Partial Remission/Complete Remission (Undetermined)	GPR/CR(U)
3	Poor Partial Remission	PPR
4	Stable	Stab.
5	Progression	Prog.
6	Treatment Related Death	TRD

1.6.5 The tumour microenvironment in FL

It is well established that interactions between FL cells and cells of the microenvironment play an important role in the development and progression of this indolent NHL (Dave et al., 2004; Yang and Ansell, 2012). Tumour infiltrating immune cells can help eradicate malignant cells but conversely may promote and maintain tumour cell survival by secreting growth factors and stimulatory cytokines (Lejeune and Alvaro, 2009; Yang and Ansell, 2012). The FL tumour microenvironment has been reported to include higher numbers of $CD4^+$ and $CD8^+$ T-cells and $CD163^+$ and $CD68^+$ macrophages (Clear et al., 2010; Lejeune and Alvaro, 2009; Yang and Ansell, 2012).

GEP analysis of 191 FL patient biopsies by Dave and colleagues demonstrated that differences in patient outcome are associated with differential expression of genes in cells of the microenvironment but not malignant cells. They identified two distinct gene signatures - immune-response 1 and immune-response 2 - which were associated with monocytes and T-cells, and macrophages and follicular dendritic cells, respectively (Dave et al., 2004). They established that patients with an immune-response 1 signature had a more favourable outcome and longer OS compared to patients with an immune-response type-2 signature (Dave et al., 2004).

1.6.6 Transformation of FL to DLBCL is associated with morphological changes and acquisition of genetic mutations

The clinical course of FL is highly variable and typically involves a number of relapses, with a large proportion of patients undergoing histological transformation to a higher grade lymphoma, typically DLBCL but sometimes acute lymphoblastic leukaemia (ALL) or Burkitts lymphoma (BL) (Lossos and Levy, 2003). The reported rate of FL-DLBCL transformation ranges from 10-60%, with differential reporting possibly due to variability in length of patient follow up, differing policies for re-biopsies and differences in the definition of transformation (Hubbard et al., 1982; Lossos and Levy, 2003; Montoto et al., 2007). The risk of transformation increases with time, with an average risk of 19.6% at 5 years and 37% at 15 years (Lossos and Levy, 2003; Montoto et al., 2007).

Morphologically, transformation is associated with loss of follicular architecture which is replaced by a more diffuse growth pattern. Clinically, it is associated with rapid disease progression, the onset of B symptoms, extranodal disease development and shorter OS (median survival <2 years) (Al-Tourah et al., 2008; Boonstra et al., 2003; Lossos and Levy, 2003; Montoto et al., 2007). Genetic abnormalities associated with transformation include mutations in the tumour suppressor gene *p53* and gain-of-function mutations in the proto-oncogene *c-Myc* (Table 1.8). It is thought that transformation is driven by multiple abnormalities which work together to promote progression from an indolent to an aggressive NHL (Boonstra et al., 2003). Transformation from FL to DLBCL can occur through direct evolution from the primary malignant *de novo* FL clone or thorough divergent, indirect evolution which is not associated with the initial FL clone (Kridel et al., 2012; Lossos and Levy, 2003; Shaffer et al., 2012).

Table 1.8 Genes frequently altered in transformation from FL to DLBCL

Gene	Function	Abnormality
TP53	Tumour Suppressor	Mutation
CDKN2A	Tumour Suppressor	Mutation; deletion
CDKN2B	Tumour Suppressor	Loss of Expression; deletion
c-Myc	Proto-Oncogene	Rearrangement; mutation; amplification
BCL-2	Anti-apoptotic	Mutation
BCL-6	Proto-Oncogene	Rearrangement; mutation

1.7 Diffuse Large B-Cell Lymphoma

1.7.1 DLBCL is an aggressive B-Cell lymphoma

DLBCL is the most common aggressive B-cell NHL, accounting for up to 40% of cases presented each year. Considered a disease of the elderly, the median age of diagnosis is 70 years and occurrence is equally common among men and women (Gurbuxani et al., 2009). Patients can present with *de novo* DLBCL or DLBCL which has arisen following transformation from a lower grade lymphoma, typically FL (Hunt and Reichard, 2008).

DLBCL cells are large B cells with nuclei twice the size of normal lymphocytes and a diffuse cellular growth pattern where normal lymph node architecture is no longer discernible (Gurbuxani et al., 2009; Hunt and Reichard, 2008). These cells typically express pan-B cell markers such as CD20 and CD19 and variably express CD38 and CD138. Germinal centre B-cell like (GCB) type DLBCL cells express markers associated with the GC including CD10 and BCL-6 and are typically $FOXP1^-$, while activated B-cell like (ABC) cells lack IRF4 expression and are $FOXP1^+$ (Gurbuxani et al., 2009; Prakash and Swerdlow, 2007; Shaffer et al., 2012).

1.7.2 DLBCL can be divided into two distinct subgroups

The level of heterogeneity observed among DLBCL patients with respect to cell morphology, clinical features and response to treatment prompted examination of the genetic profile of this aggressive lymphoma. GEP studies by Alizadeh and colleagues divided DLBCL into two distinct subgroups termed GCB and ABC which differ with regards to cell of origin, expression of B-cell genes, genetic abnormalities and clinical outcome (Alizadeh et al., 2000; Hunt and Reichard, 2008; Lossos et al., 2000).

The GEP of GCB-type DLBCL patients closely resembles that of normal GCB-cells. Cells express GC markers such as CD10 and undergo continuous immunoglobulin somatic hypermutation (Lenz and Staudt, 2010; Lossos et al., 2000; Nogai et al., 2011). ABC-type patients express genes characteristic of mitogenically activated peripheral blood B cells and so more closely resemble these cells; however their terminal differentiation to plasma cells is prohibited due to lesions in *Blimp-1* (Alizadeh et al., 2000; Lenz and Staudt, 2010; Wright et al., 2003). ABC-type DLBCL cells may arise

from pre-germinal centre (pre-GC) B cells or post-GC B cells which are IgM positive and somatic hypermutation is off in the majority of cases (Lenz and Staudt, 2010; Lossos et al., 2000; Shaffer et al., 2012). A third DLBCL subtype referred to as type 3 DLBCL or PMBL (primary mediastinal B-cell lymphoma) exists which expresses a host of different genes not particularly associated with either subtype (Lenz and Staudt, 2010; Lenz et al., 2008b).

GCB-type patients typically have a better prognosis, with a high cure rate and a survival rate of >60% at 5 years, whereas ABC-type patients have a poor prognosis and a survival rate of 16–40% at 5 years (Alizadeh et al., 2000; Shaffer et al., 2012; Wright et al., 2003). It is currently unclear which genes differentially expressed by the GCB subtype bestows them this survival advantage.

1.7.3 DLBCL is associated with a variety of genetic aberrations

Genetic aberrations observed in both the GCB and ABC DLBCL subtypes include mutations and deletions in the tumour suppressor gene *TP53*, amplification and translocation of the oncogene *Myc* and mutation of β2-microglobulin (*B2M*) (Table 1.9) (Hunt and Reichard, 2008; Lenz and Staudt, 2010; Shaffer et al., 2012).

A number of genetic lesions specific to the GCB subtype are similar to those found in FL including mutation of *EZH2* and the t(14;18) translocation (Morin et al., 2010; Nogai et al., 2011; Rosenwald et al., 2002). Amplification of the *c-rel* locus and the microRNA cluster miR-17-92 are also frequently observed in GCB DLBCL (Table 1.10) (Lenz and Staudt, 2010; Lenz et al., 2008b; Nogai et al., 2011). Genetic alterations specifically associated with the ABC DLBCL subtype include deletions/mutation of *PRDM1*and mutation of *MYD88* which results in up-regulation of the JAK-STAT3 and NF-κB signalling pathways (Table 1.9) (Ngo et al., 2011; Nogai et al., 2011). Overexpression of BCL-2 is also observed in the ABC-subtype due to amplification of the 18q21 locus (Obermann et al., 2009; Offit et al., 1989).

Table 1.9 Genetic abnormalities observed in the GCB- and ABC-subtypes of DLBCL

Gene	Frequency (%)	Function	LOF/GOF*	Subtype
B2M	12	Immune Regulator	LOF	GCB/ABC
CARD11	~10	Signalling Factor	GOF	GCB/ABC
CREBBP	17-41	Epigenetic Modifier	LOF	GCB/ABC
MLL2	24-32	Epigenetic Modifier	LOF	GCB/ABC
MYC	15-50	Transcription Factor	GOF	GCB/ABC
TP53	13-22	Genomic Integrity	LOF	GCB/ABC
BCL-2 t(14;18)	25-45	Apoptosis Regulator	GOF	GCB
c-rel Locus Amplification	16-28	Transcription Factor	GOF	GCB
EZH2	20-25	Epigenetic Modifier	GOF	GCB
miR-17-92	12-15	MicroRNA	GOF	GCB
TNFRSF14	50	Immune Regulator	LOF	GCB
BCL-2 Amplification	34	Apoptosis Regulator	GOF	ABC
CD79A; CD79B	18-20	Signalling Factor	GOF	ABC
CDKN2A	20	Cell-cycle Regulator	LOF	ABC
MYD88 L265P	30	Signalling Factor	GOF	ABC
PRDM1	25	Transcription Factor	LOF	ABC

1.7.4 Up-regulation of various signalling pathways is associated with a poor prognosis in DLBCL

Increased activity of the NF-κB pathway, frequently observed in the ABC-subtype of DLBCL, results in inhibition of apoptosis, increased tumour cell survival and a worse prognosis. Up-regulation of this pathway and it's pro-survival target genes may explain why ABC-type patients are less sensitive to chemotherapy than GCB-type patients (Shaffer et al., 2012). Up-regulation of the JAK/STAT3 pathway has also been reported in the ABC-subtype where it supports angiogenesis, tumour cell survival and metastasis (Huang et al., 2013; Yu et al., 2009). Persistent STAT3 activation may be due to increased NF-κB activity, mutations in MYD88 or increased HDAC3 expression. It has recently been shown that increased expression of phosphotyrosine-STAT3 (PY-STAT3) and an activated-STAT3 gene signature which mirrors increased mRNA levels of STAT3, correlate with a poor clinical outcome in the ABC-subtype of DLBCL (Huang et al., 2013).

Expression levels of the HIF-1 protein which regulates a cells response to hypoxia have been shown to correlate with clinical outcome in R-CHOP treated DLBCL patients (Evens et al., 2010). Expression of HIF-1 was observed in 62% of GCB- and 59% of ABC-subtype DLBCL patients and correlated with a better overall survival compared to HIF-1 negative patients (Evens et al., 2010). Autophagy induction is tightly linked with

hypoxia via HIF-1 (Mazure and Pouyssegur, 2010); however to date, autophagy status and its association with clinical outcome in DLBCL patients has not been reported.

There is currently no consensus on the prognostic significance of increased expression of BCL-2 in DLBCL (Barrans et al., 2003; Iqbal et al., 2006). The t(14;18) translocation has been reported to predict shorter overall survival in GCB-type patients carrying it while others report it has no effect on outcome. Some studies report increased BCL-2 due to locus amplification predicts a worse outcome in ABC-subtype of DLBCL although this is not always the case (Alizadeh et al., 2000; Barrans et al., 2003; Iqbal et al., 2006; Obermann et al., 2009). While increased expression of BCL-2 alone may not predict outcome double-hit DLBCL patients which carry *Myc* and *BCL-2* mutations are known to have a shorter overall survival compared to single-hit patients (Green et al., 2012).

1.7.5 Treatment of DLBCL

The standard treatment for DLBCL is the multi-drug chemotherapy regimen CHOP combined with the anti-CD20 monoclonal antibody Rituximab (R-CHOP) (Coiffier et al., 2002; Fisher et al., 1993; Glennie et al., 2007). Addition of Rituximab to CHOP treatment has significantly improved survival by several years without an added increase in toxicity (Brusamolino et al., 2006; Coiffier et al., 2010). DLBCL patients are typically treated immediately with curative intent and with varying but generally high initial success rates (Flowers et al., 2010; Mounier et al., 2003; Nastoupil et al., 2012; Tomita et al., 2013).

Not all DLBCL patients respond to R-CHOP treatment in the same way, with less than half achieving and maintaining complete remission (CR), meaning alternative treatments are required for R-CHOP refractory and relapsed patients (Alizadeh et al., 2000; Dupire and Coiffier, 2010; Fitoussi et al., 2011). First-line treatments available for R-CHOP refractory patients or second-line treatments for relapsed patients include R-ACVBP (Rituximab, cyclophosphamide, vindesine, bleomycin, prednisone), R-ICE (Rituximab, ifosfamide, carboplatin, etoposide), R-DHAP (Rituximab, dexamethasone, ara-C, cisplatin) and R-ESHAP (Rituximab, etoposide, cytarabine, cisplatinum and methylprednisolone) which are generally administered in conjunction with an

autologous stem-cell transplantation (Alizadeh et al., 2000; Flowers et al., 2010; Hagberg et al., 2006; Martin and Caballero, 2009).

To identify patients likely to respond to R-CHOP and those who may need alternative, more aggressive therapy, the International Prognostic Index (IPI) was established (Sehn et al., 2007). The IPI is similar to the FLIPI for FL and considers multiple clinical parameters such as age and ECOG (Eastern Cooperative Oncology Group) performance (Table 1.10). Patients presenting with two or less adverse prognostic factors are classified as low-moderate risk and are treated with standard R-CHOP, while patients presenting with three or more of these factors are consider high risk and so are treated more aggressively (1993; Sehn et al., 2007). A revision of the IPI to include the effect Rituximab has had on DLBCL is termed the R-IPI (Rituximab International Prognostic Index). DLBCL patient treatment response is reported in the same manner as FL (Table 1.7).

Table 1.10 Prognostic factors considered when determining an individual's IPI/R-IPI score

Prognostic Factor	Good Prognosis	Poor Prognosis
Age (years)	≤60	>60
Ann Arbor Stage	I/II	III/IV
Serum LDH Level	≤Normal	>Normal
Number of Affected Nodal Areas	≤1	>1
ECOG Performance	0/1	≥2

Over the last two decades efforts have been made to develop new drugs for the treatment of DLBCL, particularly the ABC-subtype which does not respond as well to R-CHOP as the GCB-subtype (Dunleavy et al., 2009). While to date no new chemotherapeutic agents as effective as R-CHOP have been identified, advances have been made in identification of novel agents which can synergise with R-CHOP and improve its efficacy, including Bortezomib, Bendamustine and BCL-2 inhibitors (Dunleavy et al., 2009; Dupire and Coiffier, 2010; Obermann et al., 2009). Overexpression of BCL-2 in DLBCL has been reported to promote resistance to therapy indicating that inhibition of this anti-apoptotic protein may improve the efficacy of current treatments (Barrans et al., 2003; Obermann et al., 2009). Activation of

cytoprotective autophagy as a result of BCL-2 inhibition should be considered when evaluating the utility of BCL-2 inhibitors in the treatment of DLBCL.

1.7.6 The tumour microenvironment of DLBCL

The role of the tumour microenvironment in the progression and clinical outcome of DLBCL has been firmly established (Alizadeh et al., 2000; Lenz et al., 2008a).

Gene signatures of the microenvironment have been reported predict outcome in DLBCL. Examination of 414 pre-treatment DLBCL patients identified three distinct gene-expression signatures – GC B cell, expressed by $CD19^+$ B cells, and stromal-1 and stromal-2, expressed by the $CD19^-$, microenvironment population (Lenz et al., 2008a). The stromal-1 signature is comprised of genes expressed by components of the extracellular matrix such as *MMP2*, fibronectin and osteonectin. Infiltration of cells associated with the myeloid lineage including macrophages and monocytes is characteristic of this signature which predicts a good clinical outcome (Lenz et al., 2008a). The stromal-2 signature is thought to represent an "angiogenic-switch" in DLBCL samples due to increased expression of angiogenic regulators such as VEGF and GRB10. Genes such as *EGFL7* and *FAB24*, expressed in endothelial cells and adipocytes respectively, are also associated with the stromal-2 gene signature (Lenz et al., 2008a). This signature is prognostically unfavourable in DLBCL patients. The role of autophagy in the microenvironment in DLBCL is currently unknown. Alizadeh and colleagues (Alizadeh et al., 2000; Rosenwald et al., 2002) also demonstrated that a lymph-node signature similar to normal lymph-nodes which included genes encoding for natural killer (NK) cells and macrophage markers such as CD14 and CD105 and genes involved in extracellular matrix remodelling was present in the majority of DLBCL samples.

1.8 Aims

While the pro-survival role of BCL-2 in FL and DLBCL has been established, the effect of increased expression of this anti-apoptotic protein on the autophagy pathway in these NHLs is unclear. It is also currently unknown whether autophagy is altered in FL and DLBCL and whether modulation of this pathway is associated with the clinical outcome of these diseases. Therefore, the main aims of this study are:

1.8.1 To evaluate the role of BCL-2 in autophagy in lymphoma cells

We aim to evaluate if overexpression of BCL-2 inhibits autophagy in lymphoma cells by comparing autophagy activity between BCL-2^{HIGH} and BCL-2^{LOW} DLBCL cell lines following treatment with a BCL-2 inhibitor, ABT-737. This will be done by assessing cellular levels of the autophagy markers p62 and LC3 and by evaluating if BCL-2 and Beclin-1 form an autophagy-inhibiting complex in malignant B cells. We also aim to determine whether autophagy induced following inhibition of BCL-2 functions as a cytoprotective or pro-apoptotic mechanism. Comparisons will also be made between the GEP of DLBCL cell lines following induction of autophagy to assess if BCL-2 overexpression modulates the autophagy flux at the gene level in response to autophagy stress.

1.8.2 To determine the basal level autophagy status of primary lymphoma samples

BCL-2 overexpression is common among NHLs, particularly FL patients. In order to establish if increased expression of BCL-2 inhibits autophagy, we aim to evaluate the basal level autophagy status of primary FL and DLBCL samples and lymphoma cell lines at both the gene and protein levels. We will do this by analysing the GEP of primary purified and unpurified FL and DLBCL samples and evaluating expression levels of key autophagy-related proteins including p62 in primary FL and DLBCL tissue samples.

1.8.3 To establish if expression levels of key autophagy-related proteins can be used as prognostic biomarkers in NHL

The prognostic significance of the key autophagy-related proteins p62, Beclin-1 and LC3 has been reported for a variety of malignancies. However, it is currently unclear if expression levels of these proteins, and thus the autophagy status of a sample, has prognostic value in FL and DLBCL. Using IHC and TMA technology, we aim to determine if cellular levels of these proteins can be used as independent biomarkers of clinical outcome in FL and DLBCL.

Chapter II

Materials and Methods

2.1 Cell line and cell culture

The DLBCL cell lines Su-DHL4 and CRL which are t(14;18) positive and have high BCL-2 protein expression and Su-DLH8 and Su-DHL10 which are t(14;18) negative and have low BCL-2 protein expression (Deng et al., 2007) were used in this study. Su-DHL4, Su-DHL8 and Su-DHL10 were gifted from Dr. A Letai; CRL cells were acquired from the Cancer Research UK tissue bank. Cell lines were cultured using RPMI 1640 Media supplemented with 10% heat inactivated fetal calf serum (FCS) (56°C for 1 hour), 2mM L-glutamine, 100U/ml penicillin and 100µg/ml streptomycin (Appendix I, 1.1). Cells were seeded in 75cm^2 Nunc tissue culture flasks, grown at 37°C in a 5% CO_2 humidified incubator and passaged every 2-3 days to maintain viability, which was measured using a Beckman Coulter Vi-Cell ™ XR Cell Viability Analyzer (Appendix I, 1.2).

2.2 Patient Samples

2.2.1 Ethical considerations

Ethical approval for the human biological material used in this study was obtained in accordance with the requirements of the East London and the City Ethics Committee (Ref. No. 10/H0704/65). This allowed the use of stored and newly obtained human biological samples, including lymph nodes, from patients with haematological malignancies and healthy donors. All samples were obtained from patients by informed consent. Samples were identified by vial number or hospital number only, with patient information held in a secure password protected file.

2.2.2 Patient sample selection

Samples were obtained upon request from the tissue bank located in the Centre for Haemato-Oncology, Barts Cancer Institute which is maintained according to the Human Tissue Act 2004 (Licence No. 12199). FL, DLBCL and reactive DNA samples, single cell suspensions and whole tissue samples were selected based on availability and stage. Only samples which were classified as pre-treatment at diagnosis, pre-treatment at diagnosis on expectant management or pre-treatment at diagnosis - at progression on expectant management were selected for further analysis. Due to limited sample numbers patients were not age or sex matched. The median patient age was 62 years and

55 years for FL and DLBCL patients respectively. Patients selected presented at St. Bartholomew's hospital between the years 1998-2012. Patients included on tissue microarrays (TMAs) were also diagnostic, pre-treatment samples which presented at St. Bartholomew's between the years 1968 and 2009. Further information on selection of samples for inclusion in TMAs is reported in appendix II table T and U. All clinical information was obtained upon request from the clinical database manager Mrs. Janet Matthews and was coded to protect patient identity as described above.

2.3 Preparation of cell lysates for Western blotting

Cells were spun down at 1200rpm for 5min, washed 1× with 1ml phosphate buffered saline (PBS) and centrifuged at 8000rpm for 2min after which all PBS was removed. Cell pellets were then mixed by gentle pipetting with 30-100µl cell lysis buffer containing protease inhibitor cocktail (PIC), incubated on ice for 20min and spun at 13,000rpm for 15min at 4°C. Lysates were kept on ice at all times (Appendix I, 2.1.1).

2.4 Determination of protein concentration – Bradford assay

The Bradford Assay uses the protein binding dye Coomassie® G-250 to determine protein concentration. Binding proteins induces a colour change in the dye from red to blue, shifting the absorbance maximum from 465nm to 595nm. This increase in absorption observed at 595nm is proportional to protein concentration, with samples becoming darker with increasing concentration (Bradford, 1976). Protein concentration is calculated by comparing test samples to a standard curve which is a series of defined standards that exhibit a linear absorbance profile. Samples are read at 595nm using an Opsy MR spectrophotometer and concentrations reported as µg/µl.

Procedure

A standard curve (Table 2.1) was prepared per plate using a 0.5mg/ml BSA working solution (Appendix I, 2.1.2). Increasing volumes of BSA were mixed with 100µl Bio-Rad protein assay dye reagent (Appendix I, 2.1.2) in a 96-well plate as per table 2.1. Test samples were assayed in triplicate by mixing 1µl of diluted (1:10) protein lysate with 100µl Bio-Rad reagent. Lysates were diluted prior to evaluation to ensure concentrations fall within the absorbance range of the standards and spectrophotometer.

Samples were read at 595nm on a spectrophotometer and protein concentrations calculated by linear regression using the equation y = mx + b where y is the average sample absorbance at 595nm and x is protein concentration (µg/µl).

Table 2.1 BSA Standard Curve for Bradford Assay

Row	0.5mg/ml BSA (µl)	BSA Concetnration (µg)
0	0	0
1	0.5	2.5
2	1	5
3	2	10
4	4	20

2.5 Western blotting

Western blotting allows visualisation and examination of the expression levels of cellular proteins which have been separated from one another based on their molecular weight using SDS-PAGE. The detergent SDS linearises proteins and coats them in negative charges meaning molecular weight is the only difference between them. An electrical current is applied to the gel and the negatively charged proteins migrate towards the anode, with smaller proteins migrating faster than larger proteins. Separated proteins are then transferred to a polyvinylidene difluoride (PVDF) membrane which allows the protein of interest to be detected using specific antibodies (Kurien and Scofield, 2006).

Procedure

Sample lysate was mixed with lysis buffer and loading buffer and heated at 100°C for 10min. 10µl protein molecular weight marker and 15-20µl of sample were loaded onto an Nu-PAGE ® 4-12% Bis-Tris gel, proteins separated by SDS-PAGE at 200V and transferred to a methanol-wetted PVDF membrane using a semi-dry transfer method for 1hr at 20V. Following transfer, membranes were blocked for 1hr at room temperature (RT) with agitation in 5% milk in phosphate buffered saline with Tween-20 (PBST) to avoid non-specific binding (Appendix I, 2.2). Membranes were then incubated with primary antibody (Appendix I, Table A) overnight with agitation at 4°C. Unbound primary antibody was washed off with PBST (3×10min) after which membranes were incubated with anti-rabbit/anti-mouse HRP-conjugated secondary antibody (Appendix I, Table B) for 1hr at RT with agitation. Unbound secondary antibody was washed off

with PBST (4×15min). Membranes were incubated with 1ml ECL PLUS for 5min and bands visualised using a FujiFilm LAS 4000 developer. Membranes were washed and stripped with PBST and stripping buffer and re-probed as desired. β-actin or GAPDH were used as loading controls. In some instances alternative blocking, primary and secondary antibody solutions were used which facilitate detection of weakly expressed proteins (Appendix I, 2.2).

2.6 Immunofluorescent microscopy

IFM allows detection and visualisation of a protein of interest in a tissue or cell and can be used to examine protein expression and identify co-localisation between proteins. Indirect IFM uses primary and secondary antibodies and produces more specific results than direct IFM (Ramos-Vara, 2005). Primary antibodies are raised against a specific protein/antigen and secondary antibodies against immunoglobulins of the primary antibody species. Following incubation with an unlabelled primary antibody, a secondary antibody conjugated to an enzyme maker or flurophore, which fluoresces at a certain wavelength and emits a specific colour, is used to visualise the protein of interest. The secondary antibodies used in this study were conjugated to the Alexa Fluor®488 and Alexa Fluor®546 dyes. The Alexa Fluor®488 dye has an excitation wavelength of 495nm and an emission wavelength of 519nm and produces a green fluorescence, while the Alexa Fluor®546 dye (excitation/emission wavelengths: 556nm/573nm) produces an orange-red fluorescence. If carrying out dual staining two opposing, non-overlapping wavelengths which allow both antigens to be distinctly viewed should be chosen. Alexa Fluor®488 and Alexa Fluor®546 dyes have a minimum overlap and so are suitable for dual staining (Figure. 2.1).

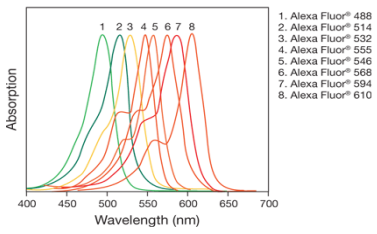

Figure 2.1 Absorption spectra of the Alexa Fluor® dyes
Note that AF-488 (1) and AF-546 (5) have minimum overlap.
http://www.invitrogen.com/site/us/en/home/References/Molecular-Probes-The-Handbook/Fluorophores-and-Their-Amine-Reactive-Derivatives/Alexa-Fluor-Dyes-Spanning-the-Visible-and-Infrared-Spectrum.html).

Procedure

10µl concentrated cell suspension was added to each chamber of a Superfrost™ slide and left to air-dry. Cells were fixed and permeabilised with 50µl Cytofix/Cytoperm for 30min at RT and rinsed with PBST. Non-specific bindings were blocked by incubation with 50µl blocking buffer (Appendix I, 3.1) for 30min at RT. Cells were then incubated with 50µl primary antibody (1hr at RT) (Appendix I, Table C), washed with PBST (3×10min), incubated with 50µl anti-mouse/anti-rabbit secondary antibody conjugated with Alexa Fluor-488 or Alexa Fluor-546 (1hr at RT) (Appendix I, Table D) and washed again with PBST (4×15min). Nuclei were counterstained by incubation with 4',6-Diamidino-2-Phenylindole, Dihydrochloride (DAPI) for 5mins (Appendix I, 3.3). Slides were allowed to dry completely, mounted using ProLong® Gold to prevent quenching and viewed using an Olympus BX40 fluorescent microscope.

Note: *Incubation with blocking buffer, primary/secondary antibodies and DAPI was carried out in a covered semi-dry box. All washes were performed with agitation and slides covered with aluminium foil to prevent flurophore quenching. 50µl volume is per chamber.*

2.7 Tissue microarray construction

TMAs are a platform on which 100s of primary tissue samples can be analysed simultaneously by established *in situ* techniques such as FISH, IHC and RNA-ISH (Simon et al., 2004). The development of TMAs allows faster, uniform analysis of multiple tissue samples at the same time under identical experimental conditions (Conway et al., 2008). TMAs are constructed by removing tissue cores 0.6mm–2mm in size from formalin-fixed paraffin embedded ‘donor’ tissue blocks and embedding these into a 'recipient' paraffin block, with each 'donor'/patient arrayed in triplicate to ensure the heterogeneous nature of the tumour is fully represented.

Procedure

TMAs used in this study were previously arrayed by our colleagues AC and AO using reactive lymph nodes, diagnostic FL and diagnostic DLBCL formalin-fixed, paraffin-embedded tissue biopsies available from St. Bartholomew's hospital. Sections of these tissue biopsies were stained with haematoxylin and eosin (H&E) and examined by our histopathologist colleague MC who identified and selected areas rich in malignant cells

which were representative of the whole tumour and suitable for sampling and inclusion on the TMAs. Using a semi-automated arraying machine (TMABooster-Alphelys, Beecher Scientific), 1mm^2 cores were 'punched' from the selected areas on the donor tissue and transferred into previously constructed holes in the recipient paraffin blocks. Each patient was arrayed in triplicate.

2.8 Immunohistochemistry

IHC allows visualisation of a protein within a tissue sample without disrupting or altering the tissue structure. It exploits the principle of antibody-antigen binding and allows these interactions to be visualised using fluorescent dyes, enzymes labels or radioactive markers (Coons, 1958). Direct IHC involves incubation of the tissue sample with a primary antibody which is conjugated to a maker (e.g. a fluorochrome) thus allowing direct antigen visualisation. Indirect IHC, which was performed in this study, involves a primary antibody acting as an antigen for a conjugated secondary antibody and is preferable to direct staining as it produces clearer results with increased sensitivity and specificity (Ramos-Vara, 2005).

In this study, the dextran polymer IHC staining method (DPM; Biogenix Supersensitive Polymer HRP) was used to identify proteins of interest, rather than the traditional avidin-biotin complex (ABC) method, which produces a high degree of non-specific background staining (Ramos-Vara, 2005). In the DPM method, samples are first incubated with an antibody directed against the antigen of interest. This antigen-antibody complex signal is amplified by binding of a multimeric compound which contains a secondary antibody targeted against the primary antibody, and a horseradish-peroxidase (HRP) conjugated polymer (SuperEnhancer™ and PolymerHRP™) (Figure 2.2). The antigen-antibody complex, which is bound by the multimeric complex, is then detected by adding a substrate that both binds to and is chemically altered by the polymer-conjugated HRP, resulting in a detectable colour change. Here, the chromogenic substrate used was 3,3'-diaminobenzidine (DAB), which when acted upon by HRP produces a dark brown colour and reflects expression of the protein of interest.

Prior to examination by IHC samples should be deparaffinised to remove excess wax, subjected to antigen-retrieval to unmask epitopes which may have been hidden during the fixing process and incubated with a blocking buffer to reduce non-specific bindings (Shi et al., 2005). Stained sections can be viewed and analysed manually or using automated commercial analysis systems such as ARIOL (Conway et al., 2008; Simon et al., 2004). The full list of antibodies used in this study can be found in the appendix (Appendix I, Table E).

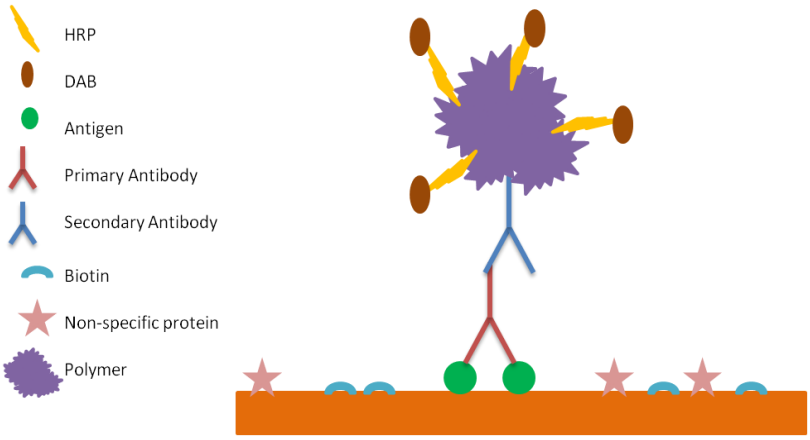

Figure 2.2 Dextran polymer indirect IHC staining method
Samples are incubated with primary antibody directed against the antigen of interest, followed by secondary antibody directed against the primary antibody. The secondary antibody is bound to a multimeric complex which contains HRP and a polymer and amplifies the signal produced by the primary antibody binding the antigen. DAB is then added which is converted to a dark brown colour by polymer-conjugated HRP if it is bound to the antigen. HRP – horseradish peroxidase; DAB – 3,3'-diaminobenzidine. Adapted from Ramos-Vara, 2005.

Procedure

Using a Leica RM2232 microtome, 3µm sections were cut from a TMA paraffin block which had been placed on an ice block for 10-15min prior to sectioning. Sections were placed on a Superfrost™ slide and placed in a 60ºC oven overnight to dry and fix. Following fixation sections were deparaffinised and non-specific bindings blocked by immersing them in 100% xylene, peroxidase blocking buffer (Appendix I, 4.1), 100% IMS and running tap water (5min per solution). Heat-induced antigen retrieval was performed by fully immersing sections in a pre-boiled unmasking solution (Appendix I,

4.2) and heating them for 10min in a pressure cooker. Sections were then marked using a hydrophobic pen and placed on an automated staining machine which was programmed to incubate slides for set periods of time with defined volumes of primary antibody (Appendix I, Table E), HRP-labelled polymer and the chromogen DAB (Appendix I, 4.4), which is chemically altered by HRP and produces a dark brown colour when the HRP-labelled polymer is bound to the antigen-antibody complex. Once stained, sections were dipped in acid alcohol (Appendix I, 4.5), counter-stained with Mayer haematoxylin which stains the nuclei of cells blue and mounted with coverslips using DPX (Distrene 80, Dibutyl phthalate and Xylene) (Appendix I, 4.6). Sections were prevented from drying out at all times by incubating with wash buffer (Appendix I, 4.7). Slides were then scanned, digitised and analysed using the automated ARIOL image analysis software. Image analysis classifiers are trained based on the saturation, intensity and hue of a colour such that only areas stained above a pre-determined threshold which reflect the highest intensity staining are included as positive staining / protein expression; background, lower level non-specific staining is excluded. For this study two classifiers were used – one which identified high intensity brown staining and was taken to represent the protein of interest, the other which reflected total area of viable tissue. Protein expression was calculated as the percent-stained viable tissue area for all proteins with the exception of CD68 which was previously analysed by our colleague RC as the percent-positive cells per viable tissue area. Poor quality cores were excluded from the analysis.

2.9 Measurement of caspase-3 activity

Induction of apoptosis results in activation of caspase-3, an essential component in the apoptotic pathway (Galluzzi et al., 2012; Porter and Janicke, 1999). Activated caspase-3 promotes the cleavage of cellular proteins including the DNA repair enzyme PARP, which it cleaves at the tetrapeptide DEVD (aspartic acid, glutamic acid, valine, aspartic acid), inhibiting its pro-survival function. Caspase-3 is also essential for apoptosis-induced DNA fragmentation and chromatin condensation (Gurtu et al., 1997; Porter and Janicke, 1999). As activated caspase-3 is a key component of apoptosis, caspase-3 activity can be used as a marker of apoptosis within cells. Conjugation of the flurophore

7-amino-4-trifluoromethylcoumarin (AFC) to the DEVD tetrapeptide forms the synthetic substrate DEVD-AFC which is cleaved by active caspase-3 during apoptosis, resulting in a shift in AFC fluorescence from blue to yellow-green. The amount of AFC cleaved from DEVD is proportional to the degree of caspase-3 activity and is defined as the amount of enzyme required to release 1µM AFC per hour.

Procedure

10µl protein lysate (Appendix I, 5.1) was mixed with 85µl reaction buffer (Appendix I, 5.2; Table F) and 5µl caspase-3-DEVD-AFC substrate (Appendix I, 5.3) giving a final volume of 100µl, protein concentration of 50µg and substrate concentration of 20µM per well. Samples were incubated at 37°C for 15min followed by 1min at -20°C and subsequently transferred from a clear 96-well culture plate to a black microtiter 96-well plate. AFC release was measured at excitation 410nm and emission 510nm using a BMG LabTech FLUOstar Omega microplate reader. Samples were analysed in triplicate. An AFC standard curve was prepared per plate according to table 2.2 using a 5µM AFC working solution (Appendix I, 5.4) and caspase-3 activity expressed as AFC release (µM/hr/mg protein).

Table 2.2 AFC Standard Curve for Caspase-3 Assay

Row	µM	5µM AFC (µl)	H_2O (µl)
0	0	0	100
1	0.1	2	98
2	0.2	4	96
3	0.3	6	94
4	0.4	8	92
5	0.5	10	90

2.10 Flow cytometry

Flow cytometry is a quantitative and qualitative assay which utilises the principles of light scattering and hydrodynamic focusing to measure and identify multiple characterises on individual cells (Brown and Wittwer, 2000; Mandy et al., 1995). Fluorescent dye -labelled cells are injected into a stream of fluid and hydrodynamically compressed, forcing them to pass one by one through a laser which results in fluorochrome excitation and emission of a photon. Emitted photons are scattered in

various directions based on cellular properties such as size and granularity, and detected by optics and filters which isolate individual wavelengths/fluorochromes (Figure 2.3) (Brown and Wittwer, 2000). Multiple fluorochromes can be used simultaneously to examine different cellular properties; however fluorochromes with minimally overlapping wavelengths should be selected.

2.10.1 Evaluation of mitochondria membrane potential and cell death

Tetramethylrhodamine, Methyl Ester, Perchlorate (TMRM) is a fluorescent lipophilic cation dye used to examine $\Delta\Psi m$ in cells (Scaduto and Grotyohann, 1999). Uptake of TMRM is an energy dependent process, meaning when $\Delta\Psi m$ is high ($\Delta\Psi m^{HIGH}$), TMRM is taken up by mitochondria. Damage to the mitochondria results in a decrease in membrane potential ($\Delta\Psi m^{LOW}$), preventing uptake and incorporation of this fluorescent dye into the mitochondria, resulting in its exclusion from cells. Therefore, a decrease in TMRM indicates low $\Delta\Psi m$ and mitochondrial damage (Nicholls and Ward, 2000). DAPI is an AT-specific, DNA binding fluorochrome used to distinguish live and dead cells (Schweizer, 1976). Due to increased membrane permeability DAPI accumulates in dead or dying cells, deemed $DAPI^{+}$, but is exclude from live cells with intact membranes, deemed $DAPI^{-}$.

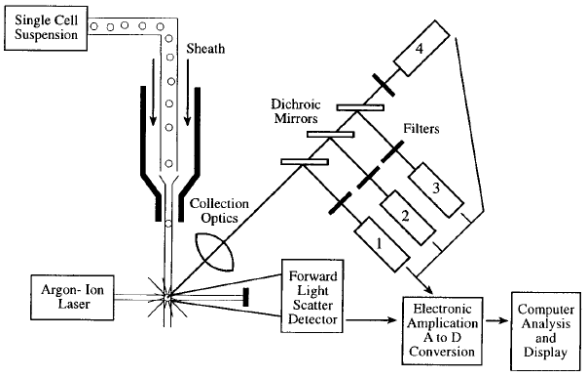

Figure 2.3 Example of typical flow cytometer

Cells in suspension are injected into the sheath fluid where they are forced into single file by hydrodynamic focusing. Upon encountering the light source (e.g. laser), light is scattered in various directions passing through collection optics, mirrors and filters. This light information is translated into digital format and produced as a read out on a computer attached to the cytometer. (http://www.clinchem.org/content/46/8/1221/F1.expansion).

Procedure

DAPI (Appendix I, 6.1) and TMRM (Appendix I, 6.2) were prepared in 10mls PBS at a concentration of 100ng/ml and 80nM, respectively, as a working solution. 400µl of working solution added to each FACs tube. Cells in suspension were added to the tubes at a ratio of 1:1 (400µl cell suspension/tube) to make final concentrations of DAPI at 50ng/ml and TMRM at 40nM. Cells were incubated for 15min at 37°C and read on an LSRFortessa cell analyser. DAPI was read under the violet laser channel (405nm) at bandpass V450/50 and TMRM under the blue laser channel (488nm) at bandpass B695/40. An unstained control containing only PBS and cell suspension in a 1:1 ratio was run prior to the fluorescently labelled samples in order to correctly define the negatively and positively stained populations. 10,000 cells were acquired per condition and data analysed using Summit Version 4.3.

2.10.2 Isolation of B cell populations by flow assisted cell sorting

Flow cytometry can identify and isolate distinct cell populations within a heterogeneous group of cells based on their immunophenotypes. Samples are incubated with antibodies labelled with fluorescent dyes directed against surface antigens expressed by the cell of interest, allowing this population to be discerned from others. Cells expressing the appropriate immunophenotype are 'gated-out', diverted from the fluid stream and collected as a homogeneous cell fraction (Ibrahim and van den Engh, 2007). While some populations can be isolated by expression of a single marker, the majority of cell types are segregated based on multiple markers. Similarly, more than one homogeneous population of cells can be obtained from a single sample at the same time. When choosing a fluorochrome panel to identify and isolate various populations care should be taken to avoid overlapping wavelengths; when this proves difficult compensation can be applied.

Procedure

Primary single cell suspensions were incubated with 0.5mg/ml DNase (Appendix I, 6.3) for 5min at RT, pelleted by centrifugation at 1,400rpm for 10min, resuspended in plain RPMI and separated into groups of 10×10^6 cells, keeping 2×10^6 cells for controls. Non-specific bindings were blocked by incubation with 2% human anti-γ-globulin antibody

(Appendix I, 6.4) for 30min on ice. Cells were then incubated with the appropriate antibodies (Appendix I, Table G) for 30min on ice in the dark, washed 1× in 2% FACS wash (Appendix I, 6.6) and resuspended in 2% FACS wash containing DNase and DAPI (Appendix I, 6.7; 1ml/10×10^6 cells). B cells were isolated using a BD FACSAria flow sorter and collected in 1ml 10% filtered FCS (Appendix I, 6.8). Isolated B cell purity was >95% in all cases. An unstained control was included for each sample and a single stain and FMO for each antibody tested. DAPI was used to discriminate live and dead cells. Following selection of DAPI negative, cells T-cells were excluded by gating on CD3 negative ($CD3^-$) cells. B cells were isolated from the $DAPI^-/CD3^-$ population based on expression of B cell markers. DLBCL and reactive B cells were identified by CD20 expression while FL B cells were isolated based on dual expression of CD19 and CD10. Purified $CD19^+/CD10^+$ FL B cells and reactive B cells were evaluated for κ/λ light chain restriction.

2.11 RNA extraction

2.11.1 Phenol-chloroform based RNA extraction (TRIzol® Reagent)

TRIzol® Reagent is a ready-to-use monophasic guanidine isothiocyanate/phenol solution used for extraction of RNA from various biological samples while maintaining RNA integrity by effectively inhibiting RNase activity (Chomczynski and Sacchi, 1987).

Procedure

RNA was extracted from solid primary tissue samples using a standard TRIzol® RNA extraction protocol. Tissue samples were placed in a 2ml eppendorf containing 1ml TRIzol® and a metal ball bearing and homogenised at 4ºC for 3min at 20Hz. The homogenised sample (~1ml) was transferred to a fresh 1.5ml eppendorf, incubated at RT for 5min, mixed vigorously with 200µl chloroform for 15sec and incubated at RT for 3min, followed by centrifugation at 12,000rpm (15min at 4°C). Centrifugation results in separation of samples into a bottom white DNA layer, a red middle protein/DNA phenol-chloroform layer and a clear top chloroform layer containing RNA. This top aqueous layer (~500µl) was transferred to a fresh 1.5ml eppendorf, mixed with 500µl isopropanol by pipetting up and down 10-15 times, incubated at RT

for 10min, centrifuged at 12,000rpm (10min at 4°C) and the supernatant completely removed. Pellets were washed 1× with 75% ethanol (Appendix I, 7.1) centrifuged at 7,500rpm for 5min at 4°C, the supernatant completely removed and pellets left to air dry for 5-10min on ice. Pellets were then re-suspended in 50-100µl RNase free water and RNA quality and quantity assessed.

2.11.2 RNA extraction using QIAGEN RNeasy® mini kit

The QIAGEN RNeasy® Mini Kit is a widely used method of RNA extraction which does not require toxic, potentially contaminating compounds such as chloroform (Morse et al., 2006).

Procedure

RNA was extracted from cells according to the QIAGEN RNeasy® Mini Kit protocol. Cells in suspension were pelleted by centrifugation at 1,500rpm for 5min, mixed with 350µl buffer RLT containing β-mercaptoethanol (Appendix I, 8.1), transferred to a QIAshredder spin column and centrifuged at full speed (~14,000rpm) for 2min. The sample flow-through was retained, mixed with 350µl 70% ethanol (Appendix I, 8.2), transferred to an RNeasy spin column and centrifuged at 9,300rpm for 15sec. An on-column DNase digestion was then performed to eliminate any residual genomic DNA. 350µl buffer RW1 was added to the RNeasy spin column and centrifuged at 9,300rpm for 15sec, after which the membrane was incubated with 80µl DNase I incubation mix (Appendix I, 8.3) for 15min at RT. 350µl buffer RW1 was then added to the membrane and centrifuged for 15sec at 9,300rpm. The membrane was washed 2× by incubation with 500µl buffer RPE (Appendix I, 8.4) for 2min at RT followed by centrifugation at 9,300rpm for 15sec or 2min and centrifugation at ~14,000rpm for 1min to dry the membrane. RNA was eluted by incubation of the membrane with 25µl RNase-free water for 2min at RT followed by centrifugation at 9,300rpm for 1min and subsequently assessed for quality and quantity.

NOTE: *Care was taken when removing the spin column from the collection tube so as to avoid carryover of ethanol. Flow through was discarded unless otherwise stated.*

2.12 RNA quantity and quality assessment

2.12.1 NanoDrop spectrophotometer

RNA concentration and quality was determined using a NanoDrop spectrophotometer which measures the amount of ultraviolet (UV) light absorbed by nucleic acids at 260nm. Nucleic acid absorbance equals optical density (OD), where taking a path length of a 1cm, 1 OD unit is equal to 50ng/µl (Cicinnati et al., 2008). Quality was assessed by determining the 260/280nm and 260/230nm absorbance ratios. The optimal 260/280nm ratio for RNA is ~2, with a lower value suggesting possible contamination with protein or other impurities which absorb strongly at 280nm (Wilfinger et al., 1997). 260/230nm ratios should be between 2 and 2.2, although no consensus has been reached as to what constitutes an acceptable cut-off. (Wilfinger et al., 1997).

Procedure

Prior to testing of samples the NanoDrop was blanked using 1µl of RNase-free water. RNA samples were tested using 1µl of RNA and the RNA quantity (ng/µl), 260/280nm and 260/230nm values recorded for each sample.

2.12.2 Agilent bioanalyser

The Agilent 2100 Bioanalyser is a microfluidics-based automated system used to establish the quality and integrity of an RNA sample (Schroeder et al., 2006) The bioanalyser generates an RNA integrity number (RIN) per sample which is calculated based on the RNAs electrophoretic trace while taking into account the presence/absence of degraded RNA products and the height of the 18S peak (Imbeaud et al., 2005; Schroeder et al., 2006). An electropherogram which shows degraded RNA products as well as the 18S and 28S ribosomal RNA peaks is produced per sample (Figure 2.4). A RIN of 1 indicates poor quality, degraded RNA while a RIN of 10 suggests good quality, intact RNA (Imbeaud et al., 2005). When carrying out RNA-based assays only samples with similar RIN should be compared.

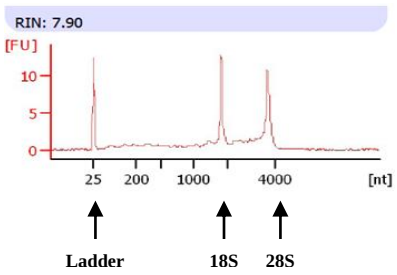

Figure 2.4 Representative Electropherogram generated by the Agilent 2100 Bioanalyser
For each sample run on the Agilent 2100 Bioanalyser an electropherogram is generated which shows the ladder, 18S subunit, 28S subunit and any degraded RNA. The sample shown has a RIN number of 7.9.

Procedure

Reagents (Agilent RNA 6000 Nano Kit) were equilibrated to RT for at least 30min prior to use (Appendix I, 9.0). The procedure was carried out according to the manufactures guidelines. 550µl RNA gel matrix was transferred to a spin filter and centrifuged at 4,000rpm for 10min. 1µl RNA dye concentrate was added to 65µl filtered gel, mixed by vortexing and spun at 11,800rpm for 10min. 9µl gel-dye mix was added to the well marked 'G' of an RNA bioanalyser chip and dispersed. A further 9µl of gel-dye mix was added to the second and third wells marked 'G' after which 5µl RNA marker was added to each well including the ladder well. Samples and the Agilent RNA 6000 ladder were denatured by heating at 70°C for 2min. 1µl RNA 6000 ladder was added to the ladder well and 1µl of sample added to each well. A further 1µl of RNA marker was added to any well which did not contain an RNA sample. The chip was then vortexed for 1min, inspected for bubbles and run on the Agilent 2100 Bioanalyser using the Eukaryote RNA Nano chip assay.

2.13 Gene expression analysis by qRT- PCR

2.13.1 Complementary DNA synthesis

RNA is not a suitable assay template as it is highly unstable and readily broken down by ubiquitous RNases (Bustin, 2002; Fleige et al., 2006). Therefore in order to examine RNA it must first be converted by the enzyme reverse-transcriptase to complementary DNA (cDNA) which acts as a stable template for RNA-based assays (Bustin, 2000). Conversion of RNA to cDNA begins with binding of primers to mRNA that act as a reference point from which reverse-transcription begins. Commonly used primers

include oligo dTs and random hexamer primers which bind RNA at the 3' poly-A tail and multiple different sites along the RNA template respectively (Bustin et al., 2005). A combination of both primers can also be used as was the case in this study. Following primer binding the reverse-transcriptase enzyme converts ssRNA to ds-cDNA which is suitable for use in RNA-based assays.

Procedure

RNA was converted to cDNA using the QIAGEN RT^2 First Strand Kit. A 10µl genomic DNA elimination (GDE) mix was prepared per sample (Appendix I, Table H). For samples where RNA volume exceeded 8µl, RNA was spun down for 3-5 min at medium speed in a 60Hz speed vac to reduce volume but maintain concentration. GDE mix was incubated at 42°C for 5min followed by at least 1min at 4°C using a thermo cycler. A reverse-transcription (ReTr) mix was prepared (Appendix I, Table I), 10µl mixed with each samples GDE mix and incubated on a thermo cycler at 42°C for 15min followed by 5min at 95°C to stop the reaction. 91µl RNase-free water was then added to each sample and mixed by gently pipetting up and down. cDNA was stored at -20°C.

2.13.2 Quantitative real-time polymerase chain reaction

qRT-PCR allows enzymatic amplification and real-time detection of specific mRNA transcripts within a given sample. This RNA-based assay utilises fluorescent molecules to determine the relative abundance of an mRNA transcript by measuring the release of a fluorescent molecule such as carboxyfluorescein (FAM) or the incorporation of a fluorescent molecule such as SYBR Green. SYBR Green based qRT-PCR begins with denaturation of ds-cDNA to a single-stranded template which is bound by primers targeted against a specific complementary mRNA sequence. Primers are extended by HotStart DNA Taq (*Thermus aquaticus*) polymerase, resulting in synthesis of a new ds-DNA complex to which SYBR Green binds, causing it to fluoresce. This cycle is repeated 40 times and amplifies the ds-cDNA exponentially, resulting in accumulation of SYBR Green fluorescence. The amount of SYBR green which accumulates is therefore proportional to the amount of newly synthesised ds-DNA and thus the amount of PCR product/mRNA initially present.

The RT^2 Profiler PCR Array combines qRT-PCR technology with a microarray format to allow rapid, simultaneous detection of multiple genes expression levels. For example the RT^2 Profiler Human Autophagy PCR Array contains primers targeted against 84 genes involved in all aspects of the autophagy pathway, from key machinery genes to regulatory genes. This array also contains primers targeted against a number of controls, namely five housekeeping genes (HKGs) used for data normalisation, along with genomic DNA (GDC), reverse-transcription (RTC) and positive PCR (PPC) controls (Figure 2.5).

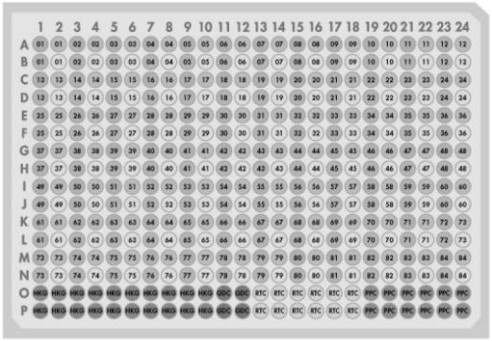

Figure 2.5 RT^2 Profiler PCR Array, 384-well plate, Format E Layout
The RT^2 Profiler PCR Array contains primers against 84 genes with each primer replicated four times (e.g. A1, A2, B1, and B2). Rows A - N contain primers directed to the autophagy-related genes, while rows O and P contain primers against various endogenous and reaction controls. HKG - housekeeping gene; GDC - genomic DNA control; RTC - reverse transcription control; PPC - positive PCR control.

Procedure

A PCR reagents mix was prepared per sample (Appendix I, Table J) using previously synthesised cDNA. Each samples' PCR-mix was placed into a loading reservoir and from here 10µl transferred to the samples designated well on the 384-well array. Once loaded the plate was sealed, centrifuged for 1min at 3,300rpm at RT and subsequently placed on ice. The Applied Biosystems 7900HT real-time cycler was then programmed according to the protocol and a dissociation curve analysis step included to verify PCR specificity (Appendix I, Table K).

2.13.3 Validation of qRT-PCR

Validation experiments were carried out in a cohort of patients to confirm a sub-set of gene expression changes observed using the RT^2 Profiler PCR Array. Following conversion of RNA to cDNA, samples were prepared for qRT-PCR (Appendix I, Table

L) and the qRT-PCR assay run under previously stipulated cycling conditions (Appendix I, Table K). All genes validated, including the HKG RPLPO, were analysed in triplicate and a no-template control (NTC) also included per gene. Primers used in validation experiments were identical to those present on the RT^2 Profiler Human Autophagy PCR Array.

2.13.4 Endogenous control selection

When performing gene expression analysis by qRT-PCR there are a number of parameters including efficiency of cDNA synthesis and technical variation which should be controlled for to ensure expression measures obtained are reliable and robust (Andersen et al., 2004). The most common way to minimise the potential effect of such variables is to normalise data to an internal HKG which ideally, should be stably expressed in all cell types and under all experimental conditions (Andersen et al., 2004; Vandesompele et al., 2002). Arbitrary selection of such a gene is advised against; instead, software programmes which use algorithms to determine the best HKG/combination of genes within and between different sample groups should be used. In this study the freely available programmes gNorm and Normfinder were used to identify the most stable HKG(s).

2.13.4.1 gNorm

gNorm identifies the most stably expressed HKG(s) within and between sample groups by using non-normalised C_T values to calculate the expression ratio between two HKGs and works on the principal that this ratio should be identical under all experimental conditions in all sample types. From this ratio the gene-stability measure M, which is the arithmetic mean of all pairwise variations of a particular gene with all other HKGs, is calculated (Vandesompele et al., 2002). A low M value is indicative of a gene with stable expression while a high M value is representative of a less stably expressed gene. gNorm compares M values between all possible combinations of genes and in a stepwise exclusion manner removes unstable genes with a high M value and retains those with similar, low M values, thus systematically identifying which gene(s) are the best to use as a housekeeping/normalisation gene (Figure 2.6) (Vandesompele et al., 2002).

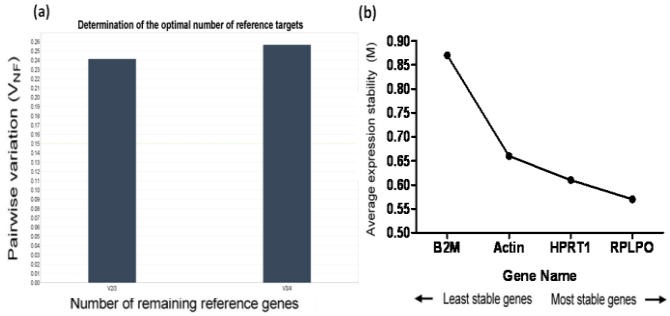

Figure 2.6 Identification of the most stable endogenous control gene(s) using gNorm software

Raw C_T values generated from qRT-PCR were imputed into the gNorm programme which analyses data and identifies the most stable HKG. gNorm returns a V_{NF} value which indicates whether or not a combination of genes is more stable than a single HKG. In this example, no pair of controls is significantly more stable than using a single gene on its own (a). gNorm also returns the M value which indicates the stability of the HKGs. The lower the M value of a HKG the more stable it is. In this example, the most stable gene is RPLPO (b).

2.13.4.2 Normfinder

Normfinder is a Microsoft Excel algorithm-based add-on which identifies the optimal HKG within any number of samples or groups (Andersen et al., 2004). It calculates a stability value for each HKG across all samples/groups by combining the intra- and intergroup variation and ranks genes according to this value. Gene(s) with a low stability value are deemed the most stable and thus the most appropriate to use as a normalisation gene (Andersen et al., 2004). Raw C_T values cannot be used for Normfinder; instead, data should be linearised relative to a user-defined calibrator sample and these values imputed.

2.13.5 Calculation of relative quantification values

The qRT-PCR assay generates cycle threshold (C_T) values which represent the abundance of mRNA transcript present for each gene in each sample. The C_T value is defined as the number of cycles required for the fluorescence signal to cross a defined threshold during the exponential phase of the PCR reaction. The threshold limit is user-defined and should be standardised across all plates within a given experiment. C_T values are inversely proportional to mRNA abundance – the greater the amount of target mRNA present the lower the C_T value. C_T values obtained from qRT-PCR assays are

non-normalised meaning direct comparison of these values within and between groups is not an accurate reflection of gene expression profiles. To allow direct comparisons, C_T values must first be converted to relative quantity (RQ) values.

Procedure

Prior to calculation of RQ values, genes with a C_T value of >35 were excluded from further analysis as this value surpasses the threshold of the qRT-PCR cycler and may not be an accurate measure of gene expression (Kreth et al., 2010). All plates within a single experiment were standardised to the same threshold. For samples analysed in triplicate the average C_T value was used provided standard deviation (SD) was <0.5. In cases where SD was >0.5, data was visualised and if a clear outlier was identified this value was excluded and the average of the remaining duplicates used.

RQ values were calculated using the formula $RQ = 2^{-\Delta\Delta C_T}$. Target C_T values were normalised to a previously selected HKG by subtracting the C_T value of the HKG from the target gene C_T, generating a delta C_T (ΔC_T) value for each gene.

$$\mathbf{C_T\ Target\ Gene - C_T\ Endogenous\ Control\ Gene = \Delta C_T}$$

The delta ΔC_T ($\Delta\Delta C_T$) value, which represents the quantity of mRNA present in each sample, was determined by subtracting the ΔC_T of a user-defined calibrator sample from the ΔC_T of test samples. In this study the average ΔC_T of reactive control samples or untreated cell lines was used as the calibrator sample on a per gene basis.

$$\mathbf{\Delta C_T\ Test\ Sample - \Delta C_T\ Calibrator\ Sample = \Delta\Delta C_T}$$

Calculation of the $\Delta\Delta C_T$ value in this manner produces data which is $\log_2$-transformed. Data was therefore transformed to a linear scale using the formula below, producing the final RQ value which is comparable across all genes and sample types in all groups.

$$\mathbf{2^{-\Delta\Delta C_T} = RQ}$$

To identify differences in gene expression levels between groups the average RQ value of each gene was calculated within each patient group. The average of one group was then divided by the average of another (e.g. average FL/average DLBCL) which generated a fold change (FC) value for each. A FC of ≥2 or ≤-2 which was statistically

($p < 0.05$) significant using a Mann-Whitney *U* test was taken to be biologically meaningful.

2.13.6 Hierarchical clustering

Hierarchical clustering is a technique commonly used in GEP to identify genes or groups of genes which are similarly expressed between samples. Using a distance metric which measures distances between observation pairs, samples are clustered based on similarities or differences in RQ values/gene expression levels. A linkage criterion is also used which groups' samples based on similarity by calculating the distance between sets of observations as a function of the pairwise distance between observations within sets and produces linkage trees or dendrograms which depict similarities between samples. In this study, hierarchical clustering was performed using the Euclidean distance measure and an average agglomeration available within the R statistical computing environment, and which determine similarity between genes and samples and calculate the distance between samples or genes respectively. All hierarchical clustering was performed by JM.

2.14 Co-Immunoprecipitation

Co-immunoprecipitation (co-IP) is used to detect protein-protein interactions within cells (Phizicky and Fields, 1995). While IP experiments aim to identify a primary target within a sample, co-IP experiments aim to identify any ligands or proteins bound to the primary antigen (www.piercenet.com). Co-IP works by incubating whole cell lysate with antibody directed against the primary target antigen. This antibody/protein complex, which will also contain proteins interacting with the primary antigen, is then captured on a solid support such as beads. This protein complex is eluted off the support, denatured and analysed by SDS-PAGE and immunoblotting (Phizicky and Fields, 1995). Secondary target antigens are probed for initially followed by detection of the primary target antigen to verify its presence (Figure 2.7) (www.piercenet.com). Normal whole cell lysate and an immunoglobulin control should be used for each sample.

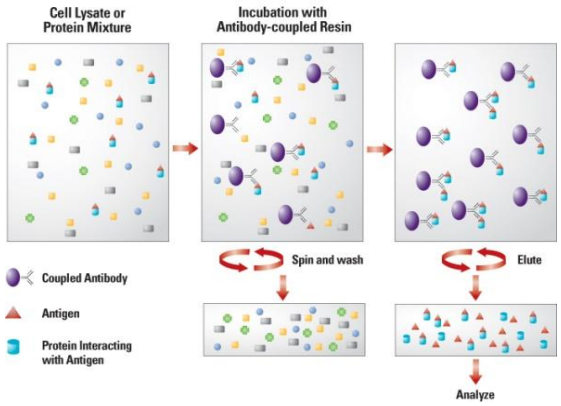

Figure 2.7 Diagrammatic representation of a co-IP experiment
Whole cell lysate is incubated with antibody target to a specific protein. A solid support (e.g. beads) is added to the mixture to capture the primary antigen and any proteins with which it interacts. The samples are spun and washed and the protein complex eluted off. Samples are analysed using SDS-PAGE. **http://www.piercenet.com/browse.cfm?fldID=9C471132-0F72-4F39-8DF0-455FB515718F.**

Procedure

Samples were prepared by mixing 300-400µg of protein with IP incubation buffer (Appendix I, Table M) to a total volume of 200µl. 2µg of mouse anti-IgG or hamster anti-BCL-2 was added to the protein/buffer mixture and samples incubated on a rotator overnight at 4°C. Samples were then incubated with 20µl of Protein A/G beads on a rotator for 1hr at RT, spun down and washed 3× with IP wash buffer (Appendix I, Table N). 20µl of eluting solution (Appendix I, 11.3) was added to each pellet and samples denatured by heating at 100°C for 5min. Proteins were separated by SDS-PAGE and Beclin-1 and BCL-2 probed for by Western blotting.

2.15 Statistical analysis

2.15.1 General statistical analysis

Data were expressed as mean ± SD of three separate experiments. A student's unpaired t-test was used to compare differences between two groups, where data was deemed to follow a normal Gaussian distribution (Shapiro-Wilk p value >0.05). To examine the effect of treatment on a single cell line, a paired student's t-test was used. Non-normally distributed data were analysed using the non-parametric Mann-Whitney *U* test. All tests performed were two-tailed. Comparisons were made between more than 2 groups using a 2-way analysis of variance (ANOVA) with Bonferroni post-test analysis for multiple comparisons. A Pearson correlation test was used to assess correlation between two data

sets. A *p* value of <0.05 (*), <0.01 (**) or <0.0001 (***) was deemed significant for all comparisons. Statistical tests were performed using Prism software Version 5.03 and Excel. Specific statistical tests used in each experiment are stated in the corresponding text or figure legend.

2.15.2 X-tile

X-tile Version 3.5 (Yale University) is a statistical software package which divides patients into two or more groups based on optimal cut-points which are derived from the variable being assessed, without the need for validated normal ranges (Camp et al., 2004). X-tile first divides the patient cohort into two independent data sets – test and validation– in a 1:2 ratio. It then determines the optimal cut-point(s) for each marker within the test set, and subsequently applies this to the validation set (Altman et al., 1994; Greaves et al., 2013).

2.15.3 Kaplan-Meier survival analysis

Kaplan-Meier survival curves were generated using Prism Version 5.03. Patients were stratified according to X-tile derived cut-points. Statistically significant differences in clinical outcome between groups, arising from differential expression of each marker or protein, were determined using a log-rank test. Outcomes compared in this study were overall survival (OS), disease-specific survival (DSS), time to transformation (TTT) and progression free survival (PFS) which were calculated according to table 2.10. Where the event (e.g. death) occurred patients were coded '1'; where the event did not occur, patients were censored and coded '0'. A *p* value of <0.05 was deemed significant.

Table 2.3 Calculation of Survival Outcomes

Outcome	Obtained
Overall Survival (OS)	Date of diagnosis to date of death or date of last follow up
Disease Specific Survival (DSS)	Date of diagnosis to date of disease related death or date of last follow up
Time to Transformation (TTT)	Date of diagnosis to date of transformation or date of last follow up
Progression Free Survival (PFS)	Date of diagnosis to date of progression/relapse

2.15.4 Continuous data analysis

Continuous univariate data analysis assesses the ability of a single variable to predict outcome using the Cox proportional hazards model (Greaves et al., 2013). This model evaluates the association between a single continuous variable and a defined event by estimating its Hazard ratio (HR) and corresponding 95% confidence intervals (CI). HR ratios represent the incremental increase in risk of an event occurring. In order for a variable to be classified as a significant prognostic marker using this analysis, *p* must be <0.05. All continuous data analysis was performed using IBM SPSS Statistics Version 22.

2.15.5 Categorical (cut-point) data analysis

Categorical data analysis stratifies patients into groups, typically 'low' and 'high', using X-tile generated cut-points (Greaves et al., 2013). Kaplan-Meier survival curves were then generated using these cut-points and significant differences between groups with respect to clinical outcome analysed using a log-rank (Mantel-Cox) test, which provides a *p* value, HR and 95% CI for each variable assessed. HR ratios represent the instantaneous risk of an event occurring in one group but not the other by the next time point. In order for a variable to be classified as a significant prognostic marker using this analysis, *p* must be <0.05, the HR must be <1 or 1>, but not equal to 1, and 95% CIs must not cross 1. Univariate categorical analysis included only one variable or two variables combined. For multivariate categorical analysis, each variable assessed was adjusted for FLIPI (FL) or IPI (DLBCL) scores. All categorical data analysis was performed using Prism Version 5.03 and IBM SPSS Statistics Version 22.

Chapter III

Evaluation of the dual roles of BCL-2 in apoptosis and autophagy in DLBCL cell lines

3.1 Introduction

The aim of conventional chemotherapy is to kill malignant cells via apoptosis so as to avoid necrosis-mediated inflammation while sparing normal, healthy cells (Kaufmann et al., 1993; Kaufmann and Earnshaw, 2000). The response of tumour cells to chemotherapy is in part governed by cellular levels of BCL-2 family proteins, with a higher ratio of anti-apoptotic to pro-apoptotic proteins known to promote resistance to chemotherapy-induced apoptosis in malignant cells (Kaufmann and Earnshaw, 2000; Malik et al., 2011).

Increased expression of BCL-2 in FL and DLBCL allows neoplastic cells to evade therapy-induced apoptosis making treatment of these haematological malignancies difficult (Campos et al., 1993; Miyashita and Reed, 1993). This obstacle may be overcome and chemotherapy-driven killing of FL and DLBCL cells improved via targeted inhibition of BCL-2 which has shown therapeutic potential in other malignancies. For example the synthetic BH3-mimetic ABT-737, which binds BCL-2 and BCL-xL via BH3-domain interactions and promotes induction of the intrinsic apoptosis pathway, has been shown to be effective as both a single and combination therapeutic agent in MCL and other malignancies (Song and Kraft, 2012; Touzeau et al., 2011).

It has been reported that the naturally occurring BH3-mimetic (-)-Gossypol can induce autophagy by binding BCL-2 via BH3-domain interactions and disrupting its binding to the pro-autophagy protein Beclin-1. Sequestration of BCL-2 by (-)-Gossypol frees Beclin-1, allowing it to promote autophagy activity within cells (Gao et al., 2010; Lian et al., 2011). As well as inducing apoptosis, ABT-737 has also been shown to mediate the autophagy pathway via different mechanisms including competitive binding of BCL-2 (Malik et al., 2011). It is currently unclear whether this BH3-mimetic can trigger autophagy while inducing apoptosis in lymphoma cells. We therefore aimed to evaluate which pro- or anti-apoptotic protein(s) determine sensitivity of our panel of DLBCL cell lines to ABT-737-induced cell death, and whether ABT-737 also induces autophagy in these cells.

3.2 Results

3.2.1 BCL-2 family proteins are differentially expressed in DLBCL cell lines

Basal expression levels of key pro- and anti-apoptotic BCL-2 family proteins were evaluated in DLBCL cell lines by Western blotting (Figure 3.1). We observed that Su-DHL4 and CRL cells expressed considerably higher levels of BCL-2 compared to Su-DHL8 and Su-DHL10 cells, which expressed little to no BCL-2 (Figure 3.1 A). This is unsurprising as both Su-DHL4 and CRL cells carry the t(14;18) translocation which results in increased, aberrant expression of BCL-2 (Deng et al., 2007; Kelly and Strasser, 2011). For this reason Su-DHL4 and CRL cells will hereafter be referred to as BCL-2^{HIGH} and Su-DHL8 and Su-DHL10 as BCL-2^{LOW} cells.

All four cell lines were found to express the anti-apoptotic proteins BCL-xL and MCL-1 (Figure 3.1 A). Expression of pro-apoptotic proteins also differed between these cell lines. Bak expression was strongest in Su-DHL4 cells while Su-DHL10 was the only cell line which did not express Bax. Similarly, both isoforms of the 'BH3'-only protein Bim (Bim EL and Bim L/S) were detected in Su-DHL4, CRL and Su-DHL10 cells but not in Su-DHL8 cells (Figure 3.1 B).

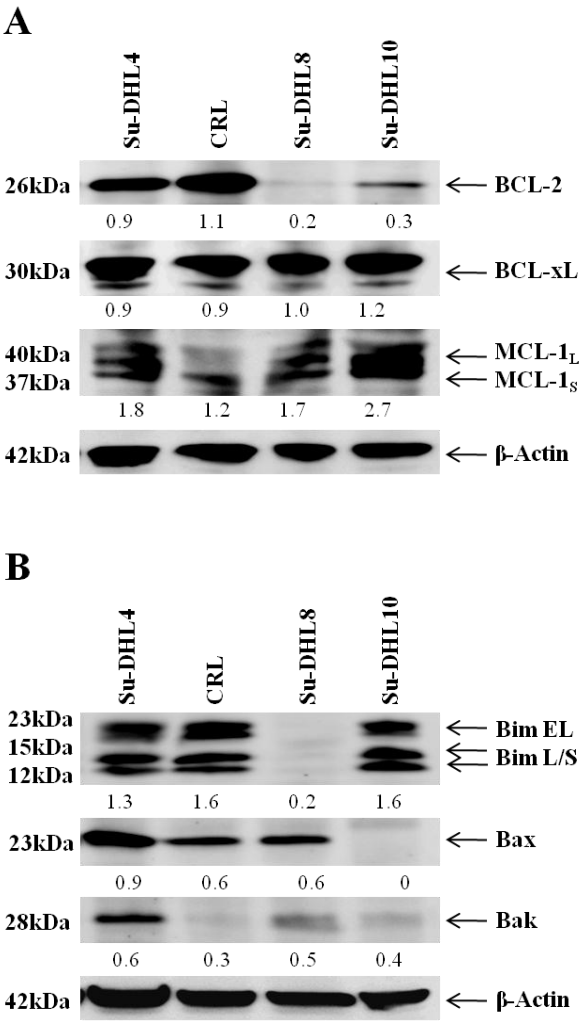

Figure 3.1 Expression of BCL-2 family proteins in DLBCL cell lines

50µg whole cell lysate was loaded onto a 4-12% Bis-Tris gel and proteins separated by SDS-PAGE. Key anti-apoptotic proteins BCL-2, BCL-xL and MCL-1 (A), and pro-apoptotic proteins Bim, Bax and Bak (B) were visualised by Western blotting; β-actin was used as a loading control. Bands are representative of a single experiment. Densitometry values were obtained using Gelscan software and represent the ratio of specific proteins to β-actin.

3.2.2 DLBCL cell lines exhibit differential sensitivity to ABT-737-induced cell death

Cellular levels of the apoptosis regulating BCL-2 family of proteins can modulate and affect cellular response to therapeutic agents. For example an increase or decrease in anti- or pro-apoptotic proteins respectively may confer resistance to malignant cells resulting in decreased therapy efficacy. To evaluate how differential expression of BCL-2 proteins among these cell lines affects their response to ABT-737 (Appendix I, 12.1), we next compared the cellular response induced by this BH3-mimetic using flow cytometry.

Levels of ABT-737-induced cell death were measured by assessing its effect on $\Delta\Psi m$ using TMRM. A decrease in TMRM levels corresponds to decreased $\Delta\Psi m$, indicating damage to the mitochondrial membrane (Hao et al., 2004; Marchetti et al., 1996). We also evaluated the effect of ABT-737 on cell viability using the DNA-intercalating dye DAPI which is taken up by dead/dying cells with permeable membranes but excluded from live cells. Therefore, an increase in the percentage of $\Delta\Psi m^{LOW}$ cells and in the percentage of $DAPI^{+}$ cells indicates increased mitochondria-dependent cell death.

Treatment of Su-DHL4 and CRL cells with 1µM ABT-737 resulted in a significant increase ($p< 0.001$) in the percentage of cells with low $\Delta\Psi m$ ($\Delta\Psi m^{LOW}$ cells) compared to untreated controls in both cell lines (*Su-DHL4:* 38.75% ± 5.1 *vs.* 11.5% ± 4; *CRL:* 58.5% ± 10.79 *vs.* 20.5% ± 5.2). Conversely, ABT-737 had no effect on the $\Delta\Psi m$ of Su-DHL8 or Su-DHL10 cells (Figure 3.2 A; Figure 3.3 B). This suggests that ABT-737 induces mitochondrial membrane depolarisation in BCL-2^{HIGH} but not BCL-2^{LOW} cells. ABT-737 also induced a significant increase in cell death in Su-DHL4 (19.25% ± 2.7 *vs.*9.25% ± 1.9) and CRL (41.25% ± 2.2.5 *vs.*16.5 ± 2.98) cells ($p< 0.05$). Viability remained unaltered between untreated and treated BCL-2^{LOW} cells (Figure 3.2 B; Figure 3.3 C). These results indicate that BCL-2^{HIGH} Su-DHL4 and CRL cell lines are more sensitive to ABT-737-induced cell death compared to BCL-2^{LOW} Su-DHL8 and Su-DHL10 cells.

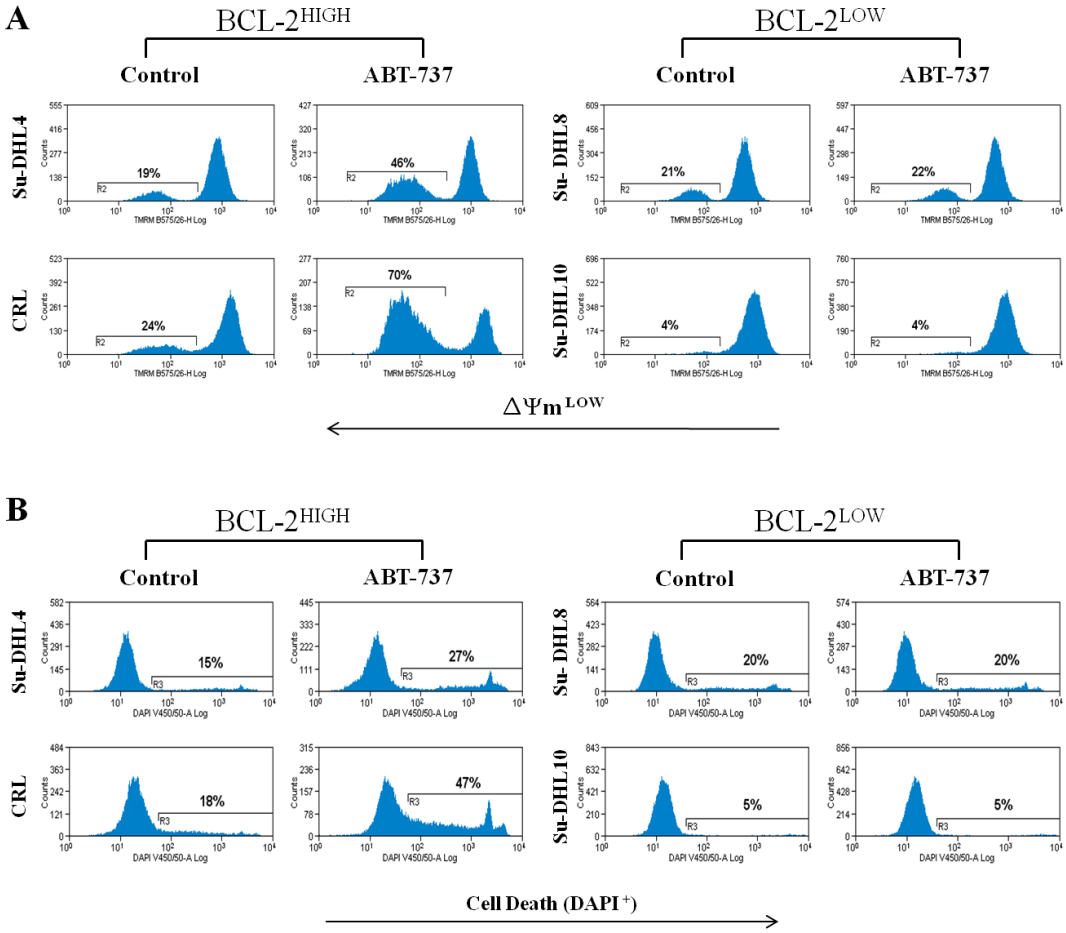

Figure 3.2 Comparison of the sensitivity of BCL-2^{HIGH} and BCL-2^{LOW} DLBCL cell lines to ABT-737

2×10^6 viable Su-DHL4, CRL, Su-DHL8 and Su-DHL10 cells were cultured with or without 1µM ABT-737 for 15hrs. Cells were incubated with 40nM TMRM and 50ng/ml DAPI for 15min at 37°C to assess the percentage of $\Delta\Psi m^{LOW}$ cells and percentage of cell death, respectively. The fluorescent density of TMRM ($\Delta\Psi m$) (A) and DAPI (cell death) (B) were evaluated by flow cytometry under the PE and Violet channels. Data was analysed using Summit software V4.3 and is displayed as the mean ± SD of three separate experiments. Histograms are representative of three separate experiments.

3.2.3 Association between expression of BCL-2 family of proteins and sensitivity to ABT-737-induced cell death

A well established hallmark of malignant cells is their ability to evade apoptosis. It has previously been shown that by evaluating the BCL-2 family profile of a malignant cell line it can be classified as exerting a particular type of apoptotic block which can then be specifically targeted and inhibited (Deng et al., 2007). According to this classification there are three types of apoptosis blocks - Class A, B and C. A class A block involves inhibition of upstream 'BH3'-only proteins such as Bim and Bad while a class B block occurs due to inhibition or loss of the pro-apoptotic multi-domain proteins Bax and Bak. Finally, a class C block occurs when there is increased expression of anti-apoptotic proteins like BCL-2 and BCL-xL, resulting in inhibition of pro-apoptotic proteins and apoptosis (Deng et al., 2007).

Combining Western blotting and flow cytometry data from Figure 3.1 and Figure 3.2, we demonstrated that the BCL-2^{HIGH} Su-DHL4 and CRL cell lines, which also express BCL-xL at a high level, exhibit a class C apoptotic block. Conversely, Su-DHL8 cells which do not express Bim are likely to evade death via a class A block, while Su-DHL10 cells lack Bax and so most likely exert a class B block (Figure 3.3 A).

While increased expression of pro-survival proteins allows tumour cells to avoid apoptosis, it has been suggested that their overexpression causes cells to be 'primed for death', meaning tumour cells are more sensitive to BH3-mimetic drugs such as ABT-737 which target these BH3-proteins. Indeed, we found that Su-DHL4 and CRL cells which express BCL-2 at high levels were more susceptible to ABT-737-mediated killing compared to BCL-2^{LOW} Su-DHL8 and Su-DHL10 cells (Figure 3.3 B and C). These data suggest that despite all cell lines evaluated expressing BCL-xL, another target of ABT-737, the sensitivity of these cells to ABT-737 is largely dependent on increased expression of BCL-2 (Figure 3.3). It is possible that Su-DHL8 and Su-DHL10 cells are resistant to ABT-737 partly due to lack of Bim and Bax respectively (Figure 3.3).

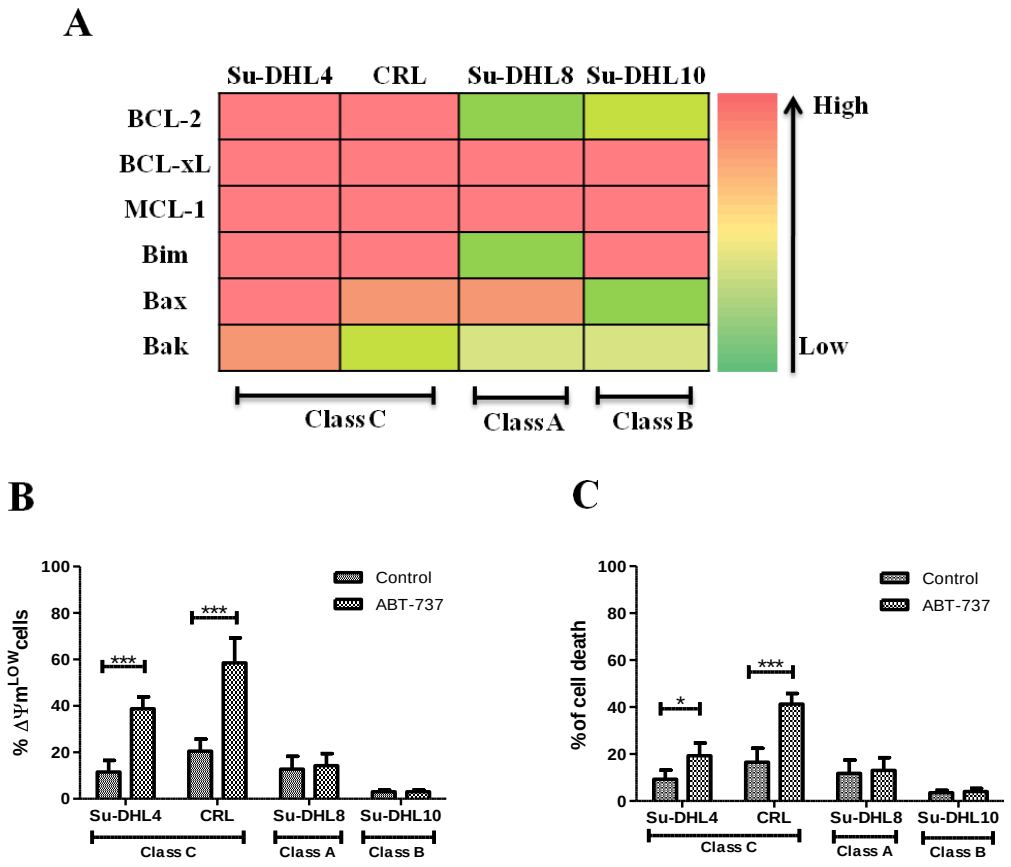

Figure 3.3 Association between expression of BCL-2 family proteins and the sensitivity of DLBCL cells to ABT-737-mediated ΔΨm reduction and cell death

Densitometry values obtained from Western blotting (Figure 3.1) were used to generate a heat-map which allows direct comparison of expression levels of BCL-2 family proteins. Protein expression levels were placed into one of five categories (0, 0.2, 0.4, 0.6, 0.8) based on their densitometry value and assigned a colour from green (0) to red (≥1) (A). Flow cytometry data previously generated (Figure 3.2) was analysed using a paired student's t-test to identify significant changes in the percentage of $\Delta\Psi m^{LOW}$ cells (B) and the percentage cell death (C) between controls and cells treated with 1μM ABT-737. Flow cytometry data are displayed as the mean ± SD of three separate experiments. Data were analysed using the statistical analysis software Prism. * $p< 0.05$, *** $p< 0.001$.

3.2.4 Evaluation of DLBCL cell lines sensitivity to ABT-737-induced Bax activation

Translocation of Bax to the mitochondria followed by a change in its conformation results in activation of this pro-apoptotic protein, and is an essential step in mitochondria-dependent apoptosis (Kelly and Strasser, 2011; Ola et al., 2011). We next aimed to evaluate whether DLBCL cell lines differ in their sensitivity to ABT-737-induced Bax activation. Bax activity was assessed by monitoring its translocation to the mitochondria and changes in its conformation following treatment with ABT-737 (Figure 3.4). Using IFM, active Bax was probed for using the anti-Bax, clone 6A7 antibody which only recognises the conformationally changed, active form of Bax (Krajewski et al., 1994).

Prior to treatment with ABT-737, Bax was present in the cytoplasm of both BCL-2^{HIGH} and BCL-2^{LOW} cells in a diffuse, smeared pattern (Figure 3.4 A and B; top panels). Following treatment with ABT-737, large, bright Bax puncta representative of its conformationally changed, active form which is situated at the mitochondria, were observed in BCL-2^{HIGH} Su-DHL4 and CRL cells (Figure 3.4 A; lower panel) but were absent from BCL-2^{LOW} cells (Figure 3.4 B; lower panel). Increased numbers of cells with condensed, fragmented nuclei, indicative of cells dying by apoptosis and consistent with Bax activation, were observed in BCL-2^{HIGH} cells following ABT-737 treatment where as Su-DHL8 and Su-DHL10 nuclei remained unaltered (Figure 3.4).

Combined, these results indicate that BCL-2^{HIGH} but not BCL-2^{LOW} cells are sensitive to ABT-737-inducued Bax activation, further confirming our previous findings that the sensitivity of DLBCL cells to ABT-737-induced cell death is dependent on BCL-2 expression.

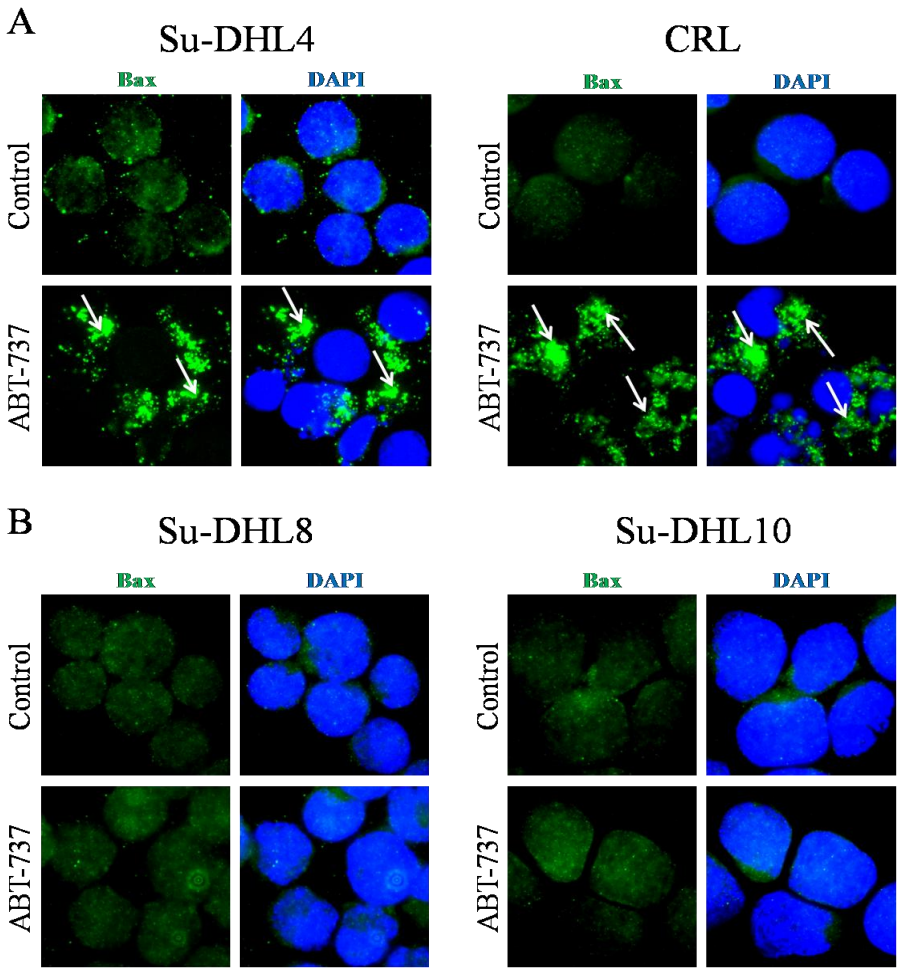

Figure 3.4 ABT-737-induced Bax activation in BCL-2^{HIGH} and BCL-2^{LOW} DLBCL cells
BCL-2^{HIGH} (A) and BCL-2^{LOW} (B) DLBCL cells were cultured with or without 1µM ABT-737 for 3hrs, harvested and fixed and permeabilised with Cytofix/Cytoperm solution. Non-specific bindings were blocked by incubation with blocking buffer containing 5% donkey serum and 0.1% saponin. Cells were stained with mouse anti-Bax antibody clone 6A7 and Alexa Fluor® 488 donkey anti-mouse secondary antibody (green). Nuclei were counterstained with DAPI (blue). Arrows highlight Bax punctate which are indicative of the active form of Bax at the mitochondria; smeared pattern represents background antibody staining.

3.2.5 Sensitivity of DLBCL cell lines to ABT-737-induced PARP cleavage

Poly(ADP-ribose) polymerase (PARP) is a 116kDa protein involved in sensing and repairing DNA-breaks and consequently maintenance of cell survival (Strosznajder et al., 2005). It is well established that during apoptosis PARP is cleaved into smaller 89kDa and 24kDa fragments by activated caspase-3, rendering the PARP enzyme inactive and unable to repair breaks in cellular DNA. Without PARP to repair DNA breaks, cells cannot survive and so undergo apoptosis (Ame et al., 2004; Boulares et al., 1999; Strosznajder et al., 2005). We next aimed to evaluate the sensitivity of BCL-2^{HIGH} and BCL-2^{LOW} DLBCL cell lines to ABT-737-induced PARP cleavage, a down-stream event in mitochondria-dependent cell death.

Following treatment with ABT-737, PARP cleavage was detected in Su-DHL4 and CRL cells but not Su-DHL8 or Su-DHL10 cells indicating BCL-2^{LOW} cells are resistant to ABT-737-induced PARP cleavage (Figure 3.5). The presence of an established apoptosis marker in BCL-2^{HIGH} cells post-ABT-737 treatment further highlights the sensitivity of these cells to ABT-737-induced apoptosis.

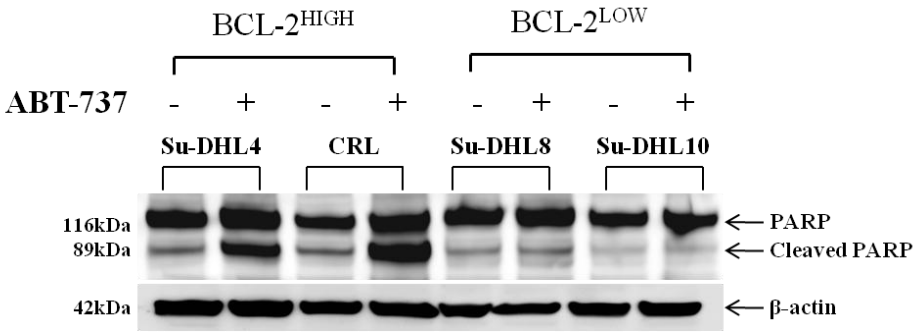

Figure 3.5 ABT-737-induced PARP cleavage in BCL-2^{HIGH} and BCL-2^{LOW} DLBCL cells
4×10^6 viable Su-DHL4, CRL, Su-DHL8 and Su-DHL10 cells were cultured with or without 1μM ABT-737 for 15hrs. 50μg whole cell lysate was loaded onto a 4-12% NuPAGE Bis-Tris gel and proteins separated by SDS-PAGE. Full-length (116kDa) and cleaved PARP (89kDa) were visualised by Western blotting. β-actin was used as a loading control. Bands are representative of a single experiment.

3.2.6 ABT-737 induces autophagy in BCL-2^{HIGH} DLBCL cell lines

Having shown that ABT-737 induces apoptosis in a BCL-2-dependent manner, we next sought to evaluate if this BH3-mimetic can induce autophagy in Su-DHL4 and CRL cell lines.

p62 is an adaptor protein that binds damaged and aggregated cellular proteins which it delivers to the autophagosome for degradation via interactions with LC3 (Ichimura et al., 2008). As a component of these cellular aggregates p62 is itself an autophagy substrate - its cellular levels decrease when autophagy is active while inactive autophagy results in accumulation of this multi-domain protein (Bjorkoy et al., 2005; Johansen and Lamark, 2011). LC3-I is a diffuse cytoplasmic protein which upon activation of autophagy is conjugated to the lipid PE and converted to a punctate form known as LC3-II, which becomes embedded in the autophagosome membrane. The presence of LC3-II puncta within a cell is the most commonly used marker of autophagy of activity; however LC3-II is also a substrate of the autophagy pathway meaning its levels can decrease due to degradation when autophagy is active (He and Klionsky, 2009; Kabeya et al., 2000). Therefore, changes in cellular levels of the key autophagy proteins p62 and LC3 were used as markers of autophagy activity in Su-DHL4 and CRL cells.

Cells were treated with increasing concentrations of ABT-737 (0µM - 1µM) in the presence or absence of the autophagy inhibitor CQ (Appendix I, 12.2) which prevents autophagic degradation, resulting in an accumulation of autophagy substrates (Amaravadi et al., 2007). Treatment of Su-DHL4 cells with ABT-737 (0.3µM - 1µM) and CRL cells with 1µM ABT-737 resulted in a decrease in p62 compared to untreated controls indicating autophagic degradation is increased following treatment with ABT-737 (Figure 3.6 A). Following the addition of CQ, p62 levels increased in these BCL-2^{HIGH} cells in an ABT-737 dose-dependent manner, further suggesting this BH3-mimetic induces autophagy within these cells (Figure 3.6 A). Consistent levels of p62 were observed in Su-DHL8 and Su-DHL10 cells following treatment with ABT-737, suggesting this BH3-mimetic does not induce autophagy in these cells (Figure 3.6 B). Treatment of these BCL-2^{LOW} cells with ABT-737 and CQ resulted in an increase in

p62 levels, indicating basal level autophagic degradation of p62 was inhibited by CQ (Figure 3.6 B).

Treatment of BCL-2^{HIGH} cells with ABT-737 resulted in a decrease in LC3-I and LC3-II levels in these cells (Figure 3.6 A). While a decrease in LC3-I may indicate increased conversion of LC3-I to LC3-II and thus increased autophagy activity, lack of a corresponding increase in LC3-II is contrary to previous reports that LC3-II levels increase during active autophagy. One possible explanation for this apparent discrepancy is the time frame in which autophagy was evaluated. Autophagy activity was examined after a 15hr incubation period during which time LC3-II may have been degraded as an autophagy substrate; LC3-I may have been converted to LC3-II which was then degraded as part of the autophagolysosome resulting in a decrease in cellular levels of both LC3-I and LC3-II in Su-DHL4 and CRL (Figure 3.6 A). Treatment with ABT-737 and CQ resulted in an increase in LC3-II levels in an ABT-737 dose-dependent manner similar to the trend observed for p62. LC3-I and LC3-II levels did not vary between untreated and ABT-737-treated Su-DHL8 and Su-DHL10 cells (Figure 3.6 B), further indicating ABT-737 does not induce autophagy in these BCL-2^{LOW} cells. LC3-II levels increased following addition of CQ; however in a similar manner to p62, no difference in LC3-II levels was observed between ABT-737 doses, indicating that this increase was due to inactive basal level autophagic degradation (Figure 3.6 B).

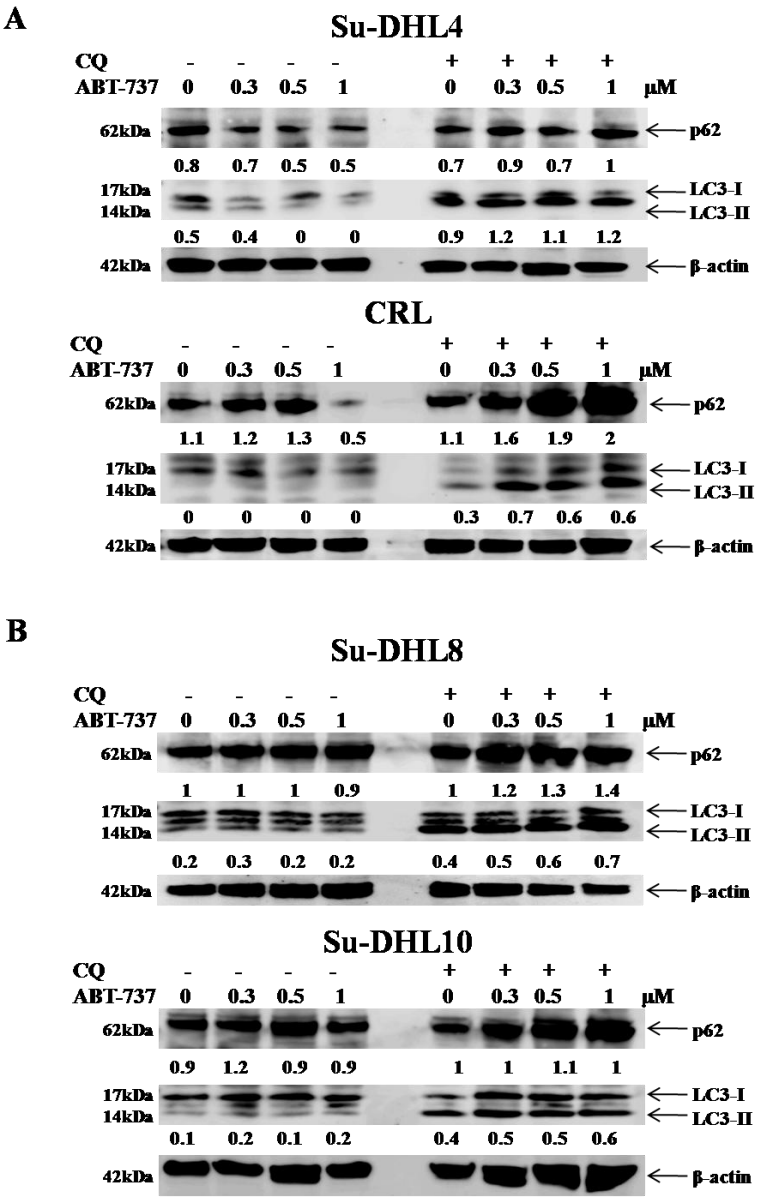

Figure 3.6 Evaluation of ABT-737-induced autophagy in BCL-2^{HIGH} and BCL-2^{LOW} DLBCL cell lines

4×10^6 cells viable BCL-2^{HIGH} (A) and BCL-2^{LOW} (B) cells were treated with increasing concentrations of ABT-737 for 15hrs in the presence or absence of CQ (50µM); untreated cells were cultured under standard growth conditions. 50µg of whole cell lysate was loaded onto a 4-12% Bis-Tris gel and proteins separated by SDS-PAGE. p62 and LC3 were visualised by Western blotting. β-actin was used as a loading control. Bands are representative of a single experiment. Densitometry values were obtained using Gelscan V5.1 and represent the ratio of p62 or LC3-II to β-actin.

Although p62 and LC3 protein levels are well established markers of autophagy activity, neither of them should be used in isolation to determine or represent autophagy activity (Klionsky et al., 2012b). Combining a decrease in p62 and LC3 (I/II) levels in response to ABT-737 with an ABT-737-dose dependent accumulation of p62 and LC3-II following autophagy inhibition suggests ABT-737 induces autophagy in BCL-2^{HIGH} DLBCL cell lines. We therefore propose that BCL-2 is a specific target for ABT-737 and treatment with this BH3-mimetic induces both apoptosis and autophagy in BCL-2^{HIGH} cells.

3.2.7 BCL-2 and Beclin-1 co-localize, but do not bind in BCL-2^{HIGH} cells

It has previously been reported that binding of BCL-2 to the autophagy essential protein Beclin-1 sequesters this pro-autophagy protein and prevents autophagy induction (Liang et al., 1998; Pattingre et al., 2005). Therefore, one possible mechanism by which ABT-737 may induce autophagy is by competitively binding BCL-2 via BH3-domain interactions, hindering its sequestration of Beclin-1. It is currently unclear whether BCL-2 binds Beclin-1 to form an autophagy inhibiting complex in lymphoma cells and if so whether ABT-737 disrupts this binding. We therefore aimed to assess BCL-2/Beclin-1 binding in the BCL-2^{HIGH} cell line Su-DHL4 and evaluate the effect of ABT-737 treatment on this interaction.

In order for BCL-2 to bind Beclin-1, both proteins must be situated at the same cellular compartment. It has been shown that BCL-2 localizes to the outer mitochondrial membrane and ER and Beclin-1 resides at the ER, TGN and mitochondria (Pattingre et al., 2005). Using dual immunofluorescent staining and microscopy, we determined whether BCL-2 and Beclin-1 co-localize at the ER and/or mitochondria in Su-DHL4 cells. The ER was identified using the 72kDa protein marker BiP (Gething, 1999), while mitochondria were identified by the well established mitochondrial marker, cytochrome *c* oxidase subunit IV (Cox IV) (Xue et al., 2001).

Dual immunofluorescent staining of Su-DHL4 cells with BCL-2 and BiP antibodies revealed a number of yellow puncta within cells, representative of co-localization between these proteins, indicating BCL-2 localizes to the ER (Figure 3.7 A). Co-staining of cells with BCL-2 and Cox IV antibodies revealed a similar yellow-punctate

pattern showing BCL-2 also resides at the mitochondria in Su-DHL4 cells (Figure 3.7 B).

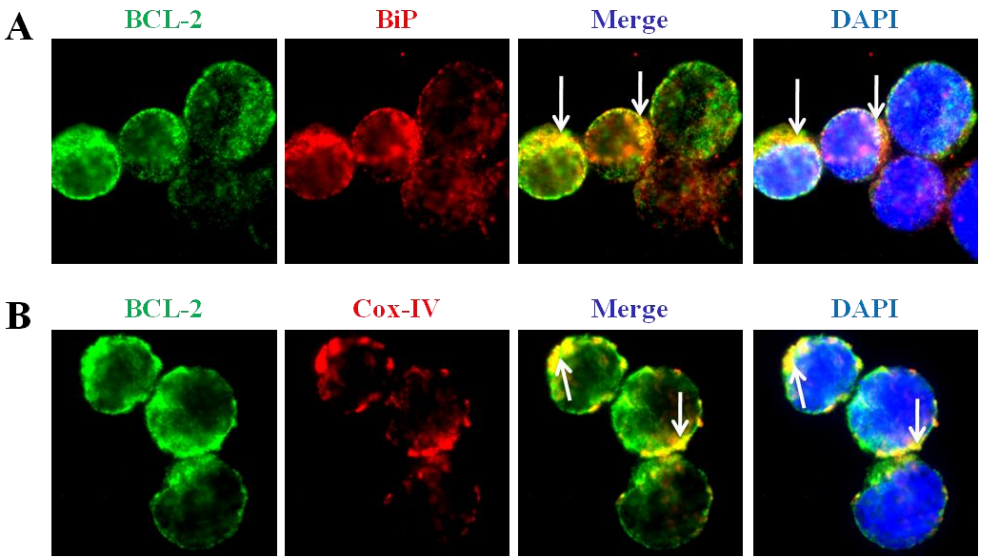

Figure 3.7 Determination of the cellular location of BCL-2 in Su-DHL4 cells
Su-DHL4 cells were fixed and permeabilised with Cytofix/Cytoperm and non-specific bindings blocked by incubation with 5% donkey serum and 0.1% saponin. Cells were co-stained for BCL-2 and BiP (A) or Cox IV (B). BCL-2 and BiP/Cox IV were probed for using Alexa Fluor® 488 donkey anti-mouse and Alexa Fluor® 546 donkey anti-rabbit secondary antibodies respectively. Nuclei were counterstained with DAPI and slides mounted and viewed using an Olympus BX40 fluorescent microscope. Arrows highlight yellow punctate, indicative of areas of co-localization between BCL-2 and BiP or Cox IV.

Co-staining of Su-DHL4 cells with Beclin-1 and either BiP or Cox IV revealed a similar localization pattern to that of BCL-2 (Figure 3.8 A and B), indicating the pro-autophagy protein localizes to both the ER and the mitochondria in these BCL-2^{HIGH} DLBCL cells.

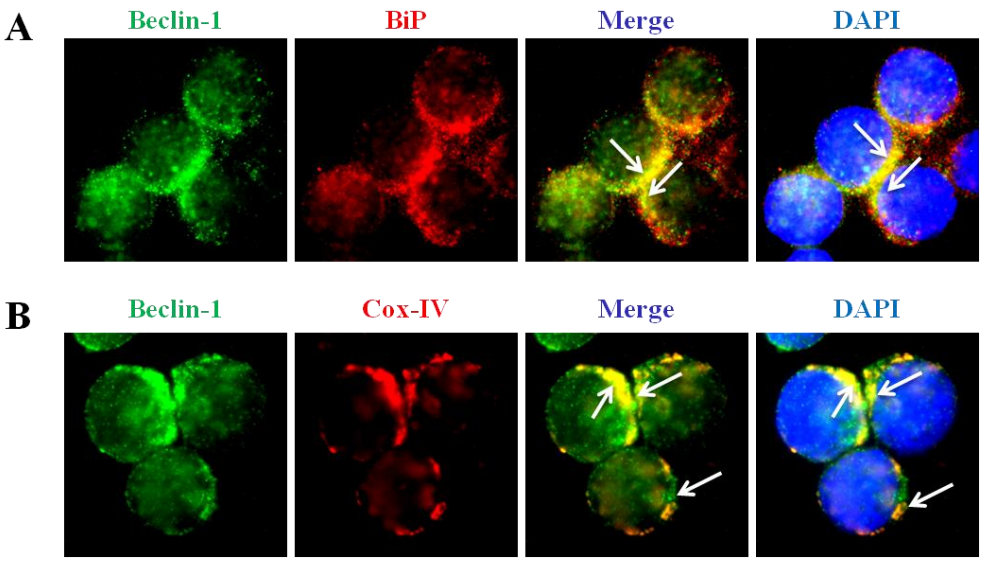

Figure 3.8 Determination of the cellular location of Beclin-1 in Su-DHL4 cells
Su-DHL4 cells were fixed and permeabilised with Cytofix/Cytoperm and non-specific bindings blocked by incubation with 5% donkey serum and 0.1% saponin. Cells were co-stained for Beclin-1 and BiP (A) or Cox IV (B) as previously described. Beclin-1 and BiP/Cox IV were probed for using Alexa Fluor® 488 donkey anti-mouse and Alexa Fluor® 546 donkey anti-rabbit secondary antibodies respectively. Nuclei were counterstained with DAPI and slides mounted and viewed as previously described. Arrows highlight yellow punctate, indicative of areas of co-localisation between Beclin-1 and BiP or Cox IV.

These results demonstrate that BCL-2 and Beclin-1 reside in the same cellular compartments in Su-DHL4 cells, indicating the potential for interaction between the two and the formation of an autophagy inhibiting complex at both organelles. Dual immunofluorescent staining of Su-DHL4 cells for BCL-2 and Beclin-1 revealed a number of yellow punctate in these cells, indicative of co-localisation between Bcl-2 and Beclin-1 at the basal level (Figure 3.9).

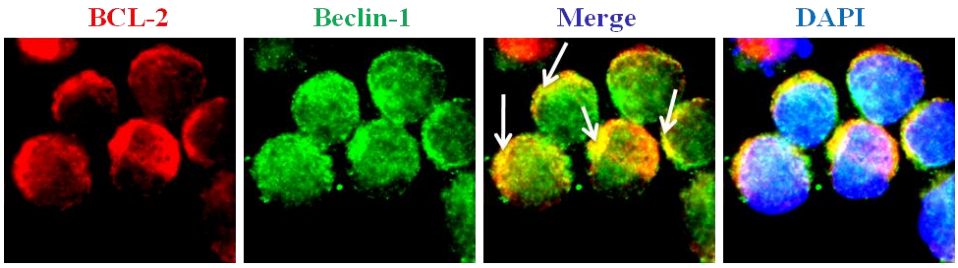

Figure 3.9 Evaluation of BCL-2 and Beclin-1 co-localisation in Su-DHL4 cells
Su-DHL4 cells were fixed and permeabilised with Cytofix/Cytoperm and non-specific bindings blocked by incubation with 5% donkey serum and 0.1% saponin. Cells were co-stained for BCL-2 and Beclin-1 as previously described. BCL-2 and Beclin-1 were probed for using Alexa Fluor® 546 donkey anti-rabbit and Alexa Fluor® 488 donkey anti-mouse secondary antibodies respectively. Nuclei were counterstained with DAPI and slides mounted and viewed as previously described. Arrows highlight yellow punctate, indicative of areas of co-localisation between BCL-2 and Beclin-1.

Co-localization between two proteins as determined by IFM does not definitively prove protein-protein interaction. Therefore, we next evaluated whether BCL-2 and Beclin-1 bind in BCL-2^{HIGH} DLBCL cells, and whether ABT-737 can disrupt this binding, using co-IP. No binding was observed between endogenous BCL-2 and endogenous Beclin-1 in Su-DHL4 DLBCL cells at the basal level, or following treatment with ABT-737 (Figure 3.10). We therefore propose that despite residing in the same cellular organelles, BCL-2 and Beclin-1 do not directly bind one another in BCL-2^{HIGH} DLBCL cells to form an autophagy inhibiting complex. Therefore, ABT-737 may not induce autophagy in these cells by disrupting binding between these proteins. Instead, induction of apoptosis by ABT-737-mediated BCL-2 inhibition may promote autophagy as a pro-survival mechanism which cells utilise to avoid death.

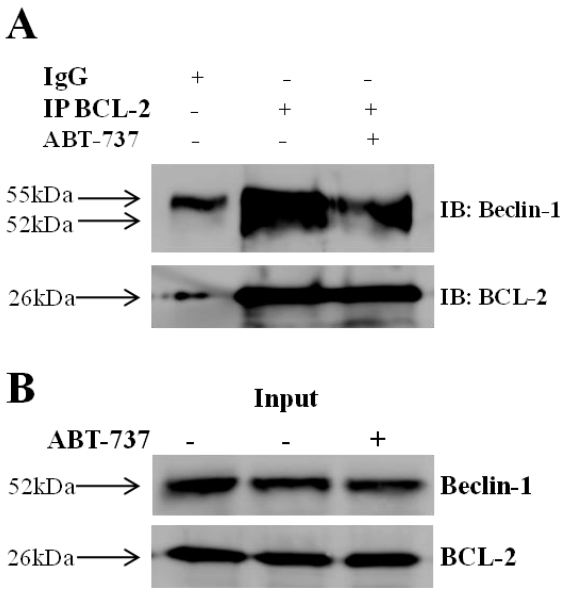

Figure 3.10 Determination of BCL-2 and Beclin-1 interaction by co-immunoprecipitation
30×10^6 viable Su-DHL4 cells were incubated with 1µM ABT-737 for 3hr; untreated cells were incubated under standard growth conditions. Proteins were extracted using 2% CHAPS buffer containing 10µl 1M DTT, PMSF and PIC. Dynabeads® Protein A was prepared at a 1:10 dilution in 2% CHAPS buffer containing DTT, PMSF and PIC. 200µl Dynabeads® Protein A were incubated with 2µg anti-rabbit IgG or anti-rabbit Bcl-2 antibody for 20 min at RT with rotation and washed 1 × 1% CHAPS buffer. 1mg cell lysate was prepared in a final volume of 200µl using 2% CHAPS buffer containing DTT and PMSF and incubated with the antibody/bead complex at RT with rotation for 20 min after which beads were washed 3× in 1% CHAPS buffer. 25µl eluting buffer was added to each sample, samples denatured at 100°C for 5min and mixed with 25µl lysis buffer. 45µl sample was loaded onto a 1.5mm 4-12% NuPAGE Bis-Tris gel and proteins separated by SDS-PAGE. Whole cell lysate samples were prepared to a 100µg concentration in 40µl. Beclin-1 and BCL-2 were visualised by Western blotting as previously described. Data are representative of a single experiment.

3.3 Discussion

In this chapter, we found that treatment with ABT-737 simultaneously induced autophagy while triggering apoptosis in BCL-2^{HIGH} lymphoma cell lines. Assessment of BCL-2/Beclin-1 interaction revealed these proteins do not bind to form an autophagy inhibiting complex in BCL-2^{HIGH} cells, indicating ABT-737 induces autophagy by another mechanism.

We found that BCL-2^{HIGH} Su-DHL4 and CRL cells are more sensitive to ABT-737-induced apoptosis compared to Su-DHL8 and Su-DHL10 cells, which express low levels of this anti-apoptotic protein. Our findings are in agreement with previous reports which state that cells expressing high levels of BCL-2 are sensitive to ABT-737-induced death (Deng et al., 2007). We also found that ABT-737 induces autophagy in BCL-2^{HIGH} Su-DHL4 and CRL cells, i.e. in a BCL-2-dependent manner.

Induction of autophagy by ABT-737 via disruption of BCL-2/Beclin-1 binding has been reported in different cell types (Kang et al., 2011; Marquez and Xu, 2012; Pattingre et al., 2005). However in our setting, we found that endogenous BCL-2 and Beclin-1 do not bind at the basal level to form an autophagy inhibiting complex, indicating ABT-737 may not induce autophagy via disruption of BCL-2/Beclin-1 binding. Treatment of DLBCL cell lines with various anti-cancer agents has been shown to induce autophagy (Jia et al., 2012). We therefore propose that induction of apoptosis by ABT-737 via BCL-2 inhibition results in an increased autophagy activity. Chemotherapy-induced autophagy can act as a cytoprotective mechanism which allows malignant cells to evade therapy-induced cell death (Kimmelman, 2011). Whether BCL-2^{HIGH} DLBCL cell lines utilise acquired autophagy as a pro-survival mechanism which confers resistance to ABT-737-induced apoptosis remains to be determined.

3.3.1 Conclusions

Treatment with ABT-737 induces mitochondria-dependent apoptosis in DLBCL cell lines in a BCL-2-dependent manner. This BH3-mimetic also induces autophagy in BCL-2^{HIGH} cells, but not via disruption of BCL-2/Beclin-1 binding.

Chapter IV

Evaluation of the role of autophagy in ABT-737-induced cell death

4.1 Introduction

Therapy-induced autophagy can promote, prevent or have no effect on the killing of malignant cells by anti-cancer drugs. While therapy-induced autophagy has been shown to potentiate the pro-death effects of chemotherapeutic-agents *in vitro* and *in vivo*, it is more commonly reported to act as a cytoprotective, pro-survival mechanism utilised by cancer cells to evade therapy-induced death (Choi et al., 2013a; Helgason et al., 2013; Kim et al., 2009). For example, treatment of CML cells with Imatinib and prostate cancer cells with tunicamycin has been reported to induce cytoprotective autophagy in malignant cells, resulting in decreased efficacy of these anti-cancer agents and decreased levels of drug-induced tumour cell death (Ding et al., 2007; Helgason et al., 2013).

It has been reported that inhibition of therapy-induced cytoprotective autophagy via ablation of key autophagy genes such as *Atg5* or using inhibitors such as CQ or HCQ, sensitizes tumour cells to chemotherapy-mediated cell death (Amaravadi et al., 2007; Bellodi et al., 2009). A number of clinical trials are currently investigating the potential use of such autophagy inhibitors in combination with standard chemotherapy agents. For example, the phase I CHOICES (CHlOrquine and IM Combination to Eliminate Stem Cells) clinical trial is currently investigating combination of HCQ with Imatinib in CML patients and is showing promising results (Helgason et al., 2013; Sinclair et al., 2013).

The BH3-mimetic compounds (-)-Gossypol and ABT-737 have been shown to induce apoptosis and cytoprotective autophagy in breast cancer and *Myc*-driven lymphoma cells (Amaravadi et al., 2007; Gao et al., 2010). We have also shown that ABT-737 can induce autophagy in BCL-2^{HIGH} DLBCL cell lines. It is unclear whether this therapy-induced, acquired autophagy functions as a pro-survival mechanism or potentiates the pro-apoptotic role of ABT-737 in BCL-2^{HIGH} lymphoma cell lines. We therefore aim to evaluate if ABT-737-induced autophagy plays a cytoprotective role in BCL-2^{HIGH} DLBCL cell lines.

4.2 Results

4.2.1 Inhibition of autophagy by chloroquine sensitises BCL-2^{HIGH} cells to ABT-737-induced cell death

To determine the effects of ABT-737-mediated autophagy on ABT-737-induced apoptosis, we examined whether inhibition of autophagy by CQ sensitizes BCL-2^{HIGH} and BCL-2^{LOW} DLBCL cells to ABT-737-induced apoptotic cell death. Cells were treated with 50μM CQ which has previously been shown to inhibit autophagic protein degradation without inducing cell death (Jia et al., 2012; Maclean et al., 2008).

Cell death was determined by flow cytometry as previously described. Treatment with ABT-737 induced a dose-dependent increase in the percentage of cell death in Su-DHL4 and CRL cells (Figure 4.1 A and B) compared to untreated controls, confirming that this BH3-mimetic induces death in BCL-2^{HIGH} cells. Blocking autophagy degradation by CQ significantly ($p< 0.05$) increased ABT-737-induced cell death in Su-DHL4 and CRL cells compared to treatment with ABT-737 alone (Figure 4.1 C and D). We also confirmed that treatment with ABT-737 or ABT-737+CQ did not have a cytotoxic effect on the BCL-2^{LOW} cell lines Su-DHL8 and Su-DHL10 (Figure 4.2).

These data suggest that ABT-737-induced autophagy acts as a cytoprotective mechanism which allows lymphoma cells to avoid drug-induced apoptosis and indicate that inhibition of this drug-induced autophagy with CQ increases sensitivity of BCL-2^{HIGH} cells to ABT-737-mediated apoptosis.

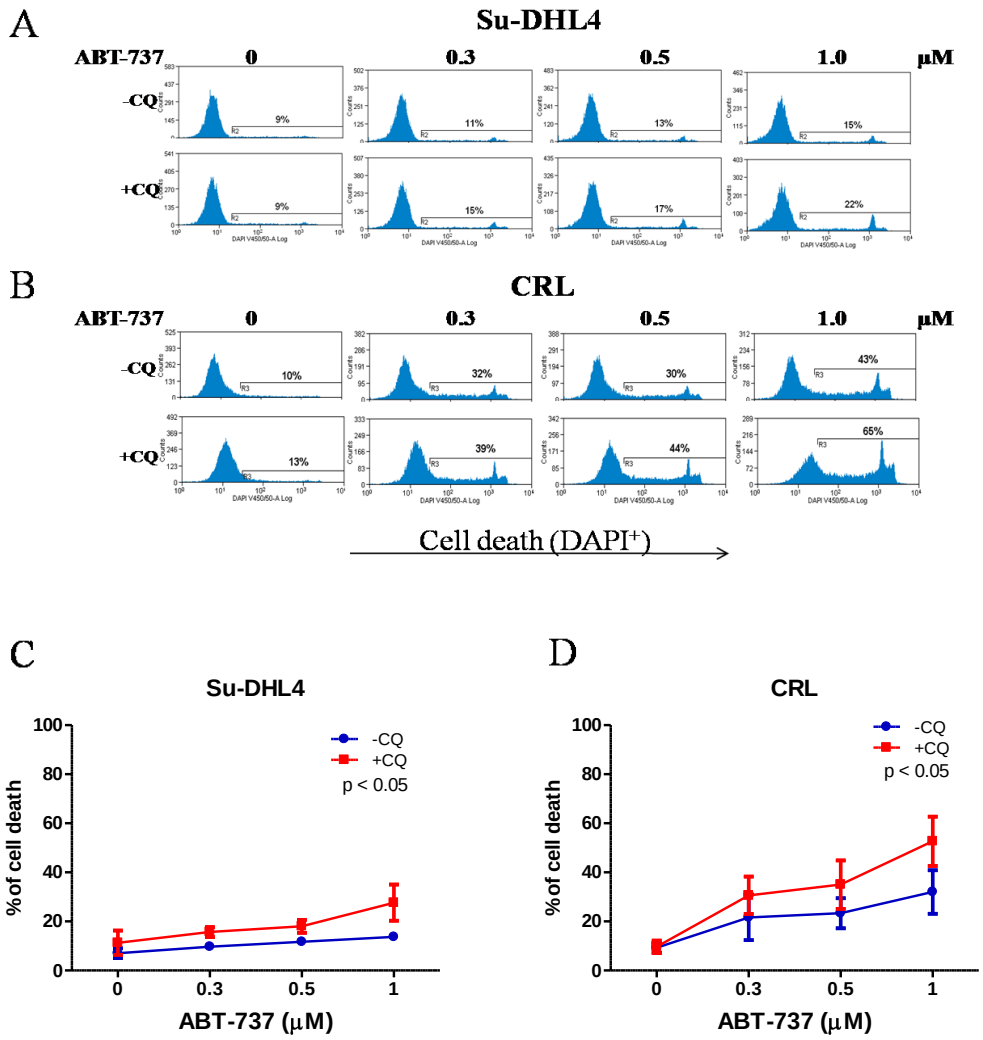

Figure 4.1 Evaluation of the effect of the autophagy inhibitor CQ on ABT-737-induced cell death in BCL-2^{HIGH} cells

2×10^6 viable Su-DHL4 and CRL cells were treated with increasing doses of ABT-737 (0µM - 1µM) for 15hr in the presence or absence of CQ (50µM); untreated cells were cultured under standard growth conditions. Cells were incubated with 100ng/ml DAPI for 15min at 37°C. The fluorescent density of DAPI was determined by flow cytometry under the Violet channel (A, B) Data were analysed using Summit software V4.3 and significant changes between treatment conditions analysed using a two-way ANOVA and the statistical software Prism (C, D). Data are displayed as the mean ± SD of three separate experiments. Histograms are representative of three separate experiments.

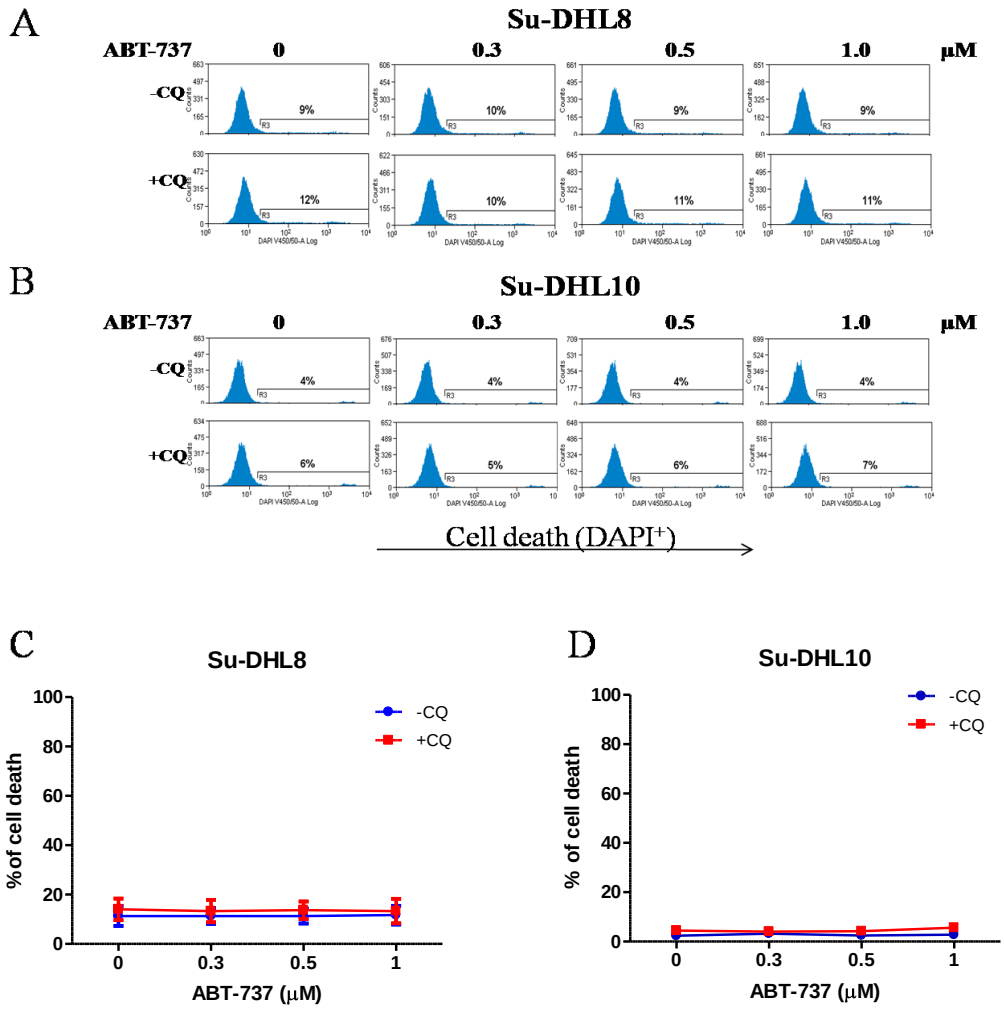

Figure 4.2 Evaluation of the effect of the autophagy inhibitor CQ on ABT-737-induced cell death in BCL-2^{HIGH} cells

2×10^6 viable Su-DHL8 (A and C) and Su-DHL10 (B and D) cells were treated with increasing doses of ABT-737 (0µM - 1µM) for 15hr in the presence or absence of CQ (50µM); untreated cells were incubated under standard growth conditions. Cell death was determined by flow cytometry as described in Figure 4.1.

We next examined the effect of CQ on ABT-737-induced reduction in ΔΨm by flow cytometry in both BCL-2^{HIGH} and BCL-2^{LOW} cell lines. Treatment of Su-DHL4 and CRL cells with ABT-737 alone resulted in a dose-dependent increase in the percentage of $\Delta\Psi m^{LOW}$ cells in both cell lines (Figure 4.3 A and B). The percentage of $\Delta\Psi m^{LOW}$ Su-DHL4 and CRL cells also significantly ($p< 0.05$) increased following dual treatment with ABT-737+CQ (Figure 4.3 C and D). As expected, and again in line with our previous findings, treatment with ABT-737 alone or in combination with CQ did not affect ΔΨm in BCL-2^{LOW} cell lines (Figure 4.4).

These results support our previous findings that inhibition of ABT-737-induced autophagy with CQ increases sensitivity of BCL-2^{HIGH} DLBCL cell lines to ABT-737-induced apoptosis.

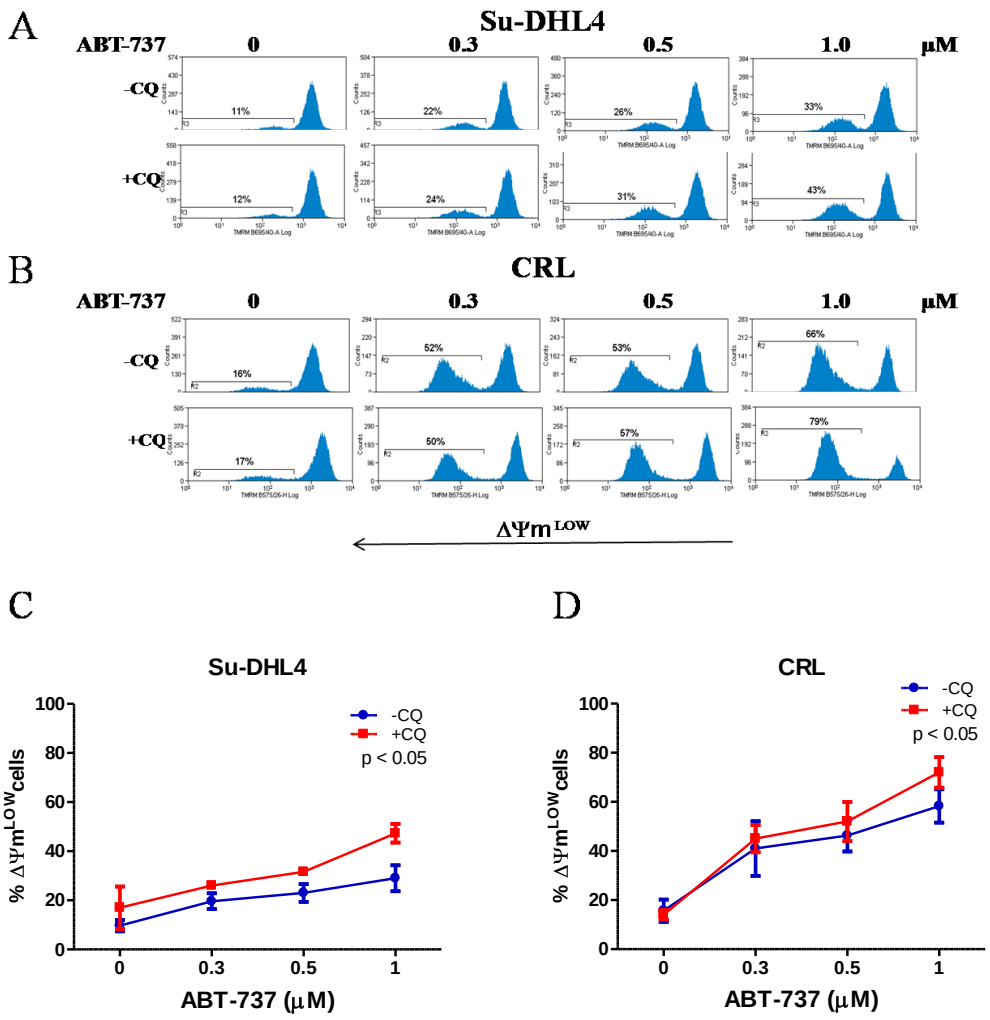

Figure 4.3 Effect of the autophagy inhibitor CQ on ABT-737-induced ΔΨm depolarization in BCL-2^{HIGH} DLBCL cells

2×10^6 viable Su-DHL4 and CRL cells were treated with increasing doses of ABT-737 (0µM - 1µM) for 15hr in the presence or absence of CQ (50µM); untreated cells were cultured under standard growth conditions. Cells were incubated with 40nM TMRM for 15min at 37°C. The fluorescent density of TMRM (ΔΨm) was determined by flow cytometry under the PE channel (A and B). Data were analysed using Summit software V4.3 and significant changes between treatment conditions analysed using a two-way ANOVA and the statistical software Prism (C and D). Data are displayed as the mean ± SD of three separate experiments. Histograms are representative of three separate experiments.

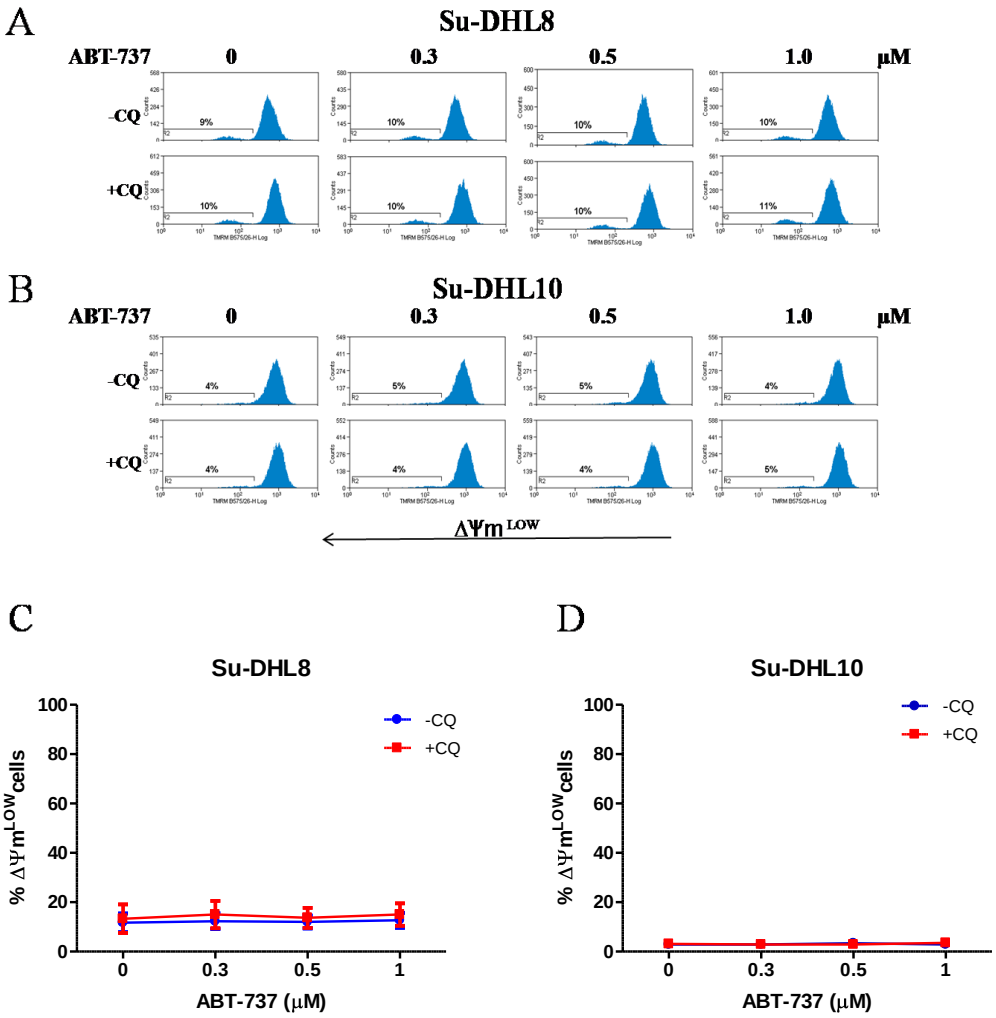

Figure 4.4 Effect of the autophagy inhibitor CQ on ABT-737-induced ΔΨm in BCL-2^{LOW} DLBCL cells

2×10^6 viable Su-DHL8 (A and C) and Su-DHL10 (B and D) cells were treated with increasing doses of ABT-737 (0μM - 1μM) for 15hr in the presence or absence of CQ (50μM); untreated cells were incubated under standard growth conditions. Experimental conditions are as same as described in the legend of Figure 4.3.

4.2.2 Inhibition of autophagy by CQ sensitises BCL-2^{HIGH} cells to ABT-737-induced PARP cleavage

We have shown that ABT-737 induces PARP cleavage in a BCL-2 dependent manner and that inhibition of autophagy with CQ further sensitises BCL-2^{HIGH} cells to ABT-737-induced cell death. We next examined the effect of ABT-737+CQ on PARP cleavage in BCL-2^{HIGH} cell lines.

DLBCL cell lines were treated with increasing doses of ABT-737 (0µM - 1µM) with or without CQ (50µM) and PARP cleavage evaluated by Western blotting. We found that treatment with ABT-737+CQ resulted in increased PARP cleavage in the BCL-2^{HIGH} cell lines Su-DHL4 and CRL compared with treatment with ABT-737 alone (Figure 4.5 A and B). PARP cleavage was not observed in BCL-2^{LOW} cell lines following ABT-737 or combination treatment (Figure 4.5 C and D).

These data support our previous findings that inhibition of ABT-737-induced autophagy further sensitises BCL-2^{HIGH} cells to ABT-737-induced apoptosis.

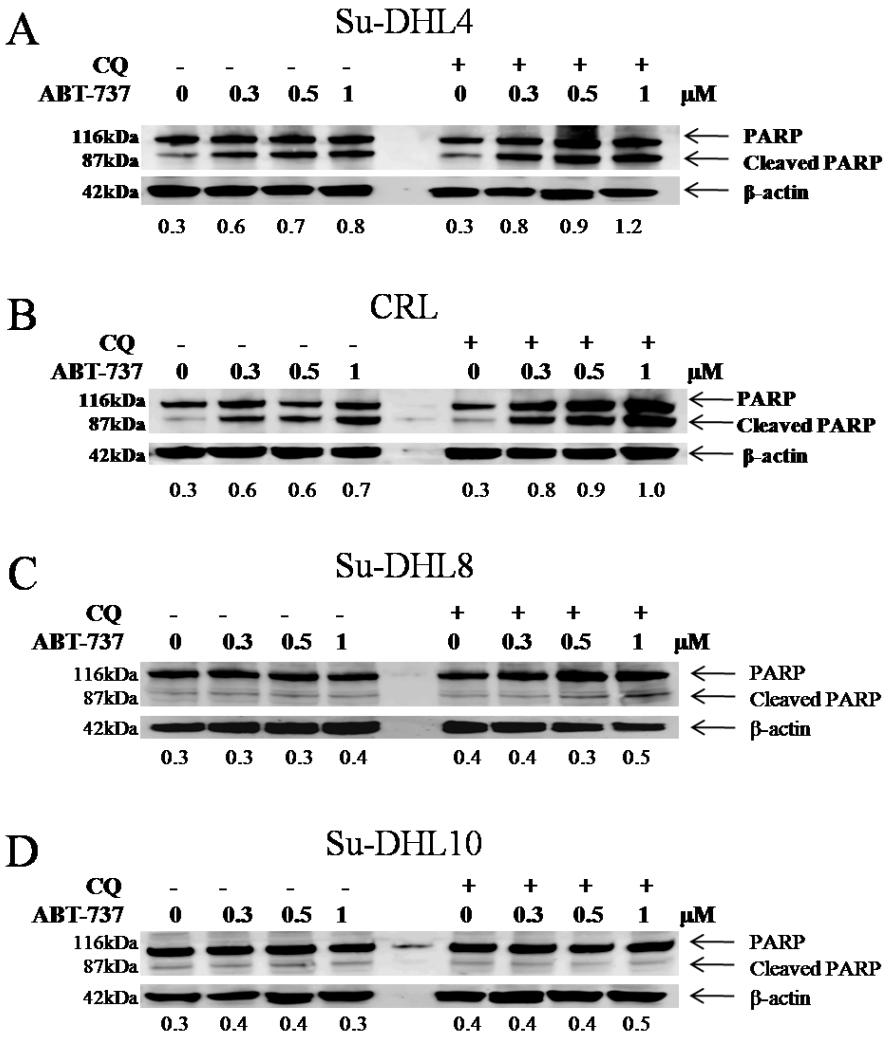

Figure 4.5 Evaluation of the effect of autophagy inhibition on ABT-737-induced PARP cleavage in BCL-2^{HIGH} and BCL-2^{LOW} DLBCL cell lines

4×10^6 viable Su-DHL4 (A), CRL (B), Su-DHL8 (C) and Su-DHL10 (D) cells were treated with increasing concentrations of ABT-737 (0µM -1µM) for 15hr in the presence or absence of CQ (50µM). 50µg whole cell lysate was loaded onto a 4-12% NuPAGE Bis-Tris gel and proteins separated by SDS-PAGE. Full length (116kDa) and cleaved (89kDa) PARP were visualised by western blotting; β-actin was used as a loading control. Bands are representative of a single experiment. Densitometry values were obtained using Gelscan software and represent the ratio of cleaved PARP to β-actin.

4.2.3 Inhibition of caspase activation blocks ABT-737 and ABT-737+CQ-induced apoptosis in BCL-2^{HIGH} DLBCL cell lines

We next aimed to evaluate if ABT-737+CQ-induced cell death is caspase-dependent by assessing caspase-3 activity in cells treated with ABT-737 ± CQ in the presence or absence of the pan-caspase inhibitor N-Benzyloxycarbonyl-Val-Ala-Asp(O-Me) fluromethyl ketone (Z-VAD.fmk).

Incubation of Su-DHL4 and CRL cells with CQ alone (25µM or 50µM) did not increase caspase-3 activity in these cells, confirming that treatment with CQ does not induce caspase activation. We also confirmed that treatment of these BCL-2^{HIGH} cells with 0.5µM ABT-737 for 3hr results in increased caspase-3 activity indicating that this BH3-mimetic induces caspase-dependent apoptosis (Figure 4.6).

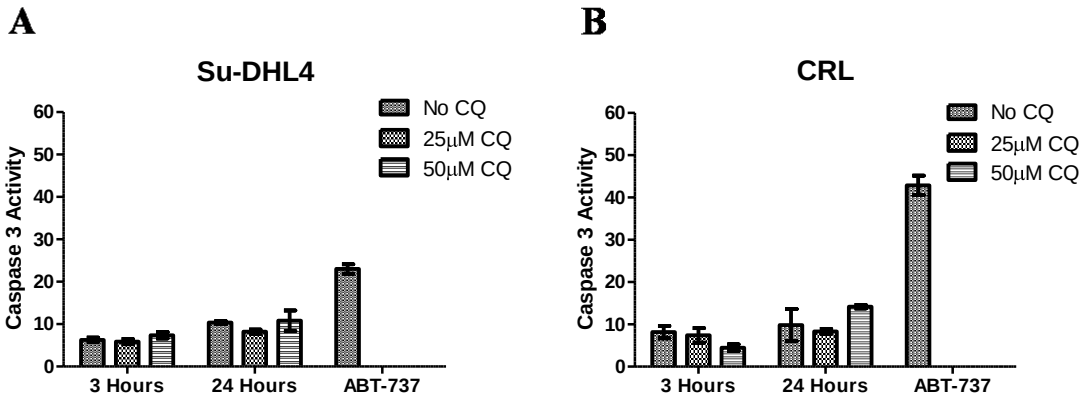

Figure 4.6 Comparison of the effect of CQ and ABT-737 on caspase-3 activation in BCL-2^{HIGH} DLBCL cell lines

2×10^6 viable Su-DHL4 (A) or CRL (B) cells were treated with 25µM or 50µM CQ for 3hr or 24hr or 0.5µM ABT-737 for 3hr at 37°C; untreated cells were cultured under standard growth conditions. 50µg protein lysate was incubated with reaction buffer and caspase-3-DEVD-AFC substrate for 15min at 37ºC followed by 1min at -20ºC. AFC release was measured at excitation 410nm and emission 510nm using a BMG LabTech FLUOstar Omega plate reader. Samples were analysed in triplicate and caspase-3 activity calculated as the average AFC release per sample (µM/hr/mg protein). Data were analysed using Prism software.

We first identified which concentration of Z-VAD.fmk (Appendix I, 12.3) completely inhibits caspase activation. TRAIL-induced caspase-3 activation and PARP cleavage were examined in Su-DHL4 cells treated with TRAIL alone or in combination with Z-VAD.fmk (20µM or 50µM) (Figure 4.7).

Treatment of Su-DHL4 cells with TRAIL induced a remarkable increase in caspase-3 activity compared with untreated controls. TRAIL-induced caspase-3 activation was dramatically decreased in the presence of 20µM or 50µM Z-VAD.fmk (Figure 4.7 A). Similarly, treatment with TRAIL resulted in an increase in PARP cleavage which was ablated following incubation with Z-VAD.fmk (Figure 4.7 B). These results indicate that incubation of cells with 20µM or 50µM Z-VAD.fmk completely inhibits TRAIL-induced caspase-3 activation and PARP cleavage.

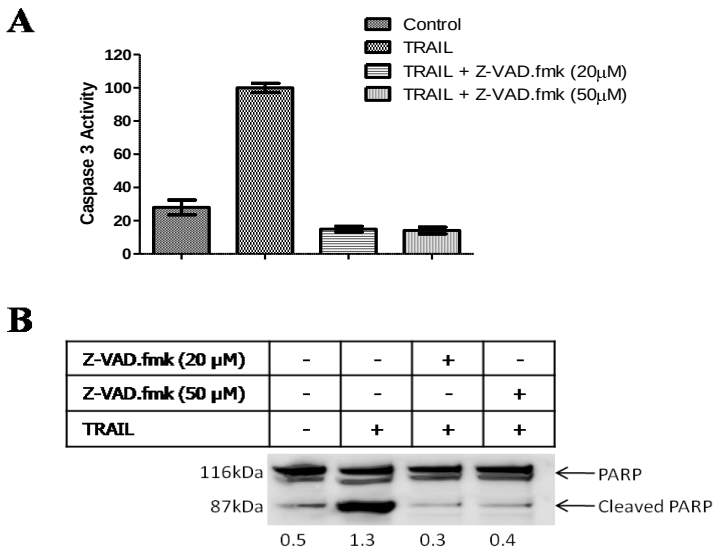

Figure 4.7 Inhibitory effect of Z-VAD.fmk on TRAIL-induced caspase-3 activation and PARP cleavage

2×10^6 viable Su-DHL4 cells were treated with 10µM TRAIL in the presence or absence of 20µM or 50µM Z-VAD.fmk for 3hr at 37°C; untreated cells were cultured under standard growth conditions. 50µg protein lysate was incubated with reaction buffer and caspase-3-DEVD-AFC substrate for 15min at 37ºC followed by 1min at -20ºC and caspase-3 activity calculated as previously described (A). 50µg whole cell lysate was loaded onto a 4-12% Bis-Tris gel and proteins separated by SDS-PAGE. Cleaved PARP was probed for and bands visualised as previously described. Densitometry values were obtained using Gelscan software and calculated as the ratio of cleaved PARP to full length PARP (B).

We next determined whether ABT-737+CQ-induced cell death is caspase-dependent. Su-DHL4 and CRL cells were treated with ABT-737 alone or in combination with CQ in the presence or absence of Z-VAD.fmk. Caspase-3 activity was determined using a fluoregenic assay.

We found that treatment with ABT-737 alone induced significantly ($p< 0.001$) increased caspase-3 activity in Su-DHL4 and CRL cells, while dual treatment with ABT-737+CQ resulted in a further significant ($p< 0.001$) increase in caspase-3 activity in these BCL-2^{HIGH} cells (Figure 4.8). Incubation of cells with Z-VAD.fmk did not alter caspase-3 activity in untreated or CQ treated BCL-2^{HIGH} cells; however levels of caspase-3 activity were significantly decreased ($p< 0.001$) in both cell lines following treatment with ABT-737 or ABT-737+CQ in the presence of this pan-caspase inhibitor (Figure 4.8).

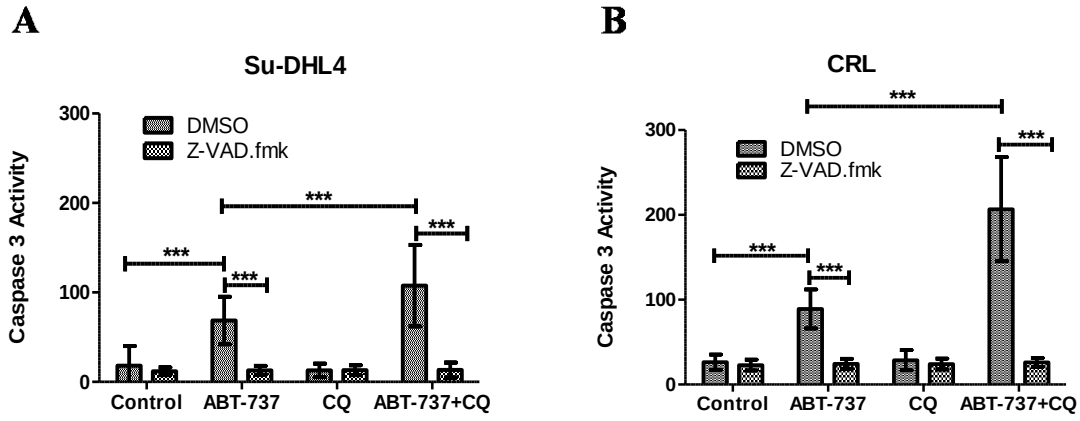

Figure 4.8 Effect of Z-VAD.fmk on ABT-737+CQ-induced caspase-3 activation
2×10^6 viable Su-DHL4 (A) or CRL (B) cells were treated with 0.5µM ABT-737 with or without 50µM CQ in the presence or absence of 20µM Z-VAD.fmk for 3hr at 37°C; untreated cells were cultured under standard growth conditions. Data represent mean ± SD of three independent experiments. Significant changes between treatment conditions analysed using student t-test. *** $p< 0.001$.

We also evaluated the effect of caspase inhibition on PARP cleavage in Su-DHL4 cells treated with ABT-737 or ABT-737+CQ. The 89kDa cleaved PARP fragment was observed in cells treated with ABT-737 alone and to a greater extent in cells treated with ABT-737+CQ (Figure 4.9). Following administration of Z-VAD.fmk, levels of cleaved PARP were comparable between treated and untreated cells, indicating that pan-caspase inhibition can inhibit ABT-737+CQ-induced PARP cleavage and thus, apoptosis (Figure 4.9).

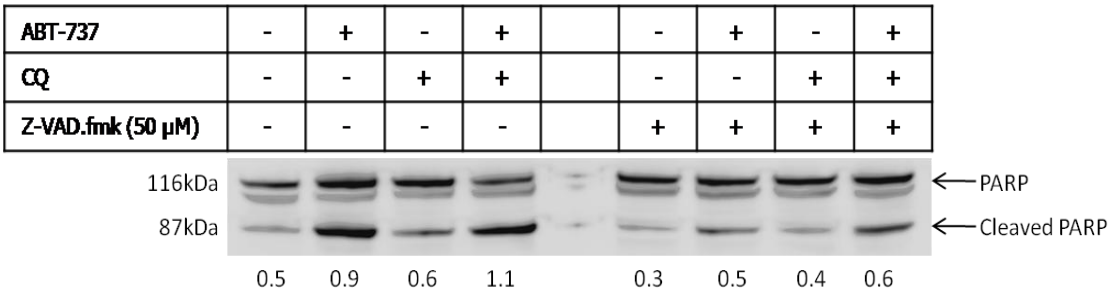

Figure 4.9 Inhibition of caspase activation blocks ABT-737+CQ-induced PARP cleavage
2×10^6 viable Su-DHL4 cells were treated with 0.5µM ABT-737 with or without 50µM CQ in the presence or absence of 20µM Z-VAD.fmk for 3hr at 37°C; untreated cells were cultured under standard growth conditions. PARP was probed for as previously described.

Combined, these results show that inhibition of caspase activity in BCL-2^{HIGH} DLBCL cell lines using the pan-caspase inhibitor Z-VAD.fmk ablates ABT-737+CQ-induced apoptosis, indicating that this treatment combination induces the intrinsic caspase-dependent apoptosis pathway in BCL-2^{HIGH} DLBCL cell lines.

4.2.4 Inhibition of caspase activation showed less inhibitory effect on ABT-737+CQ induced ΔΨm depolarization

It has been reported that BH3-mimetics such as ABT-737 exert their pro-apoptotic effects at the mitochondria where they bind BCL-2 allowing Bax/Bak mediated apoptosis to proceed (Maiuri et al., 2007b). While Z-VAD.fmk can prevent activation of the caspase cascade, this pan-caspase inhibitor does not necessarily inhibit upstream events of apoptosis. We therefore sought to evaluate if treatment with Z-VAD.fmk affects ΔΨm depolarization and cell viability in ABT-737+CQ treated cells.

Cells were treated with ABT-737 with or without CQ in the presence or absence of Z-VAD.fmk and cell viability and ΔΨm depolarization evaluated as previously described. We found that ABT-737 and ABT-737+CQ-induced cell death was significantly ($p< 0.001$) inhibited by Z-VAD.fmk in Su-DHL4 and CRL cells as demonstrated by the dramatic decrease in the percentage of $DAPI^+$ cells (Figure 4.10). Z-VAD.fmk also had a limited but significant ($p< 0.01$) inhibitory effect on ABT-737+CQ-mediated ΔΨm depolarization (Figure 4.11) reflected by a decrease in percentage of $\Delta\Psi m^{LOW}$ cells. This suggests that despite inhibition of caspase activation treatment with ABT-737+CQ results in damage in the mitochondria.

These data suggest that ABT-737+CQ-induced caspase activation occurs downstream of mitochondrial damage, confirming mitochondria as a primary target of ABT-737.

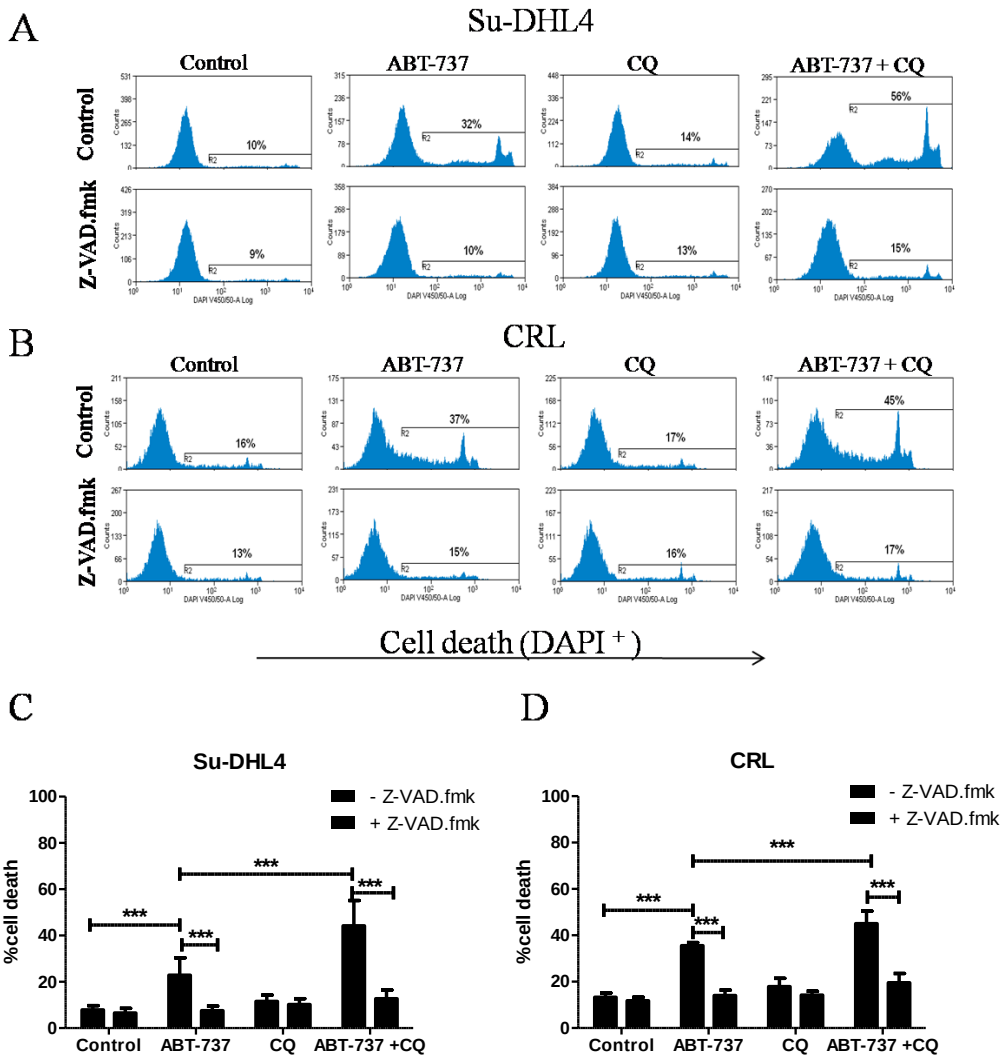

Figure 4.10 Evaluation of the effect of caspase inhibition on ABT-737+CQ-induced cell death in Su-DHL4 and CRL cells

2×10^6 viable Su-DHL4 (A) and CRL (B) cells were treated with 0.5µM ABT-737 with or without 50µM CQ in the presence or absence of 20µM Z-VAD.fmk for 3hr at 37°C; untreated cells were cultured under standard growth conditions. Data were analysed using Summit software V4.3 and significant changes between treatment conditions analysed using student t-test. Data are displayed as the mean ± SD of three separate experiments. Histograms are representative of three separate experiments. *** $p < 0.001$.

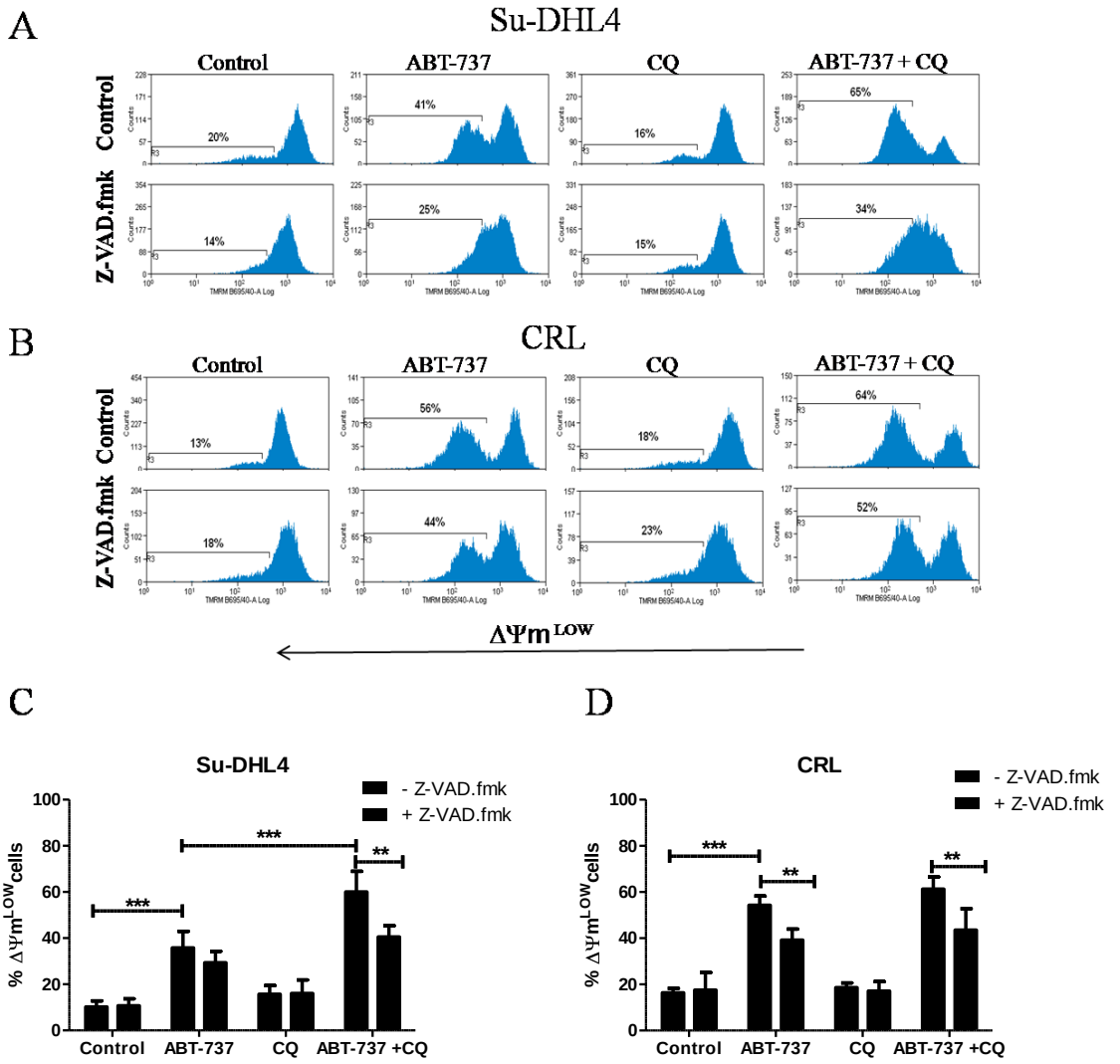

Figure 4.11 Evaluation of the effect of caspase inhibition on ABT-737+CQ-induced ΔΨm in Su-DHL4 and CRL cells

2×10^6 viable Su-DHL4 (A and C) and CRL (B and D) cells were treated with 0.5μM ABT-737 with or without 50μM CQ in the presence or absence of 20μM Z-VAD.fmk for 3hr at 37°C; untreated cells were cultured under standard growth conditions. Significant changes between treatment conditions analysed using student t-test. Data are displayed as the mean ± SD of three separate experiments. Histograms are representative of three separate experiments. ** $p < 0.01$; *** $p < 0.001$.

4.3 Discussion

In this chapter we aimed to evaluate if ABT-737-induced autophagy acts as a cytoprotective mechanism which allows tumour cells to escape death. We found that inhibition of acquired autophagy with CQ resulted in increased levels of ABT-737-induced ΔΨm depolarization, caspase-3 activation, PARP cleavage and cell death in Su-DHL4 and CRL cells, demonstrating that blocking autophagy sensitizes BCL-2^{HIGH} DLBCL cell lines to ABT-737-induced cell death.

Inhibition of caspases was found to result in significantly decreased levels of cell death following dual treatment, indicating that activation of the caspase-cascade is essential for ABT-737+CQ-induced apoptosis. To a lesser extent, ΔΨm depolarization also decreased upon caspase inhibition, indicating treatment with ABT-737+CQ induces mitochondrial damage upstream of caspase activation, confirming the mitochondria as a primary target for ABT-737.

These findings indicate that ABT-737-acquired autophagy is used by cells as a pro-survival mechanism to escape ABT-737-induced apoptosis. Combining autophagy inhibitors with standard chemotherapy drugs is showing promising results in a number of ongoing clinical trials across a variety of malignancies (Helgason et al., 2013). Our data demonstrate that the use of such inhibitors in the treatment of FL and DLBCL patients warrants further investigation and may improve treatment outcome.

4.3.1 Conclusions

Inhibition of autophagy with CQ sensitises BCL-2^{HIGH} DLBCL cell lines to ABT-737-induced apoptosis. ABT-737+CQ-induced cell death is caspase-dependent. Damage to mitochondria by ABT-737 occurs upstream of caspase activation confirming the mitochondria as a primary target of ABT-737. We propose that acquired treatment resistance can be partly overcome by inhibition of autophagy.

Chapter V

Evaluation of the effect of increased BCL-2 expression on the autophagy status and autophagy flux in lymphoma cells

5.1 Introduction

The roles of autophagy in cancer are paradoxical (Choi et al., 2013a). On the one hand, autophagy can inhibit tumourigenesis by removing old and damaged organelles, which prevents DNA damage and maintains genomic stability. Autophagy can also suppress tumourigenesis by preventing the inflammatory response induced by necrotic cell death (Rosenfeldt and Ryan, 2011). On the other hand, autophagy can promote tumourigenesis and tumour cell survival by allowing malignant cells to adapt to stresses such as nutrient deprivation and hypoxia (Kimmelman, 2011). It is also now known that autophagy can mitigate tumour cells response to chemotherapeutic agents and either promote or hinder their pro-death role (Choi et al., 2013a).

As well as inhibiting apoptosis, BCL-2 has been shown to inhibit autophagy by binding and sequestering the autophagy essential protein Beclin-1, which is involved in assembling the pre-autophagosomal structure that gives rise to the autophagosome (Kang et al., 2011; Marquez and Xu, 2012). Overexpression of this anti-apoptotic protein is observed in the majority of FL and ~20% of DLBCL patients (Kelly and Strasser, 2011). While increased expression of BCL-2 in FL and DLBCL is known to promote tumour growth by inhibiting apoptosis, the role of BCL-2 in autophagy regulation in NHL is currently unclear. Gene expression profile (GEP) studies have been carried out in FL and DLBCL in a bid to identify markers of progression and clinical heterogeneity (Alizadeh et al., 2000; Dave et al., 2004). However to date, there is no report of examination of the autophagy-related GEP of primary FL or DLBCL samples which overexpress BCL-2.

To study the role of BCL-2 in autophagy, we compared the autophagy-related GEP of BCL-2^{HIGH} DLBCL cell lines with BCL-2^{LOW} DLBCL cell lines, and primary FL or DLBCL samples with reactive lymph-nodes (RA).

5.2 Results

5.2.1 BCL-2^{HIGH} DLBCL cells have higher basal level autophagy activity compared to BCL-2^{LOW} DLBCL cells

We first aimed to assess if increased expression of BCL-2 inhibits basal level autophagy by comparing expression levels of key autophagy-related proteins and the autophagy-related GEP of BCL-2^{HIGH} Su-DHL4 and BCL-2^{LOW} Su-DHL8 cells.

Using Western blotting we confirmed increased expression of BCL-2 in Su-DHL4 cells and found expression of BCL-xL and Beclin-1 to be similar in both cell lines. Expression of p62 and total levels of LC3 (LC3-I/LC3-II) were lower in BCL-2^{HIGH} cells compared to BCL-2^{LOW} cells (Figure 5.1), suggesting increased degradation of these autophagy substrates and a higher basal level of autophagy activity in BCL-2^{HIGH} cells. Lower levels of LC3-I observed in Su-DHL4 may reflect its increased conversion to LC3-II, further suggesting basal level autophagy is increased within BCL-2^{HIGH} cells.

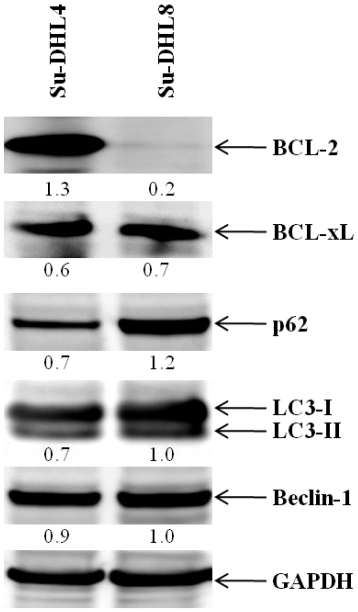

Figure 5.1 Evaluation of expression of key autophagy-related proteins in Su-DHL4 and Su-DHL8 DLBCL cell lines

50µg whole cell lysate was loaded onto a 4-12% Bis-Tris gel and proteins separated by SDS-PAGE. Proteins were transferred to PVDF membrane and probed overnight at 4°C for the key autophagy-related proteins BCL-2, BCL-xL, p62, LC3 and Beclin-1; GAPDH was used as a loading control. Bands are representative of a single experiment. Densitometry values were obtained using Gelscan software and represent the ratio of specific proteins to GAPDH; LC3 values represent the ratio of LC3-I to GAPDH.

We next evaluated the autophagy status of these BCL-2^{HIGH} and BCL-2^{LOW} cell lines by examining their basal level autophagy-related GEP. mRNA levels of 84 autophagy-related genes were examined and compared between Su-DHL4 and Su-DHL8 cell lines using the RT^2 Profiler PCR Array. This PCR array analyses mRNA levels of 84 genes involved in all aspects of the autophagy pathway. Like whole genome microarrays, qRT-PCR allows evaluation of mRNA/gene expression levels but it differs in its method of data normalisation. While analysis of microarray data uses a global normalisation approach, qRT-PCR data are normalised to an individual endogenous control which is selected based on its stability across all samples under all experimental conditions (Andersen et al., 2004).

RNA was extracted from each cell line (three replicates per cell line), assessed for quality, converted to cDNA and analysed by qRT-PCR. RIN and 260/280 values were comparable across all samples and were within the accepted ranges for good quality RNA (Appendix II, Table O). C_T values generated by the qRT-PCR reaction, which represent mRNA transcript levels and reflect the number of cycles taken for the fluorescence signal to cross a user-defined threshold, were normalised to RPLPO which was identified as the most stably expressed HKG using gNorm and Normfinder programmes. Normalised C_T values were converted to RQ values using the formula $2^{-\Delta\Delta Ct}$. RQ values reflect expression of a gene relative to an internal control gene and allow direct comparison of mRNA levels across samples, meaning a standard curve is not required for each condition. Fold changes (FC) were calculated by dividing the mean Su-DHL4 RQ value by the mean Su-DHL8 RQ value on a per gene basis. A gene was classified as being significantly differentially expressed between cell lines if it had a FC $\geq$2 or $\leq$-2 and a *p* value <0.05.

Both autophagy-machinery (Table 5.1) and autophagy-regulatory (Table 5.2) genes were identified as being significantly differentially expressed in Su-DHL4 cells compared to Su-DHL8 cells (Figure 5.2). A supervised hierarchical clustering analysis performed using RQ values of significantly differentially expressed genes successfully resolved these cell lines into two groups (Figure 5.2 A). The autophagy-machinery genes *Atg10* (10.5-fold) and *Atg4C* (3.8-fold) were among the 13 genes significantly up-

regulated in BCL-2^{HIGH} Su-DHL4 cells compared to BCL-2^{LOW} Su-DHL8 cells, while *CTSS* (-2.4-fold) and *MAP1LC3A* (-9.3-fold) were two of the six autophagy-machinery genes significantly down-regulated in Su-DHL4 cells (Figure 5. 2 B). *GAA* (-2.2-fold) and *HTT* (3-fold) were among the autophagy-regulatory genes significantly differentially expressed by these BCL-2^{HIGH} cells (Figure 5. 2 C). BCL-2 expression was shown to be up-regulated 59-fold in Su-DHL4 cells (Figure 5.2 C) which is unsurprising as this cell line carries the t(14;18) translocation. Successful identification of a gene previously known to be differentially expressed between these cell lines demonstrates the validity and applicability of the RT^2 Profiler PCR array in the evaluation of the autophagy-related GEP of these cells. An unsupervised clustering analysis incorporating all genes, irrespective of significance or FC, also successfully separated Su-DHL4 and Su-DHL8 cell lines into two groups (Appendix II, Figure 1).

These results show that BCL-2^{HIGH} DLBCL cell lines have a higher basal level of autophagy activity compared to BCL-2^{LOW} cells as demonstrated by increased expression of multiple autophagy-related genes in Su-DHL4 cells. Increased degradation of autophagy substrates in Su-DHL4 cells also indicates a higher rate of autophagy-flux in these BCL-2^{HIGH} cells, indicating that despite its increased expression, BCL-2 does not inhibit basal level autophagy activity in these cells.

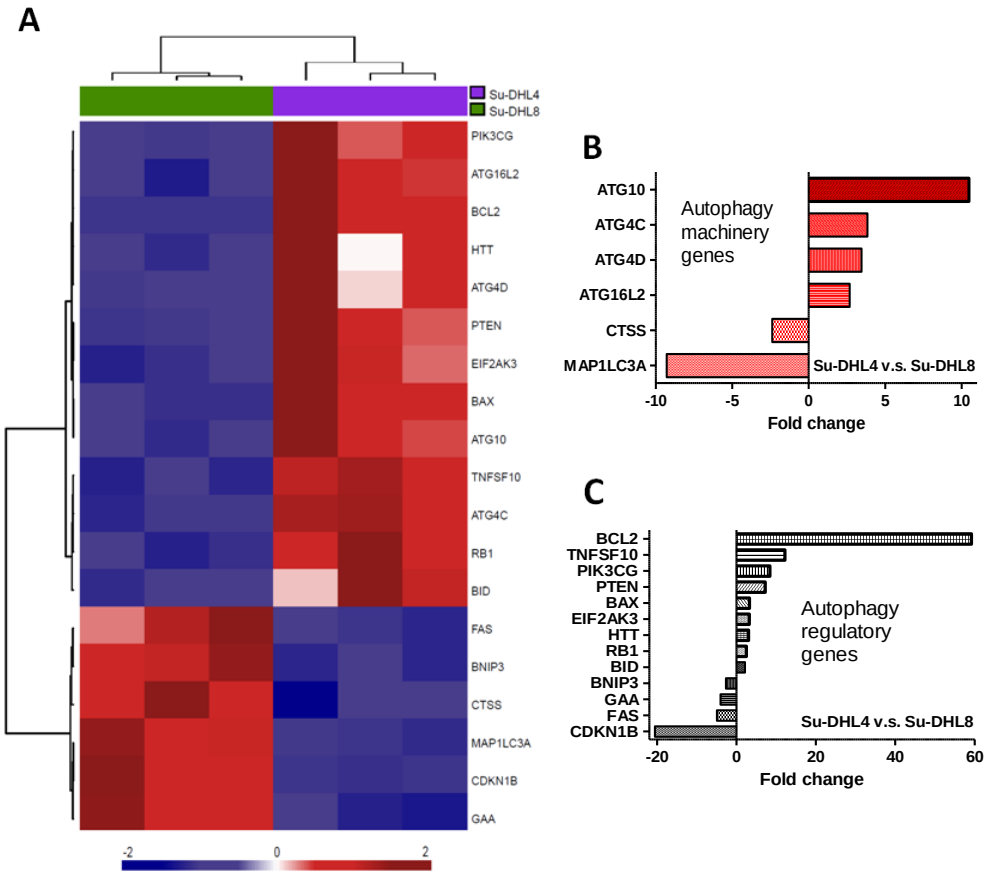

Figure 5.2 Su-DHL4 and Su-DHL8 cells differ in their expression of autophagy-related genes

1µg RNA extracted from untreated Su-DHL4 and Su-DHL8 cell lines (three replicates per cell line) was converted to cDNA and analysed using the RT^2 Profiler PCR Array according to the manufactures protocol. C_T values were normalised to the HKG RPLPO and genes with a FC ≥2 or ≤-2 and a p value <0.05 were deemed to be significantly differentially expressed between cell lines. *P* values were calculated using an unpaired student t-test. A supervised hierarchical clustering analysis was performed by JM using a Euclidean distance measure and an average agglomeration where each row represents a gene and each column an RQ value. Gene expression levels are represented on a scale of blue to red colour indicative of low to high expression (A). Graphs depict fold-changes of autophagy-machinery (B) and autophagy-regulatory (C) genes significantly differentially expressed in Su-DHL4 cells compared to Su-DHL8 cells.

Table 5.1 Autophagy-machinery genes

Gene Name	Full name	Function
AMBRA1	Autophagy/Beclin-1 regulator 1	Autophagic vacuole formation
ATG12	Autophagy related protein 12	Autophagic vacuole formation/co-regulator for autophagy and apoptosis
ATG16L1	Autophagy related protein 16-1	Autophagic vacuole formation/protein transport
ATG4 A, B, C, D	Autophagy related protein 4 A, B, C, D	Autophagic vacuole formation/protein targeting to vacuole/protein transport/with protease activity
ATG5	Autophagy related protein 5	Autophagic vacuole formation
ATG9A	Autophagy related protein 9A	Autophagic vacuole formation/protein transport
ATG9B	Autophagy related protein 9B	Autophagic vacuole formation
BECN1	Beclin-1	Autophagic vacuole formation/co-regulator of autophagy and apoptosis
GABARAP	GABA(A) receptor-associated protein	Autophagic vacuole formation/protein targeting to vacuole/protein transport/linking to lysosome
GABARAPL1	GABA(A) receptor-associated protein-like 1	Autophagic vacuole formation
GABARAPL2	GABA(A) receptor-associated protein-like 2	Autophagic vacuole formation/protein transport
IRGM	Immunity-related GTPase family,M	Autophagic vacuole formation
MAP1LC3A	Microtubule-associated protein 1 light chain 3-α (LC3A)	Autophagic vacuole formation
MAP1LC3B	Microtubule-associated protein 1 light chain 3- (LC3B)	Autophagic vacuole formation
RGS19	Regulator of G-protein signalling 19	Autophagic vacuole formation
ULK1	Serine/threonine-protein kinase ULK1 (ATG1)	Autophagic vacuole formation
WIPI1	WD repeat domain, phosphoinositide interacting 1	Autophagic vacuole formation
ATG10	Autophagy related protein 10	Protein transport
ATG16L2	Autophagy related protein 16-2	Protein transport
ATG3	Autophagy related protein 3	Protein transport/ubiquitination
ATG7	Autophagy related protein 7	Protein transport/ubiquitination
RAB24	RAB24	Protein transport
DRAM1	DNA-damage regulated autophagy modulator 1	Linking to lysosome/co-regulator of autophagy and apoptosis
LAMP1	Lysosomal-associated membrane protein 1	Linking to lysosome; autophagy induction
NPC1	Niemann-Pick disease, type C1	Linking to lysosome
CTS B, D, S	Cathepsin B, D, S	Linking to lysosome
HDAC6	Histone Deacetylase 6	Protein Ubiquitination

Table 5.2 Autophagy-regulatory genes

Gene Name	Full name	Function
AKT1	v-akt murine thymoma viral oncogene homolog 1	Co-regulator of autophagy and apoptosis
APP	Amyloid beta (A4) precursor protein	Co-regulator of autophagy and apoptosis
ATG5	Autophagy related protein 5	Co-regulator of autophagy and apoptosis
BAD	BCL-2-associated agonist of cell death (Bad)	Co-regulator of autophagy and apoptosis
BAK1	BCL-2 antagonist/killer 1	Co-regulator of autophagy and apoptosis
BAX	BCL-2 associated X protein	Co-regulator of autophagy and apoptosis
BCL2	B-cell CLL/lymphoma 2	Co-regulator of autophagy and apoptosis
BCL2L1	BCL-2 like 1	Co-regulator of autophagy and apoptosis
BID	BH3 interacting domain death agonist	Co-regulator of autophagy and apoptosis
BNIP3	BCL-2/adenovirus E1B 19kDa interacting protein 3	Co-regulator of autophagy and apoptosis
CASP3, 8	Caspase-3, 8	Co-regulator of autophagy and apoptosis
CDKN1B	Cyclin-dependent kinase inhibitor 1B (p27)	Co-regulator of autophagy and apoptosis and cell cycle
CDKN2A	Cyclin-dependent kinase inhibitor 2A (p16)	Co-regulator of autophagy and apoptosis and cell cycle
CLN3	Battenin	Co-regulator of autophagy and apoptosis
CXCR4	Chemokine (C-X-C motif) receptor 4	Co-regulator of autophagy and apoptosis
DAPK1	Death-associated protein kinase 1	Co-regulator of autophagy and apoptosis
EIF2AK3	Eukaryotic translation initiation factor 2 alpha kinase 3	Co-regulator of autophagy and apoptosis and autophagy induction
FADD	Fas (TNFRSF6)-associated via death domain	Co-regulator of autophagy and apoptosis
FAS	Fas cell surface death receptor	Co-regulator of autophagy and apoptosis
HDAC1	Histone deacetylase 1	Co-regulator of autophagy and apoptosis
HTT	Huntingtin	Co-regulator of autophagy and apoptosis
IFNG	Interferon γ	Co-regulator of autophagy and apoptosis and cell cycle and autophagy induction
INS	Insulin	Co-regulator of autophagy and apoptosis
MAPK8	Mitogen-activated protein kinase 8	Co-regulator of autophagy and apoptosis
MTOR	Mechanistic target of rapamycin	Co-regulator of autophagy and apoptosis
NFKB1	Nuclear factor of kappa light polypeptide gene enhancer in B-cells 1	Co-regulator of autophagy and apoptosis
PIK3CG	Phosphatidylinositol-4,5-bisphosphate 3-kinase, catalytic subunit γ	Co-regulator of autophagy and apoptosis
PRKAA1	Protein Kinase, AMP-Activated, Alpha 1	Co-regulator of autophagy and apoptosis
PTEN	Phosphatase and tensin homolog	Co-regulator of autophagy and apoptosis and cell cycle
SNCA	synuclein, alpha	Co-regulator of autophagy and apoptosis
SQSTM1	Sequestosome 1 (p62)	Co-regulator of autophagy and apoptosis
TGFB1	Transforming growth factor beta 1	Co-regulator of autophagy and apoptosis and cell cycle
TGM2	Transglutaminase 2	Co-regulator of autophagy and apoptosis
TNF	Tumour necrosis factor	Co-regulator of autophagy and apoptosis
TNFSF10	Tumour necrosis factor (ligand)	Co-regulator of autophagy and apoptosis

	superfamily, member 10	
TP53	Tumour p53	Co-regulator of autophagy and apoptosis and cell cycle
RB1	Retinoblastoma 1	Co-regulator of autophagy and cell cycle
EIF4G1	Eukaryotic translation initiation factor 4 gamma, 1	Autophagy in response to other intracellular signals
ESR1	Estrogen receptor 1	Autophagy in response to other intracellular signals
GAA	Glucosidase, α; acid	Autophagy in response to other intracellular signals
HGS	Hepatocyte growth factor-regulated tyrosine kinase substrate	Autophagy in response to other intracellular signals
MAPK14	Mitogen-activated protein kinase 14	Autophagy in response to other intracellular signals
PIK3C3	Phosphatidylinositol 3-kinase, catalytic subunit, type 3	Autophagy in response to other intracellular signals
PIK3R4	Phosphatidylinositol 3-kinase, regulatory subunit 4	Autophagy in response to other intracellular signals
RPS6KB1	Ribosomal protein S6 kinase, 70kDa, polypeptide 1	Autophagy in response to other intracellular signals
TMEM74	Transmembrane protein 74	Autophagy in response to other intracellular signals
ULK2	Unc-51 like autophagy activating kinase 2	Autophagy in response to other intracellular signals
UVRAG	UV radiation resistance associated gene	Autophagy in response to other intracellular signals
HSP90AA1	Heat shock protein 90 alpha class A1	Chaperone-mediated autophagy
HSPA8	Heat shock protein 8	Chaperone-mediated autophagy

5.2.2 Increased expression of BCL-2 does not inhibit the autophagy flux

We next aimed to assess if BCL-2 expression levels affect the autophagy-flux. Expression levels of autophagy-related proteins and genes were evaluated and compared following modulation of the autophagy flux in BCL-2^{HIGH} and BCL-2^{LOW} DLBCL cell lines. The autophagy-flux was either inhibited with CQ or induced by culturing cells in HANKS Balanced Salt Solution (HBSS), a starvation media established to induce autophagy (Alers et al., 2012; Shang et al., 2011). Cellular levels of the key autophagy proteins p62, LC3 and Beclin-1 were evaluated in Su-DHL4 and Su-DHL8 cells which were cultured for up to 6hrs in normal media with or without CQ or cultured in HBSS.

Inhibition of the autophagy flux by incubation with 50μM CQ resulted in a time-dependent increase in levels of p62, LC3-I and LC3-II in both Su-DHL4 and Su-DHL8 cells, indicative of a block in autophagy degradation and accumulation of these autophagy substrates (Figure 5.3 A). Beclin-1 levels remained stable following addition

of CQ (Figure 5.3 A) and incubation in HBSS for up to 6hrs (Figure 5.3 B), indicating this protein may not be a substrate of autophagic degradation.

Nutrient deprivation caused LC3 and p62 levels to fluctuate within cell lines (Figure 5.3 B). Cellular levels of LC3-I decreased in Su-DHL4 and Su-DHL8 cells during the 6hr starvation period. Similarly, aside from an initial increase in Su-DHL4 cells following 2hr starvation, LC3-II levels also decreased in a time-dependent manner during the starvation period (Figure 5.3 B). A decrease in LC3-I may be due to its conversion to LC3-II, while a decrease in LC3-II may be caused by increased autophagic degradation.

p62 levels initially decreased in both cell lines following 2-4hr starvation, indicative of its degradation by active autophagy. However levels of this adaptor protein increased after 4-6hrs starvation (Figure 5.3 B). An increase in p62 at the protein level seems to conflict with increased autophagy activity. However, in a similar finding to ours, Sahani and colleagues observed an initial decrease in p62 levels in MEF and HepG2 cell lines following 1-2hr starvation. but levels of p62 were found to increase again under conditions of prolonged (4-8hr) starvation, which was due to an increase in p62 at the mRNA/gene level (Sahani et al., 2014).

These data indicate that increased expression of BCL-2 does not inhibit the autophagy-flux in BCL-2^{HIGH} cells. Despite differences in their basal level autophagy activity, BCL-2^{HIGH} and BCL-2^{LOW} cells appear to regulate their autophagy-flux in a similar way in response to modulation of autophagy activity.

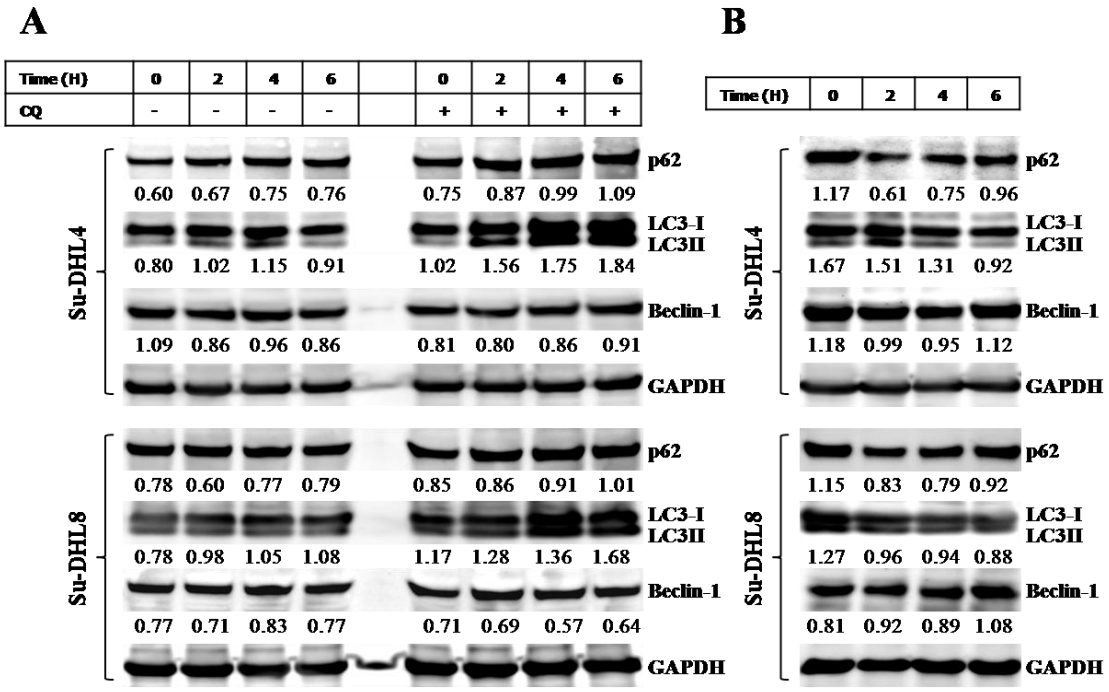

Figure 5.3 Incubation with HBSS induces autophagy in Su-DHL4 and Su-DHL8 cell lines
Cells were cultured under standard growth conditions in normal media with or without 50μM CQ (A) or in HBSS (B) for 0, 2, 4 or 6hr. 50μg whole cell lysate was loaded onto a 4-12% Bis-Tris gel and proteins separated by SDS-PAGE. Proteins were transferred to PVDF membrane and probed overnight at 4°C for the key autophagy-related proteins p62, LC3 and Beclin-1; GAPDH was used as a loading control. Bands are representative of a single experiment. Densitometry values were obtained as previously described; LC3 densitometry values represent the ratio of LC3-I and LC3-II to GAPDH.

We next examined the effects of nutrient deprivation on the autophagy-related GEP of Su-DHL4 and Su-DHL8 cells. The GEP of starved cells was compared to cells cultured under nutrient replete conditions, referred to as untreated cells. RNA was extracted from cells (three replicates per cell line) (Appendix II, Table O) and analysed by qRT-PCR. FC differences were calculated by dividing the mean HBSS RQ value by the mean untreated RQ value within each cell line.

A supervised clustering analysis successfully resolved starved and untreated cells into two groups in Su-DHL4 (Figure 5.4 A) and Su-DHL8 (Figure 5.4 B) cell lines. Starvation up-regulated autophagy at the gene level in BCL-2^{HIGH} and BCL-2^{LOW} cells as demonstrated by increased expression of a number of key autophagy-related genes in both cell lines (Figure 5.4 C and D). Three autophagy-regulatory genes *CDKN1B,*

UVRAG and *SQSTM1/p62* were significantly up-regulated in starved Su-DHL4 and Su-DHL8 cells compared to untreated controls (Figure 5.4). An increase in p62 mRNA levels explains our previous observation of increased expression of p62 at the protein level following 6hr starvation and is in agreement with the findings of Sahani and colleagues (Sahani et al., 2014). *GABARAPL1* and *GABARAPL2*, mammalian homologs of *Atg8*, were also up-regulated in starved Su-DHL4 cells (Figure 5.4 A and C). The autophagy-machinery genes *Atg7*, *Atg16L2* and *Atg9B* were significantly down-regulated in Su-DHL4 and/or Su-DHL8 cells following nutrient withdrawal despite an increase in the autophagy flux (Figure 5.4). An unsupervised clustering analysis also resolved starved and untreated cells in both cell lines (Appendix II, Figure 2 and 3)

Increased expression of autophagy-machinery and autophagy-regulatory genes in both starved BCL-2^{HIGH} and BCL-2^{LOW} cell lines indicates BCL-2 expression may not affect autophagy induction or the autophagy flux at the gene level. More genes were found to be significantly up-regulated in Su-DHL4 cells compared to Su-DHL8 cells, suggesting increased autophagy activity in BCL-2^{HIGH} cells following nutrient deprivation.

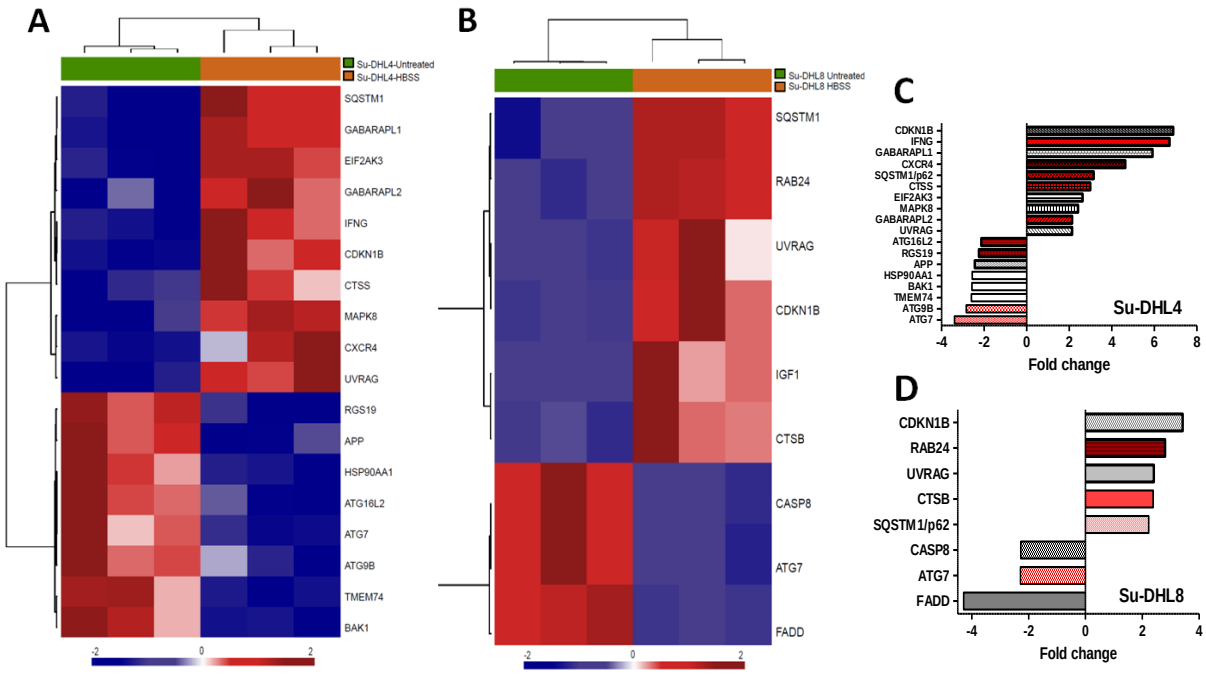

Figure 5.4 HBSS-induced starvation alters the autophagy-related GEP of Su-DHL4 and Su-DHL8 cell lines

1µg RNA was extracted from Su-DHL4 (A and C) and Su-DHL8 (B and D) cell lines cultured in normal media (untreated) or cultured in HBSS for 6hr, converted to cDNA and analysed by qRT-PCR according to the manufactures protocol. C_T values were normalised to RPLPO and genes with a FC ≥2 or ≤-2 and a *P* value <0.05 deemed significantly different. *P* values were calculated using a paired student t-test. A supervised hierarchical clustering analysis was performed by JM using a Euclidean distance measure and an average agglomeration where each row represents a gene and each column an RQ value. Gene expression levels are represented on a scale of blue to red colour indicative of low to high expression (A and B). Graphs depict fold-changes of autophagy related genes significantly differentially expressed in Su-DHL4 (C) and Su-DHL8 (D) HBSS cultured cells compared to cells cultured in normal supplemented media. Red bars indicate changes in autophagy machinery genes; black and white bars indicate changes in autophagy regulatory genes.

5.2.3 Purification of B cells from primary FL, DLBCL and reactive control samples for gene expression analysis

Autophagy is a cellular process which occurs in the majority of cell types. Therefore, in order to determine the autophagy status of malignant FL and DLBCL cells specifically, we isolated B cells from primary FL and DLBCL single-cell suspensions using cell sorting by flow cytometry. B cells isolated from RA were used as controls.

We first selected the viable, non-T cell fraction of cells by gating on $DAPI^-/CD3^-$ cells (Figure 5.5). B cells were then isolated from this dual negative population based on their expression of well established B cell markers. DLBCL and RA B cells were identified by expression of the pan-B cell marker CD20 (Figure 5.5 A; middle and bottom panels) (Shaffer et al., 2012) while FL B cells were isolated according to co-expression of the pan-B cell marker CD19 and the germinal centre B cell marker CD10 (Figure 5.5 A; top panel) (Dogan et al., 2000; Gurbuxani et al., 2009). B cells were isolated from all samples with >95% purity.

In healthy individuals, normal B cells are polyclonal and express both kappa and lambda light chains, typically in a kappa: lambda ratio of 2:1 or 1.5:1 (Katzmann et al., 2005; Schmid et al., 2011), while FL B cells are monoclonal and express either kappa or lambda at a high levels (~>90%), skewing the kappa: lambda ratio (Schmid et al., 2011; Warnke and Levy, 1978). Healthy B cells are therefore light-chain unrestricted while malignant B cells are light-chain restricted (Katzmann et al., 2005; Schmid et al., 2011). Evaluation of light-chain restriction in our population of $CD19^+/CD10^+$ isolated FL B cells revealed expression of either the kappa (Figure 5.5 B; top panel) or the lambda (Figure 5.5 B; middle panel) light-chain only, indicative of light-chain restriction and a monoclonal, neoplastic population of B cells. In comparison, reactive B cells expressed kappa and lambda at approximately equal levels (kappa: lambda - 0.92:1) indicating a polyclonal B cell population (Figure 5.5; bottom panel). This demonstrates that isolation of B cells from primary FL samples based on dual expression of CD19 and CD10 successfully identifies the malignant cell population.

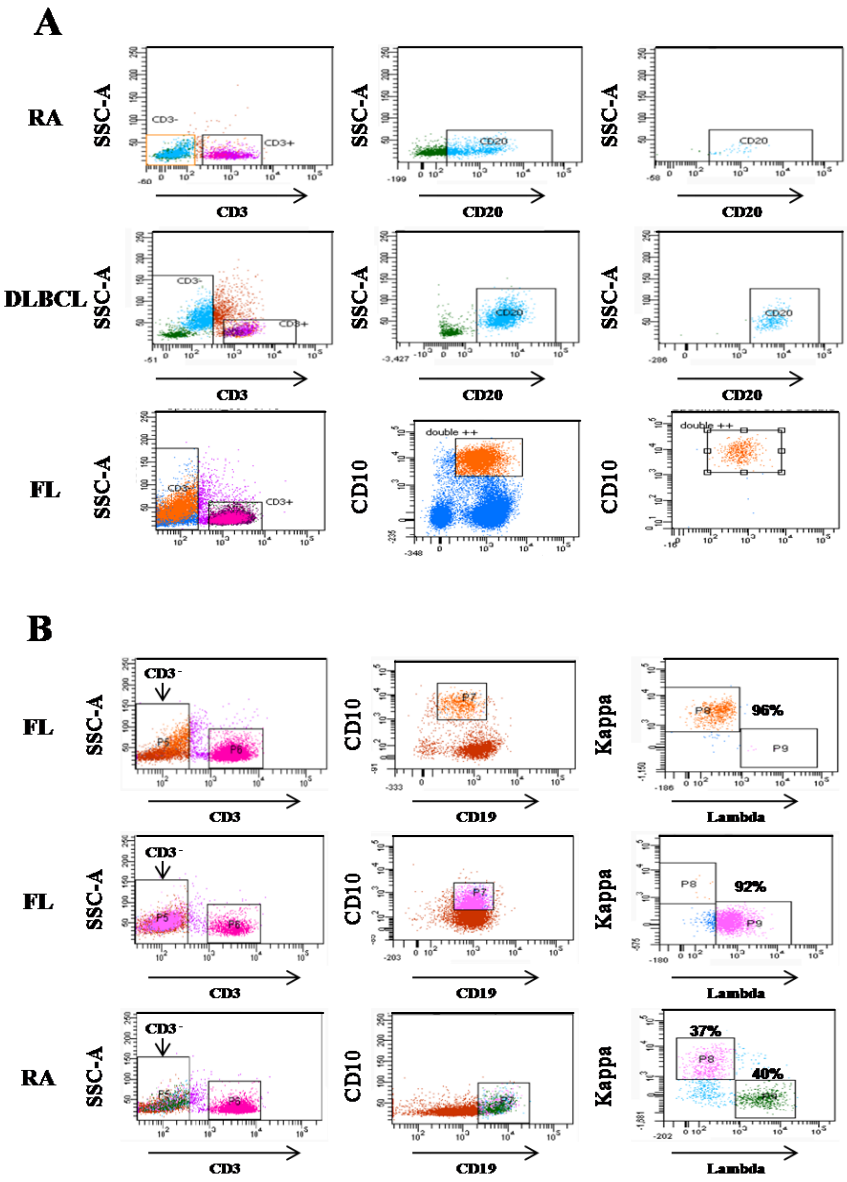

Figure 5.5 Flow sorting strategy for purification of B cells from primary FL, DLBCL and RA single cell suspensions

FL, DLBCL and RA samples were prepared as described in materials and methods. Following exclusion of $DAPI^+$ dead cells, $CD3^+$ T cells and $CD3^-$ cells were identified and B cells isolated from the live, non-T cell ($DAPI^-/CD3^-$) population. FL B cells were isolated according to co-expression of CD19 and CD10 ($CD3^-/CD19^+/CD10^+$); DLBCL and RA B cells were identified based on expression of CD20 ($CD3^-/CD20^+$) (A). $CD3^-/CD19^+/CD10^+$ FL B cells were further evaluated for kappa/lambda light chain restriction. $CD19^+$ RA B cells were used as a positive control for the normal kappa: lambda ratio (B). Purity of isolated B cells was >95% in all cases. Fluorochromes were visualised under the following channels: DAPI - *Violet-Blue*; CD3 - *FITC*; CD20 - *APC-H7*; CD19 - *APC-Cy7*; CD10 - *PE*; Kappa - *APC*; Lambda - *PerCP-Cy5.5*. Further antibody information is listed in appendix I, 7.5; table *I*.

5.2.4 FL samples displayed higher autophagy activity despite increased expression of BCL-2

Next, we compared the autophagy-related GEP of purified primary FL and DLBCL B cells to those of RA non-malignant B cells. RNA was extracted from five FL, two DLBCL and three RA primary purified samples. Full patient information is given in the appendix (Appendix II, Table P and Q). RINs were comparable across all samples ranging from 7-10, and were considered high enough to deem the RNA as non-degraded and of good quality. 260/280 values were also within the accepted range and were comparable across samples (Appendix II, Table R). Expression levels of autophagy-related genes were assessed using the RT^2 Profiler Human Autophagy PCR array and RQ values calculated as previously described. FC values were obtained by dividing the mean FL or mean DLBCL RQ value by the mean RA RQ value on a per gene basis. Genes with a fold change ≥ 3 or ≤ -3 or a FC ≥ 2 or ≤ -2 and a *p* value <0.05 were taken to be biologically meaningful.

An unsupervised hierarchical clustering analysis successfully separated purified RA B cells from purified FL and DLBCL B cells (Figure 5.6 A). Of the five FL samples studied, three had similar autophagy-related gene expression profiles and expressed a number of genes at higher levels compared to RA controls; DLBCL sample T2628 was similar to these FL patients. FL sample T6697 resembled RA B cells, while T6713, which showed up-regulation of a number of genes compared to sample T6697, clustered separately to all other FL samples (Figure 5.6 A). DLBCL sample T3531 expressed autophagy genes at low levels comparable to RA controls, suggesting decreased autophagy activity in this sample. These data indicate that despite increased expression of BCL-2, purified primary FL B cells have increased basal level autophagy activity compared to non-malignant B cells and DLBCL B cells. The autophagy-related GEP and status of DLBCL B cells was heterogeneous and so could not be definitively defined; a greater number of purified DLBCL samples are therefore required to establish aberrant expression of autophagy genes in this aggressive disease.

Among those genes significantly up-regulated in FL B cells were the early and late autophagy-machinery genes *Atg9A*, *LAMP1* and *GABARAPL1* (Table 5.3), the latter of

which was also up-regulated in Su-DHL4 cells following starvation (Figure 5.4). *MAP1LC3A* was up-regulated in both FL and DLBCL B cells, as was the autophagy-regulatory gene *CDKN2A* (Table 5.3 and 5.4). *SQSTM1*, which encodes for p62, was up-regulated in three of the five FL samples evaluated (T5728, T0167, T6713), although this increase did not reach statistical significance. Unsurprisingly, expression of *BCL-2* was increased in FL B cells compared to RA B cells (Table 5.4).

The median, overall expression of autophagy-related genes was comparable between purified RA B cells suggesting similar expression of autophagy-related genes and autophagy activity between these samples (Figure 5.6 B). Global expression of autophagy genes varied among purified FL and DLBCL B cells indicating heterogeneity amongst lymphoma patients with respect to their expression of autophagy-related genes and their autophagy pathway activity. However, we observed that with the exception of sample T6697, FL B cells expressed autophagy-related genes at a higher level compared to RA B cells (Figure 5.6 B), suggesting increased autophagy activity in these malignant B cells.

Up-regulation of autophagy-machinery and autophagy-regulatory genes in purified FL B cells indicates higher basal level autophagy activity in these cells despite increased expression of BCL-2. This suggests that overexpression of BCL-2 does not inhibit autophagy in FL B cells.

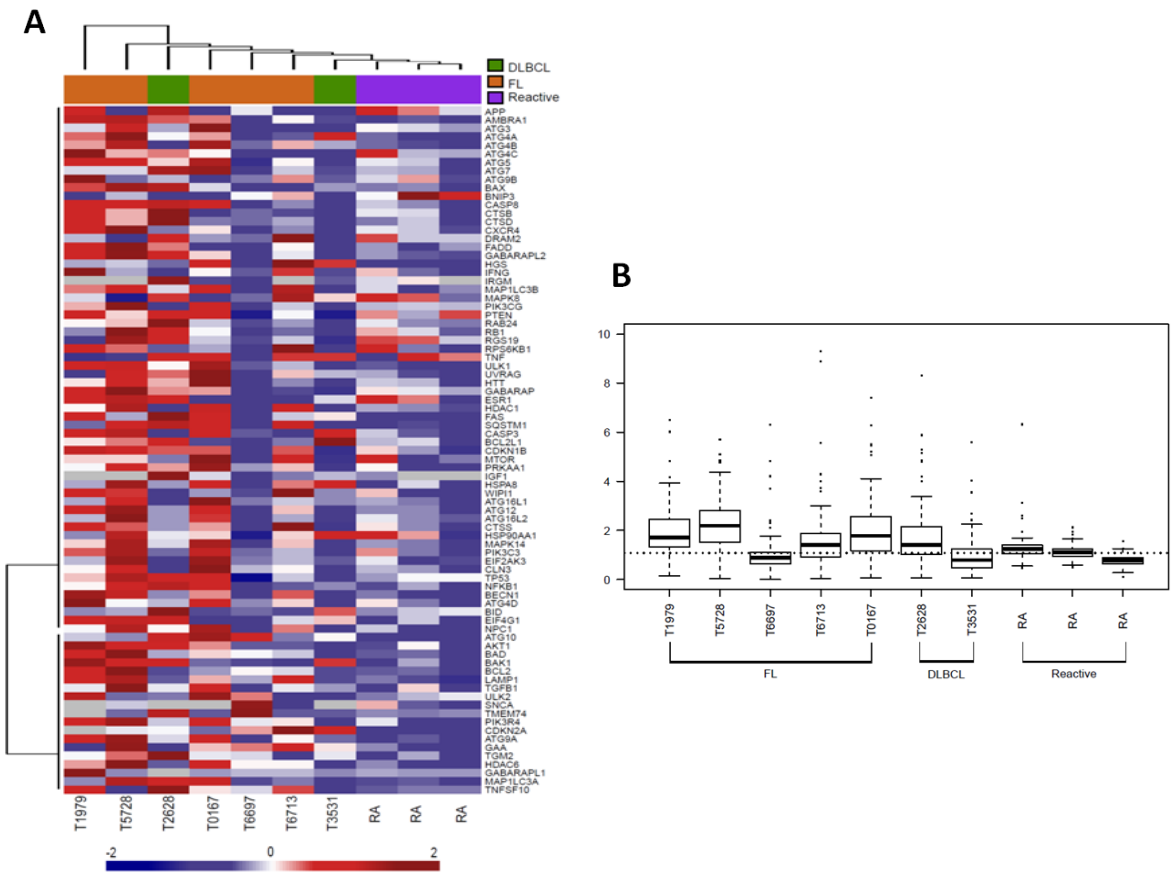

Figure 5.6 Evaluation of the autophagy-related GEP of primary FL, DLBCL and RA B cells

300ng RNA extracted from diagnostic primary FL, DLBCL and RA B cells previously isolated by flow sorting was converted to cDNA and analysed by qRT-PCR according to the manufactures protocol C_T values were normalised to RPLPO and genes with a FC ≥2 or ≤-2 and a *p* value <0.05 deemed significantly different. *p* values were calculated using a Mann Whitney *U* test. An un-supervised hierarchical clustering analysis was performed by JM using a Euclidean distance measure and an average agglomeration. Heat-map shows RQ values where each column represents a patient and each row a gene. Gene expression levels are represented as a gradient of blue to red colour indicating low and high expression respectively; gray indicates missing data (A). Data were visualised based on their total global expression level of those genes included in the un-supervised hierarchical clustering; mid-line represents the median for each sample; box-limits - 25th-75th percentiles; whiskers - 5th - 95th percentiles (B). Dashed line reflects median global expression of autophagy-related genes across RA samples.

While examination of autophagy at the mRNA level in purified B cells gives us an understanding of this pathways activity in malignant cells, it does not provide information on activity of this pro-survival process in cells of the tumour microenvironment. We therefore evaluated the autophagy-related GEP of primary FL, DLBCL and RA tissue biopsies, classified as un-purified, to establish if FL samples can still be distinguished as having increased expression of autophagy genes. The autophagy-related GEP of eight FL and ten DLBCL un-purified samples were compared to eight un-purified primary RA controls (Appendix II, Table P and Q). RINs and 260/280 values were comparable between samples and were within the acceptable limits to deem the RNA of good quality (Appendix II, Table S).

Unsupervised hierarchical clustering grouped seven of the eight FL samples together, with sample F9713 behaving differently. The DLBCL sample T1486 also clustered with these FL samples (Figure 5.7 A). The remaining nine DLBCL samples clustered with RA controls and expressed autophagy-related genes at low levels compared to FL samples (Figure 5.7 A). Based on this unsupervised clustering, un-purified FL samples appear to up-regulate a number of autophagy-related genes compared to RA and DLBCL samples, indicating increased autophagy in these samples. Similarities in expression levels of autophagy genes between DLBCL samples and RA controls suggest lower basal level autophagy in DLBCL compared to FL. Multiple autophagy-machinery and autophagy-regulatory genes were significantly up-regulated in un-purified FL samples compared to RA controls (Table 5.3 and 5.4). For example *Atg9A*, *Atg16L1* and *MAP1LC3A*, previously shown to have increased expression in purified FL B cells, were up-regulated in this larger cohort of un-purified FL samples. Similarly *UVRAG* and *GABARAPL2*, both previously identified as being significantly up-regulated in Su-DHL4 cells following starvation, were expressed at significantly higher levels in un-purified FL samples. *SQSTM1* expression was variable among un-purified FL samples, with half of the samples evaluated showing increased expression compared to RA controls. A greater number of autophagy genes were found to have altered expression in un-purified FL samples compared to purified B cells, indicating that expression of autophagy genes may also be altered in cells of the tumour microenvironment. Only three autophagy-regulatory genes *CTSD*, *DRAM1* and *TGM2*

were significantly differentially expressed in un-purified DLBCL samples compared to RA (Table 5.3 and 5.4).

Comparing samples based on their overall median expression levels of autophagy-related genes, FL samples showed global up-regulation of autophagy genes compared to DLBCL and control samples (Figure 5.7 B). Autophagy activity varied among DLBCL samples although generally, the global autophagy-related GEP of un-purified DLBCL samples were similar to RA controls (Figure 5.7 B).

These data demonstrate that autophagy activity is higher in FL tumour cells and cells in the surrounding microenvironment, suggesting overexpression of BCL-2 does not inhibit autophagy in this indolent NHL.

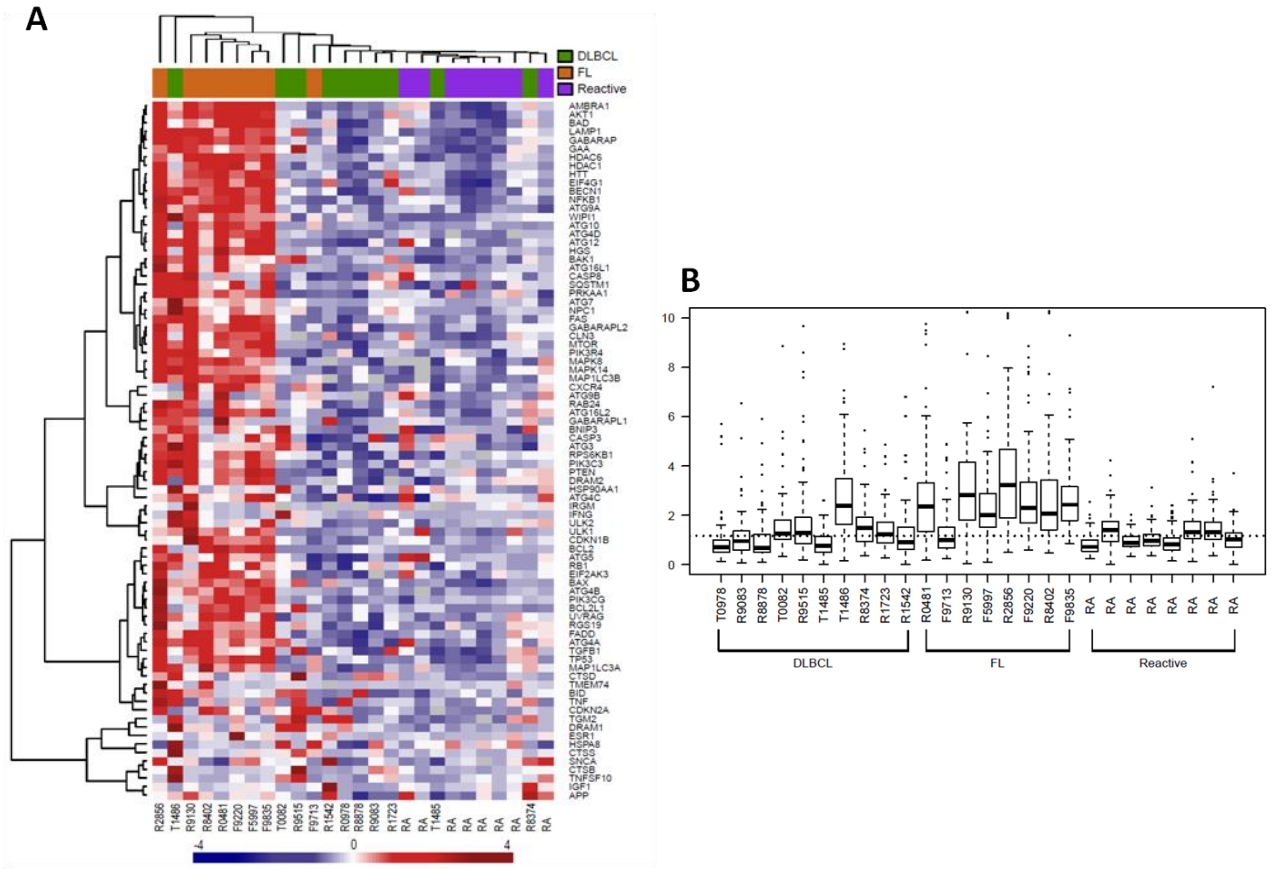

Figure 5.7 Evaluation of the autophagy-related GEP of primary FL, DLBCL and RA whole tumour samples

400ng RNA extracted from diagnostic primary FL, DLBCL and RA whole tissue biopsies was converted to cDNA and analysed by qRT-PCR according to the manufactures protocol C_T values were normalised to RPLPO and genes with a FC ≥2 or ≤-2 and a *p* value < 0.05 deemed significantly different. p values were calculated using a Mann Whitney *U* test. An un-supervised hierarchical clustering analysis was performed by JM using a Euclidean distance measure and an average agglomeration. Heat-map shows RQ values where each column represents a patient and each row a gene. Gene expression levels are represented as a gradient of blue to red colour indicating low and high expression respectively; gray indicates missing data (A). Data were visualised based on their total global expression level of those autophagy genes included in the clustering analysis; mid-line represents the median for each sample; box-limits - 25th -75th percentiles; whiskers - 5th - 95th percentiles (B). Dashed line reflects median global expression of autophagy-related genes across RA samples.

Table 5.3 Autophagy-machinery genes differentially regulated in primary lymphoma samples compared to RA controls

Gene name and function	FL				DLBCL			
	F.C (UP)	P value	F.C (P)	P value	F.C (UP)	P value	F.C (P)	P value
BECN1	2.07	<0.005						
RGS19	2.14	<0.05						
AMBRA1	2.23	<0.005						
ATG16L1	2.42	<0.05	3.00	0.24				
MAP1LC3A	2.60	<0.005	5.38	0.2			5.22	0.33
GABARAPL1			7.98	0.65				
GABARAPL2	2.64	<0.005						
GABARAP	2.06	<0.005						
ATG9A	3.26	<0.005	2.56	<0.05				
ATG4D	3.75	<0.005						
ATG4B	4.66	<0.005						
ULK1			3.29	0.06				
WIPI1	3.97	<0.005						
ATG16L2	2.047	<0.05						
RAB24	2.38	<0.05						
ATG7	2.39	<0.005						
ATG10	7.21	<0.005						
DRAM1	2.38	<0.05			4.24	<0.05	10.77	0.27
CTSD	2.41	<0.005			4.14	<0.05		
LAMP1	2.65	<0.05	2.02	<0.05				
HDAC6	3.91	<0.005	2.23	<0.05				

F.C. - Fold change; UP - unpurified; P - purified

Table 5.4 Autophagy-regulatory genes differentially regulated in primary lymphoma samples compared to RA controls

Gene name and function	FL				DLBCL			
	F.C (UP)	P value	F.C (P)	P value	F.C (UP)	P value	F.C (P)	P value
BNIP3			-2.8	0.05			-15.37	0.12
FADD	2.07	<0.005						
BAD	2.12	<0.005						
BID							3.96	0.11
FAS	2.16	<0.05	3.58	0.10			7.16	0.08
MTOR	2.18	<0.005						
MAPK8	2.31	<0.05						
BAK1	2.31	<0.05						
CLN3	2.33	<0.005						
CXCR4	2.25	<0.05						
AKT1	2.69	<0.005						
BAX	2.95	<0.05						
IFNG			3.04	0.34	6.54	0.1	-5	0.44
HTT	3.20	<0.005						
HDAC1	3.23	<0.005					-2.0	<0.05
PIK3CG	3.33	<0.005					-8.07	<0.005
BCL2L1	3.81	<0.005						
DAPK1	5.04	<0.05						
BCL2	8.88	<0.005	7.03	0.1				
TGM2					2.99	<0.05	4.56	0.16
TP53	2.98	<0.005						
CDKN1B	2.11	<0.05						
CDKN2A	6.19	<0.05	4.22	0.11	3.27	0.12	4.12	<0.05
EIF4G1	2.16	<0.005						
UVRAG	2.33	<0.005						
RPS6KB1	2.36	<0.005						
MAPK14	2.50	<0.05						
ESR1	2.52	<0.05						
GAA	2.95	<0.005						
TMEM74	3.56	0.31	3.71	0.51			5.69	0.33
HGS	7.38	<0.05						

F.C. - Fold change; UP - unpurified; P - purified

The experiments described above were performed using biological rather than technical replicates due to limited availability of RNA, particularly amongst purified samples. We therefore validated a cohort of genes previously identified as being significantly differentially expressed among purified and/or un-purified lymphoma samples and included triplicate technical replicates and a NTC for each gene in each sample. Validation was carried out in a subset of un-purified primary samples for which sufficient amounts of good quality RNA were available. In total, validation was carried out in five RA, five FL and five DLBCL samples. Prior to calculation of RQ values triplicate C_T values returned for each gene following qRT-PCR were compared for similarity by assessing their SD. Only replicates with a SD of ≤ 0.5 were carried forward for further analysis meaning in some instances duplicate rather than triplicate C_T values were used to generate the average C_T of a gene. Data were normalised to averaged RPLPO and RQ and FC values calculated as previously described.

Five genes previously identified as being significantly up-regulated in lymphoma samples were selected for validation. *MAP1LC3A* was validated as it was found to be up-regulated in purified FL and DLBCL B cells and un-purified FL samples (Table 5.3) while *DRAM1* was validated due to its increased expression in un-purified DLBCL and FL and purified DLBCL samples (Table 5.4). *CTSD*, *BECN1* and *Atg4B* were also included in the validation cohort due to their high FC in one or more population (Table 5.3).

Expression levels of *MAP1LC3A*, *Atg4B* and *DRAM1* were found to be significantly up-regulated in un-purified FL and DLBCL samples respectively compared to RA controls (Table 5.5), confirming our previous findings. *CTSD* was also found to be significantly up-regulated in both patient cohorts, again in line with our previous findings (Table 5.5). *BECN1* and *DRAM1* were not up-regulated ≥2-fold in this un-purified FL cohort which may be due to a smaller sample size. Unsurprisingly, *BECN1*, *Atg4B* and *MAP1LC3A*, which were not previously identified as being significantly differentially expressed in DLBCL patients, were not up-regulated in this validation cohort (Table 5.5).

Table 5.5 Validation of differential expression of autophagy-related genes in FL and DLBCL samples compared to RA controls

Gene name and function	FL				DLBCL			
	F.C (Array)	P value	F.C (V)	P value	F.C (Array)	P value	F.C (V)	P value
BECN1	2.07	<0.005	1.46	0.06			1.23	0.46
MAP1LC3A	2.60	<0.005	2.08	<0.05			1.59	0.32
ATG4B	4.66	<0.005	2.72	<0.05			1.78	0.13
DRAM1	2.38	<0.05	1.05	0.18	4.24	<0.05	5.77	0.05
CTSD	2.41	<0.05	2.27	<0.05	4.13	<0.05	8.99	<0.05

F.C. - Fold change; P - purified; Array - microarray; V - validation

These validation experiments confirmed differential expression of autophagy-related genes in a smaller cohort of un-purified primary FL and DLBCL samples, indicating that our previous experiments accurately identified differentially expressed autophagy-related genes despite lack of technical replicates.

Having shown FL has higher basal level autophagy at the gene level, we next evaluated if increased mRNA levels of autophagy-related genes translates into increased protein expression. Using Western blotting, we examined protein expression levels of *Atg4B* and *ULK1*, which were previously identified as being up-regulated in purified and/or un-purified FL samples. Protein expression levels were evaluated in un-purified lymphoma and RA samples previously included in qRT-PCR analysis.

Based on densitometry values, expression levels of Atg4B and ULK1 were significantly higher in FL compared to DLBCL samples and RA controls (Figure 5.8). These data indicate increased expression of autophagy-related genes in FL patients translates into increased protein expression and that basal level autophagy is higher in FL patients at both the gene and protein level, further indicating overexpression of BCL-2 does not inhibit autophagy in these patients.

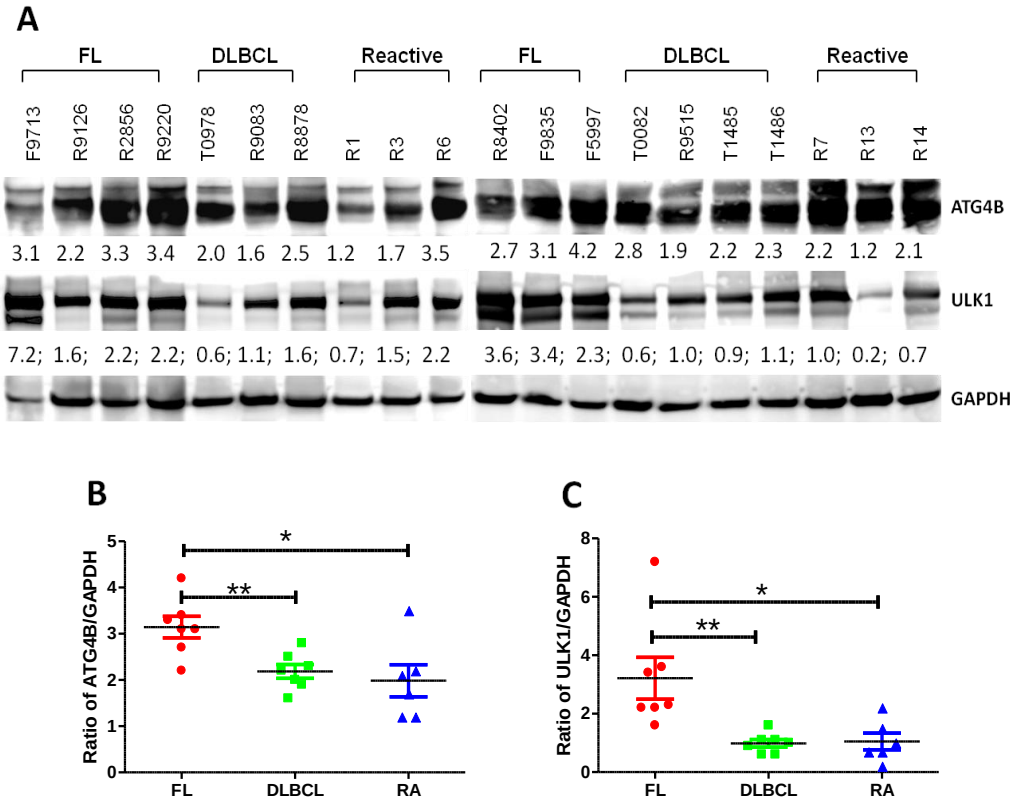

Figure 5.8 Analysis of expression levels of autophagy-related proteins in un-purified primary FL, DLBCL and RA tissues

50µg whole cell lysates extracted from primary tissue samples were loaded onto a 4-12% Bis-Tris gel and proteins separated by SDS-PAGE. Autophagy-related proteins Atg4B and ULK1 were visualised by Western blotting; GAPDH was used as a loading control. Bands are representative of a single experiment. Densitometry values were obtained as previously described and represent the ratio of specific proteins to GAPDH (A). Differences in expression levels/densitometry values were compared using a student t-test (B, C). Data representative of a single experiment. * p< 0.05, ** p< 0.05, *** p< 0.001.

5.2.5 Autophagy-related genes are up-regulated in cells of the tumour microenvironment

CTSD and *TGM2*, which are predominantly expressed by stromal cells, fibroblasts and macrophages (Martinez et al., 2013; O'Donoghue et al., 1995), were significantly up-regulated at the mRNA level in un-purified FL and DLBCL and purified DLBCL B cells (Table 5.3 and 5.4) We therefore aimed to assess which cell type(s) express these proteins in lymphoma samples, and if their expression levels differ between patient samples and controls.

Primary RA and diagnostic FL and DLBCL samples on TMAs were stained for CTSD or TGM2 using IHC. We first assessed the morphology of cells expressing CTSD (Figure 5.9 A; top panel) and TGM2 (Figure 5.9 A; bottom panel) and found both proteins to be expressed by large elongated cells with an irregular shape, a morphology which does not resemble that of B cells. To confirm these proteins are primarily expressed by cells in the microenvironment, we stained DLBCL and RA samples on TMAs for the pan-macrophage marker CD68 (Figure 5.9 D) (Greaves et al., 2013) and observed that $CD68^{+}$, $CTSD^{+}$ and $TGM2^{+}$ cells were morphologically similar. Cells which highly expressed CTSD and TGM2 were confirmed to be macrophages by our histopathologist colleagues MC and RC. Expression of CTSD (Figure 5.9 E) and TGM2 (Figure 5.9 F) was significantly positively correlated with CD68 expression in 144 DLBCL patients, further confirming these lysosomal enzymes are expressed by macrophages, not B cells.

We also assessed if these proteins are differentially expressed between FL and DLBCL patients and RA controls. Using the automated ARIOL analysis system we quantified brown positive staining, indicative of CTSD or TGM2 expression, as the percent-stained area of viable tissue within cores. As each patient was arrayed in triplicate an average of these cores was taken as the percent stained area for CTSD or TGM2. Expression of CTSD was significantly higher in DLBCL patients (n=144) compared to RA controls (n=21; $p < 0.05$) (Figure 5.9 B), whereas protein levels of TGM2 were significantly lower (Figure 5.9 C). Both CTSD and TGM2 expressed at significantly

lower levels in FL patients compared to DLBCL patients and RA controls (Figure 5.9 B and C).

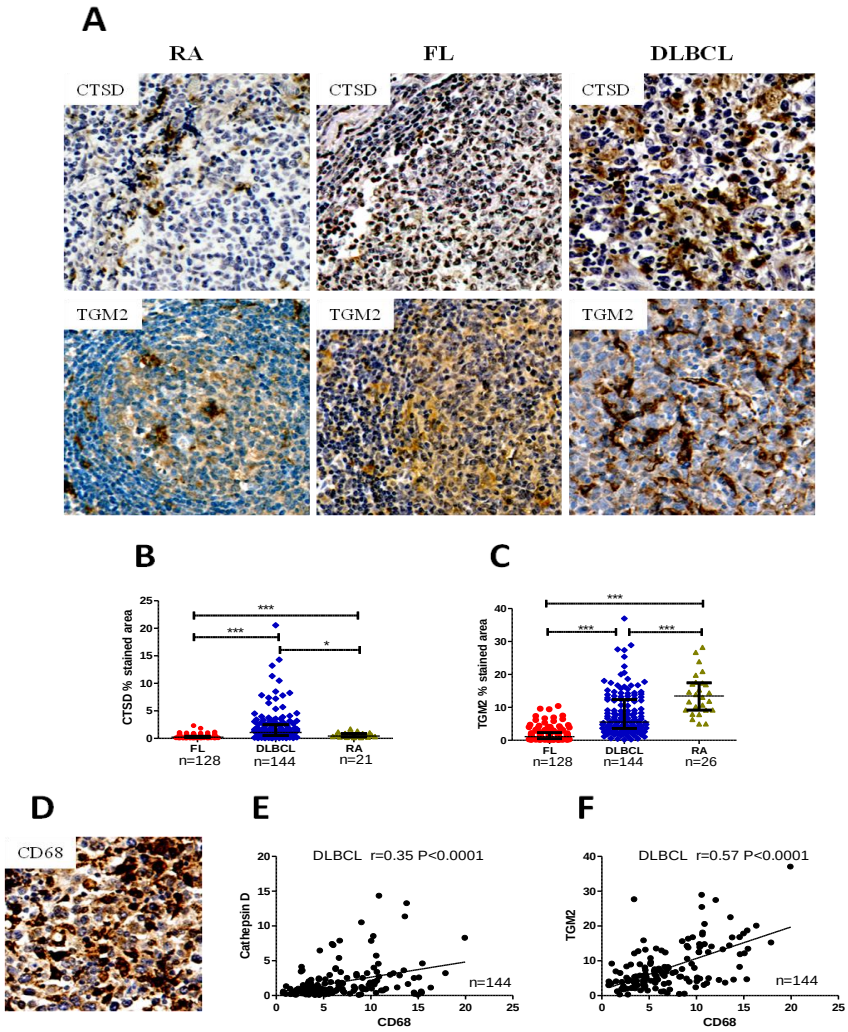

Figure 5.9 Analysis of CTSD and TGM2 expression in primary lymphoma samples using IHC

RA, diagnostic FL and diagnostic DLBCL TMAs previously constructed by AC and AO were stained for CTSD and TGM2, RA and DLBCL TMAs stained for CD68 and nuclei counterstained with haematoxylin. CD68 staining was previously carried out by RC and AC. Expression of these proteins is shown by HRP-DAB immunostaining and was analysed using the automated ARIOL analysis system which was trained to recognise areas of viable tumour and brown-positive staining. Positive brown staining was taken to be that staining which was strongest; non-specific, background staining was excluded. Representative images of CTSD and TGM2 staining in FL, DLBCL and RA tissue cores (A). CTSD and TGM2 expression was calculated as the average percent stained viable area for each patient and differences in expression levels of these proteins compared between samples using a student's t-test (B, C). Representative image of CD68 staining in a DLBCL tissue core (D). CD68 expression was analysed by RC as the average number of positive cells per patient within a viable tissue area. Expression levels of CTSD (E) and TGM2 (F) were correlated with CD68 expression in DLBCL patients using a Pearson's product-moment correlation method.

Next, we evaluated if cellular levels of CTSD or TGM2 could predict OS in our FL or DLBCL patient cohorts by performing a univariate, categorical analysis. X-tile software was used to generate optimal cut-points which divided FL and DLBCL patients into two groups based on CTSD or TGM2 levels. Kaplan-Meier curves were generated and significant differences in OS between groups evaluated using a log-rank (Mantel-Cox) test.

Increased expression of CTSD has previously been reported to predict a poor outcome in NHLs (Nicotra et al., 2010a). In agreement with these findings, we found that higher expression of CTSD was associated with shorter OS in FL and DLBCL (Figure 5.10 A and C). TGM2 did not predict outcome in either patient cohort (Figure 5.10 B and D), despite being identified as a prognostic marker in other malignancies (Miyoshi et al., 2010; Park et al., 2010).

These results show that CTSD and TGM2 proteins are primarily expressed by tumour-associated macrophages (TAMs), not malignant B cells. Evaluation of autophagy activity in un-purified tumour samples reflects expression of autophagy-related genes in not only tumour cells, but also tumour infiltrating cells. This may affect or skew accurate interpretation of autophagy gene expression levels and thus autophagy activity within a sample.

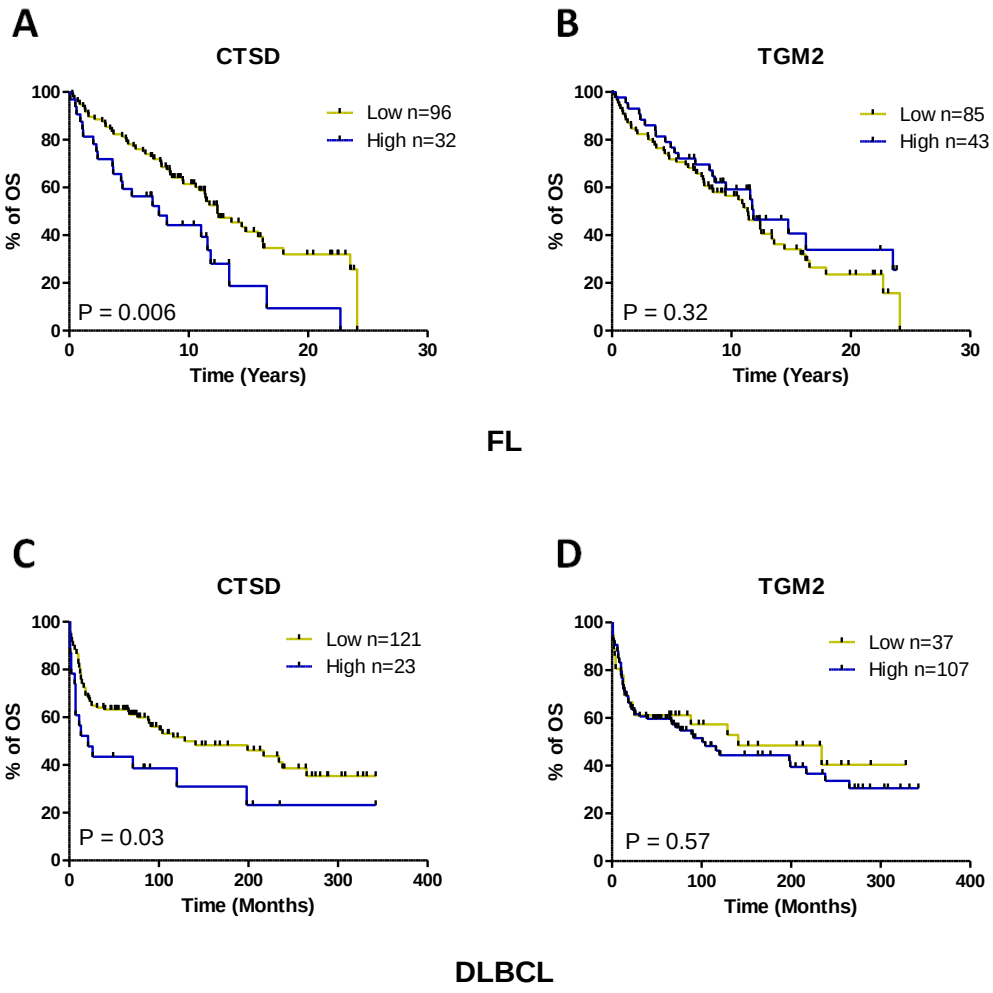

Figure 5.10 Higher levels of CTSD are associated with a poor prognosis in FL and DLBCL
Evaluation of OS in 128 FL and 144 DLBCL patients based on low and high (percent-stained viable tissue area) CTSD (A and C) and TGM2 (B and D) expression using Kaplan-Meier survival analysis. Patients were stratified into low and high protein expressing groups using optimal cut-points generated by the statistical software X-tile. Generation of Kaplan-Meier curves and evaluation of differences in survival between groups using a log-rank (Mantel-Cox) test were performed using GraphPad Prism software. *p* value of <0.05 was deemed significant. OS= overall survival; n= number.

5.3 Discussion

In this chapter we have demonstrated that overexpression of BCL-2 does not modulate the autophagy status or inhibit basal level autophagy flux in B-cell lymphomas. FL, which frequently overexpresses BCL-2 showed higher expression of autophagy-related genes compared to RA-LN controls. We therefore propose that despite increased expression of BCL-2, autophagy activity may be up-regulated in FL samples.

As BCL-2 has previously been shown to inhibit autophagy in a cardiac BCL-2 transgenic mouse model (Pattingre et al., 2005), we reasoned that overexpression of BCL-2 in B-cell NHLs might lead to autophagy inhibition. We therefore evaluated the autophagy status and autophagy flux of BCL-2^{HIGH} and BCL-2^{LOW} DLBCL cell lines at the protein and gene level to assess the effect of BCL-2 overexpression on autophagy activity in B-cell lymphomas. We found that BCL-2^{HIGH} Su-DHL4 cells had increased expression of a number of autophagy-related genes at the basal level compared to BCL-2^{LOW} Su-DHL8 cells. We also demonstrated that BCL-2^{HIGH} and BCL-2^{LOW} cells modulate the autophagy flux in a similar way following autophagy induction by starvation or inhibition with CQ, as demonstrated by similar patterns of p62 and LC3 accumulation and degradation respectively. Starvation-induced autophagy resulted in up-regulation of a greater number of genes in BCL-2^{HIGH} cells, suggesting that despite its increased expression BCL-2 does not inhibit the autophagy flux in BCL-2^{HIGH} cells at the basal level or following autophagy stress. Instead, BCL-2^{HIGH} cells appear to have higher basal level autophagy activity compared to BCL-2^{LOW} cells. A possible explanation for this is that inhibition of apoptosis by BCL-2 increases autophagy activity as a pro-survival mechanism to remove old and damaged cellular organelles and proteins which have accumulated within cells. It is also possible that increased expression of BCL-2 promotes increased basal level autophagy in cells where it is overexpressed, although the mechanistic route through which is may occur is currently unclear.

We also compared the autophagy-related GEP of primary NHL samples to RA to evaluate the role of BCL-2 in autophagy in the primary setting. B cells were purified from FL and DLBCL samples to assess the autophagy-associated gene signature of the

malignant cell population compared to RA B cells; the autophagy-related GEP of un-purified lymphoma and RA samples were also evaluated. As expected, *BCL-2* was expressed at a higher level in purified and un-purified FL samples compared to DLBCL samples and RA controls. Unsupervised hierarchical clustering identified FL B cells as having increased basal level expression of autophagy-related genes compared to DLBCL and RA samples. Among those genes significantly up-regulated in FL B cells were *ATG9A*, *MAP1LC3A* and *LAMP1*, which are involved in protein transport, vacuole formation and lysosomal degradation respectively. This suggests that despite overexpression of BCL-2, basal level autophagy is higher in FL B cells compared to DLBCL and RA controls. The autophagy status of DLBCL B cells varied; however due to limited sample numbers, autophagy activity within these malignant cells could not be fully elucidated.

Comparison of the autophagy-related GEP of un-purified FL, DLBCL and RA samples again identified FL samples as having higher autophagy-related GEPs and increased expression of autophagy-related genes compared to DLBCL and RA controls. Genes aberrantly expressed in FL samples included the autophagy-machinery genes *MAP1LC3A* and *LAMP1*, previously found to have increased expression in purified FL B cells and *CDKN2A*, *UVRAG* and *GABARAPL2* which were also up-regulated in BCL-2^{HIGH} Su-DHL4 cells following starvation-induced autophagy. These results again suggest that basal level autophagy activity is higher in FL samples, and that both DLBCL and RA samples have low basal level autophagy activity. Interestingly, a greater number of autophagy-related genes were significantly differentially expressed in un-purified FL samples compared to purified FL B cells, which suggests autophagy activity might also be altered in cells of the FL microenvironment.

Fewer genes were differentially expressed in DLBCL, irrespective of sample purity. *CTSD* and *TGM2*, which are involved in regulation of the autophagy flux through the lysosome and the autophagy-dependent clearance of ubiquitinated proteins respectively, were two of the three genes significantly up-regulated un-purified DLBCL samples. IHC staining showed that CTSD and TMG2 proteins in DLBCL were expressed by $CD68^{+}$ TAMs, not B cells. Both proteins were expressed at significantly lower levels in

FL, while CTSD was expressed at significantly higher levels in DLBCL compared to RA controls. In line with previous findings (Nicotra et al., 2010a), increased expression of CTSD was associated a shorter OS in FL and DLBCL patients. TGM2 was not identified as a prognostic marker in either NHL patient cohort, despite previously being shown to predict outcome in non-small cell lung cancer and colorectal cancer (Miyoshi et al., 2010; Park et al., 2010). Aberrant expression of *CTSD* and *TGM2* in DLBCL did not reflect their altered expression in malignant B cells but rather cells of the tumour microenvironment. We therefore propose that determination of autophagy-related gene expression using un-purified samples may be distorted by TAMs and other tumour-infiltrating cells.

The role of BCL-2 in autophagy in NHL is currently unclear. Here, we have shown that BCL-2^{HIGH} lymphoma cells, FL samples and cells of the FL microenvironment express autophagy-related genes at a higher basal level and have increased autophagy activity compared to RA controls, despite overexpression of BCL-2. The mechanism by which FL cells up-regulate autophagy at the gene level is currently unknown and may be due to multiple factors. One possibility is that inhibition of apoptosis by BCL-2 up-regulates autophagy to promote elimination of old, damaged organelles and proteins. It is also unclear if the autophagy status and autophagy activity of FL and DLBCL patients is associated with clinical outcome.

5.3.1 Conclusions

BCL-2 does not inhibit the autophagy flux at the basal level or in response to autophagy stress in BCL-2^{HIGH} lymphoma cell lines or primary FL samples. Increased expression of autophagy-related genes and autophagy activity in BCL-2^{HIGH} lymphoma cells may be a consequence of BCL-2-mediated inhibition of apoptotic cell death.

Chapter VI

Evaluation of the prognostic significance of autophagy-related proteins in non-Hodgkin’s lymphomas

6.1 Introduction

The clinical course of FL and DLBCL is highly variable (Shankland et al., 2012). FL and DLBCL patients are risk-stratified based on their FLIPI and IPI scores respectively. These are prognostic indexes based on clinical risk factors including age, Ann Arbor stages, numbers of extranodal sites, and serum LDH levels. Patients are classified as high risk if they present with more than three adverse clinical factors, for example Ann Arbor stage >III/IV, age >60 years and LDH levels >480U/L. However, these risk factor based indexes provide no information or understanding about the underlying biology of these indolent and aggressive malignancies (Johnson et al., 2012; Shankland et al., 2012). DLBCL can also be stratified by GEP into GCB- and ABC-subtypes, which have markedly different clinical outcomes (Alizadeh et al., 2000). While GCB/ABC stratification provides information on the biology of this aggressive malignancy, and can help explain the clinical heterogeneity observed among DLBCL patients, routine segregation of patients using GEP is currently not feasible in the clinical setting. However, advances in technology which allow for rapid turnover and declining costs mean that routine GEP analysis of patient tumour samples may soon become a reality (Alizadeh et al., 2000). Therefore, it is desirable to identify biomarkers which can stratify patients based on clinical outcome, are feasible for clinical use, and provide an understanding of disease biology.

Autophagy, whose activity varies among cancer types, can be tumour promoting or tumour suppressing (Choi et al., 2013a). The roles of this degradation pathway in NHL are currently unclear. Expression levels of the key autophagy-related proteins Beclin-1, LC3 and p62 have previously been shown to predict clinical outcome in a variety of malignancies. For example, accumulation of p62 due to defective autophagy has been shown to promote tumourigenesis and is associated with a worse prognosis in patients with oral cancer and adenocarcinoma (Inoue et al., 2012; Inui et al., 2013). Decreased expression of Beclin-1 has been identified as a poor prognostic marker in squamous cell carcinoma and extranodal natural killer T-cell lymphoma (Chen et al., 2009; Huang et al., 2010), while its increased expression was associated with a good clinical outcome in

a small cohort of FL and DLBCL patients (Huang et al., 2011; Nicotra et al., 2010b). It is unclear if Beclin-1 levels directly reflect autophagy activity.

The anti-apoptotic protein BCL-2, a co-regulator of apoptosis and autophagy, is overexpressed in ~85% of FL and ~20% of DLBCL patients (Kridel et al., 2012; Marquez and Xu, 2012; Obermann et al., 2009). The role of BCL-2 in autophagy regulation in FL and DLBCL is currently unknown. Similarly, whether expression levels of the key autophagy proteins p62, LC3 and Beclin-1 are altered in NHL, and whether their levels can predict clinical outcome in NHL, has not been reported. We therefore aimed to assess the basal level autophagy status of primary FL and DLBCL tissue biopsies at the protein level by evaluating expression levels of p62, LC3, Beclin-1 and BCL-2 using IHC and TMA technology. We also evaluated if expression levels of these proteins can be used as prognostic biomarkers to risk-stratify FL and/or DLBCL patients at diagnosis.

6.2 Results

6.2.1 p62, LC3 and Beclin-1 proteins are expressed at lower levels in primary FL tissue biopsies

Using IHC, we first determined expression levels of the key autophagy-related proteins p62, LC3 and Beclin-1 in primary FL, DLBCL and RA tissue biopsies present on TMAs to evaluate the autophagy status of FL and DLBCL compared to RA controls. TMAs used in this study were constructed using un-treated diagnostic tissue biopsy material from FL and DLBCL patients and non-malignant individuals.

Sequential FL, DLBCL and RA TMA sections were stained for the proteins of interest and expression levels, defined as the percent-stained viable tissue area, quantified using ARIOL (Lieca Microsystems) automated digital analysis software. An advantage of using this automated software is that user error, bias, variability and fatigue are avoided, ensuring consistent, uniform analysis of all samples. A user-defined classifier was created for each protein which selected only high intensity brown staining as positive protein expression; non-specific background staining was excluded (Figure 6.1 A; red arrows). A second classifier was created to determine the total viable tissue area per core. Protein expression levels, classified as the percent-stained viable tissue area, were then calculated by combining these classifiers. FL and RA samples were also stained with CD10 antibody, a marker of germinal centre (GC) B cells, to distinguish GC/intra-follicular areas ($CD10^+$) from non-GC/inter-follicular areas ($CD10^-$) (Figure 6.1 B). Diffuse cytoplasmic LC3-I was not distinguishable from membrane-bound LC3-II puncta using IHC; therefore, 'LC3' refers to total cellular levels of LC3.

Due to technical difficulties and tissue loss, not all patients present on the original TMAs were included in the final analysis. To ensure those patients used for further analysis were representative of the total patient population, clinical characteristics were compared between 'included' and 'excluded' patients. Using a chi-squared (χ^2) test, no significant difference was observed between staging and FLIPI scores of FL patients. A difference was observed between these groups with respect to clinical grade; however as this variable is incorporated into the FLIPI score which did not differ between groups, this subset of patients can still be considered representative of the total population.

DLBCL patient groups differed with respect to staging but not IPI scores, which include this variable. No significant difference was observed between DLBCL groups with respect to B symptoms or ECOG performance.

Comparison of protein expression levels between FL follicles, DLBCL whole cores and RA whole cores revealed that expression levels of p62, LC3 and Beclin-1 were significantly lower in FL follicles (Figure 6.2 A, C and E), while only Beclin-1 expression was significantly decreased in DLBCL samples (Figure 6.2 E). LC3 and Beclin-1 expression levels were heterogeneous among FL and DLBCL samples, whereas p62 was expressed at a homogeneously low level in FL (Figure 6.2 A, C and E). Significantly decreased expression of p62, LC3 and Beclin-1 was also observed in FL inter-follicular regions compared to $CD10^-$ areas in RA controls (Figure 6.2 B, D and F).

In this study, positive protein expression was defined as the highest, most intense brown cytoplasmic staining, indicative of protein accumulation and lower autophagy activity. Therefore, decreased expression of the autophagy substrates p62 and LC3 in FL follicles suggests an increased autophagy activity in FL compared to DLBCL and RA controls. Decreased expression of these autophagy-related proteins in inter-follicular regions of FL samples suggests autophagy activity is also increased in the microenvironment. We have previously shown that Beclin-1 expression levels were not altered in response to autophagy stress (Figure 5.3), indicating that it may not be an autophagy substrate. Therefore, differential expression of Beclin-1 in FL and DLBCL is unlikely to reflect altered autophagy activity in these NHLs.

These data indicate that basal level autophagy is higher in FL compared to DLBCL and RA controls, based on decreased expression/increased degradation of the autophagy substrates p62 and LC3. Our findings also suggest autophagy activity is increased in tumour-infiltrating cells of the microenvironment as well as tumour cells.

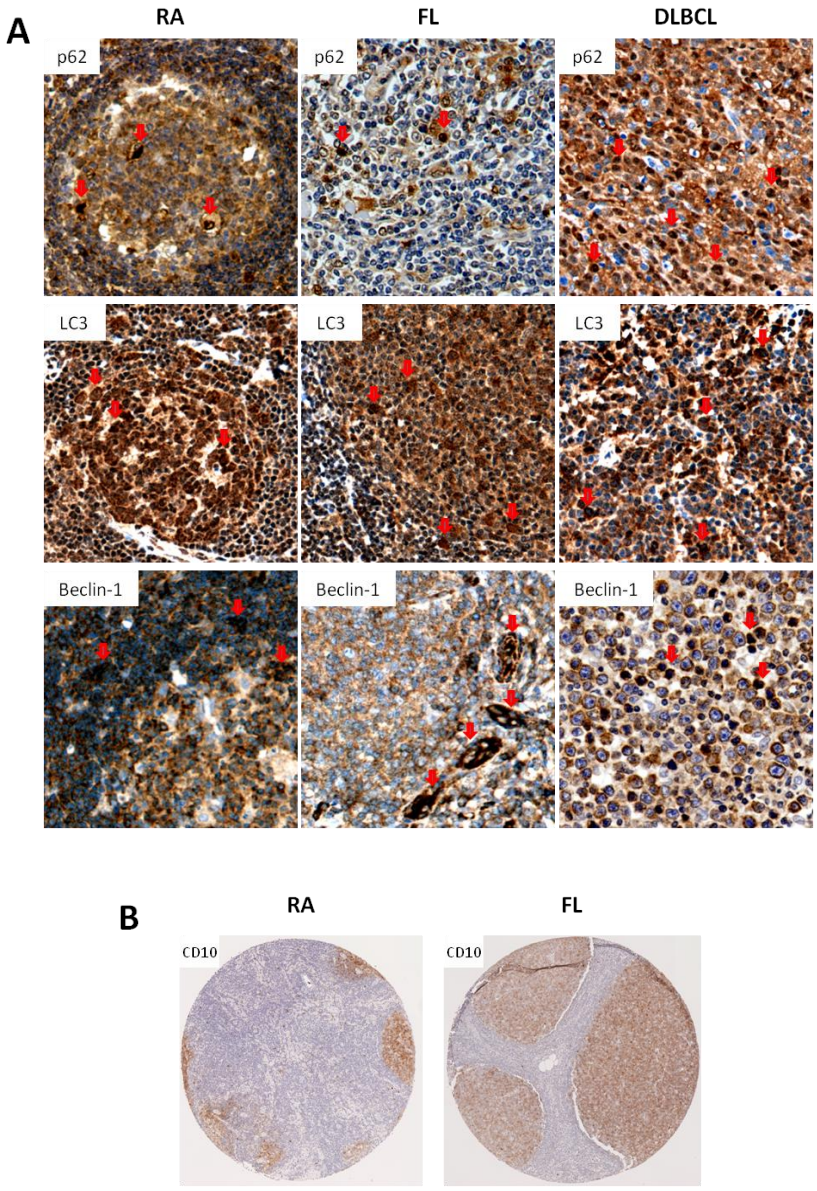

Figure 6.1 Representative images of immunohistochemical staining of p62, LC3, Beclin-1 and CD10 in primary RA, FL and DLBCL tissue

Representative images of p62, LC3 and Beclin-1 IHC staining in primary RA, diagnostic FL and diagnostic DLBCL tissue biopsies (A). RA, FL and DLBCL TMAs previously constructed by AC and AO were stained with polyclonal p62, polyclonal LC3B and mouse anti-Beclin-1 under optimised conditions; nuclei were counterstained with haematoxylin. Proteins were visualised using a peroxidase-labelled system which uses 3,3'-diaminobenzidine (DAB) as the chromogen (Super-Sensitive Polymer-HRP IHC Detection System, BioGenex). Positive brown staining was taken to be high-intensity, strong staining indicated by red arrows; weak, non-specific background staining was excluded. Representative images of CD10 staining in RA and FL tissue samples (B). CD10 was visualised using the DAB chromogen. GC/intra-follicular regions were selected based on $CD10^{+}$ staining and clear GC morphology; non-GC/inter-follicular regions were $CD10^{-}$.

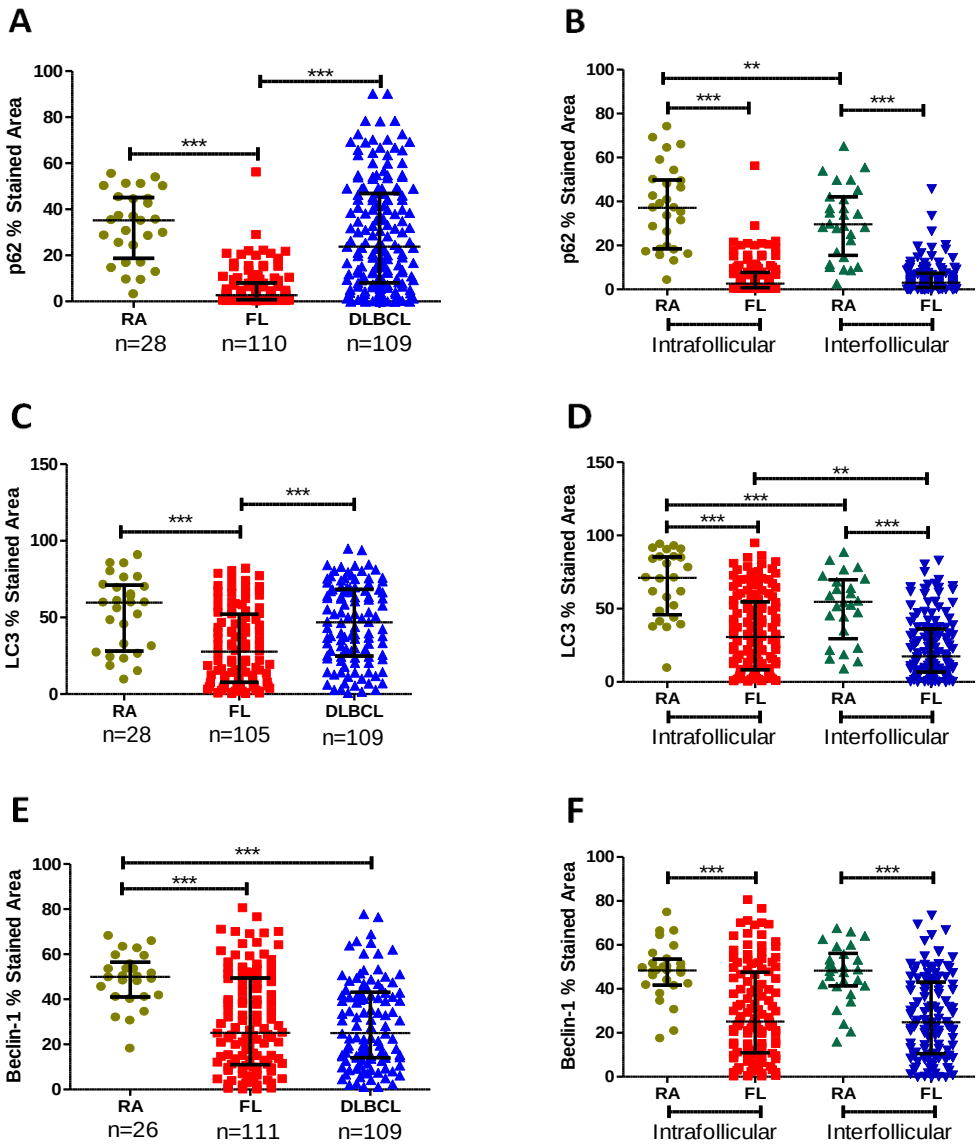

Figure 6.2 Comparison of p62, LC3 and Beclin-1 protein expression in primary RA, FL and DLBCL tissue samples

Expression levels of p62, LC3 and Beclin-1 previously stained by IHC (Figure 6.1) were analysed and quantified using the digital analysis software ARIOL, which was trained with the help of AC to recognise areas of brown positive staining as stipulated in figure 6.1 (classifier 1) and viable tumour areas (classifier 2) based on protein hue, saturation and intensity levels. Protein expression levels were calculated as the percent-stained viable tissue area by combining these classifiers and an average expression value obtained for each patient. Significant differences in protein expression levels, i.e. percent-stained viable tissue area, were compared between whole RA and DLBCL cores and FL $CD10^{+}$ follicles (A, C and E) and between inter- and intra-follicular regions in RA and FL samples (B, D and F) using a Mann Whitney U test. Data are presented as the median ± SD. Sample numbers are reported below each group; sample numbers for RA and FL in B, D and F were the same as in A, C and E. **p <0.01; *** p <0.001.

We also evaluated expression levels of the anti-apoptotic protein BCL-2 in FL, DLBCL and RA tissue biopsies (Figure 6.3). Using the ARIOL analysis system we calculated the percent BCL-2-positive cells in FL follicles, and RA and DLBCL whole cores. BCL-2 was strongly expressed in the inter-follicular regions of RA samples, ubiquitously expressed among DLBCL samples and strongly expressed in FL follicles (Figure 6.3 A). Samples were classified as overexpressing BCL-2 if >30% of cells were BCL-2 positive. As expected, the majority of FL samples (~90%) had significantly increased expression of BCL-2 in their follicles compared to DLBCL and RA controls, while expression was heterogeneous among DLBCL samples (Figure 6.3 B).

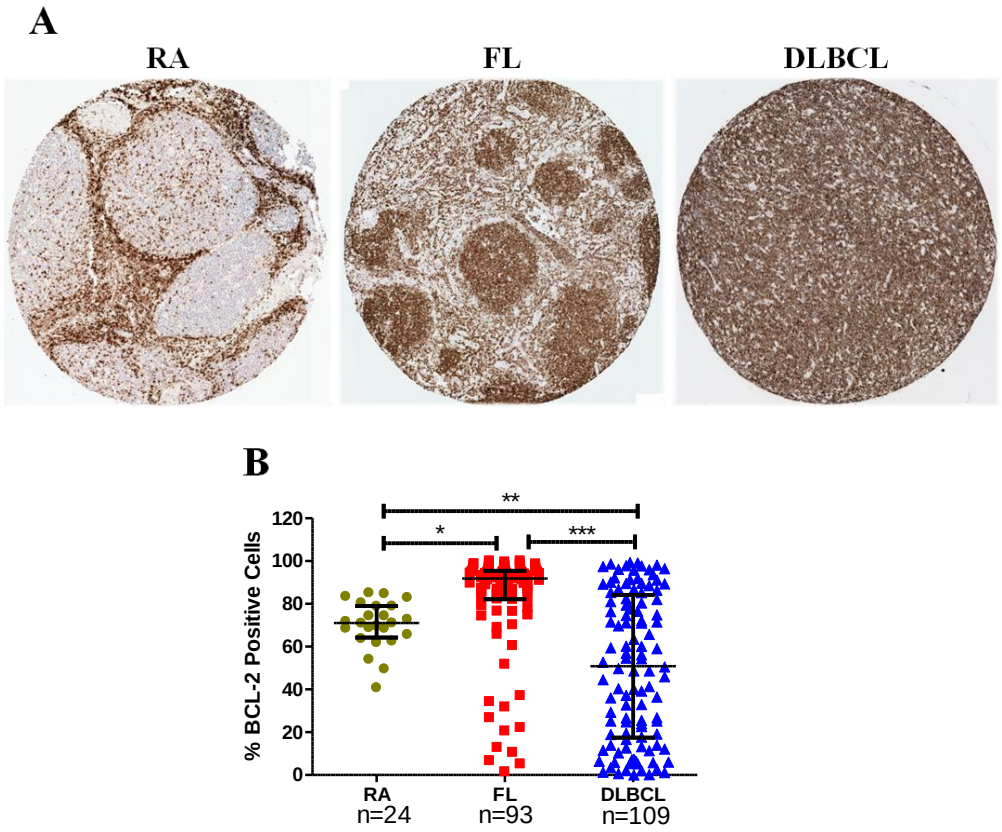

Figure 6.3 Evaluation of BCL-2 expression in primary RA, FL and DLBCL tissue biopsies
Representative images of BCL-2 IHC staining in primary RA, FL and DLBCL tissue cores (A). TMAs were stained for BCL-2 and nuclei counterstained with haematoxylin. BCL-2 expression visualised using the DAB chromogen and analysed using the ARIOL analysis system. Positive cells were taken to be cells with high-intensity, strong brown staining; weak, non-specific background staining was excluded. Samples in which >30% of cells expressed BCL-2 were taken to be BCL-2 positive. Significant differences in the percent BCL-2-positive cells were compared between whole RA and DLBCL cores and FL $CD10^{+}$ follicles using a Mann Whitney U test (B). Data are presented as the median ± SD; sample numbers are reported below each group. * $p < 0.05$; ** $p < 0.01$; *** $p < 0.001$.

6.2.2 Expression levels of p62, LC3 and Beclin-1 were correlated in FL and DLBCL

In order to understand whether these autophagy-related proteins are associated with each other, we next assessed correlation between p62, LC3, Beclin-1 and BCL-2 expression levels in FL and DLBCL

Using the Pearson product-moment correlation method, we found that expression levels of p62 and LC3 were significantly positively correlated in FL ($p < 0.0001$; $\gamma = 0.536$), DLBCL ($p < 0.0001$; $\gamma = 0.589$) and RA ($p < 0.0001$; $\gamma = 0.659$) samples (Table 6.1). During active autophagy, p62 binds membrane-bound LC3 to facilitate delivery of autophagy substrates, including themselves, to the autophagosome for degradation. Observation of a positive correlation between these proteins suggests that cellular levels of p62 and LC3, individually or in combination, can be used as a marker of autophagy activity. However, in all sample types the correlation coefficient (γ) was low, indicating that the correlation was weak (Table 6.1). p62 also correlated with Beclin-1 in all three sample groups, while Beclin-1 levels were correlated with LC3 expression in DLBCL and FL samples but not RA controls (Table 6.1 B and C). There was a weak negative correlation between BCL-2 and p62 protein expression in FL samples ($p < 0.05$; $\gamma = -0.342$), which suggests that higher BCL-2 is correlated with lower p62, implying this anti-apoptotic protein does not inhibit autophagy in FL (Table 6.1 B). A significant positive correlation was observed between BCL-2 and p62, LC3 and Beclin-1 in DLBCL samples ($p < 0.01$; $\gamma < 0.5$) (Table 6.1 C).

These results demonstrate that expression levels of p62 and LC3 proteins can be used as markers of autophagy activity in primary FL and DLBCL samples. Increased expression of BCL-2 may not inhibit autophagy in FL.

Table 6.1 Evaluation of correlation between autophagy-related proteins in primary RA (A), FL (B) and DLBCL (C) tissue samples

A

Protein	Beclin-1	LC3	p62	Correlation parameters
BCL-2	0.079	0.140	0.166	γ
	>0.05	>0.05	>0.05	*P* value
	Beclin-1	0.005	0.453	γ
		>0.05	<0.05	*P* value
		LC3	0.659	γ
			<0.0001	*P* value

B

Protein	Beclin-1	LC3	p62	Correlation parameters
BCL-2	0.207	-0.087	-0.342	γ
	>0.05	>0.05	<0.05	*P* value
	Beclin-1	0.417	0.390	γ
		<0.01	<0.01	*P* value
		LC3	0.536	γ
			<0.0001	*P* value

C

Protein	Beclin-1	LC3	p62	Correlation parameters
BCL-2	0.359	0.281	0.275	γ
	<0.01	<0.01	<0.01	*P* value
	Beclin-1	0.573	0.359	γ
		<0.0001	<0.0001	*P* value
		LC3	0.589	γ
			<0.0001	*P* value

6.2.3 Decreased expression of p62 is associated with a worse prognosis in DLBCL

Having shown p62, LC3, Beclin-1 and BCL-2 proteins are differentially expressed in FL compared to DLBCL and RA samples, we next assessed if expression levels of these autophagy-related proteins, individually or in combination with BCL-2, can be used to predict outcome in FL and/or DLBCL patients at diagnosis.

Continuous and categorical univariate survival analysis was carried out in 117 FL and 109 DLBCL patients for whom FLIPI and IPI scores were available. Full patient information is given in the appendix (Appendix II, Table T and U).

The Cox proportional hazards model was used to evaluate the association between a continuous variable and a defined event, e.g. death, and estimate the Hazard ratio (HR) and its corresponding 95% confidence intervals (CI) for each variable. For a continuous variable, the HR represents the incremental increase of the event happening per unit increase in the variable. In order for a continuous variable to be classified as a prognostic marker the p value must be <0.05 and the HR must be greater than or less than, but not equal to 1.

Categorical univariate analysis divides patients into groups based on protein expression levels. First, X-tile software is used to identify the optimal cut-point at which patients separate into two groups with differential outcome. X-tile does this by dividing patients into training and validation sets in a ratio of 1:2, identifying the point at which patients in the training set separate into two groups and applying this cut-point to the validation set. Patients are then stratified into two groups, typically low and high, based on this cut-point and Kaplan-Meier curves generated to visualise differences in survival between groups. Significant differences in outcome due to differential protein expression are then evaluated using the log-rank (Mantel-Cox) test. HR and 95% CI are also generated in categorical survival analysis. Here, the HR represents the instantaneous risk of an event occurring in one group but not the other by the next time point; for example a HR of 2 would indicate that the event, e.g. death, is twice as likely to occur in one group over the other. The clinical outcomes evaluated in this study were

OS, DSS, TT and PFS which were measured from the date of diagnosis to the date of event occurrence or date of last follow-up.

Using univariate continuous and categorical analysis, we confirmed FLIPI and IPI to be prognostic markers of OS and DSS in FL and DLBCL, respectively. As expected, both FL (Appendix II, Table V) and DLBCL (Appendix II, Table W) patients with a FLIPI or IPI score >3 (i.e. FLIPI/IPI^{HIGH}) had significantly shorter OS and DSS rates compared to patients with low FLIPI/IPI scores (Appendix II, Figure 4). TT was also significantly lower in FLIPI^{LOW} patients.

We assessed expression levels of p62, LC3, Beclin-1 and BCL-2 for their ability to predict outcome in FL and DLBCL. In a continuous, univariate analysis we found that p62 expression levels were prognostically significant in DLBCL for OS (p= 0.015) and DSS (p= 0.037) (Table 6.2) and that the HR was lower than 1, with a negative regression coefficient, indicating that lower expression of p62 is associated with a worse clinical outcome. This result indicates that p62 is an independent prognostic biomarker for DLBCL. LC3, Beclin-1 and BCL-2 expression levels were not associated with outcome in DLBCL (Table 6.2). None of these autophagy-related proteins were identified as prognostic biomarkers for OS, DSS or TT in FL using continuous data analysis (Table 6.3).

Table 6.2 Univariate Cox-regression analysis of autophagy-related proteins as continuous variables in DLBCL

Variable	Overall survival		Disease-specific survival		Progression-free survival	
	HR (95% CI)	***P***	**HR (95% CI)**	***P***	**HR (95% CI)**	***P***
p62	0.98 (0.97-1.00)	0.015	0.98 (0.97-1.00)	0.037	0.99 (0.97-1.00)	0.090
LC3	0.99 (0.98-1.00)	0.256	1.00 (0.98-1.01)	0.610	0.99 (0.98-1.00)	0.125
Beclin-1	0.99 (1.00-1.01)	0.245	0.99 (0.97-1.01)	0.210	0.99 (0.97-1.01)	0.398
BCL-2	1.00 (1.00-1.01)	0.282	1.00 (0.99-1.01)	0.385	1.00 (0.99-1.00)	0.082

HR= Hazard ratio; CI= Confidence interval

Table 6.3 Univariate Cox-regression analysis of autophagy-related proteins as continuous variables in FL

Variable	Overall survival		Disease-specific survival		Time to Transformation	
	HR (95% CI)	***P***	**HR (95% CI)**	***P***	**HR (95% CI)**	***P***
p62	1.02 (0.98-1.06)	0.432	1.02 (0.97-1.07)	0.360	1.03 (0.97-1.09)	0.358
LC3	1.00 (0.99-1.01)	0.665	1.00 (0.99-1.01)	0.901	1.00 (0.99-1.02)	0.771
Beclin-1	0.99 (0.98-1.01)	0.474	0.99 (0.97-1.01)	0.214	1.00 (0.99-1.02)	0.795
BCL-2	1.00 (0.99-1.01)	0.893	1.00 (0.99-1.02)	0.548	0.99 (0.98-1.00)	0.146

HR= Hazard ratio; CI= Confidence interval

We next evaluated the prognostic significance of these autophagy-related proteins using a univariate categorical analysis. FL and DLBCL patients were divided into two groups with low and high expression of autophagy-related proteins (e.g. $p62^{LOW}$ and $p62^{HIGH}$) for each outcome evaluated using X-tile generated cut-points (Appendix II, Table X). Separation of groups was visualised using Kaplan-Meier curves and significant differences in outcome arising from differential protein expression analysed using a log-rank (Mantel Cox) test.

Lower expression of p62 ($p62^{LOW}$) in DLBCL patients was significantly associated with shorter OS, DSS and PFS rates compared with $p62^{HIGH}$ patients (Figure 6.4 A-C). 5 year survival rates were worse for patients expressing lower levels of p62 (Appendix II, Table Y). This finding indicates that increased autophagy activity is associated with a poor prognosis in DLBCL and confirms that p62 is a prognostic biomarker of clinical outcome in this aggressive lymphoma.

Although decreased expression of p62 was associated with a shorter TT (p= 0.07) among FL patients, its levels did not reach prognostic significance. Similarly, OS and DSS rates did not differ between $p62^{HIGH}$ and $p62^{LOW}$ patients (Figure 6.5 A-C) (Appendix II, Table Z). This suggests that despite FL expressing p62 at significantly lower levels compared to DLBCL samples and RA controls, levels of this autophagy substrate do not impact or predict clinical outcome in this indolent lymphoma.

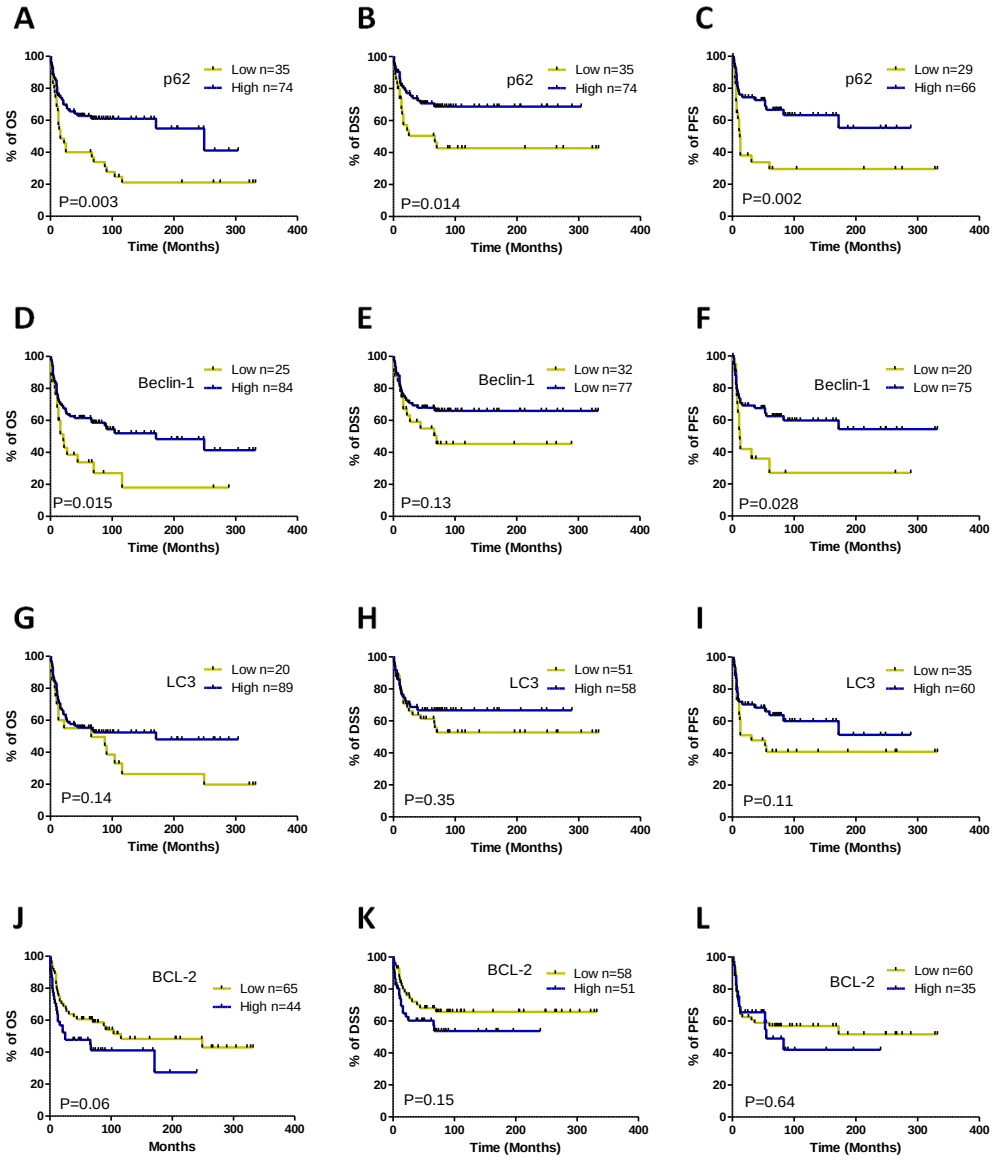

Figure 6.4 Decreased expression of key autophagy-related proteins in DLBCL predicts a worse clinical outcome

Evaluation of OS, DSS and PFS in DLBCL patients based on low and high expression of the key autophagy related proteins p62 (A-C), Beclin-1 (D-F), LC3 (G-I) and BCL-2 (J-L). Patients were stratified into low and high protein groups using optimal cut-points generated by the statistical software X-tile. X-tile generated cut-points are listed in appendix II, Table X. Generation of Kaplan-Meier curves and evaluation of differences in survival between groups using a log-rank (Mantel-Cox) test was performed using GraphPad Prism software. OS= overall survival; DSS= disease specific survival; PFS= progression free survival; n= number.

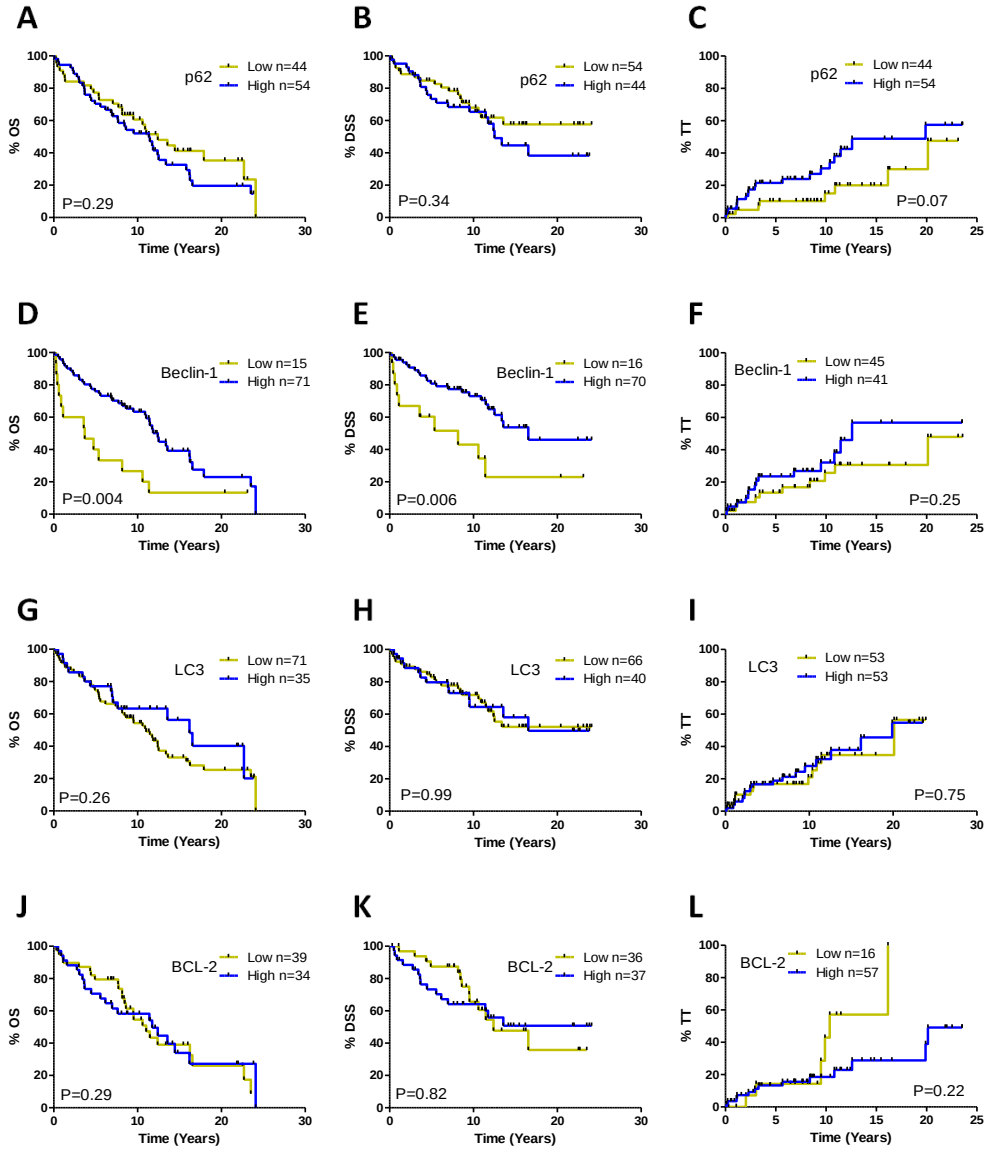

Figure 6.5 Decreased expression of Beclin-1 predicts shorter overall and disease specific survival in FL

Evaluation of OS, DSS and TTT in FL patients based on low and high expression of the key autophagy related proteins p62 (A-C), Beclin-1 (D-F), LC3 (G-I) and BCL-2 (J-L). Patients were stratified into low and high protein expressing groups as previously described. X-tile generated cut-points are listed in appendix II, Table X. Kaplan-Meier curves were generated and differences in survival compared as previously described. OS= overall survival; DSS= disease specific survival; TT= Time to transformation; n= number.

Multivariate proportional hazards model analysis was performed to further confirm p62 is an independent prognostic biomarker of clinical outcome in DLBCL. This multivariate analysis evaluates the prognostic significance of p62 following adjustment for IPI scores and LC3, BCL-2 and Beclin-1 expression levels. The prognostic value of p62 in FL was not evaluated by multivariate analysis as it was not identified as a significant biomarker using univariate analysis.

Following adjustment by IPI scores, p62 retained its prognostic significance for OS and DSS, further confirming that p62 can be used as an independent biomarker of clinical outcome in DLBCL (Table 6.4). For both parameters evaluated, the HR returned for p62 was >1 (OS: HR= 2.06; DSS: HR= 1.97). As comparisons were made between $p62^{LOW}$ and $p62^{HIGH}$ patients following adjustment for IPI scores, these HR values confirm that patients expressing low levels of p62 have a worse prognosis compared to patients expressing this protein at high levels. Adjustment of p62 by LC3, Beclin-1 or BCL-2 expression levels confirmed this autophagy-substrate is a prognostic biomarker in DLBCL independent of LC3, Beclin-1 or BCL-2 expression.

These results demonstrate for the first time that p62 is a novel independent biomarker for clinical outcome in patients with DLBCL, and that decreased expression of this autophagy substrate predicts a worse outcome. It will be important to validate these findings in an independent patient cohort, and it would also be desirable to evaluate if p62 retains its prognostic significance following adjustment for GCB/ABC-subtype classification.

Table 6.4 Categorical multivariate proportional hazard model analysis for IPI, p62, LC3, Beclin-1 and BCL-2 in DLBCL and for Beclin-1 in FL

Disease	Covariates	OS		DSS	
		HR (95% CI)	***P***	**HR (95% CI)**	***P***
DLBCL	**IPI**[a]	0.47 (0.25-0.89)	0.02	0.40 (0.19-0.84)	0.02
	p62 [b]	2.41 (1.35-4.28)	0.003	2.40 (1.19-4.85)	0.014
	BCL-2 [b]	0.59 (0.33-1.02)	0.060	0.63 (0.33-1.19)	0.151
	Beclin-1 [b]	2.29 (1.17-4.47)	0.015	1.73 (0.85-3.51)	0.130
	LC3 [b]	1.66 (0.84-3.25)	0.143	1.36 (0.72-2.56)	0.346
	IPI[a]	0.53 (0.30-0.92)	0.02	0.47 (0.25-0.89)	0.02
	p62[b]	2.06 (1.22-3.47)	0.007	1.97 (1.05-3.70)	0.04
	IPI[a]	0.56 (0.32-0.98)	0.04	0.50 (0.26-0.94)	0.03
	BCL-2[b]	0.70 (0.41-1.18)	0.18	0.76 (0.41-1.42)	0.40
	IPI[a]	0.57 (0.33-1.00)	0.05	0.51 (0.27-0.97)	0.04
	Beclin-1[b]	1.67 (0.94-2.97)	0.08	1.64 (0.83-3.24)	0.16
	IPI[a]	0.52 (0.30-0.91)	0.02	0.47 (0.25-0.89)	0.02
	LC3 [b]	1.61 (0.87-2.96)	0.13	1.41 (0.64-3.05)	0.40
	p62 [b]	2.15 (1.67-3.95)	0.01	2.67 (1.25-5.72)	0.01
	BCL-2 [b]	0.49 (0.28-0.87)	0.01	0.53 (0.28-1.01)	0.05
	Beclin-1 [b]	1.74 (0.98-3.10)	0.06	1.69 (0.87-3.29)	0.12
	LC3 [b]	1.22 (0.61-2.42)	0.58	0.80 (0.37-1.69)	0.55
FL	**FLIPI**[C]	0.44 (0.25-0.76)	0.003	0.46 (0.23-0.92)	0.03
	Beclin-1 [b]	3.39 (1.47-7.83)	0.004	3.94 (1.47-10.6)	0.006
	FLIPI[c]	0.43 (0.25-0.76)	0.003	0.46 (0.23-0.93)	0.03
	Beclin-1[b]	2.47 (1.31-4.67)	0.005	2.63 (1.21-5.73)	0.02

'a': comparison was low (IPI 0-2) *vs.* high (IPI 3-4); 'b': comparison was low expression *vs.* high expression for each protein; 'c': comparison was low (FLIPI 1-2) *vs.* high (FLIPI 3-4). DLBCL: n=109. FL: n=86. Data shown were either as single risk factor or in combination with other factor(s) in the same panel. OS= overall survival; DSS= disease specific survival; PFS= progression free survival; n= number

6.2.4 Beclin-1 is an independent biomarker of clinical outcome in FL

We next evaluated the prognostic significance of Beclin-1 in FL and DLBCL using categorical analysis. Patients were classified as Beclin-1^{LOW} or Beclin-1^{HIGH} as previously described (Appendix II, 4.0 Table X) and differences in survival analysed using a log-rank (Mantel Cox) test.

In agreement with its role as a tumour suppressing protein, decreased expression of Beclin-1 was significantly associated with shorter OS and PFS in our DLBCL patient cohort (Figure 6.4 D-F). Unsurprisingly, 5 year OS and PFS rates were significantly lower in Beclin-1^{LOW} DLBCL patients (Appendix II, Table Y). After adjusting for IPI scores, Beclin-1 lost its prognostic significance in DLBCL (Table 6.4). This demonstrates that while its expression levels are associated with clinical outcome, Beclin-1 is not an independent prognostic marker of outcome in DLBCL. Lower levels of Beclin-1 were significantly associated with shorter OS and DSS in FL (Figure 6.5 D-F) (Appendix II, Table Z). Using multivariate analysis, Beclin-1 retained its prognostic significance, indicating that it is an independent prognostic biomarker of clinical outcome in FL patients, irrespective of patients FLIPI scores (Table 6.4).

These findings indicate that although Beclin-1 expression may not reflect autophagy activity within a sample, levels of this autophagy-essential tumour suppression protein, which were decreased in both FL and DLBCL, can be as an independent biomarker for predicting clinical outcome in patients with FL but not DLBCL.

6.2.5 LC3 or BCL-2 alone do not predict clinical outcome in patients with FL or DLBCL

Although a trend was observed between decreased expression of LC3 and shorter OS, DSS and PFS, its levels were not found to be prognostically significant in DLBCL, as analysed by univariate and multivariate analysis (Figure 6.4 G-I, Table 6.4). Similarly, although it was expressed at significantly lower levels in FL patients compared to RA-LN controls, LC3 expression did not impact or predict clinical outcome in FL (Figure 6.5 G-I). This suggests that levels of this autophagy-substrate may not be of prognostic value in NHL.

Previous studies have reported BCL-2 as being a prognostic marker in DLBCL, with BCL-2^{LOW} patients having a more favourable outcome compared to BCL-2^{HIGH} patients (Gascoyne et al., 1997). We found that in our DLBCL cohort, while there was a trend towards a poor prognosis among BCL-2^{HIGH} patients, expression levels of this anti-apoptotic protein alone did not predict outcome in DLBCL (Figure 6.4 J-L); however in the multivariate analysis, BCL-2 gained statistical significance when it was adjusted by p62, LC3 and Beclin-1 expression levels (Table 6.4). This indicates that the prognostic value of BCL-2 in DLBCL is dependent on other autophagy-related biomarkers. No difference in survival rates was observed between BCL-2^{HIGH} and BCL-2^{LOW} FL patients, indicating BCL-2 expression levels do not impact on survival in this indolent NHL (Figure 6.5 J-L). This finding is in agreement with previous reports (Llanos et al., 2001).

These results demonstrate that neither LC3 nor BCL-2 alone predict clinical outcome in DLBCL or FL, and that BCL-2 is a dependent marker of survival in this aggressive NHL.

6.2.6 Lower levels of autophagy-related proteins combined with high BCL-2 expression predicts a worse outcome in DLBCL

The results above show that the prognostic value of BCL-2 in DLBCL is dependent on other biomarkers. We therefore evaluated the impact of BCL-2 expression levels on autophagy status and clinical outcome based on combined expression levels of the autophagy related proteins p62, LC3 and Beclin-1 with BCL-2.

Using cut-points previously generated in X-tile (Appendix II, Table X), patients were divided into four groups based on expression levels of BCL-2 and p62: BCL-2^{LOW}/$p62^{LOW}$; BCL-2^{LOW}/$p62^{HIGH}$; BCL-2^{HIGH}/$p62^{LOW}$; BCL-2^{HIGH}/$p62^{HIGH}$. Patients were categorised in the same way based on BCL-2/LC3 expression and BCL-2/Beclin-1 expression. We then compared OS and DSS between these four groups using the Kaplan-Meier method and a multivariate Cox-regression analysis. This analysis was carried out in DLBCL patents only, as ~90% of FL patients overexpressed BCL-2 (Figure 6.3), meaning too few BCL-2^{LOW} cases were available with which meaningful comparisons could be made.

We found that patients with high levels of autophagy-related proteins and low levels of BCL-2 had a favourable clinical outcome compared to patients with high BCL-2 and low levels of p62, LC3 or Beclin-1 (Figure 6.6). BCL-2^{HIGH}/$p62^{LOW}$ patients showed the shortest OS and DSS compared to all other groups, particularly BCL-2^{LOW}/$p62^{HIGH}$ patients (Figure 6.6 A and B). A multivariate Cox-regression analysis confirmed a significant difference in survival rates between BCL-2^{HIGH}/$p62^{LOW}$ and BCL-2^{LOW}/$p62^{HIGH}$ patients (Table 6.5 A). Combining BCL-2 and Beclin-1 expression levels, BCL-2^{HIGH}/Beclin-1^{LOW} and BCL-2^{LOW}/Beclin-1^{LOW} patients were shown to have significantly shorter OS compared with BCL-2^{LOW}/Beclin-1^{HIGH} patients (Figure 6.6 C). BCL-2^{HIGH}/Beclin-1^{LOW} patients also had significantly shorter DSS (Figure 6.6 D; Table 6.5 B). Similarly, patients categorised as BCL-2^{HIGH}/$LC3^{LOW}$ were found to have significantly shorter OS and DSS compared to BCL-2^{LOW}/$LC3^{HIGH}$ patients (Figure 6.6 E and F; Table 6.5 C).

These data indicate that inhibition of apoptosis due to increased BCL-2 expression, combined with decreased expression of the autophagy-substrates p62 and LC3, an

indicator of increased autophagy activity, predicts a worse outcome in DLBCL. As the number of patients analysed in some groups was limited, it will be important to validate these findings in a larger, independent cohort of patients.

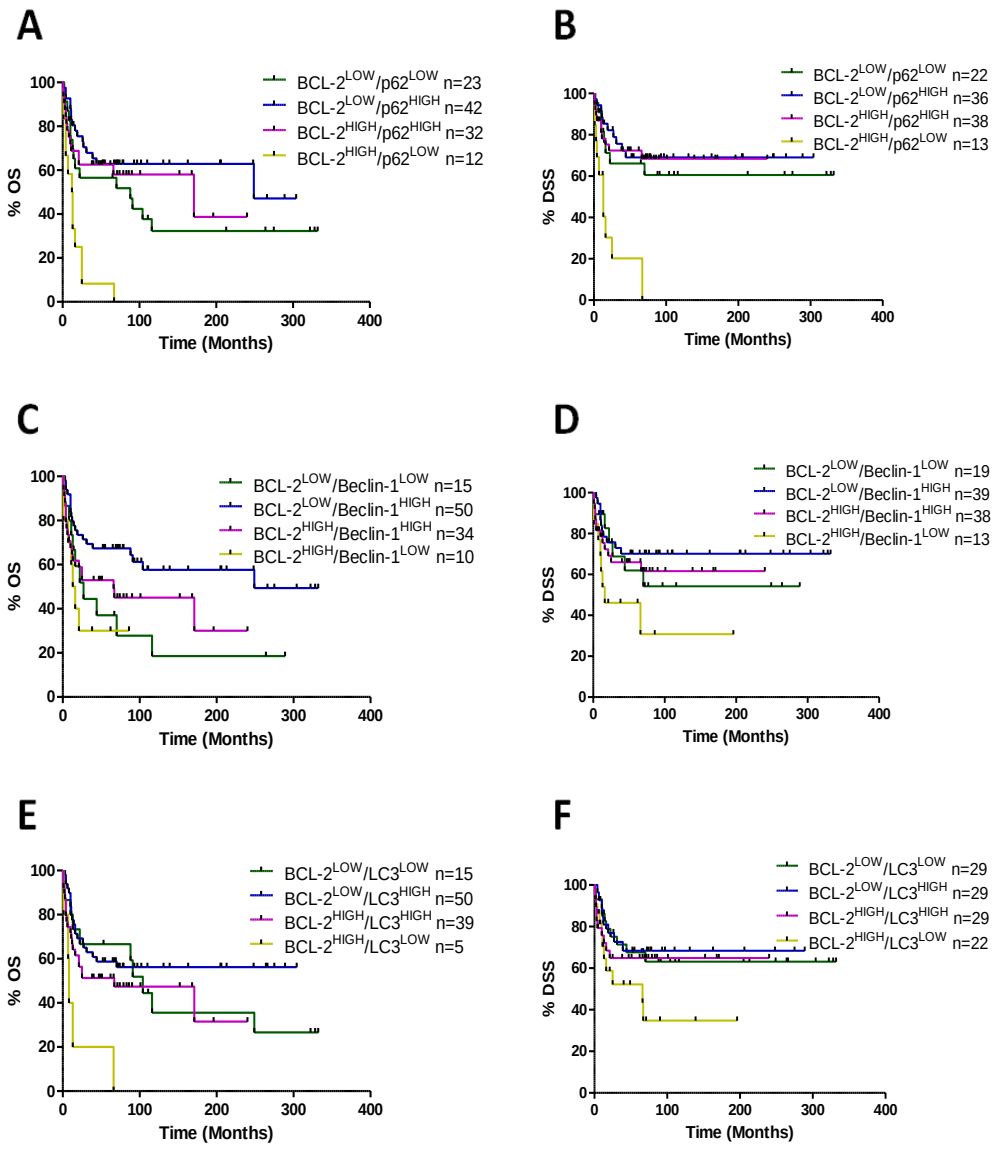

Figure 6.6 Decreased expression of p62 combined with BCL-2 overexpression predicts a worse outcome in DLBCL

Evaluation of OS and DSS in DLBCL patients based on low and high expression of the key autophagy related proteins p62 (A and B), Beclin-1 (C and D) and LC3 (E and F) in combination with BCL-2. Patients were stratified into four groups, using optimal cut-points previously generated using X-tile software (Appendix II, Table X), based on low or high expression of autophagy-related proteins and low or high BCL-2 expression. Kaplan-Meier curves were generated using GraphPad Prism software and differences in survival outcomes evaluated using a Cox-regression analysis and SPSS software. OS= overall survival; DSS= disease specific survival; n= number.

Table 6.5 Categorical multivariate analysis of expression levels of autophagy-related proteins in combination with BCL-2 expression levels in primary DLBCL samples

A

Variable	Overall survival		Disease-specific survival	
	HR (95% CI)	***P***	**HR (95% CI)**	***P***
BCL-2^{LOW}/p62^{HIGH}		<0.0001		0.001
BCL-2^{HIGH}/p62^{HIGH}	1.27 (0.63-2.59)	0.65	1.02 (0.44-2.35)	0.97
BCL-2^{LOW}/p62^{LOW}	1.61 (0.79-3.23)	0.30	1.23 (0.49-3.05)	0.66
BCL-2^{HIGH}/p62^{LOW}	4.95 (2.32-10.61)	<0.0001	4.69 (1.96-11.29)	<0.0001

BCL-2^{LOW} /p62^{HIGH} = Reference against which all other groups were compared

B

Variable	Overall survival		Disease-specific survival	
	HR (95% CI)	***P***	**HR (95% CI)**	***P***
BCL-2^{LOW}/ Beclin-1^{HIGH}		0.045		0.19
BCL-2^{HIGH}/ Beclin-1^{HIGH}	1.75 (0.93-3.27)	0.08	0.37 (0.15-0.92)	0.51
BCL-2^{LOW}/ Beclin-1^{LOW}	2.17 (1.05-4.52)	0.04	0.49 (0.2-1.18)	0.59
BCL-2^{HIGH}/ Beclin-1^{LOW}	2.89 (1.21-6.93)	0.02	0.48 (0.18-1.34)	0.03

BCL-2^{LOW} /Beclin-1^{HIGH} = Reference against which all other groups were compared

C

Variable	Overall survival		Disease-specific survival	
	HR (95% CI)	***P***	**HR (95% CI)**	***P***
BCL-2^{LOW}/LC3^{HIGH}		0.22		0.15
BCL-2^{LOW}/LC3^{LOW}	1.36 (0.64-2.89)	0.42	1.02 (0.42-2.52)	0.97
BCL-2^{HIGH}/LC3^{HIGH}	1.5 (0.82-2.74)	0.19	1.17 (0.48-2.88)	0.65
BCL-2^{HIGH}/LC3^{LOW}	4.69 (1.75-12.58)	0.002	2.04 (0.84-4.93)	0.04

BCL-2^{LOW} /LC3^{HIGH} = Reference against which all other groups were compared

These results indicate that decreased levels of the autophagy substrates p62 and LC3, which indicates active autophagy, coupled with inhibition of apoptosis due to BCL-2 overexpression, predicts a worse outcome in DLBCL. These data also suggest that increased expression of BCL-2 does not affect autophagy activity or the autophagy status of DLBCL samples.

6.3 Discussion

In this chapter, we have shown that autophagy activity is increased in FL compared to RA controls and DLBCL samples as demonstrated by decreased expression/increased degradation of the autophagy substrates p62 and LC3. We also found that despite being significantly differentially expressed in FL, these autophagy-related proteins were not associated with the outcome of this indolent lymphoma. Most importantly, we identified p62 is as a novel independent prognostic biomarker in DLBCL. We therefore propose that overexpression of BCL-2 does not inhibit autophagy activity in both FL and DLBCL.

Using continuous and categorical univariate analysis and multivariate analysis, we identified that p62 is an independent biomarker of clinical outcome in patients with DLBCL. We found that patients with decreased expression of this autophagy-substrate had significantly shorter survival rates compared to patients expressing this protein at high levels. This suggests that increased autophagy activity, as demonstrated by increased p62 degradation, predicts a worse outcome in DLBCL. While this finding is at odds with some previous reports (Luo et al., 2013), it is in agreement with the observation of Ellis *et al* who identified decreased expression of p62 as being a poor prognostic marker in melanoma (Ellis et al., 2014).

Decreased expression of p62 in combination with increased BCL-2 predicted the worst outcome in DLBCL, with BCL-2^{HIGH}/$p62^{LOW}$ patients having the shortest OS and DSS rates compared to all other groups. Simultaneous inhibition of apoptosis by BCL-2 and an increase in autophagy activity are associated with a poor clinical outcome in DLBCL. These results further indicate overexpression of BCL-2 does not negatively regulate autophagy activity in NHLs. In both patient cohorts, decreased expression of Beclin-1 predicted a worse outcome, a finding which is in line with previous reports (Nicotra et al., 2010b). In particular, Beclin-1 expression levels had greater prognostic significance in FL.

A caveat of using p62 and LC3 expression levels as biomarkers of autophagy activity is that accumulation or increased expression of these autophagy substrates can indicate either enhanced autophagosome formation and thus active autophagy or, impaired

autophagic degradation of substrates and autophagosomes due to autophagy inhibition (Klionsky et al., 2008b). Decreased expression of these substrates would suggest their degradation by active autophagy pathway; however it may also indicate decreased delivery of substrates to the autophagosome and reduced autophagosome formation, meaning lower levels of autophagy. As p62, LC3 and other autophagy-substrates are degraded by lysosomal hydrolayses, dual staining of samples for p62 or LC3 and a lysosomal marker may clarify this confusion; that is, establish if the autophagy flux is increased or if autophagic degradation is inhibited. However, double staining using IHC is difficult and can often produce a large number of false positives or false negatives making accurate interpretation of results difficult. As with all IHC-based analysis, it will be important to validate these findings in an independent cohort of patients, ideally at another institution. It will also be important to confirm p62 as a prognostic marker independently of patients GCB/ABC-subtype classification. However, this may be difficult as GEP information is not available or easily obtainable for samples present on TMAs, especially the historic cases. While it is possible to stratify patients into these subtypes using IHC-based algorithms, there is poor concordance among these different algorithms as to what truly classifies a patient as GCB or ABC (Coutinho et al., 2013).

We have shown that basal level autophagy activity is increased in primary FL samples despite increased expression of BCL-2 and increased autophagy activity is not directly associated with clinical outcome in this indolent lymphoma. We have also shown that Beclin-1 can be used as an independent biomarker in FL and that decreased expression of p62 independently predicts a poor outcome in DLBCL. DLBCL patients with decreased expression of p62 in combination with increased BCL-2 showed the lowest survival rates, indicating that inhibition of apoptosis and increased autophagy activity predicts a worse prognosis in DLBCL.

6.3.1 Conclusions

Here we show that FL has increased autophagy activity as detected at the protein level, which is in agreement with an increased autophagy-related GEP in the same disease. Overexpression of BCL-2 did not appear to have an inhibitory effect on autophagy in NHL. Increased expression of Beclin-1 predicts a favourable outcome in FL and

DLBCL. Decreased expression of p62 independently, and in conjunction with increased expression of BCL-2 predicts poor survival rates in DLBCL.

Chapter VII

Discussion

7.1 The main findings of this study

In this study, we report for the first time that expression levels of p62 can be used as an independent biomarker of overall, disease specific and progression free survival in DLBCL but not FL. We have shown that basal level autophagy activity is higher in primary FL samples, as demonstrated by global up-regulation of the autophagy-related gene expression profile and decreased expression of the autophagy substrate p62 at the protein level. This suggests that overexpression of BCL-2 in FL does not inhibit basal level autophagy in this indolent lymphoma.

Expression levels of autophagy-related genes were also up-regulated in BCL-2^{HIGH} DLBCL cell lines compared to BCL-2^{LOW} cells at the basal level and in response to autophagy stress. Inhibition of BCL-2 by ABT-737 induced both apoptosis and cytoprotective autophagy in BCL-2^{HIGH} lymphoma cell lines.

7.2 Autophagy plays paradoxical roles in cancer development

As autophagy is regulated by a number of oncogenes and tumour suppressors, it is unsurprising that this degradation process is involved in cancer development. However, the role of autophagy in cancer is complex and paradoxical, and is dependent on tumour stage, type and genetic content (Kimmelman, 2011; White, 2012).

Defective autophagy due to activation of autophagy inhibiting oncogenes provides indirect evidence for the tumour suppressing role of this pathway. PI3K activating mutations and Akt amplifications which activate mTOR and lead to autophagy inhibition are frequently observed in a variety of cancers (Diaz-Troya et al., 2008; Kimmelman, 2011). Similarly in some instances, BCL-2 has been shown to bind and sequester Beclin-1, leading to autophagy inhibition (Kimmelman, 2011; Pattingre et al., 2005). The direct evidence for the tumour suppressing role of autophagy came from work by Liang *et al*, who reported that monoallelic deletion of *Beclin-1* lead to autophagy inhibition and predisposed mice to a variety of tumours (Liang et al., 1999). Indeed, a large number of ovarian and breast cancers are heterozygous for the *Beclin-1* gene, which is classified as a haploinsufficient tumour suppressor (Marquez and Xu, 2012; Yue et al., 2003). Ablation of *Atg5* has also been shown to promote the

development of hepatocarcinomas (Takamura et al., 2011). Active autophagy is thought to suppress tumourigenesis by mitigating genomic instability and DNA damage and preventing accumulation of ROS (Kimmelman, 2011).

While autophagy inhibition appears to be important for the initiation of tumourigenesis, active autophagy is thought to be necessary for cancer progression and maintenance of established tumour cells. Indeed, a tumour promoting role of autophagy has been described in a variety of malignancies (Kimmelman, 2011; Kroemer et al., 2010). Increased autophagy has been shown to potentiate survival of tumour cells under conditions of nutrient deprivation and hypoxia, stresses frequently encountered by evolving tumours (Karantza-Wadsworth et al., 2007; White, 2012). It has also been reported that active autophagy allows malignant cells evade death induced by anti-cancer agents, thus promoting therapy resistance (Carella et al., 2012; Sinclair et al., 2013; Verschooten et al., 2012). Evidence is emerging which supports the concept of a cell autonomous role for autophagy in tumour cell maintenance. Yang *et al* and White and colleagues have reported that the survival of RAS-driven tumours is dependent on active autophagy (Guo et al., 2011; Lock et al., 2011; Yang et al., 2011). Elevated autophagy activity has been proposed to act as a mechanism which allows rapidly dividing tumour cells to meet their increased metabolic requirements and energy needs (Eng and Abraham, 2011), but that this stress-induced autophagy differs from basal level autophagy which degrades substrates in a more specific manner (Kimmelman, 2011) . In this study, we report that basal level autophagy is increased in the indolent NHL FL compared to faster growing DLBCL. Autophagy may be up-regulated in slow growing FL cells to prolong their survival by facilitating the removal of old, damaged aggregates and organelles. We found that autophagy activity varies largely among DLBCL samples, and that higher levels of autophagy activity are associated with a worse clinical outcome in DLBCL. Therefore, it is possible that increased autophagy activity in both FL and DLBCL favours tumour cell survival.

The proposed model for the role of autophagy in tumourigenesis is that in normal tissue, autophagy maintains homeostasis and is involved in quality control of proteins and organelles. Inhibition of autophagy disrupts this homoeostasis, resulting in DNA

damage, genomic instability and aneuploidy, which leads to tumour initiation. Once established, tumour cells re-activate the autophagy pathway, allowing them to meet their metabolic needs, promote survival and growth, and often, resistance to therapy.

7.3 Do key autophagy markers reflect autophagy activity in lymphoma cells?

The autophagy status and activity of a sample is typically determined by evaluating expression levels and cellular patterns of the key autophagy-related proteins p62, LC3 and sometimes Beclin-1, whose modulation is known to reflect progress through the autophagy flux.

7.3.1 p62 is a marker of autophagy activity in lymphoma cells

The adaptor protein p62 was identified as an autophagy substrate and marker by Bjorkoy *et al* in 2005. Using HeLa cells, IFM and Western blotting, they observed a decrease in p62 levels following Rapamycin-induced autophagy, and found that inhibition of autophagic degradation with Bafilomycin A1 resulted in p62 accumulation (Bjorkoy et al., 2005). p62 is now well established as an autophagy substrate whose cellular levels decrease when the autophagy flux is active (Pankiv et al., 2007; White, 2012), and its accumulation/increased expression has proven to be an accurate marker of defective/inactive autophagic degradation in a number of cell types including iBMK cells (Mathew et al., 2009), neuronal cells (Bartlett et al., 2011) and mouse liver cells (Komatsu et al., 2007). A recent study by Sahani *et al* has however highlighted that care should be taken when using p62 as an autophagy marker. They report that following an initial decrease in p62 protein levels during starvation-induced autophagy, prolonged starvation and autophagy resulted in reappearance of p62 in MEF and HepG2 cells (Sahani et al., 2014). In line with these findings, using Western blotting we found that starvation-induced autophagy resulted in a decrease in p62 protein levels over a short time period, followed by a reappearance of p62 to the basal level after prolonged nutrient deprivation. We confirmed re-expression of p62 was due to increased mRNA expression. Blocking autophagy degradation with CQ resulted in p62 accumulation in BCL-2^{HIGH} and BCL-2^{LOW} DLBCL cell lines. Therefore, p62 can be used as a marker of

autophagy activity in lymphoma cells, but with caution and taking timing and the method of autophagy induction into account.

p62 expression levels have also been evaluated by IHC in a variety of tissues. Lee *et al* (Lee et al., 2012) assessed whether evaluation of p62 expression by IHC could be used as a diagnostic marker for drug-induced autophagic vaculoar myopathies such as Danon disease. Staining of formalin-fixed paraffin embedded (FFPE) tissue from patients treated with CQ or HCQ revealed darkly stained p62 puncta which reflected accumulation of this autophagy substrate and protein aggregates, indicative of defective autophagy degradation. On the other hand, p62 puncta were absent from normal tissues not treated with either drug (Lee et al., 2012). Doi and colleagues also used IHC to evaluate p62 expression, however not in the context of autophagy, and showed strong, dark, nuclear staining to reflect p62 expression in skeletal muscle (Doi et al., 2013). These findings suggest p62 expression levels can be assessed by IHC and in turn, can be used as a maker of autophagy activity.

In this study strong, dark brown DAB staining which included only areas stained above a pre-determined threshold, was taken to represent the highest intensity staining, and was classified as p62 positive. Low level background staining was excluded. Similar to Lee *et al*, this p62 staining pattern was taken to reflect higher expression of p62 due to autophagy inhibition. Using this scoring method, we found p62 expression is significantly lower in FL intra- and inter-follicular regions compared to RA controls and DLBCL samples, indicating degradation and accumulation of p62 in FL and DLBCL respectively, and suggesting increased autophagy activity in FL. Our findings also indicate that evaluation of p62 expression levels using IHC, and indeed Western blotting, is a valid method by which to assess the autophagy status of a lymphoma sample.

7.3.2 Active autophagy results in decreased expression of LC3 in lymphoma cells

Kabeya *et al* first described LC3-II as a marker of active autophagy in 2000 (Kabeya et al., 2000). Using Western blotting, they showed that following starvation-induced autophagy levels of LC3-II, a 16kDa processed form of LC3, were increased in HeLa

cells compared to non-starved controls. Greater numbers of LC3-II-positive puncta were also observed under starvation conditions using IFM (Kabeya et al., 2000). Increased expression of LC3-II and increased numbers of LC3-II puncta have since been reported to reflect increased autophagy activity in MEFs (Klionsky et al., 2012b), HEK293 (Tanida et al., 2005) and MPC cell lines (Asanuma et al., 2003) among many others.

However, care should be taken when utilising LC3 as an autophagy marker. It has been reported that autophagy-induced increases in LC3-II are tissue and cell type dependent (Klionsky et al., 2012b; Mizushima et al., 2004), and that increased expression of LC3-II can reflect inhibition of autophagic degradation rather than increased autophagy activity (Kabeya et al., 2000; Pankiv et al., 2007). Pankiv *et al* (Pankiv et al., 2007) reported that LC3-II is a substrate of the autophagy pathway. They reported that membrane-bound LC3-II binds p62 via its LIR and facilitates the delivery of autophagy substrates to the autophagosome. Using a mCherry/GFP tag construct, they then demonstrated that as a component of the aggregates it delivers for degradation, LC3-II is itself degraded in the autophagolysosome. They also described an increase in LC3-II levels following lysosomal inhibition and subsequent inhibition of autophagy degradation with Bafilomycin A1, confirming LC3-II is degraded by active autophagy (Pankiv et al., 2007). Increased LC3-II as a result of defective autophagy has also been described in breast cancer (Maycotte et al., 2012), squamous cell carcinoma (Verschooten et al., 2012) and numerous other cell lines (Klionsky et al., 2012b).

Therefore while LC3 levels are modulated during an active autophagy flux, using this protein as an autophagy marker is not straight forward. On the one hand, increased LC3-II expression may be due to conversion of LC3-I to LC3-II by an active autophagy flux; on the other, it may be due to a block in autophagy degradation which results in accumulation of this membrane-bound autophagy substrate (Klionsky et al., 2012b; Mizushima and Yoshimori, 2007). We found that treatment of BCL-2^{HIGH} and BCL-2^{LOW} DLBCL cell lines with the late autophagy inhibitor CQ resulted in an accumulation of LC3-II under nutrient replete conditions, indicative of a block in autophagic degradation. Evaluation of LC3 in these cell lines following starvation-induced autophagy revealed a time dependent decrease in both LC3-I and LC3-II

expression levels, which suggests conversion of LC3-I to LC3-II and subsequent degradation of LC3-II, i.e. an active autophagy flux. In this study, we therefore considered decreased expression of total LC3 (i.e. LC3-I and LC3-II) to reflect active autophagy. On the other hand, increased LC3-II combined with slightly increased LC3-I expression was used as a marker of inactive autophagy in lymphoma cells.

Cellular levels of endogenous LC3 have also been assessed in a variety of malignancies using IHC, including lymphomas (Huang et al., 2010; Nicotra et al., 2010b), colorectal carcinoma (Giatromanolaki et al., 2010) and breast cancer (Sivridis et al., 2010). We have evaluated LC3 primarily for its prognostic significance but also its ability to predict autophagy activity. While IHC is becoming an increasingly common technique with which to evaluate LC3 levels, there are a number of caveats which can make it difficult to interpret the results of this assay correctly. For example, staining tissue for LC3 can produce a number of different patterns which are hard to differentiate and distinguish from one another. These patterns are also reported to vary between cell and tissue types (Klionsky et al., 2012b; Sivridis et al., 2010). Also, LC3 can localise to structures other than autophagosomes within cells (e.g. lipid droplets), meaning increased LC3 puncta does not always reflect increased numbers of autophagosomes (Shibata et al., 2009). It is also quite difficult to differentiate between LC3-I and LC3-II using this assay.

Sivridis *et al* evaluated LC3 staining and expression levels in 102 breast cancer cases, and identified three distinct staining patterns for this autophagy-essential protein - cytoplasmic, cytoplasmic/juxta-nuclear, and "stone-like" pattern (SLS). The latter of these appeared as dense, strongly stained structures and were taken to be reflective of autophagosomes and increased autophagy activity in tumour cells (Sivridis et al., 2010). Similar patterns of staining were also observed in colorectal carcinomas and xenograft models (Giatromanolaki et al., 2010). On the other hand, the study previously described by Lee *et al* which evaluated p62 staining using IHC also evaluated LC3 expression and staining (Lee et al., 2012). Similar to their p62 finding, they observed increased LC3-positive puncta in patients treated with the late autophagy inhibitors CQ or HCQ. They

therefore took large, densely stained LC3 aggregates to be reflective of an accumulation of autophagosomes due to blocked autophagy degradation (Lee et al., 2012).

To evaluate LC3 expression in our FL and DLBCL patient cohorts, we employed a similar scoring system to that previously described for p62. Dark, strong staining was identified as being LC3 positive, and in a similar manner to Lee *et al*, was taken to reflect high expression/accumulation of LC3, indicative of an inactive autophagy flux. It is important to note that in this study, evaluation of 'LC3' in tissue biopsies refers to total LC3, i.e. LC3-I and LC3-II, as these isoforms could not be distinguished by IHC. We believe that the scoring method used in this study is valid and comprehensive as it takes the total autophagy flux, not just LC3-II formation, into account. Also, without using autophagy inhibitors such as CQ it is difficult to tell, particularly by IHC, if 'LC3-II aggregates' are due to increased autophagy activity or a block in autophagic degradation. We therefore propose that LC3 may not be the most suitable marker by which to evaluate autophagy activity in lymphoma cells, particularly using IHC, and that if it is to be used it should be in conjunction with a more robust marker such as p62.

7.3.3 Beclin-1 is not a marker of the autophagy flux in lymphoma cells

Beclin-1 is an essential component of the autophagy initiating complex which functions to promote autophagosome formation and elongation (Marquez and Xu, 2012). While Beclin-1 is known to be involved in the early stages of the autophagy flux, it is less well established if this protein is a substrate of the autophagy pathway, and if its cellular levels can be used as a general marker of autophagy activity in a similar manner as p62 and LC3.

Beclin-1 macroaggregates identified in the Golgi apparatus of neuronal cells using TEM and IFM have been proposed to reflect autophagy induction in these cells, and suggests Beclin-1 may be used as a marker of autophagy activity (Castino et al., 2010; Castino et al., 2011; Yue et al., 2002). We found that Beclin-1 expression levels did not fluctuate in BCL-2^{HIGH} or BCL-2^{LOW} DLBCL cell lines following autophagy induction by starvation or inhibition of autophagic degradation with CQ. This finding indicates that Beclin-1 is most likely not a substrate of the autophagy flux in lymphoma cells and

suggests its expression levels should not be used as a direct marker of autophagy activity within these cells.

Expression levels of Beclin-1 have been evaluated by IHC in malignancies including colon cancer (Koukourakis et al., 2010), nasopharyngeal carcinoma (Wan et al., 2010) and lymphomas (Nicotra et al., 2010b). As with p62 and LC3, in this study positive Beclin-1 staining was characterised as the most intense, darkest staining and low level background staining was excluded. In line with others, we found that Beclin-1 staining is primarily cytoplasmic when examined using IHC. While we observed a difference in Beclin-1 expression levels between FL, DLBCL and RA samples using this assay, this was not taken to reflect differential autophagy activity between sample types as our previous findings demonstrated that Beclin-1 levels do not vary during the autophagy flux. We did however find that expression levels of Beclin-1 protein are positively correlated with p62 levels in FL and DLBCL - lower expression of p62, indicative of active autophagy, is associated with decreased Beclin-1 expression, suggesting that autophagy activity in NHLs is not dependent on the Beclin-1 protein.

7.4 The autophagy-related GEP of lymphoma cells reflects their autophagy status

It has been reported that in some instances, an active autophagy flux is accompanied by an increase in the mRNA levels of autophagy-related genes (Klionsky et al., 2012b; Moussay et al., 2011). Transcription levels of *Atg5* and *Atg7* for example have been reported to increase in neutrophils and during neurogenesis when the autophagy flux is active (Rodriguez-Muela et al., 2012; Vazquez et al., 2012). Similarly, up-regulation of *Atg12* and *GABARAPL1* has been reported in C2C5, MEF (Kouroku et al., 2007) and neuronal cells (Le Grand et al., 2013) following ER-induced autophagy (Klionsky et al., 2012b). Increased knowledge of the autophagy pathway at the gene level will improve our understanding of the role this degradation process plays in cancer development. Evaluation of the autophagy-related GEP should be done on a per cell-type basis as changes in autophagy-related genes mRNA levels is reported to be cell type and stimulus specific (Klionsky et al., 2012b; Klionsky et al., 2008a).

7.4.1 p62 mRNA levels increase when autophagy is induced

It has been reported that during active autophagy, mRNA levels of *SQSTM1* are up-regulated, which often results in increased expression of p62 at the protein level (Bjorkoy et al., 2005; Fujita et al., 2011; Ishii et al., 1997). For example Puissant *et al* reported that resveratrol-induced autophagy resulted in increased expression of p62 at the mRNA and protein level in CML cells (Puissant et al., 2010). Sahani and colleagues recently demonstrated that this is also the case in MEF and HepG2 cells, but not HeLa or HEK293 cell lines, following starvation-induced autophagy (Sahani et al., 2014). They found that pro-longed starvation promoted transcriptional up-regulation of *SQSTM1* in MEF and HepG2 cells, and that up-regulation of p62 at the mRNA level was accompanied by an increase at the protein level (Sahani et al., 2014). Up-regulation of *SQSTM1* during active autophagy is thought to occur to ensure sufficient levels of p62 are available within cells for autophagy to continue. p62 is degraded as part of the autophagolysosome; however it is also essential for the delivery of substrates to the autophagosome. Therefore, by up-regulating *SQSTM1* at the mRNA level, cells maintain a pool of p62 to replace that which is degraded by autophagy, and so allow continued activity of the autophagy process (Klionsky et al., 2012b; Sahani et al., 2014).

On the other hand, accumulation of p62 due to defective autophagy is independent of changes at the mRNA level. In their study, Matthew *et al* described how increased expression of p62 in autophagy defective iBMK cells was due to its accumulation at the protein level rather than up-regulation of *SQSTM1*, and demonstrated that p62 mRNA levels were comparable between wild-type and autophagy-null cells (Mathew et al., 2009). In a similar finding, Komatsu and colleagues reported no change in *SQSTM1* mRNA levels in *Atg7*-defecient/autophagy inactive liver cells, despite increased expression of p62 at the protein level (Komatsu et al., 2007).

In line with the findings of Sahani *et al*, we found that *SQSTM1* was up-regulated in BCL-2^{HIGH} and BCL-2^{LOW} DLBCL cell lines following 6 hrs' starvation. We believe this shows differential expression of *SQSTM1*, and indeed other autophagy-related genes at the mRNA level can be taken to reflect changes in the autophagy flux and

autophagy status of lymphoma cells. Expression of *SQSTM1* was also increased in a number of purified and un-purified primary FL samples compared to DLBCL and RA-LN controls, which coupled with decreased expression of p62 at the protein level indicative of its degradation, further suggests increased autophagy in this indolent NHL. Moussay *et al* have reported a similar finding in endothelial cell lines (Moussay et al., 2011).

7.4.2 LC3 and Beclin-1 mRNA levels can be used as a marker of autophagy activity

Previous studies have reported an increase in *LC3* at the mRNA level when autophagy is active (Klionsky et al., 2012b; Moussay et al., 2011). Nara and colleagues described how following starvation-induced autophagy *LC3* was up-regulated, which resulted in increased synthesis of the LC3 protein (Nara et al., 2002). In their study, Rouschop *et al* (Rouschop et al., 2010) also reported an increase in *LC3* mRNA levels in various cell lines including MCF7 and HT29 cells under hypoxic conditions, and found that *LC3* increased to differing degrees from one cell type to another. LC3 is essential to the autophagy pathway as it recruits substrates to the autophagosome for degradation; however as it is an autophagy substrate its levels are depleted when autophagy is active. Therefore in a similar manner to p62, it is postulated that *LC3* is up-regulated at the gene level to ensure sufficient amounts of LC3 are produced to replenish protein that is degraded by autophagy, and in doing so, ensures autophagy activity can be maintained. Modulation of LC3 is autophagy-stimulus and cell-type dependent (Klionsky et al., 2012b; Klionsky et al., 2008a), indicating that its mRNA levels should be evaluated on a cancer-by-cancer basis.

It is well established that monoallelic deletion of the *BECN1* results in autophagy inhibition and leads to the development of spontaneous breast and ovarian tumours in mice (Sahni et al., 2014; Yue et al., 2003). Similarly, increased expression of Beclin-1 has been reported in a panel of pancreatic cancer cell lines where autophagy activity was increased (Yang et al., 2011). Moussay *et al* also reported an increase in Beclin-1 mRNA levels, along with LC3 and p62, in endothelial cells (Moussay et al., 2011).

In this study, starvation-induced autophagy did not result in increased expression of *LC3* or *BECN1* at the mRNA level in BCL-2^{HIGH} or BCL-2^{LOW} DLBCL cell lines when compared to cells cultured under nutrient replete conditions. We did however observe increased expression of *GABARAPL1* and *GABARAPL2*, the other mammalian homologs of *Atg8*. On the other hand, *BECN1* and *MAP1LC3A* mRNA levels were increased in primary FL samples compared to RA controls, which again suggests increased autophagy activity in these lymphoma cells.

7.5 Does overexpression of BCL-2 inhibit autophagy in lymphoma cells?

7.5.1 BCL-2 inhibits apoptosis but not autophagy in lymphoma cells

The role of BCL-2 as an anti-apoptotic protein is well established (Galluzzi et al., 2012; Llambi and Green, 2011). By binding pro-death proteins such as Bax or Bim, BCL-2 inhibits permeablisation of the mitochondrial membrane which prevents the release of apoptotic factors such as cytochrome c, and subsequent induction of the apoptotic cascade (Kroemer et al., 2007; Ola et al., 2011). While inhibition of cell death is considered to be its primary function, over the last decade it has been demonstrated that BCL-2 can also inhibit the autophagy pathway through binding and sequestration of the autophagy essential protein Beclin-1 (Marquez and Xu, 2012; Pattingre et al., 2005). Interaction between BCL-2 and Beclin-1 prevents the latter from forming the IC, an essential step in autophagy initiation, and thus prevents autophagy induction (Kang et al., 2011).

While binding between BCL-2 and Beclin-1 was first described by Liang *et al* in 1998 (Liang et al., 1998), it was Pattingre and colleagues who demonstrated that this interaction plays a role in regulating the autophagy process (Pattingre et al., 2005) . By evaluating accumulation of transfected GFP-LC3 by IFM, Pattingre and colleagues showed that artificially induced overexpression of BCL-2 and Beclin-1 in HT-29 and MEF cell lines inhibited and increased autophagy activity respectively. They also showed by co-immunoprecipitation that endogenous BCL-2 and Beclin-1 bind to form an autophagy inhibiting complex in HeLa cells, and that BCL-2 is a negative regulator of starvation-induced autophagy in these cells (Pattingre et al., 2005). Similar

experiments in the cardiac muscle of BCL-transgenic mice showed that BCL-2 overexpression inhibits autophagy under conditions of prolonged starvation *in vivo* (Pattingre et al., 2005). Inhibition of the autophagy flux due to BCL-2/Beclin-1 binding has also been reported by other groups in pancreatic adenocarcinoma, colorectal and breast cancer cell lines (Marquez and Xu, 2012; Tang et al., 2010; Wei et al., 2008).

While a number of studies describe how binding between BCL-2 and Beclin-1 can result in autophagy inhibition, a recent study by Lindqvist *et al* suggests that BCL-2 and other pro-survival proteins do not directly affect autophagy activity, but rather indirectly modulate this cellular process through their anti-apoptotic function (Lindqvist et al., 2014). Using apoptosis defective ($Bax^{-/-}$ $Bak^{-/-}$) MEF and factor-dependent myeloid (FDM) cells, Lindqvist and colleagues found that treatment with ABT-737 did not increase basal level or stress-induced autophagy, but that autophagy was active in apoptosis competent cells treated with this BH3-mimetic. These results indicate that BCL-2 does not directly inhibit autophagy via Beclin-1 binding, as treatment with ABT-737, a BH3-mimetic that would disrupt this interaction, only affected autophagy when the mitochondria-dependent apoptosis pathway was intact. Lindqvist *et al* also evaluated the possibility that BCL-2/Beclin-1 interactions are too weak to have a discernible effect on autophagy by evaluating its activity in cells where BCL-2 was overexpressed, and found that overexpression of BCL-2 or any other anti-apoptotic protein did not inhibit the autophagy flux in $Bax^{-/-}$ $Bak^{-/-}$ cells. They therefore propose that BCL-2 indirectly modulates autophagy activity through its anti-apoptotic/pro-survival function, rather than directly through binding and sequestration of Beclin-1(Lindqvist et al., 2014).

As interest in the role of autophagy in cancer development increases, it is important to understand how BCL-2 regulates this pathway in different cells. Prior to this study, it was unknown if BCL-2 inhibits autophagy as well as apoptosis in FL and DLBCL. Using techniques including IHC, Western blotting and qRT-PCR, we aimed to determine whether increased BCL-2 expression inhibits autophagy in FL and DLBCL. We evaluated the autophagy status and basal level activity in primary FL and DLBCL tissues and DLBCL cell lines based on their endogenous autophagy-related GEP. Our

results show that endogenous BCL-2 is unlikely to inhibit basal level autophagy in primary lymphomas and BCL-2 positive DLBCL cell lines.

7.5.2 ABT-737 induces cytoprotective autophagy in lymphoma cell lines

BH3-mimetic compounds bind anti-apoptotic members of the BCL-2 family of proteins via BH3-domain interactions with varying degrees of affinity (Souers et al., 2013; Vogler et al., 2009). By binding these pro-survival proteins, BH3-mimetics promote the release of pro-death proteins such as Bax, which induce apoptosis (Davids and Letai, 2013; Kang and Reynolds, 2009; White, 2012). Binding of these compounds to BCL-2 has also been shown to promote autophagy activity by precluding BCL-2s autophagy-inhibiting interactions with Beclin-1 (Levine et al., 2008; Marquez and Xu, 2012). Induction of autophagy following treatment with BH3-mimetics, and indeed other anti-cancer drugs, has been shown to both promote and hinder the pro-death role of these anti-neoplastic agents (Kimmelman, 2011). In their study, Pattingre *et al* reported that while binding between BCL-2 and Beclin-1 occurs at the mitochondria and the ER, only disruption of this interaction at the ER promotes autophagy (Kang et al., 2011; Pattingre et al., 2005).

In this study, we confirmed that ABT-737 induces apoptosis in BCL-2^{HIGH} but not BCL-2^{LOW} DLBCL cell lines, irrespective of BCL-xL expression levels, as demonstrated by increased PARP cleavage and a change in Bax conformation to its active form. Our findings are in line with those of Deng *et al* and various other studies (Deng et al., 2007; Konopleva et al., 2006; Vandenberg and Cory, 2013). Sensitivity of BCL-2^{HIGH} DLBCL cell lines to ABT-737 is not surprising as increased expression of this pro-survival protein has been reported to 'prime' cells for death (Davids and Letai, 2013; Deng et al., 2007). Treatment of BCL-2^{HIGH} DLBCL cell lines with ABT-737 resulted in increased autophagy activity, as demonstrated by degradation of the autophagy substrates p62 and LC3. IFM experiments showed that endogenous BCL-2 and endogenous Beclin-1 proteins co-localise in BCL-2^{HIGH} cells. Cellular fractionation experiments were not performed to determine the sub-cellular location at which this interaction occurred. However, co-immunoprecipitation experiments showed no binding between these proteins at the basal level. Co-localisation was not reduced following

treatment with ABT-737, indicating that while BCL-2 and Beclin-1 localise to the same cellular organelle(s) they do not bind to form an autophagy-inhibiting complex in lymphoma cells.

Treatment with CQ sensitised BCL-2^{HIGH} cells to ABT-737-mediated apoptosis, indicating that ABT-737-induced autophagy functions as a cytoprotective mechanism utilised by cells to avoid death. While ABT-737 induces autophagy in BCL-2^{HIGH} DLBCL cell lines, it appears unlikely to be due to disruption of BCL-2/Beclin-1 binding. Instead, inhibition of BCL-2 may induce autophagy as a pro-survival, stress-response mechanism. Indeed, induction of autophagy in DLBCL cell lines in response to drug treatment has previously been reported (Jia et al., 2012). Our findings indicate that overexpression of BCL-2 does not inhibit basal level autophagy in lymphoma cells, and that acquired autophagy is a survival response utilised by tumour cells to cope with induction of apoptosis. It is important to note that we evaluated BCL-2/Beclin-1 binding at the endogenous, basal level, not following modulation of protein expression levels or transfection, the process of which could itself induce autophagy.

BH3-mimetcis are widely used as anti-cancer agents in the clinical setting (Davids and Letai, 2013; Souers et al., 2013; Wilson et al., 2010). Navitoclax (ABT-263), an orally available second generation ABT-737 derivative, has shown anti-tumour activity in various solid malignancies, CLL and FL, both as a single agent and in combination with standard chemotherapeutic agents (Davids and Letai, 2012; Touzeau et al., 2014; Wilson et al., 2010). Similarly, the third generation BH3-mimetic ABT-199 which only binds BCL-2, effectively promotes tumour cell death in CLL, multiple myeloma and other tumours, but with the distinct advantage of not inducing thrombocytopenia, a side-effect of Navitoclax (Davids and Letai, 2013; Souers et al., 2013; Touzeau et al., 2014). As BH3-mimetics are increasingly being used as therapeutic agents in NHLs, our results indicate that inclusion of autophagy-inhibiting drugs such as CQ and HCQ in current FL and DLBCL treatment regimens should be considered.

7.5.3 Overexpression of BCL-2 does not inhibit autophagy in primary FL samples

We have shown that decreased expression of p62 and LC3 at the protein level can be used as markers of increased autophagy flux in lymphoma cells. An increase in mRNA levels of the genes encoding for these proteins (*SQSTM1* and *MAP1LC3*) and indeed other key autophagy-related genes, also mirrors active autophagy. Evaluation of endogenous p62 and LC3 levels and the autophagy-related GEP of primary FL and DLBCL tissues revealed that autophagy activity is increased in FL samples compared to RA controls and DLBCL samples. Expression of the global autophagy-related GEP was higher in FL samples, while p62 and LC3 protein levels were decreased, indicative of their degradation. We therefore propose that these data indicate that despite its overexpression at the gene and protein levels, BCL-2 does not inhibit basal level autophagy in primary lymphoma samples. Similarly, overexpression of BCL-2 in DLBCL cell lines did not appear to inhibit basal level or stress-induced autophagy. These findings are contrary to previous studies which suggest that BCL-2 inhibits autophagy through binding and sequestration of Beclin-1 (Pattingre et al., 2005; Tang et al., 2010). There are a number of possibilities which may explain our findings.

As previously stated, autophagy activity is cell-type dependent, meaning observations made in one cell type do not necessarily hold true for all others (Kimmelman, 2011; White, 2012). Therefore, while BCL-2 overexpression has been shown to inhibit autophagy in other malignancies, we report here for the first time that this does not appear to be the case in primary purified FL B cells and un-purified tissue biopsies. Similarly, previous studies have reported BCL-2 to be a negative regulator of starvation-induced autophagy which is described as being mechanistically different to basal level autophagy (Kimmelman, 2011). Our study differs in that we evaluated the autophagy status of primary lymphoma samples at the basal level by assessing endogenous expression levels of autophagy-related proteins and genes, while most other studies use transgenic murine-models and artificially-induced BCL-2 or Beclin-1 expression to evaluate BCL-2s role in autophagy.

While our findings contradict the dogma that BCL-2 overexpression inhibits autophagy, and disprove our initial hypothesis that increased expression of this protein negatively regulates autophagy in human NHLs, it is important to note that our methods of assessing autophagy activity have previously been shown to be suitable for evaluation of autophagy within lymphoma cells. In this study, and as previously described (Bjorkoy et al., 2005; Klionsky et al., 2012b; Mathew et al., 2009; Pankiv et al., 2007), increased expression of p62 at the protein level as evaluated by Western blotting and IHC, was taken to indicate inactive autophagy degradation, while its decreased expression suggested active autophagy. Similarly, in accordance with previous reports increased expression of autophagy-related genes such as *Atg9A*, *Atg16L1*, *MAP1LC3* and *UVRAG*, was taken to reflect increased autophagy flux. Our methods did differ with respect to the utility of LC3 as an accurate autophagy marker in lymphoma cells. While some studies report accumulation of LC3 to reflect LC3-II puncta and thus increased autophagy activity (Mizushima and Yoshimori, 2007; Sivridis et al., 2010; Tanida et al., 2005), it is difficult to prove that increased LC3 expression is not due to impaired degradation without using autophagy inhibitors such as CQ (Klionsky et al., 2012b). It is also difficult to distinguish LC3-I from LC3-II using IHC. Following experiments with CQ, we took a decrease in global LC3 levels (i.e. LC3-I and LC3-II) to reflect conversion of LC3-I to LC3-II, degradation of LC3-II by autophagy and hence an active autophagy flux. Therefore while our findings differ to others, the assays employed in this study have been shown both here, and by others, to be valid methods with which to evaluate autophagy activity in lymphoma cells.

Based on our findings we propose that overexpression of BCL-2 does not inhibit the autophagy flux in primary FL samples. Instead, basal level autophagy activity is increased in these lymphoma samples compared to RA-LN controls. FL cells are slow growing cells with a low proliferation rate; therefore, autophagy activity may be up-regulated in these cells to facilitate the removal of old, potentially toxic aggregates and provide nutrients under conditions of starvation. Our finding fits with the proposed model of the role of autophagy in cancer development which describes how established tumour cells utilise autophagy as a pro-survival mechanism (Guo et al., 2011;

Kimmelman, 2011; Kroemer et al., 2010). It is important to distinguish this from the theory that autophagy inhibition promotes tumourigenesis (Kimmelman, 2011; Liang et al., 1998; Mathew et al., 2009). In this study, we did not evaluate the role of BCL-2 or autophagy in tumourigenesis or tumour cell progression, but rather their function in already developed tumour cells. Therefore, while BCL-2 may inhibit autophagy during FL development, we have demonstrated that its overexpression does not negatively impact autophagy activity in established FL cells. The mechanism by which FL cells up-regulate autophagy is unknown. One possibility is that inhibition of apoptosis by BCL-2 results in accumulation of aged organelles and misfolded proteins which triggers autophagy. Rapidly dividing, aggressive lymphomas have previously been reported to up-regulate autophagy in order to meet their metabolic needs (Guo et al., 2011; Kimmelman, 2011). In this study, we found autophagy activity is ubiquitously increased in FL samples but varies among DLBCL samples.

7.5.4 Inhibition of apoptosis by BCL-2 promotes autophagy in lymphoma cells

Initially thought of as two distinct cellular processes, it is now clear that a high level of cross-talk occurs between the autophagy and apoptosis pathways (Eisenberg-Lerner et al., 2009; Mukhopadhyay et al., 2014).These processes are inter-connected as they share a number of common regulators including BCL-2, Beclin-1, AMBRA1 and Bim, which can regulate each pathway in a similar or different way. For example UVRAG is pro-autophagic but anti-apoptotic (Mukhopadhyay et al., 2014). The inter-play between autophagy and apoptosis is complex and at times contradictory. Broadly speaking, these pathways can act in synergy to promote one another's activity or behave antagonistically, where activation of one blocks the other (Denton et al., 2012; Eisenberg-Lerner et al., 2009; Maiuri et al., 2007c; Mukhopadhyay et al., 2014).

Inhibition of apoptosis has been shown to result in the induction of autophagic cell death. For example in Bax^{-}/Bak^{-} apoptosis defective MEF cells, an initial increase in autophagy was followed by delayed autophagy-associated cell death (Maiuri et al., 2007c; Shimizu et al., 2004). On the other hand, increased autophagy under conditions of inhibited apoptosis has been shown to promote tumour cell survival. Upon removal of interluekin-3 (IL3), Bax^{-}/Bak^{-} defective immortalised IL3-dependent cell lines increased their autophagy activity which acted in a cytoprotective manner and promoted and maintained tumour cell survival (Lum et al., 2005a; Lum et al., 2005b). These reports indicate that in a similar manner to the autophagy pathway itself, cross-talk between autophagy and apoptosis is stimulus and cell-type dependent, as is the outcome of this cross-talk (Denton et al., 2012; Eisenberg-Lerner et al., 2009; Mukhopadhyay et al., 2014).

BCL-2 is known to inhibit apoptosis in FL and DLBCL tumour cells where it is frequently overexpressed (Campos et al., 1993). In our study, we have shown that BCL-2 does not simultaneously inhibit autophagy in these lymphoma cells, but rather that autophagy activity is increased in FL samples and a proportion of DLBCL samples. We therefore propose that inhibition of apoptosis by BCL-2 results in up-regulation of the

autophagy process, which functions as a pro-survival mechanism. Increased autophagy in apoptosis-defective FL and DLBCL cells is likely to facilitate and promote the elimination of damaged, old cellular proteins, organelles and aggregates which if allowed accumulate could induce necrotic cell death. Therefore FL and some DLBCL tumours maintain their growth survival advantage by concurrently preventing cell death and increasing cell survival. This further supports our previous suggestion that inclusion of autophagy inhibitors to current NHL treatment regimens should be considered and evaluated.

7.6 Autophagy activity is increased in cells of the tumour microenvironment

It is well established that interactions between FL and DLBCL B cells and cells of the tumour microenvironment are involved in the development and progression of these lymphomas (Alizadeh et al., 2000; Clear et al., 2010; Rosenwald et al., 2002; Yang and Ansell, 2012). Increased numbers of $CD4^+$ T cells and $CD163^+$ macrophages have been described in FL tissue samples (Clear et al., 2010; Lee et al., 2006), while greater numbers of macrophages and adipocytes have been reported in DLBCL tissues (Lenz et al., 2008a; Rosenwald et al., 2002) compared to normal controls. The role of the microenvironment in these NHLs has also been clearly demonstrated by GEP studies (Alizadeh et al., 2000; Dave et al., 2004; Lenz et al., 2008a; Rosenwald et al., 2002). In a large cohort of DLBCL patients, Lenz *et al* identified three distinct gene signatures as being predictive of outcome and modulating cells response to therapy, two of which were associated with CD19- stromal cells including macrophages and endothelial cells (Lenz et al., 2008a). Similar studies have demonstrated that survival among FL patients is linked with altered expression of genes associated with immune cells including T-cells and follicular dendritic cells (Dave et al., 2004).

In this study, we found a greater number of autophagy-related genes to be aberrantly expressed in un-purified FL samples compared to purified B cells, while genes differentially expressed in un-purified DLBCL samples were expressed by tumour-infiltrating macrophages, not malignant B cells. These results, which demonstrate up-regulation of autophagy-related genes in cells of the microenvironment of primary FL

and DLBCL samples, suggest autophagy activity is not only increased in malignant B cells but also in tumour-infiltrating cells. To our knowledge, this is the first report which describes the autophagy pathway as being differentially regulated in the FL and DLBCL microenvironment.

These results also indicate that while studying the autophagy pathway in cell lines is important and essential to our continued understanding of this complex process, examination of autophagy in primary samples is more relevant and informative as it reflects activity of this pathway in the whole tumour setting including the microenvironment, which is not possible with cell lines.

7.7 Can expression levels of key autophagy-related proteins predict outcome in FL and/or DLBCL?

7.7.1 Low levels of p62 predict a worse outcome in DLBCL

It has previously been reported that accumulation of p62 due to defective autophagy can contribute to tumourigenesis by altering regulation of the NF-κB pathway and its target genes (Mathew et al., 2009). It is therefore unsurprising that the prognostic value of this protein has been assessed in a variety of tumours. Some studies report increased expression of p62 as having no bearing on clinical outcome (Park et al., 2012), while others have shown that increased expression of this adaptor protein due to inactive autophagy predicts a worse prognosis (Choi et al., 2013b; Rolland et al., 2007).

Luo and colleagues found p62 was overexpressed in 51 cases of triple-negative breast cancer (TNBC) patients (Luo et al., 2013). Comparison of survival and metastasis-free survival rates between patients expressing low and high levels of p62 showed patients with increased p62 expression as having a worse prognosis compared to p62-negative patients (Luo et al., 2013). In particular, high levels of p62 were identified as an independent marker of decreased DFS rates. Higher levels of p62 were also predictive of a poor outcome and chemo-radiotherapeutic resistance in a cohort of oral carcinoma cases (Inui et al., 2013). On the other hand, lower levels of p62, taken to be indicative of active autophagy, have been reported to predict shorter survival in melanoma patients (Ellis et al., 2014). Ellis and colleagues report that in a cohort of 121 primary cutaneous

melanomas, DFS was significantly shorter among the 66 patients classified as p62 low, while a non-significant trend towards increased melanoma-specific mortality (MSM) was also observed in this group (Ellis et al., 2014).

To our knowledge, the prognostic value of p62 in NHL has not been previously described. In this study, we found that despite being expressed at significantly lower levels compared to RA controls, p62 was not associated with clinical outcome in FL. A possible explanation for p62 lacking of prognostic value may stem from the fact that it is expressed at homogeneously low levels in all FL samples; therefore, in a similar manner to BCL-2, while low level p62 expression may be characteristic of FL it does not appear to impact on survival. On the other hand, we found that p62 expression levels are an independent biomarker of clinical outcome in our DLBCL patient cohort. Among the 109 DLBCL cases evaluated, the 74 patients classified as $p62^{HIGH}$ had longer OS, DSS and PFS rates compared to the 35 $p62^{LOW}$ patients. In line with the studies described above, in this study low levels of p62 were taken to reflect its degradation and thus increased autophagy activity. However, unlike those studies who report that accumulation of p62 and inhibition of autophagy predicts worse survival in various solid cancers and is associated with tumourigenesis, but in line with the findings of Ellis *et al* (Ellis et al., 2014), we found that degradation of p62 and up-regulation of the autophagy pathway predicts a poor outcome in this aggressive lymphoma, but not in indolent FL.

Our findings show that high p62 expression levels and inactive autophagy predicts a favourable clinical outcome in DLBCL. We believe this finding fits with the proposed theory that increased autophagy activity, as demonstrated by decreased p62 levels, promotes tumour cell survival, resulting in a worse clinical outcome. As mentioned before, the autophagy pathway and its role in tumourigenesis and cancer development is highly tumour specific, meaning an observation in one malignancy does not necessarily hold true for another. Also, the microenvironment plays an important role in the development and progression of DLBCL, and as we have demonstrated in this study, autophagy activity is altered in cells of the DLBCL, and FL, tumour microenvironment.

We therefore propose that p62 is a valid and important independent biomarker for clinical outcome in DLBCL, where its decreased expression predicts a worse prognosis.

7.7.2 Low levels of Beclin-1 are associated with shorter survival rates in FL and DLBCL

The prognostic significance of Beclin-1 in various malignancies is well reported. As it is classified as a haploinsufficient tumour suppressor gene (Liang et al., 1999; Marquez and Xu, 2012), it is unsurprising that in the majority of studies, increased expression of Beclin-1 is reported to be associated with a good prognosis, while decreased expression of this autophagy-essential protein predicts shorter survival rates (Chen et al., 2009; Huang et al., 2010). For example, Geng *et al* found that in a cohort of 271 lymph-node positive gastric cancers, OS was significantly higher in the 229 patients with increased expression of Beclin-1 (Geng et al., 2012). However, there are some reports which describe higher levels of Beclin-1 as being a marker of poor outcome (Wan et al., 2010). The prognostic significance of Beclin-1 as an independent marker of outcome in NHLs has previously been described (Huang et al., 2011; Nicotra et al., 2010b). In a study of 102 NHL patients which included 21 FL cases and 32 cases of DLBCL, ~60% of patients, including 16 FL and 15 DLBCL, had high (≥20%) levels of Beclin-1 as identified by tissue immunofluorescence. Evaluation of clinical outcome identified Beclin-1 as an independent prognostic marker, and showed increased survival among Beclin-1^{HIGH} patients following chemotherapy compared to patients with decreased expression (Nicotra et al., 2010b). In a similar finding, Huang and colleagues (Huang et al., 2011) confirmed Beclin-1 to be an independent marker of prognosis in a larger (118) cohort of newly diagnosed DLBCL patients. They reported an association between decreased expression of Beclin-1 and high IPI scores, B-symptoms and an overall worse outcome; comparatively CR rates were higher in patients expressing high levels of Beclin-1 (Huang et al., 2011). In these studies, positive Beclin-1 expression was identified as aggregates (Nicotra et al., 2010b) and strong, cytoplasmic staining (Huang et al., 2011) respectively. As previously described, in this study Beclin-1-positive staining was identified as the most intense, dark cytoplasmic staining. Using this scoring method we confirmed Beclin-1 to be an independent prognostic marker in 86 FL and 109 DLBCL patients. Increased expression of Beclin-1 was associated with

longer OS and DSS in the 71 Beclin-1^{HIGH} FL patients, and OS and PFS in the 84 Beclin-1^{HIGH} cases of DLBCL. While we were unable to stratify patients as GCB or ABC-subtype, Huang *et al* have previously reported that Beclin-1 expression is similar among these subtypes (Huang et al., 2011). These results demonstrate that our IHC technique and scoring method are valid as they confirm previously reported findings.

7.7.3 LC3 does not predict outcome in NHL

The prognostic ability and significance of LC3 varies depending on tumour type (Lee et al., 2013). Some studies describe increased expression of LC3 as being a marker of poor prognosis (Han et al., 2011; Karpathiou et al., 2011), while others found low levels of LC3 to be associated with an unfavourable clinical outcome and tumourigenesis (He et al., 2013; Zhu et al., 2012). Others again report LC3 expression does not predict outcome (Sivridis et al., 2011).

In a study of 163 TNBC patients, He and colleagues (He et al., 2013) identified decreased expression of LC3 as being an independent marker for disease-free survival (DFS), with shorter 10-year DFS rates observed among LC3^{LOW} patients compared to LC3^{HIGH} patients. They describe low levels of LC3 as being indicative of low levels of autophagy, and so propose that defective autophagy is associated with an aggressive form of TNBC, increased risk of metastasis and a worse prognosis (He et al., 2013). In a conflicting study, Han and colleagues (Han et al., 2011) evaluated LC3 expression and its prognostic ability in 70 melanoma patients. They found increased expression of LC3 and LC3-containing vacuoles, reflective of greater numbers of autophagosomes and thus active autophagy, predicted a worse outcome in these patients. They therefore propose that high levels of autophagy may be promote metastasis of melanoma (Han et al., 2011). Lee *et al* (Lee et al., 2013) have also shown that LC3 is an independent prognostic marker in hepatocellular carcinoma (HCC), where its increased expression predicts longer OS. However they highlight that as IHC cannot clearly differentiate between LC3-I and LC3-II, IHC staining for this protein may not accurately reflect autophagic flux.

Nicotra *et al* reported that increased LC3-II expression and the presence of LC3-positive puncta are indicative of active autophagy and predictive of a better outcome in their NHL patient cohort (Nicotra et al., 2010b). They found that in the 36 cases stained for LC3, 7 of which were FL and 13 of which were DLBCL, there was a high concordance between LC3 and Beclin-1 positive staining in the majority of cases. As they also observed a negative correlation between Beclin-1, LC3 and BCL-2 expression, their data supports previous reports of increased basal levels autophagy in leukaemic cells following decreased BCL-2 expression (Nicotra et al., 2010b; Saeki et al., 2000). This study therefore indicates that in NHLs increased expression of LC3 reflects increased autophagy activity and in combination with high levels of Beclin-1, predicts a better outcome (Nicotra et al., 2010b).

The findings in our study regarding the prognostic significance of LC3 somewhat conflict with those of Nicotra and colleagues. Using IHC, and consistent with the p62 expression pattern, we found that LC3 expression is significantly decreased in our cohort of 86 FL patients, which was taken to reflective conversion of LC3-I to LC3-II and/or increased LC3-II degradation, and hence increased autophagy activity. We did not find LC3 expression levels to be associated with clinical outcome in either FL or DLBCL (109) patients; however there was a trend among DLBCL patients for longer OS, DSS and PFS when LC3 expression was high. While Nicotra and colleagues also report increased expression of LC3 to be predictive of a favourable clinical outcome, these findings have opposing meanings. In our study, increased LC3 expression indicates inactive autophagy, meaning lower autophagy activity is associated with a better outcome; on the other hand, Nicotra *et al* suggest that increased LC3 puncta reflects active autophagy and so an active autophagy flux is associated with a better outcome. Possible explanations for these opposing observations include differences in sample population size, the IHC scoring method employed, and potentially even the antibody used. These findings again highlight the lack of consistency encountered when using LC3 as an autophagy marker not only in lymphoma cells, but in general.

7.7.4 BCL-2 expression alone does not predict outcome in FL or DLBCL

The BCL-2 protein is overexpressed in the majority of FL and a large proportion of DLBCL tumours, specifically the GCB sub-type (Nogai et al., 2011; Shaffer et al., 2012). However, the impact of BCL-2 overexpression on clinical outcome varies between these malignancies. In FL, despite initial reports that increased expression of this anti-apoptotic protein predicted a worse outcome (Yunis et al., 1989), it is now established that overexpression of BCL-2 at the protein level, and the presence of the t(14;18) translocation, does not negatively impact on survival in this indolent NHL (Llanos et al., 2001; Pezzella et al., 1992). On the other hand, increased expression of BCL-2 has been reported to predict a worse outcome in DLBCL. In their study of 151 DLBCL patients, Hermine *et al* found that BCL-2 is overexpressed in 44% of patients, and that this increased expression was associated with shorter overall and disease specific survival rates (Hermine et al., 1996). Gascoyne and colleagues reported similar findings in a cohort of 116 DLBCL patients and also showed relapse-free survival to be decreased in patients with high BCL-2 expression (Gascoyne et al., 1997). More recently, Iqbal *et al* have described that BCL-2 overexpression preferentially predicts a poor outcome in the ABC-subgroup of DLBCL patients (Iqbal et al., 2006).

In line with previous reports, we found that BCL-2 is not a prognostic marker of clinical outcome in FL. However, contrary to other studies, increased expression of BCL-2 was not identified as an independent marker of poor survival among DLBCL patients using univariate analysis. After dividing DLBCL patients into four groups based on their combined BCL-2/p62 expression levels, we found that BCL-2^{HIGH}/$p62^{LOW}$ patients showed significantly shorter OS and DSS compared to all other groups, suggesting increased expression of BCL-2 negatively impacts survival when combined low levels of p62. Using a multivariate analysis, BCL-2 gained significance as a prognostic marker, indicating that its prognostic value is dependent on other autophagy-related markers.

7.8 Conclusion

In conclusion, we have shown that p62 is a novel, independent prognostic biomarker for DLBCL but not FL. Patients with decreased p62 expression had a poor prognosis,

indicating that increased basal level autophagy has an adverse effect on clinical outcome in this aggressive lymphoma. Overexpression of BCL-2 had no inhibitory effect on basal level autophagy in primary FL samples, but instead may increase its activity through inhibition of apoptosis. Other, as yet unidentified mechanisms are also likely to be involved in the up-regulation of this process in FL. It is unclear if increased autophagy is associated with disease progression as well as tumour cell maintenance. Autophagy activity was also increased in tumour-infiltrating cells, particularly tumour-associated macrophages. Up-regulation of autophagy in lymphoma cells could be cytoprotective and conferring a survival advantage to FL cells. We therefore propose that the inclusion of autophagy inhibitors in current FL, and possibly DLBCL treatment options should be considered.

7.9 Future Work

The main aims of our future work are:

- To validate p62 is an independent prognostic marker of clinical outcome in DLBCL in an independent patient cohort using the same staining and analysis methods employed in this study. TMAs containing a further 80 patients in whom this analysis can be performed are available to us through our collaboration with the Portuguese Institute of Oncology; further patients may also be available through collaborations with the LLMPP consortium. While it would be important to confirm p62 is a prognostic marker in DLBCL independent of GCB/ABC-subtype classification, this would be difficult to do as this information is not available for historic cases present on TMAs, and there is poor concordance among IHC-based algorithms as to how patients should be categorised as GCB or ABC using IHC.

- To determine if increased autophagy activity confers a survival advantage to lymphoma cells. This would be done by evaluating and comparing survival and proliferation rates between autophagy active and inactive lymphoma cells and non-malignant controls. Autophagy would be repressed genetically using siRNA targeted against autophagy essential genes identified as being differentially expressed in primary lymphoma cells and cell lines. Proliferation and viability

assays would be carried out to evaluate the effects of inactive autophagy on B cell growth and survival compared to autophagy active lymphoma cells. These experiments would be difficult to perform in primary FL and DLBCL samples meaning cell lines would have to be utilised. However, this may be difficult as while there are well established DLBCL cell lines available, no FL cell lines are available which accurately mimic the biology and growth process of this indolent lymphoma.

- To evaluate if increased autophagy activity in B-cell lymphomas is associated with disease progression and in particular if it is involved in the progression and transformation of FL to DLBCL. This would be assessed *in vivo* so as to fully determine the role of autophagy in the development and pathogenesis of FL and DLBCL. Murine models of B-cell lymphomas in which these experiments could be carried out include VavP-BCL-2 and Eμ-BRD2 which mimic FL (Egle et al., 2004) and DLBCL (Greenwald et al., 2004) respectively. The Eμ-*Myc* murine model could also be used to study the role of autophagy in progression from FL to DLBCL in a time dependent manner (Donnou et al., 2012). Autophagy activity would also be evaluated in relapsed FL patients based on p62, LC3 and Beclin-1 expression levels to elucidate the role of this pathway in disease progression. We would also aim to construct a TMA containing transformed FL patients to determine if increased autophagy activity is involved in the transformation process.

References

(1993). A predictive model for aggressive non-Hodgkin's lymphoma. The International Non-Hodgkin's Lymphoma Prognostic Factors Project. N Engl J Med *329*, 987-994.

Abida, W.M., and Gu, W. (2008). p53-Dependent and p53-independent activation of autophagy by ARF. Cancer Res *68*, 352-357.

Adams, J.M., and Cory, S. (1998). The Bcl-2 protein family: arbiters of cell survival. Science *281*, 1322-1326.

Al-Tourah, A.J., Gill, K.K., Chhanabhai, M., Hoskins, P.J., Klasa, R.J., Savage, K.J., Sehn, L.H., Shenkier, T.N., Gascoyne, R.D., and Connors, J.M. (2008). Population-based analysis of incidence and outcome of transformed non-Hodgkin's lymphoma. J Clin Oncol *26*, 5165-5169.

Alers, S., Loffler, A.S., Wesselborg, S., and Stork, B. (2012). Role of AMPK-mTOR-Ulk1/2 in the regulation of autophagy: cross talk, shortcuts, and feedbacks. Mol Cell Biol *32*, 2-11.

Alizadeh, A.A., Eisen, M.B., Davis, R.E., Ma, C., Lossos, I.S., Rosenwald, A., Boldrick, J.C., Sabet, H., Tran, T., Yu, X., *et al.* (2000). Distinct types of diffuse large B-cell lymphoma identified by gene expression profiling. Nature *403*, 503-511.

Altman, B.J., Jacobs, S.R., Mason, E.F., Michalek, R.D., MacIntyre, A.N., Coloff, J.L., Ilkayeva, O., Jia, W., He, Y.W., and Rathmell, J.C. (2011). Autophagy is essential to suppress cell stress and to allow BCR-Abl-mediated leukemogenesis. Oncogene *30*, 1855-1867.

Altman, D.G., Lausen, B., Sauerbrei, W., and Schumacher, M. (1994). Dangers of using "optimal" cutpoints in the evaluation of prognostic factors. Journal of the National Cancer Institute *86*, 829-835.

Amaravadi, R.K., Yu, D., Lum, J.J., Bui, T., Christophorou, M.A., Evan, G.I., Thomas-Tikhonenko, A., and Thompson, C.B. (2007). Autophagy inhibition enhances therapy-induced apoptosis in a Myc-induced model of lymphoma. J Clin Invest *117*, 326-336.

Ame, J.C., Spenlehauer, C., and de Murcia, G. (2004). The PARP superfamily. Bioessays *26*, 882-893.

Andersen, C.L., Jensen, J.L., and Orntoft, T.F. (2004). Normalization of real-time quantitative reverse transcription-PCR data: a model-based variance estimation approach to identify genes suited for normalization, applied to bladder and colon cancer data sets. Cancer Res *64*, 5245-5250.

Ardeshna, K.M., Smith, P., Norton, A., Hancock, B.W., Hoskin, P.J., MacLennan, K.A., Marcus, R.E., Jelliffe, A., Vaughan, G., Hudson, *et al.* (2003). Long-term effect of a watch and wait policy versus immediate systemic treatment for asymptomatic advanced-stage non-Hodgkin lymphoma: a randomised controlled trial. Lancet *362*, 516-522.

Armitage, J.O., and Weisenburger, D.D. (1998). New approach to classifying non-Hodgkin's lymphomas: clinical features of the major histologic subtypes. Non-Hodgkin's Lymphoma Classification Project. J Clin Oncol *16*, 2780-2795.

Asanuma, K., Tanida, I., Shirato, I., Ueno, T., Takahara, H., Nishitani, T., Kominami, E., and Tomino, Y. (2003). MAP-LC3, a promising autophagosomal marker, is processed during the differentiation and recovery of podocytes from PAN nephrosis. FASEB J *17*, 1165-1167.

Azad, M.B., Chen, Y., and Gibson, S.B. (2009). Regulation of autophagy by reactive oxygen species (ROS): implications for cancer progression and treatment. Antioxid Redox Signal *11*, 777-790.

Barrans, S.L., Evans, P.A., O'Connor, S.J., Kendall, S.J., Owen, R.G., Haynes, A.P., Morgan, G.J., and Jack, A.S. (2003). The t(14;18) is associated with germinal center-derived diffuse large B-cell lymphoma and is a strong predictor of outcome. Clin Cancer Res *9*, 2133-2139.

Bartlett, B.J., Isakson, P., Lewerenz, J., Sanchez, H., Kotzebue, R.W., Cumming, R.C., Harris, G.L., Nezis, I.P., Schubert, D.R., Simonsen, A., *et al.* (2011). p62, Ref(2)P and ubiquitinated proteins are conserved markers of neuronal aging, aggregate formation and progressive autophagic defects. Autophagy *7*, 572-583.

Bellodi, C., Lidonnici, M.R., Hamilton, A., Helgason, G.V., Soliera, A.R., Ronchetti, M., Galavotti, S., Young, K.W., Selmi, T., Yacobi, R., *et al.* (2009). Targeting autophagy potentiates tyrosine kinase inhibitor-induced cell death in Philadelphia chromosome-positive cells, including primary CML stem cells. J Clin Invest *119*, 1109-1123.

Bellot, G., Garcia-Medina, R., Gounon, P., Chiche, J., Roux, D., Pouyssegur, J., and Mazure, N.M. (2009). Hypoxia-induced autophagy is mediated through hypoxia-inducible factor induction of BNIP3 and BNIP3L via their BH3 domains. Mol Cell Biol *29*, 2570-2581.

Ben Sahra, I., Le Marchand-Brustel, Y., Tanti, J.F., and Bost, F. (2010). Metformin in cancer therapy: a new perspective for an old antidiabetic drug? Mol Cancer Ther *9*, 1092-1099.

Benjamin, D., Colombi, M., Moroni, C., and Hall, M.N. (2011). Rapamycin passes the torch: a new generation of mTOR inhibitors. Nat Rev Drug Discov *10*, 868-880.

Bjorkoy, G., Lamark, T., Brech, A., Outzen, H., Perander, M., Overvatn, A., Stenmark, H., and Johansen, T. (2005). p62/SQSTM1 forms protein aggregates degraded by autophagy and has a protective effect on huntingtin-induced cell death. J Cell Biol *171*, 603-614.

Bodor, C., Grossmann, V., Popov, N., Okosun, J., O'Riain, C., Tan, K., Marzec, J., Araf, S., Wang, J., Lee, A.M., *et al.* (2013). EZH2 mutations are frequent and represent an early event in follicular lymphoma. Blood *122*, 3165-3168.

Boonstra, R., Bosga-Bouwer, A., Mastik, M., Haralambieva, E., Conradie, J., van den Berg, E., van den Berg, A., and Poppema, S. (2003). Identification of chromosomal copy number changes associated with transformation of follicular lymphoma to diffuse large B-cell lymphoma. Hum Pathol *34*, 915-923.

Boulares, A.H., Yakovlev, A.G., Ivanova, V., Stoica, B.A., Wang, G., Iyer, S., and Smulson, M. (1999). Role of poly(ADP-ribose) polymerase (PARP) cleavage in apoptosis. Caspase 3-resistant PARP mutant increases rates of apoptosis in transfected cells. J Biol Chem *274*, 22932-22940.

Boya, P., Reggiori, F., and Codogno, P. (2013). Emerging regulation and functions of autophagy. Nat Cell Biol *15*, 713-720.

Bradford, M.M. (1976). A rapid and sensitive method for the quantitation of microgram quantities of protein utilizing the principle of protein-dye binding. Anal Biochem *72*, 248-254.
Brahimi-Horn, M.C., Chiche, J., and Pouyssegur, J. (2007). Hypoxia and cancer. J Mol Med (Berl) *85*, 1301-1307.

Brown, M., and Wittwer, C. (2000). Flow cytometry: principles and clinical applications in hematology. Clin Chem *46*, 1221-1229.

Brusamolino, E., Rusconi, C., Montalbetti, L., Gargantini, L., Uziel, L., Pinotti, G., Fava, S., Rigacci, L., Pagnucco, G., Pascutto, C., *et al.* (2006). Dose-dense R-CHOP-14 supported by pegfilgrastim in patients with diffuse large B-cell lymphoma: a phase II study of feasibility and toxicity. Haematologica *91*, 496-502.

Buske, C., Hoster, E., Dreyling, M., Hasford, J., Unterhalt, M., and Hiddemann, W. (2006). The Follicular Lymphoma International Prognostic Index (FLIPI) separates high-risk from intermediate- or low-risk patients with advanced-stage follicular lymphoma treated front-line with rituximab and the combination of cyclophosphamide, doxorubicin, vincristine, and prednisone (R-CHOP) with respect to treatment outcome. Blood *108*, 1504-1508.

Bustin, S.A. (2000). Absolute quantification of mRNA using real-time reverse transcription polymerase chain reaction assays. J Mol Endocrinol *25*, 169-193.

Bustin, S.A. (2002). Quantification of mRNA using real-time reverse transcription PCR (RT-PCR): trends and problems. J Mol Endocrinol *29*, 23-39.

Bustin, S.A., Benes, V., Nolan, T., and Pfaffl, M.W. (2005). Quantitative real-time RT-PCR--a perspective. J Mol Endocrinol *34*, 597-601.

Camp, R.L., Dolled-Filhart, M., and Rimm, D.L. (2004). X-tile: a new bio-informatics tool for biomarker assessment and outcome-based cut-point optimization. Clin Cancer Res *10*, 7252-7259.

Campo, E., Swerdlow, S.H., Harris, N.L., Pileri, S., Stein, H., and Jaffe, E.S. (2011). The 2008 WHO classification of lymphoid neoplasms and beyond: evolving concepts and practical applications. Blood *117*, 5019-5032.

Campos, L., Rouault, J.P., Sabido, O., Oriol, P., Roubi, N., Vasselon, C., Archimbaud, E., Magaud, J.P., and Guyotat, D. (1993). High expression of bcl-2 protein in acute myeloid leukemia cells is associated with poor response to chemotherapy. Blood *81*, 3091-3096.

Carella, A.M., Beltrami, G., Pica, G., Carella, A., and Catania, G. (2012). Clarithromycin potentiates tyrosine kinase inhibitor treatment in patients with resistant chronic myeloid leukemia. Leukemia & lymphoma *53*, 1409-1411.

Castino, R., Bellio, N., Follo, C., Murphy, D., and Isidoro, C. (2010). Inhibition of PI3k class III-dependent autophagy prevents apoptosis and necrosis by oxidative stress in dopaminergic neuroblastoma cells. Toxicol Sci *117*, 152-162.

Castino, R., Fiorentino, I., Cagnin, M., Giovia, A., and Isidoro, C. (2011). Chelation of lysosomal iron protects dopaminergic SH-SY5Y neuroblastoma cells from hydrogen peroxide toxicity by precluding autophagy and Akt dephosphorylation. Toxicol Sci *123*, 523-541.

Castle, V.P., Heidelberger, K.P., Bromberg, J., Ou, X., Dole, M., and Nunez, G. (1993). Expression of the apoptosis-suppressing protein bcl-2, in neuroblastoma is associated with unfavorable histology and N-myc amplification. Am J Pathol *143*, 1543-1550.

Chen, L., Willis, S.N., Wei, A., Smith, B.J., Fletcher, J.I., Hinds, M.G., Colman, P.M., Day, C.L., Adams, J.M., and Huang, D.C. (2005). Differential targeting of prosurvival Bcl-2 proteins by their BH3-only ligands allows complementary apoptotic function. Mol Cell *17*, 393-403.

Chen, Y., Lu, Y., Lu, C., and Zhang, L. (2009). Beclin-1 expression is a predictor of clinical outcome in patients with esophageal squamous cell carcinoma and correlated to hypoxia-inducible factor (HIF)-1alpha expression. Pathol Oncol Res *15*, 487-493.

Cheung, K.J., Johnson, N.A., Affleck, J.G., Severson, T., Steidl, C., Ben-Neriah, S., Schein, J., Morin, R.D., Moore, R., Shah, S.P., *et al.* (2010). Acquired TNFRSF14 mutations in follicular lymphoma are associated with worse prognosis. Cancer Res *70*, 9166-9174.

Choi, A.M., Ryter, S.W., and Levine, B. (2013a). Autophagy in human health and disease. N Engl J Med *368*, 1845-1846.

Choi, J., Jung, W., and Koo, J.S. (2013b). Expression of autophagy-related markers beclin-1, light chain 3A, light chain 3B and p62 according to the molecular subtype of breast cancer. Histopathology *62*, 275-286.

Chomczynski, P., and Sacchi, N. (1987). Single-step method of RNA isolation by acid guanidinium thiocyanate-phenol-chloroform extraction. Anal Biochem *162*, 156-159.

Cicinnati, V.R., Shen, Q., Sotiropoulos, G.C., Radtke, A., Gerken, G., and Beckebaum, S. (2008). Validation of putative reference genes for gene expression studies in human hepatocellular carcinoma using real-time quantitative RT-PCR. BMC Cancer *8*, 350.

Cimmino, A., Calin, G.A., Fabbri, M., Iorio, M.V., Ferracin, M., Shimizu, M., Wojcik, S.E., Aqeilan, R.I., Zupo, S., Dono, M., *et al.* (2005). miR-15 and miR-16 induce apoptosis by targeting BCL2. Proc Natl Acad Sci U S A *102*, 13944-13949.

Clear, A.J., Lee, A.M., Calaminici, M., Ramsay, A.G., Morris, K.J., Hallam, S., Kelly, G., Macdougall, F., Lister, T.A., and Gribben, J.G. (2010). Increased angiogenic sprouting in poor prognosis FL is associated with elevated numbers of CD163+ macrophages within the immediate sprouting microenvironment. Blood *115*, 5053-5056.

Coiffier, B., Lepage, E., Briere, J., Herbrecht, R., Tilly, H., Bouabdallah, R., Morel, P., Van Den Neste, E., Salles, G., Gaulard, P., *et al.* (2002). CHOP chemotherapy plus rituximab compared with CHOP alone in elderly patients with diffuse large-B-cell lymphoma. N Engl J Med *346*, 235-242.

Coiffier, B., Thieblemont, C., Van Den Neste, E., Lepeu, G., Plantier, I., Castaigne, S., Lefort, S., Marit, G., Macro, M., Sebban, C., *et al.* (2010). Long-term outcome of patients in the LNH-98.5 trial, the first randomized study comparing rituximab-CHOP to standard CHOP

chemotherapy in DLBCL patients: a study by the Groupe d'Etudes des Lymphomes de l'Adulte. Blood *116*, 2040-2045.

Conway, C., Dobson, L., O'Grady, A., Kay, E., Costello, S., and O'Shea, D. (2008). Virtual microscopy as an enabler of automated/quantitative assessment of protein expression in TMAs. Histochem Cell Biol *130*, 447-463.

Coons, A.H. (1958). Fluorescent antibody methods. Gen Cytochem Methods *1*, 399-422.

Coutinho, R., Clear, A.J., Owen, A., Wilson, A., Matthews, J., Lee, A., Alvarez, R., Gomes da Silva, M., Cabecadas, J., Calaminici, M., *et al.* (2013). Poor concordance among nine immunohistochemistry classifiers of cell-of-origin for diffuse large B-cell lymphoma: implications for therapeutic strategies. Clin Cancer Res *19*, 6686-6695.

Dave, S.S., Wright, G., Tan, B., Rosenwald, A., Gascoyne, R.D., Chan, W.C., Fisher, R.I., Braziel, R.M., Rimsza, L.M., Grogan, T.M., *et al.* (2004). Prediction of survival in follicular lymphoma based on molecular features of tumor-infiltrating immune cells. N Engl J Med *351*, 2159-2169.

Davids, M.S., and Letai, A. (2012). Targeting the B-cell lymphoma/leukemia 2 family in cancer. J Clin Oncol *30*, 3127-3135.

Davids, M.S., and Letai, A. (2013). ABT-199: taking dead aim at BCL-2. Cancer Cell *23*, 139-141.

Degenhardt, K., Mathew, R., Beaudoin, B., Bray, K., Anderson, D., Chen, G., Mukherjee, C., Shi, Y., Gelinas, C., Fan, Y., *et al.* (2006). Autophagy promotes tumor cell survival and restricts necrosis, inflammation, and tumorigenesis. Cancer Cell *10*, 51-64.

Del Gaizo Moore, V., Brown, J.R., Certo, M., Love, T.M., Novina, C.D., and Letai, A. (2007). Chronic lymphocytic leukemia requires BCL2 to sequester prodeath BIM, explaining sensitivity to BCL2 antagonist ABT-737. J Clin Invest *117*, 112-121.

Deng, J., Carlson, N., Takeyama, K., Dal Cin, P., Shipp, M., and Letai, A. (2007). BH3 profiling identifies three distinct classes of apoptotic blocks to predict response to ABT-737 and conventional chemotherapeutic agents. Cancer Cell *12*, 171-185.

Denton, D., Nicolson, S., and Kumar, S. (2012). Cell death by autophagy: facts and apparent artefacts. Cell Death Differ *19*, 87-95.

Deretic, V., Saitoh, T., and Akira, S. (2013). Autophagy in infection, inflammation and immunity. Nature reviews Immunology *13*, 722-737.

Deter, R.L., Baudhuin, P., and De Duve, C. (1967). Participation of lysosomes in cellular autophagy induced in rat liver by glucagon. J Cell Biol *35*, C11-16.

Diaz-Troya, S., Perez-Perez, M.E., Florencio, F.J., and Crespo, J.L. (2008). The role of TOR in autophagy regulation from yeast to plants and mammals. Autophagy *4*, 851-865.

Dikic, I., Johansen, T., and Kirkin, V. (2010). Selective autophagy in cancer dev
elopment and therapy. Cancer Res *70*, 3431-3434.

Ding, W.X., Ni, H.M., Gao, W., Hou, Y.F., Melan, M.A., Chen, X., Stolz, D.B., Shao, Z.M., and Yin, X.M. (2007). Differential effects of endoplasmic reticulum stress-induced autophagy on cell survival. J Biol Chem *282*, 4702-4710.

Djavaheri-Mergny, M., Amelotti, M., Mathieu, J., Besancon, F., Bauvy, C., Souquere, S., Pierron, G., and Codogno, P. (2006). NF-kappaB activation represses tumor necrosis factor-alpha-induced autophagy. J Biol Chem *281*, 30373-30382.

Dogan, A., Bagdi, E., Munson, P., and Isaacson, P.G. (2000). CD10 and BCL-6 expression in paraffin sections of normal lymphoid tissue and B-cell lymphomas. Am J Surg Pathol *24*, 846-852.

Doi, H., Adachi, H., Katsuno, M., Minamiyama, M., Matsumoto, S., Kondo, N., Miyazaki, Y., Iida, M., Tohnai, G., Qiang, Q., *et al.* (2013). p62/SQSTM1 differentially removes the toxic mutant androgen receptor via autophagy and inclusion formation in a spinal and bulbar muscular atrophy mouse model. J Neurosci *33*, 7710-7727.

Donnou, S., Galand, C., Touitou, V., Sautes-Fridman, C., Fabry, Z., and Fisson, S. (2012). Murine models of B-cell lymphomas: promising tools for designing cancer therapies. Adv Hematol *2012*, 701704.

Dreyling, M., Ghielmini, M., Marcus, R., Salles, G., Vitolo, U., and Group, E.G.W. (2011). Newly diagnosed and relapsed follicular lymphoma: ESMO Clinical Practice Guidelines for diagnosis, treatment and follow-up. Ann Oncol *22 Suppl 6*, vi59-63.

Dunleavy, K., Pittaluga, S., Czuczman, M.S., Dave, S.S., Wright, G., Grant, N., Shovlin, M., Jaffe, E.S., Janik, J.E., Staudt, L.M., *et al.* (2009). Differential efficacy of bortezomib plus chemotherapy within molecular subtypes of diffuse large B-cell lymphoma. Blood *113*, 6069-6076.

Dupire, S., and Coiffier, B. (2010). Targeted treatment and new agents in diffuse large B cell lymphoma. Int J Hematol *92*, 12-24.

Duran, A., Linares, J.F., Galvez, A.S., Wikenheiser, K., Flores, J.M., Diaz-Meco, M.T., and Moscat, J. (2008). The signaling adaptor p62 is an important NF-kappaB mediator in tumorigenesis. Cancer Cell *13*, 343-354.

Duran, A., Serrano, M., Leitges, M., Flores, J.M., Picard, S., Brown, J.P., Moscat, J., and Diaz-Meco, M.T. (2004). The atypical PKC-interacting protein p62 is an important mediator of RANK-activated osteoclastogenesis. Dev Cell *6*, 303-309.

Egle, A., Harris, A.W., Bath, M.L., O'Reilly, L., and Cory, S. (2004). VavP-Bcl2 transgenic mice develop follicular lymphoma preceded by germinal center hyperplasia. Blood *103*, 2276-2283.

Eisenberg-Lerner, A., Bialik, S., Simon, H.U., and Kimchi, A. (2009). Life and death partners: apoptosis, autophagy and the cross-talk between them. Cell Death Differ *16*, 966-975.

Eisenberg-Lerner, A., and Kimchi, A. (2009). The paradox of autophagy and its implication in cancer etiology and therapy. Apoptosis *14*, 376-391.

Ellis, R.A., Horswell, S., Ness, T., Lumsdon, J., Tooze, S.A., Kirkham, N., Armstrong, J.L., and Lovat, P.E. (2014). Prognostic Impact of p62 Expression in Cutaneous Malignant Melanoma. J Invest Dermatol *134*, 1476-1478.

Eng, C.H., and Abraham, R.T. (2011). The autophagy conundrum in cancer: influence of tumorigenic metabolic reprogramming. Oncogene *30*, 4687-4696.

Eskelinen, E.L. (2008a). Fine structure of the autophagosome. Methods in molecular biology *445*, 11-28.

Eskelinen, E.L. (2008b). To be or not to be? Examples of incorrect identification of autophagic compartments in conventional transmission electron microscopy of mammalian cells. Autophagy *4*, 257-260.

Eskelinen, E.L., Reggiori, F., Baba, M., Kovacs, A.L., and Seglen, P.O. (2011). Seeing is believing The impact of electron microscopy on autophagy research. Autophagy *7*, 935-956.

Evens, A.M., Sehn, L.H., Farinha, P., Nelson, B.P., Raji, A., Lu, Y., Brakman, A., Parimi, V., Winter, J.N., Schumacker, P.T., *et al.* (2010). Hypoxia-inducible factor-1 {alpha} expression predicts superior survival in patients with diffuse large B-cell lymphoma treated with R-CHOP. J Clin Oncol *28*, 1017-1024.

Feng, Z., Hu, W., de Stanchina, E., Teresky, A.K., Jin, S., Lowe, S., and Levine, A.J. (2007). The regulation of AMPK beta1, TSC2, and PTEN expression by p53: stress, cell and tissue specificity, and the role of these gene products in modulating the IGF-1-AKT-mTOR pathways. Cancer Res *67*, 3043-3053.

Feng, Z., Zhang, H., Levine, A.J., and Jin, S. (2005). The coordinate regulation of the p53 and mTOR pathways in cells. Proc Natl Acad Sci U S A *102*, 8204-8209.

Fisher, R.I., Gaynor, E.R., Dahlberg, S., Oken, M.M., Grogan, T.M., Mize, E.M., Glick, J.H., Coltman, C.A., Jr., and Miller, T.P. (1993). Comparison of a standard regimen (CHOP) with three intensive chemotherapy regimens for advanced non-Hodgkin's lymphoma. N Engl J Med *328*, 1002-1006.

Fitoussi, O., Belhadj, K., Mounier, N., Parrens, M., Tilly, H., Salles, G., Feugier, P., Ferme, C., Ysebaert, L., Gabarre, J., *et al.* (2011). Survival impact of rituximab combined with ACVBP and upfront consolidation autotransplantation in high-risk diffuse large B-cell lymphoma for GELA. Haematologica *96*, 1136-1143.

Fleige, S., Walf, V., Huch, S., Prgomet, C., Sehm, J., and Pfaffl, M.W. (2006). Comparison of relative mRNA quantification models and the impact of RNA integrity in quantitative real-time RT-PCR. Biotechnol Lett *28*, 1601-1613.

Flowers, C.R., Sinha, R., and Vose, J.M. (2010). Improving outcomes for patients with diffuse large B-cell lymphoma. CA Cancer J Clin *60*, 393-408.

Freedman, A. (2012). Follicular lymphoma: 2012 update on diagnosis and management. Am J Hematol *87*, 988-995.

Friedberg, J.W. (2011). Rituximab maintenance in follicular lymphoma: PRIMA. Lancet *377*, 4-6.

Fujita, K., Maeda, D., Xiao, Q., and Srinivasula, S.M. (2011). Nrf2-mediated induction of p62 controls Toll-like receptor-4-driven aggresome-like induced structure formation and autophagic degradation. Proc Natl Acad Sci U S A *108*, 1427-1432.

Fukuhara, S., Rowley, J.D., Variakojis, D., and Golomb, H.M. (1979). Chromosome abnormalities in poorly differentiated lymphocytic lymphoma. Cancer Res *39*, 3119-3128.

Fulda, S. (2012). Autophagy and cell death. Autophagy *8*, 1250-1251.

Galluzzi, L., Vitale, I., Abrams, J.M., Alnemri, E.S., Baehrecke, E.H., Blagosklonny, M.V., Dawson, T.M., Dawson, V.L., El-Deiry, W.S., Fulda, S., *et al.* (2012). Molecular definitions of cell death subroutines: recommendations of the Nomenclature Committee on Cell Death 2012. Cell Death Differ *19*, 107-120.

Galteland, E., Sivertsen, E.A., Svendsrud, D.H., Smedshammer, L., Kresse, S.H., Meza-Zepeda, L.A., Myklebost, O., Suo, Z., Mu, D., Deangelis, P.M., *et al.* (2005). Translocation t(14;18) and gain of chromosome 18/BCL2: effects on BCL2 expression and apoptosis in B-cell non-Hodgkin's lymphomas. Leukemia *19*, 2313-2323.

Gao, P., Bauvy, C., Souquere, S., Tonelli, G., Liu, L., Zhu, Y., Qiao, Z., Bakula, D., Proikas-Cezanne, T., Pierron, G., *et al.* (2010). The Bcl-2 homology domain 3 mimetic gossypol induces both Beclin 1-dependent and Beclin 1-independent cytoprotective autophagy in cancer cells. J Biol Chem *285*, 25570-25581.

Gascoyne, R.D., Adomat, S.A., Krajewski, S., Krajewska, M., Horsman, D.E., Tolcher, A.W., O'Reilly, S.E., Hoskins, P., Coldman, A.J., Reed, J.C., *et al.* (1997). Prognostic significance of Bcl-2 protein expression and Bcl-2 gene rearrangement in diffuse aggressive non-Hodgkin's lymphoma. Blood *90*, 244-251.

Geng, Q.R., Xu, D.Z., He, L.J., Lu, J.B., Zhou, Z.W., Zhan, Y.Q., and Lu, Y. (2012). Beclin-1 expression is a significant predictor of survival in patients with lymph node-positive gastric cancer. PLoS One *7*, e45968.

Gething, M.J. (1999). Role and regulation of the ER chaperone BiP. Semin Cell Dev Biol *10*, 465-472.

Giammarioli, A.M., Gambardella, L., Barbati, C., Pietraforte, D., Tinari, A., Alberton, M., Gnessi, L., Griffin, R.J., Minetti, M., and Malorni, W. (2012). Differential effects of the glycolysis inhibitor 2-deoxy-D-glucose on the activity of pro-apoptotic agents in metastatic melanoma cells, and induction of a cytoprotective autophagic response. Int J Cancer *131*, E337-347.

Giatromanolaki, A., Koukourakis, M.I., Harris, A.L., Polychronidis, A., Gatter, K.C., and Sivridis, E. (2010). Prognostic relevance of light chain 3 (LC3A) autophagy patterns in colorectal adenocarcinomas. J Clin Pathol *63*, 867-872.

Glas, A.M., Kersten, M.J., Delahaye, L.J., Witteveen, A.T., Kibbelaar, R.E., Velds, A., Wessels, L.F., Joosten, P., Kerkhoven, R.M., Bernards, R., *et al.* (2005). Gene expression profiling in

follicular lymphoma to assess clinical aggressiveness and to guide the choice of treatment. Blood *105*, 301-307.

Glass, A.G., Karnell, L.H., and Menck, H.R. (1997). The National Cancer Data Base report on non-Hodgkin's lymphoma. Cancer *80*, 2311-2320.

Glennie, M.J., French, R.R., Cragg, M.S., and Taylor, R.P. (2007). Mechanisms of killing by anti-CD20 monoclonal antibodies. Mol Immunol *44*, 3823-3837.

Gonzalez-Polo, R.A., Boya, P., Pauleau, A.L., Jalil, A., Larochette, N., Souquere, S., Eskelinen, E.L., Pierron, G., Saftig, P., and Kroemer, G. (2005). The apoptosis/autophagy paradox: autophagic vacuolization before apoptotic death. J Cell Sci *118*, 3091-3102.

Goy, A., Younes, A., McLaughlin, P., Pro, B., Romaguera, J.E., Hagemeister, F., Fayad, L., Dang, N.H., Samaniego, F., Wang, M., *et al.* (2005). Phase II study of proteasome inhibitor bortezomib in relapsed or refractory B-cell non-Hodgkin's lymphoma. J Clin Oncol *23*, 667-675.

Greaves, P., Clear, A., Coutinho, R., Wilson, A., Matthews, J., Owen, A., Shanyinde, M., Lister, T.A., Calaminici, M., and Gribben, J.G. (2013). Expression of FOXP3, CD68, and CD20 at diagnosis in the microenvironment of classical Hodgkin lymphoma is predictive of outcome. J Clin Oncol *31*, 256-262.

Green, T.M., Young, K.H., Visco, C., Xu-Monette, Z.Y., Orazi, A., Go, R.S., Nielsen, O., Gadeberg, O.V., Mourits-Andersen, T., Frederiksen, M., *et al.* (2012). Immunohistochemical double-hit score is a strong predictor of outcome in patients with diffuse large B-cell lymphoma treated with rituximab plus cyclophosphamide, doxorubicin, vincristine, and prednisone. J Clin Oncol *30*, 3460-3467.

Greenwald, R.J., Tumang, J.R., Sinha, A., Currier, N., Cardiff, R.D., Rothstein, T.L., Faller, D.V., and Denis, G.V. (2004). Eμ-BRD2 transgenic mice develop B-cell lymphoma and leukemia. Blood *103*, 1475-1484.

Guo, J.Y., Chen, H.Y., Mathew, R., Fan, J., Strohecker, A.M., Karsli-Uzunbas, G., Kamphorst, J.J., Chen, G., Lemons, J.M., Karantza, V., *et al.* (2011). Activated Ras requires autophagy to maintain oxidative metabolism and tumorigenesis. Genes Dev *25*, 460-470.

Gurbuxani, S., Anastasi, J., and Hyjek, E. (2009). Diffuse large B-cell lymphoma--more than a diffuse collection of large B cells: an entity in search of a meaningful classification. Arch Pathol Lab Med *133*, 1121-1134.

Gurtu, V., Kain, S.R., and Zhang, G. (1997). Fluorometric and colorimetric detection of caspase activity associated with apoptosis. Anal Biochem *251*, 98-102.

Hagberg, H., Gisselbrecht, C., and group, C.s. (2006). Randomised phase III study of R-ICE versus R-DHAP in relapsed patients with CD20 diffuse large B-cell lymphoma (DLBCL) followed by high-dose therapy and a second randomisation to maintenance treatment with rituximab or not: an update of the CORAL study. Ann Oncol *17 Suppl 4*, iv31-32.

Han, C., Sun, B., Wang, W., Cai, W., Lou, D., Sun, Y., and Zhao, X. (2011). Overexpression of microtubule-associated protein-1 light chain 3 is associated with melanoma metastasis and vasculogenic mimicry. Tohoku J Exp Med *223*, 243-251.

Hanada, M., Delia, D., Aiello, A., Stadtmauer, E., and Reed, J.C. (1993). bcl-2 gene hypomethylation and high-level expression in B-cell chronic lymphocytic leukemia. Blood *82*, 1820-1828.

Hanahan, D., and Weinberg, R.A. (2011). Hallmarks of cancer: the next generation. Cell *144*, 646-674.

Hao, J.H., Yu, M., Liu, F.T., Newland, A.C., and Jia, L. (2004). Bcl-2 inhibitors sensitize tumor necrosis factor-related apoptosis-inducing ligand-induced apoptosis by uncoupling of mitochondrial respiration in human leukemic CEM cells. Cancer Res *64*, 3607-3616.

He, C., and Klionsky, D.J. (2009). Regulation mechanisms and signaling pathways of autophagy. Annu Rev Genet *43*, 67-93.

He, C., and Levine, B. (2010). The Beclin 1 interactome. Current opinion in cell biology *22*, 140-149.

He, J.H., Luo, R.Z., Cai, M.Y., Li, M., Lu, J.B., and Yuan, Z.Y. (2013). Decreased expression of light chain 3 (LC3) increased the risk of distant metastasis in triple-negative breast cancer. Med Oncol *30*, 468.

Helgason, G.V., Mukhopadhyay, A., Karvela, M., Salomoni, P., Calabretta, B., and Holyoake, T.L. (2013). Autophagy in chronic myeloid leukaemia: stem cell survival and implication in therapy. Curr Cancer Drug Targets *13*, 724-734.

Hermine, O., Haioun, C., Lepage, E., d'Agay, M.F., Briere, J., Lavignac, C., Fillet, G., Salles, G., Marolleau, J.P., Diebold, J., *et al.* (1996). Prognostic significance of bcl-2 protein expression in aggressive non-Hodgkin's lymphoma. Groupe d'Etude des Lymphomes de l'Adulte (GELA). Blood *87*, 265-272.

Hiddemann, W., Kneba, M., Dreyling, M., Schmitz, N., Lengfelder, E., Schmits, R., Reiser, M., Metzner, B., Harder, H., Hegewisch-Becker, S., *et al.* (2005). Frontline therapy with rituximab added to the combination of cyclophosphamide, doxorubicin, vincristine, and prednisone (CHOP) significantly improves the outcome for patients with advanced-stage follicular lymphoma compared with therapy with CHOP alone: results of a prospective randomized study of the German Low-Grade Lymphoma Study Group. Blood *106*, 3725-3732.

Huang, J.J., Li, H.R., Huang, Y., Jiang, W.Q., Xu, R.H., Huang, H.Q., Lv, Y., Xia, Z.J., Zhu, X.F., Lin, T.Y., *et al.* (2010). Beclin 1 expression: a predictor of prognosis in patients with extranodal natural killer T-cell lymphoma, nasal type. Autophagy *6*, 777-783.

Huang, J.J., Zhu, Y.J., Lin, T.Y., Jiang, W.Q., Huang, H.Q., and Li, Z.M. (2011). Beclin 1 expression predicts favorable clinical outcome in patients with diffuse large B-cell lymphoma treated with R-CHOP. Hum Pathol *42*, 1459-1466.

Huang, X., Meng, B., Iqbal, J., Ding, B.B., Perry, A.M., Cao, W., Smith, L.M., Bi, C., Jiang, C., Greiner, T.C., *et al.* (2013). Activation of the STAT3 signaling pathway is associated with poor survival in diffuse large B-cell lymphoma treated with R-CHOP. J Clin Oncol *31*, 4520-4528.

Hubbard, S.M., Chabner, B.A., DeVita, V.T., Jr., Simon, R., Berard, C.W., Jones, R.B., Garvin, A.J., Canellos, G.P., Osborne, C.K., and Young, R.C. (1982). Histologic progression in non-Hodgkin's lymphoma. Blood *59*, 258-264.

Hunt, K.E., and Reichard, K.K. (2008). Diffuse large B-cell lymphoma. Arch Pathol Lab Med *132*, 118-124.

Ibrahim, S.F., and van den Engh, G. (2007). Flow cytometry and cell sorting. Adv Biochem Eng Biotechnol *106*, 19-39.

Ichimura, Y., Kominami, E., Tanaka, K., and Komatsu, M. (2008). Selective turnover of p62/A170/SQSTM1 by autophagy. Autophagy *4*, 1063-1066.

Imbeaud, S., Graudens, E., Boulanger, V., Barlet, X., Zaborski, P., Eveno, E., Mueller, O., Schroeder, A., and Auffray, C. (2005). Towards standardization of RNA quality assessment using user-independent classifiers of microcapillary electrophoresis traces. Nucleic Acids Res *33*, e56.

Inoue, D., Suzuki, T., Mitsuishi, Y., Miki, Y., Suzuki, S., Sugawara, S., Watanabe, M., Sakurada, A., Endo, C., Uruno, A., *et al.* (2012). Accumulation of p62/SQSTM1 is associated with poor prognosis in patients with lung adenocarcinoma. Cancer Sci *103*, 760-766.

Inui, T., Chano, T., Takikita-Suzuki, M., Nishikawa, M., Yamamoto, G., and Okabe, H. (2013). Association of p62/SQSTM1 excess and oral carcinogenesis. PLoS One *8*, e74398.

Iqbal, J., Neppalli, V.T., Wright, G., Dave, B.J., Horsman, D.E., Rosenwald, A., Lynch, J., Hans, C.P., Weisenburger, D.D., Greiner, T.C., *et al.* (2006). BCL2 expression is a prognostic marker for the activated B-cell-like type of diffuse large B-cell lymphoma. J Clin Oncol *24*, 961-968.

Ishii, T., Yanagawa, T., Yuki, K., Kawane, T., Yoshida, H., and Bannai, S. (1997). Low micromolar levels of hydrogen peroxide and proteasome inhibitors induce the 60-kDa A170 stress protein in murine peritoneal macrophages. Biochem Biophys Res Commun *232*, 33-37.

Jia, L., Dourmashkin, R.R., Allen, P.D., Gray, A.B., Newland, A.C., and Kelsey, S.M. (1997). Inhibition of autophagy abrogates tumour necrosis factor alpha induced apoptosis in human T-lymphoblastic leukaemic cells. Br J Haematol *98*, 673-685.

Jia, L., Gopinathan, G., Sukumar, J.T., and Gribben, J.G. (2012). Blocking Autophagy Prevents Bortezomib-Induced NF-kappaB Activation by Reducing I-kappaBalpha Degradation in Lymphoma Cells. PLoS One *7*, e32584.

Johansen, T., and Lamark, T. (2011). Selective autophagy mediated by autophagic adapter proteins. Autophagy *7*, 279-296.

Johnson, N.A., Slack, G.W., Savage, K.J., Connors, J.M., Ben-Neriah, S., Rogic, S., Scott, D.W., Tan, K.L., Steidl, C., Sehn, L.H., *et al.* (2012). Concurrent expression of MYC and BCL2

in diffuse large B-cell lymphoma treated with rituximab plus cyclophosphamide, doxorubicin, vincristine, and prednisone. J Clin Oncol *30*, 3452-3459.

Jung, C.H., Ro, S.H., Cao, J., Otto, N.M., and Kim, D.H. (2010). mTOR regulation of autophagy. FEBS Lett *584*, 1287-1295.

Kabeya, Y., Kawamata, T., Suzuki, K., and Ohsumi, Y. (2007). Cis1/Atg31 is required for autophagosome formation in Saccharomyces cerevisiae. Biochem Biophys Res Commun *356*, 405-410.

Kabeya, Y., Mizushima, N., Ueno, T., Yamamoto, A., Kirisako, T., Noda, T., Kominami, E., Ohsumi, Y., and Yoshimori, T. (2000). LC3, a mammalian homologue of yeast Apg8p, is localized in autophagosome membranes after processing. EMBO J *19*, 5720-5728.

Kaminski, M.S., Tuck, M., Estes, J., Kolstad, A., Ross, C.W., Zasadny, K., Regan, D., Kison, P., Fisher, S., Kroll, S., *et al.* (2005). 131I-tositumomab therapy as initial treatment for follicular lymphoma. N Engl J Med *352*, 441-449.

Kang, M.H., and Reynolds, C.P. (2009). Bcl-2 inhibitors: targeting mitochondrial apoptotic pathways in cancer therapy. Clin Cancer Res *15*, 1126-1132.

Kang, M.H., Wan, Z., Kang, Y.H., Sposto, R., and Reynolds, C.P. (2008). Mechanism of synergy of N-(4-hydroxyphenyl)retinamide and ABT-737 in acute lymphoblastic leukemia cell lines: Mcl-1 inactivation. Journal of the National Cancer Institute *100*, 580-595.

Kang, M.R., Kim, M.S., Oh, J.E., Kim, Y.R., Song, S.Y., Kim, S.S., Ahn, C.H., Yoo, N.J., and Lee, S.H. (2009). Frameshift mutations of autophagy-related genes ATG2B, ATG5, ATG9B and ATG12 in gastric and colorectal cancers with microsatellite instability. J Pathol *217*, 702-706.

Kang, R., Livesey, K.M., Zeh, H.J., Loze, M.T., and Tang, D. (2010). HMGB1: a novel Beclin 1-binding protein active in autophagy. Autophagy *6*, 1209-1211.

Kang, R., Zeh, H.J., Lotze, M.T., and Tang, D. (2011). The Beclin 1 network regulates autophagy and apoptosis. Cell Death Differ *18*, 571-580.

Karantza-Wadsworth, V., Patel, S., Kravchuk, O., Chen, G., Mathew, R., Jin, S., and White, E. (2007). Autophagy mitigates metabolic stress and genome damage in mammary tumorigenesis. Genes Dev *21*, 1621-1635.

Karpathiou, G., Sivridis, E., Koukourakis, M.I., Mikroulis, D., Bouros, D., Froudarakis, M.E., and Giatromanolaki, A. (2011). Light-chain 3A autophagic activity and prognostic significance in non-small cell lung carcinomas. Chest *140*, 127-134.

Katzmann, J.A., Abraham, R.S., Dispenzieri, A., Lust, J.A., and Kyle, R.A. (2005). Diagnostic performance of quantitative kappa and lambda free light chain assays in clinical practice. Clin Chem *51*, 878-881.

Kaufmann, S.H., Desnoyers, S., Ottaviano, Y., Davidson, N.E., and Poirier, G.G. (1993). Specific proteolytic cleavage of poly(ADP-ribose) polymerase: an early marker of chemotherapy-induced apoptosis. Cancer Res *53*, 3976-3985.

Kaufmann, S.H., and Earnshaw, W.C. (2000). Induction of apoptosis by cancer chemotherapy. Exp Cell Res *256*, 42-49.

Kelly, P.N., and Strasser, A. (2011). The role of Bcl-2 and its pro-survival relatives in tumourigenesis and cancer therapy. Cell Death Differ *18*, 1414-1424.

Kerr, J.F., Wyllie, A.H., and Currie, A.R. (1972). Apoptosis: a basic biological phenomenon with wide-ranging implications in tissue kinetics. Br J Cancer *26*, 239-257.

Khan, S.B., Maududi, T., Barton, K., Ayers, J., and Alkan, S. (2004). Analysis of histone deacetylase inhibitor, depsipeptide (FR901228), effect on multiple myeloma. Br J Haematol *125*, 156-161.

Kihara, A., Kabeya, Y., Ohsumi, Y., and Yoshimori, T. (2001). Beclin-phosphatidylinositol 3-kinase complex functions at the trans-Golgi network. EMBO reports *2*, 330-335.

Kim, J., Kundu, M., Viollet, B., and Guan, K.L. (2011). AMPK and mTOR regulate autophagy through direct phosphorylation of Ulk1. Nat Cell Biol *13*, 132-141.

Kim, K.W., Moretti, L., Mitchell, L.R., Jung, D.K., and Lu, B. (2009). Combined Bcl-2/mammalian target of rapamycin inhibition leads to enhanced radiosensitization via induction of apoptosis and autophagy in non-small cell lung tumor xenograft model. Clin Cancer Res *15*, 6096-6105.

Kimmelman, A.C. (2011). The dynamic nature of autophagy in cancer. Genes Dev *25*, 1999-2010.

Kirkin, V., McEwan, D.G., Novak, I., and Dikic, I. (2009). A role for ubiquitin in selective autophagy. Mol Cell *34*, 259-269.

Klionsky, D.J. (2007). Autophagy: from phenomenology to molecular understanding in less than a decade. Nat Rev Mol Cell Biol *8*, 931-937.

Klionsky, D.J., Abdalla, F.C., Abeliovich, H., Abraham, R.T., Acevedo-Arozena, A., Adeli, K., Agholme, L., Agnello, M., Agostinis, P., Aguirre-Ghiso, J.A., *et al.* (2012a). Guidelines for the use and interpretation of assays for monitoring autophagy. Autophagy *8*, 445-544.

Klionsky, D.J., Abdalla, F.C., Abeliovich, H., Abraham, R.T., Acevedo-Arozena, A., Adeli, K., Agholme, L., Agnello, M., Agostinis, P., Aguirre-Ghiso, J.A., *et al.* (2012b). Guidelines for the use and interpretation of assays for monitoring autophagy. Autophagy *8*, 445-544.

Klionsky, D.J., Abeliovich, H., Agostinis, P., Agrawal, D.K., Aliev, G., Askew, D.S., Baba, M., Baehrecke, E.H., Bahr, B.A., Ballabio, A., *et al.* (2008a). Guidelines for the use and interpretation of assays for monitoring autophagy in higher eukaryotes. Autophagy *4*, 151-175.

Klionsky, D.J., Cuervo, A.M., and Seglen, P.O. (2007). Methods for monitoring autophagy from yeast to human. Autophagy *3*, 181-206.

Klionsky, D.J., Elazar, Z., Seglen, P.O., and Rubinsztein, D.C. (2008b). Does bafilomycin A1 block the fusion of autophagosomes with lysosomes? Autophagy *4*, 849-850.

Komatsu, M., Kageyama, S., and Ichimura, Y. (2012). p62/SQSTM1/A170: physiology and pathology. Pharmacol Res *66*, 457-462.

Komatsu, M., Kurokawa, H., Waguri, S., Taguchi, K., Kobayashi, A., Ichimura, Y., Sou, Y.S., Ueno, I., Sakamoto, A., Tong, K.I., *et al.* (2010). The selective autophagy substrate p62 activates the stress responsive transcription factor Nrf2 through inactivation of Keap1. Nat Cell Biol *12*, 213-223.

Komatsu, M., Waguri, S., Koike, M., Sou, Y.S., Ueno, T., Hara, T., Mizushima, N., Iwata, J., Ezaki, J., Murata, S., *et al.* (2007). Homeostatic levels of p62 control cytoplasmic inclusion body formation in autophagy-deficient mice. Cell *131*, 1149-1163.

Konopleva, M., Contractor, R., Tsao, T., Samudio, I., Ruvolo, P.P., Kitada, S., Deng, X., Zhai, D., Shi, Y.X., Sneed, T., *et al.* (2006). Mechanisms of apoptosis sensitivity and resistance to the BH3 mimetic ABT-737 in acute myeloid leukemia. Cancer Cell *10*, 375-388.

Korolchuk, V.I., Menzies, F.M., and Rubinsztein, D.C. (2010). Mechanisms of cross-talk between the ubiquitin-proteasome and autophagy-lysosome systems. FEBS Lett *584*, 1393-1398.

Koukourakis, M.I., Giatromanolaki, A., Sivridis, E., Pitiakoudis, M., Gatter, K.C., and Harris, A.L. (2010). Beclin 1 over- and underexpression in colorectal cancer: distinct patterns relate to prognosis and tumour hypoxia. Br J Cancer *103*, 1209-1214.

Kouroku, Y., Fujita, E., Tanida, I., Ueno, T., Isoai, A., Kumagai, H., Ogawa, S., Kaufman, R.J., Kominami, E., and Momoi, T. (2007). ER stress (PERK/eIF2alpha phosphorylation) mediates the polyglutamine-induced LC3 conversion, an essential step for autophagy formation. Cell Death Differ *14*, 230-239.

Krajewski, S., Krajewska, M., Shabaik, A., Miyashita, T., Wang, H.G., and Reed, J.C. (1994). Immunohistochemical determination of in vivo distribution of Bax, a dominant inhibitor of Bcl-2. Am J Pathol *145*, 1323-1336.

Kreth, S., Heyn, J., Grau, S., Kretzschmar, H.A., Egensperger, R., and Kreth, F.W. (2010). Identification of valid endogenous control genes for determining gene expression in human glioma. Neuro Oncol *12*, 570-579.

Kridel, R., Sehn, L.H., and Gascoyne, R.D. (2012). Pathogenesis of follicular lymphoma. J Clin Invest *122*, 3424-3431.

Kroemer, G., Galluzzi, L., and Brenner, C. (2007). Mitochondrial membrane permeabilization in cell death. Physiol Rev *87*, 99-163.

Kroemer, G., Marino, G., and Levine, B. (2010). Autophagy and the integrated stress response. Mol Cell *40*, 280-293.

Kurien, B.T., and Scofield, R.H. (2006). Western blotting. Methods *38*, 283-293.

Kuwana, T., Bouchier-Hayes, L., Chipuk, J.E., Bonzon, C., Sullivan, B.A., Green, D.R., and Newmeyer, D.D. (2005). BH3 domains of BH3-only proteins differentially regulate Bax-

mediated mitochondrial membrane permeabilization both directly and indirectly. Mol Cell *17*, 525-535.

Lamark, T., Perander, M., Outzen, H., Kristiansen, K., Overvatn, A., Michaelsen, E., Bjorkoy, G., and Johansen, T. (2003). Interaction codes within the family of mammalian Phox and Bem1p domain-containing proteins. J Biol Chem *278*, 34568-34581.

Launay, E., Pangault, C., Bertrand, P., Jardin, F., Lamy, T., Tilly, H., Tarte, K., Bastard, C., and Fest, T. (2012). High rate of TNFRSF14 gene alterations related to 1p36 region in de novo follicular lymphoma and impact on prognosis. Leukemia *26*, 559-562.

Le Grand, J.N., Bon, K., Fraichard, A., Zhang, J., Jouvenot, M., Risold, P.-Y., Boyer-Guittaut, M., and Delage-Mourroux, R. (2013). Specific distribution of the autophagic protein GABARAPL1/GEC1 in the developing and adult mouse brain and identification of neuronal populations expressing GABARAPL1/GEC1. PloS one *8*, e63133.

Lee, A.M., Clear, A.J., Calaminici, M., Davies, A.J., Jordan, S., MacDougall, F., Matthews, J., Norton, A.J., Gribben, J.G., Lister, T.A., *et al.* (2006). Number of CD4+ cells and location of forkhead box protein P3-positive cells in diagnostic follicular lymphoma tissue microarrays correlates with outcome. J Clin Oncol *24*, 5052-5059.

Lee, H.S., Daniels, B.H., Salas, E., Bollen, A.W., Debnath, J., and Margeta, M. (2012). Clinical utility of LC3 and p62 immunohistochemistry in diagnosis of drug-induced autophagic vacuolar myopathies: a case-control study. PLoS One *7*, e36221.

Lee, Y.J., Ha, Y.J., Kang, Y.N., Kang, K.J., Hwang, J.S., Chung, W.J., Cho, K.B., Park, K.S., Kim, E.S., Seo, H.Y., *et al.* (2013). The autophagy-related marker LC3 can predict prognosis in human hepatocellular carcinoma. PLoS One *8*, e81540.

Lejeune, M., and Alvaro, T. (2009). Clinicobiological, prognostic and therapeutic implications of the tumor microenvironment in follicular lymphoma. Haematologica *94*, 16-21.

Lenz, G., and Staudt, L.M. (2010). Aggressive lymphomas. N Engl J Med *362*, 1417-1429.

Lenz, G., Wright, G., Dave, S.S., Xiao, W., Powell, J., Zhao, H., Xu, W., Tan, B., Goldschmidt, N., Iqbal, J., *et al.* (2008a). Stromal gene signatures in large-B-cell lymphomas. N Engl J Med *359*, 2313-2323.

Lenz, G., Wright, G.W., Emre, N.C., Kohlhammer, H., Dave, S.S., Davis, R.E., Carty, S., Lam, L.T., Shaffer, A.L., Xiao, W., *et al.* (2008b). Molecular subtypes of diffuse large B-cell lymphoma arise by distinct genetic pathways. Proc Natl Acad Sci U S A *105*, 13520-13525.

Letai, A., Bassik, M.C., Walensky, L.D., Sorcinelli, M.D., Weiler, S., and Korsmeyer, S.J. (2002). Distinct BH3 domains either sensitize or activate mitochondrial apoptosis, serving as prototype cancer therapeutics. Cancer Cell *2*, 183-192.

Levine, B., and Klionsky, D.J. (2004). Development by self-digestion: molecular mechanisms and biological functions of autophagy. Dev Cell *6*, 463-477.

Levine, B., and Kroemer, G. (2008). Autophagy in the pathogenesis of disease. Cell *132*, 27-42.

Levine, B., Sinha, S., and Kroemer, G. (2008). Bcl-2 family members: dual regulators of apoptosis and autophagy. Autophagy *4*, 600-606.

Li, L., Chen, Y., and Gibson, S.B. (2013). Starvation-induced autophagy is regulated by mitochondrial reactive oxygen species leading to AMPK activation. Cell Signal *25*, 50-65.

Lian, J., Wu, X., He, F., Karnak, D., Tang, W., Meng, Y., Xiang, D., Ji, M., Lawrence, T.S., and Xu, L. (2011). A natural BH3 mimetic induces autophagy in apoptosis-resistant prostate cancer via modulating Bcl-2-Beclin1 interaction at endoplasmic reticulum. Cell Death Differ *18*, 60-71.

Liang, X.H., Jackson, S., Seaman, M., Brown, K., Kempkes, B., Hibshoosh, H., and Levine, B. (1999). Induction of autophagy and inhibition of tumorigenesis by beclin 1. Nature *402*, 672-676.

Liang, X.H., Kleeman, L.K., Jiang, H.H., Gordon, G., Goldman, J.E., Berry, G., Herman, B., and Levine, B. (1998). Protection against fatal Sindbis virus encephalitis by beclin, a novel Bcl-2-interacting protein. J Virol *72*, 8586-8596.

Lindqvist, L.M., Heinlein, M., Huang, D.C., and Vaux, D.L. (2014). Prosurvival Bcl-2 family members affect autophagy only indirectly, by inhibiting Bax and Bak. Proc Natl Acad Sci U S A *111*, 8512-8517.

Ling, J., Kang, Y., Zhao, R., Xia, Q., Lee, D.F., Chang, Z., Li, J., Peng, B., Fleming, J.B., Wang, H., *et al.* (2012). KrasG12D-induced IKK2/beta/NF-kappaB activation by IL-1alpha and p62 feedforward loops is required for development of pancreatic ductal adenocarcinoma. Cancer Cell *21*, 105-120.

Lipford, E., Wright, J.J., Urba, W., Whang-Peng, J., Kirsch, I.R., Raffeld, M., Cossman, J., Longo, D.L., Bakhshi, A., and Korsmeyer, S.J. (1987). Refinement of lymphoma cytogenetics by the chromosome 18q21 major breakpoint region. Blood *70*, 1816-1823.

Liu, D., Yang, Y., Liu, Q., and Wang, J. (2011). Inhibition of autophagy by 3-MA potentiates cisplatin-induced apoptosis in esophageal squamous cell carcinoma cells. Med Oncol *28*, 105-111.

Llambi, F., and Green, D.R. (2011). Apoptosis and oncogenesis: give and take in the BCL-2 family. Curr Opin Genet Dev *21*, 12-20.

Llanos, M., Alvarez-Arguelles, H., Aleman, R., Oramas, J., Diaz-Flores, L., and Batista, N. (2001). Prognostic significance of Ki-67 nuclear proliferative antigen, bcl-2 protein, and p53 expression in follicular and diffuse large B-cell lymphoma. Med Oncol *18*, 15-22.

Lock, R., Roy, S., Kenific, C.M., Su, J.S., Salas, E., Ronen, S.M., and Debnath, J. (2011). Autophagy facilitates glycolysis during Ras-mediated oncogenic transformation. Mol Biol Cell *22*, 165-178.

Lossos, I.S., Alizadeh, A.A., Eisen, M.B., Chan, W.C., Brown, P.O., Botstein, D., Staudt, L.M., and Levy, R. (2000). Ongoing immunoglobulin somatic mutation in germinal center B cell-like but not in activated B cell-like diffuse large cell lymphomas. Proc Natl Acad Sci U S A *97*, 10209-10213.

Lossos, I.S., and Levy, R. (2003). Higher grade transformation of follicular lymphoma: phenotypic tumor progression associated with diverse genetic lesions. Semin Cancer Biol *13*, 191-202.

Lu, M., Nakamura, R.M., Dent, E.D., Zhang, J.Y., Nielsen, F.C., Christiansen, J., Chan, E.K., and Tan, E.M. (2001). Aberrant expression of fetal RNA-binding protein p62 in liver cancer and liver cirrhosis. Am J Pathol *159*, 945-953.

Lucin, K.M., and Wyss-Coray, T. (2013). Targeting autophagy for disease therapy. Nat Biotechnol *31*, 322-323.

Lum, J.J., Bauer, D.E., Kong, M., Harris, M.H., Li, C., Lindsten, T., and Thompson, C.B. (2005a). Growth factor regulation of autophagy and cell survival in the absence of apoptosis. Cell *120*, 237-248.

Lum, J.J., DeBerardinis, R.J., and Thompson, C.B. (2005b). Autophagy in metazoans: cell survival in the land of plenty. Nat Rev Mol Cell Biol *6*, 439-448.

Luo, R.Z., Yuan, Z.Y., Li, M., Xi, S.Y., Fu, J., and He, J. (2013). Accumulation of p62 is associated with poor prognosis in patients with triple-negative breast cancer. Onco Targets Ther *6*, 883-888.

Maclean, K.H., Dorsey, F.C., Cleveland, J.L., and Kastan, M.B. (2008). Targeting lysosomal degradation induces p53-dependent cell death and prevents cancer in mouse models of lymphomagenesis. J Clin Invest *118*, 79-88.

Maiuri, M.C., Criollo, A., Tasdemir, E., Vicencio, J.M., Tajeddine, N., Hickman, J.A., Geneste, O., and Kroemer, G. (2007a). BH3-only proteins and BH3 mimetics induce autophagy by competitively disrupting the interaction between Beclin 1 and Bcl-2/Bcl-X(L). Autophagy *3*, 374-376.

Maiuri, M.C., Galluzzi, L., Morselli, E., Kepp, O., Malik, S.A., and Kroemer, G. (2010). Autophagy regulation by p53. Curr Opin Cell Biol *22*, 181-185.

Maiuri, M.C., Le Toumelin, G., Criollo, A., Rain, J.C., Gautier, F., Juin, P., Tasdemir, E., Pierron, G., Troulinaki, K., Tavernarakis, N., *et al.* (2007b). Functional and physical interaction between Bcl-X(L) and a BH3-like domain in Beclin-1. EMBO J *26*, 2527-2539.

Maiuri, M.C., Zalckvar, E., Kimchi, A., and Kroemer, G. (2007c). Self-eating and self-killing: crosstalk between autophagy and apoptosis. Nat Rev Mol Cell Biol *8*, 741-752.

Malik, S.A., Orhon, I., Morselli, E., Criollo, A., Shen, S., Marino, G., BenYounes, A., Benit, P., Rustin, P., Maiuri, M.C., *et al.* (2011). BH3 mimetics activate multiple pro-autophagic pathways. Oncogene *30*, 3918-3929.

Mandy, F.F., Bergeron, M., and Minkus, T. (1995). Principles of flow cytometry. Transfus Sci *16*, 303-314.

Marchetti, P., Hirsch, T., Zamzami, N., Castedo, M., Decaudin, D., Susin, S.A., Masse, B., and Kroemer, G. (1996). Mitochondrial permeability transition triggers lymphocyte apoptosis. J Immunol *157*, 4830-4836.

Marcus, R., Imrie, K., Solal-Celigny, P., Catalano, J.V., Dmoszynska, A., Raposo, J.C., Offner, F.C., Gomez-Codina, J., Belch, A., Cunningham, D., *et al.* (2008). Phase III study of R-CVP compared with cyclophosphamide, vincristine, and prednisone alone in patients with previously untreated advanced follicular lymphoma. J Clin Oncol *26*, 4579-4586.

Marquez, R.T., and Xu, L. (2012). Bcl-2:Beclin 1 complex: multiple, mechanisms regulating autophagy/apoptosis toggle switch. Am J Cancer Res *2*, 214-221.

Martin, A., and Caballero, M.D. (2009). R-ESHAP as salvage therapy for patients with relapsed or refractory diffuse large B-cell lymphoma: influence of prior autologous stem-cell transplantation on outcome. Haematologica *94*, 744.

Martinez, F.O., Helming, L., Milde, R., Varin, A., Melgert, B.N., Draijer, C., Thomas, B., Fabbri, M., Crawshaw, A., Ho, L.P., *et al.* (2013). Genetic programs expressed in resting and IL-4 alternatively activated mouse and human macrophages: similarities and differences. Blood *121*, e57-69.

Masir, N., Campbell, L.J., Goff, L.K., Jones, M., Marafioti, T., Cordell, J., Clear, A.J., Lister, T.A., Mason, D.Y., and Lee, A.M. (2009). BCL2 protein expression in follicular lymphomas with t(14;18) chromosomal translocations. Br J Haematol *144*, 716-725.

Mathew, R., Karp, C.M., Beaudoin, B., Vuong, N., Chen, G., Chen, H.Y., Bray, K., Reddy, A., Bhanot, G., Gelinas, C., *et al.* (2009). Autophagy suppresses tumorigenesis through elimination of p62. Cell *137*, 1062-1075.

Matsuura, A., Tsukada, M., Wada, Y., and Ohsumi, Y. (1997). Apg1p, a novel protein kinase required for the autophagic process in Saccharomyces cerevisiae. Gene *192*, 245-250.

Maycotte, P., Aryal, S., Cummings, C.T., Thorburn, J., Morgan, M.J., and Thorburn, A. (2012). Chloroquine sensitizes breast cancer cells to chemotherapy independent of autophagy. Autophagy *8*, 200-212.

Mazure, N.M., and Pouyssegur, J. (2010). Hypoxia-induced autophagy: cell death or cell survival? Curr Opin Cell Biol *22*, 177-180.

McDonnell, T.J., Deane, N., Platt, F.M., Nunez, G., Jaeger, U., McKearn, J.P., and Korsmeyer, S.J. (1989). bcl-2-immunoglobulin transgenic mice demonstrate extended B cell survival and follicular lymphoproliferation. Cell *57*, 79-88.

McDonnell, T.J., and Korsmeyer, S.J. (1991). Progression from lymphoid hyperplasia to high-grade malignant lymphoma in mice transgenic for the t(14; 18). Nature *349*, 254-256.

Miyashita, T., and Reed, J.C. (1993). Bcl-2 oncoprotein blocks chemotherapy-induced apoptosis in a human leukemia cell line. Blood *81*, 151-157.

Miyoshi, N., Ishii, H., Mimori, K., Tanaka, F., Hitora, T., Tei, M., Sekimoto, M., Doki, Y., and Mori, M. (2010). TGM2 is a novel marker for prognosis and therapeutic target in colorectal cancer. Ann Surg Oncol *17*, 967-972.

Mizushima, N., Levine, B., Cuervo, A.M., and Klionsky, D.J. (2008). Autophagy fights disease through cellular self-digestion. Nature *451*, 1069-1075.

Mizushima, N., Sugita, H., Yoshimori, T., and Ohsumi, Y. (1998). A new protein conjugation system in human. The counterpart of the yeast Apg12p conjugation system essential for autophagy. J Biol Chem *273*, 33889-33892.

Mizushima, N., Yamamoto, A., Matsui, M., Yoshimori, T., and Ohsumi, Y. (2004). In vivo analysis of autophagy in response to nutrient starvation using transgenic mice expressing a fluorescent autophagosome marker. Mol Biol Cell *15*, 1101-1111.

Mizushima, N., and Yoshimori, T. (2007). How to interpret LC3 immunoblotting. Autophagy *3*, 542-545.

Montoto, S., Davies, A.J., Matthews, J., Calaminici, M., Norton, A.J., Amess, J., Vinnicombe, S., Waters, R., Rohatiner, A.Z., and Lister, T.A. (2007). Risk and clinical implications of transformation of follicular lymphoma to diffuse large B-cell lymphoma. J Clin Oncol *25*, 2426-2433.

Morin, R.D., Johnson, N.A., Severson, T.M., Mungall, A.J., An, J., Goya, R., Paul, J.E., Boyle, M., Woolcock, B.W., Kuchenbauer, F., *et al.* (2010). Somatic mutations altering EZH2 (Tyr641) in follicular and diffuse large B-cell lymphomas of germinal-center origin. Nat Genet *42*, 181-185.

Morin, R.D., Mendez-Lago, M., Mungall, A.J., Goya, R., Mungall, K.L., Corbett, R.D., Johnson, N.A., Severson, T.M., Chiu, R., Field, M., *et al.* (2011). Frequent mutation of histone-modifying genes in non-Hodgkin lymphoma. Nature *476*, 298-303.

Morschhauser, F., Radford, J., Van Hoof, A., Vitolo, U., Soubeyran, P., Tilly, H., Huijgens, P.C., Kolstad, A., d'Amore, F., Gonzalez Diaz, M., *et al.* (2008). Phase III trial of consolidation therapy with yttrium-90-ibritumomab tiuxetan compared with no additional therapy after first remission in advanced follicular lymphoma. J Clin Oncol *26*, 5156-5164.

Morse, S.M., Shaw, G., and Larner, S.F. (2006). Concurrent mRNA and protein extraction from the same experimental sample using a commercially available column-based RNA preparation kit. Biotechniques *40*, 54, 56, 58.

Moscat, J., and Diaz-Meco, M.T. (2009). p62 at the crossroads of autophagy, apoptosis, and cancer. Cell *137*, 1001-1004.

Moscat, J., and Diaz-Meco, M.T. (2012). p62: a versatile multitasker takes on cancer. Trends Biochem Sci *37*, 230-236.

Mounier, N., Briere, J., Gisselbrecht, C., Emile, J.F., Lederlin, P., Sebban, C., Berger, F., Bosly, A., Morel, P., Tilly, H., *et al.* (2003). Rituximab plus CHOP (R-CHOP) overcomes bcl-2--associated resistance to chemotherapy in elderly patients with diffuse large B-cell lymphoma (DLBCL). Blood *101*, 4279-4284.

Moussay, E., Kaoma, T., Baginska, J., Muller, A., Van Moer, K., Nicot, N., Nazarov, P.V., Vallar, L., Chouaib, S., Berchem, G., *et al.* (2011). The acquisition of resistance to TNFalpha in breast cancer cells is associated with constitutive activation of autophagy as revealed by a transcriptome analysis using a custom microarray. Autophagy *7*, 760-770.

Mukhopadhyay, S., Panda, P.K., Sinha, N., Das, D.N., and Bhutia, S.K. (2014). Autophagy and apoptosis: where do they meet? Apoptosis *19*, 555-566.

Nakamura, K., Kimple, A.J., Siderovski, D.P., and Johnson, G.L. (2010). PB1 domain interaction of p62/sequestosome 1 and MEKK3 regulates NF-kappaB activation. J Biol Chem *285*, 2077-2089.

Nakaso, K., Yoshimoto, Y., Nakano, T., Takeshima, T., Fukuhara, Y., Yasui, K., Araga, S., Yanagawa, T., Ishii, T., and Nakashima, K. (2004). Transcriptional activation of p62/A170/ZIP during the formation of the aggregates: possible mechanisms and the role in Lewy body formation in Parkinson's disease. Brain Res *1012*, 42-51.

Nara, A., Mizushima, N., Yamamoto, A., Kabeya, Y., Ohsumi, Y., and Yoshimori, T. (2002). SKD1 AAA ATPase-dependent endosomal transport is involved in autolysosome formation. Cell Struct Funct *27*, 29-37.

Nastoupil, L.J., Rose, A.C., and Flowers, C.R. (2012). Diffuse large B-cell lymphoma: current treatment approaches. Oncology *26*, 488-495.

Nathwani, B.N., Anderson, J.R., Armitage, J.O., Cavalli, F., Diebold, J., Drachenberg, M.R., Harris, N.L., MacLennan, K.A., Muller-Hermelink, H.K., Ullrich, F.A., *et al.* (1999). Clinical significance of follicular lymphoma with monocytoid B cells. Non-Hodgkin's Lymphoma Classification Project. Hum Pathol *30*, 263-268.

Nazio, F., Strappazzon, F., Antonioli, M., Bielli, P., Cianfanelli, V., Bordi, M., Gretzmeier, C., Dengjel, J., Piacentini, M., Fimia, G.M., *et al.* (2013). mTOR inhibits autophagy by controlling ULK1 ubiquitylation, self-association and function through AMBRA1 and TRAF6. Nat Cell Biol *15*, 406-416.

Ngo, V.N., Young, R.M., Schmitz, R., Jhavar, S., Xiao, W., Lim, K.H., Kohlhammer, H., Xu, W., Yang, Y., Zhao, H., *et al.* (2011). Oncogenically active MYD88 mutations in human lymphoma. Nature *470*, 115-119.

Nicholls, D.G., and Ward, M.W. (2000). Mitochondrial membrane potential and neuronal glutamate excitotoxicity: mortality and millivolts. Trends Neurosci *23*, 166-174.

Nicotra, G., Manfroi, F., Follo, C., Castino, R., Fusco, N., Peracchio, C., Kerim, S., Valente, G., and Isidoro, C. (2010a). High expression of cathepsin D in non-Hodgkin's lymphomas negatively impacts on clinical outcome. Dis Markers *28*, 167-183.

Nicotra, G., Mercalli, F., Peracchio, C., Castino, R., Follo, C., Valente, G., and Isidoro, C. (2010b). Autophagy-active beclin-1 correlates with favourable clinical outcome in non-Hodgkin lymphomas. Mod Pathol *23*, 937-950.

Nogai, H., Dorken, B., and Lenz, G. (2011). Pathogenesis of non-Hodgkin's lymphoma. J Clin Oncol *29*, 1803-1811.

Novikoff, A.B., and Essner, E. (1962). Cytolysomes and mitochondrial degeneration. J Cell Biol *15*, 140-146.

O'Donoghue, A.E., Poller, D.N., Bell, J.A., Galea, M.H., Elston, C.W., Blamey, R.W., and Ellis, I.O. (1995). Cathepsin D in primary breast carcinoma: adverse prognosis is associated with expression of cathepsin D in stromal cells. Breast Cancer Res Treat *33*, 137-145.

Obermann, E.C., Csato, M., Dirnhofer, S., and Tzankov, A. (2009). BCL2 gene aberration as an IPI-independent marker for poor outcome in non-germinal-centre diffuse large B cell lymphoma. J Clin Pathol *62*, 903-907.

Offit, K., Koduru, P.R., Hollis, R., Filippa, D., Jhanwar, S.C., Clarkson, B.C., and Chaganti, R.S. (1989). 18q21 rearrangement in diffuse large cell lymphoma: incidence and clinical significance. Br J Haematol *72*, 178-183.

Ola, M.S., Nawaz, M., and Ahsan, H. (2011). Role of Bcl-2 family proteins and caspases in the regulation of apoptosis. Mol Cell Biochem *351*, 41-58.

Pankiv, S., Clausen, T.H., Lamark, T., Brech, A., Bruun, J.A., Outzen, H., Overvatn, A., Bjorkoy, G., and Johansen, T. (2007). p62/SQSTM1 binds directly to Atg8/LC3 to facilitate degradation of ubiquitinated protein aggregates by autophagy. J Biol Chem *282*, 24131-24145.

Papandreou, I., Lim, A.L., Laderoute, K., and Denko, N.C. (2008). Hypoxia signals autophagy in tumor cells via AMPK activity, independent of HIF-1, BNIP3, and BNIP3L. Cell Death Differ *15*, 1572-1581.

Park, J.M., Huang, S., Wu, T.-T., Foster, N.R., and Sinicrope, F.A. (2012). Prognostic impact of Beclin 1, p62/sequestosome 1 and LC3 protein expression in colon carcinomas from patients receiving 5-fluorouracil as adjuvant chemotherapy. Cancer biology & therapy *14*, 100-107.

Park, K.-S., Kim, H.-K., Lee, J.-H., Choi, Y.-B., Park, S.-Y., Yang, S.-H., Kim, S.-Y., and Hong, K.-M. (2010). Transglutaminase 2 as a cisplatin resistance marker in non-small cell lung cancer. Journal of cancer research and clinical oncology *136*, 493-502.

Pasqualucci, L., Dominguez-Sola, D., Chiarenza, A., Fabbri, G., Grunn, A., Trifonov, V., Kasper, L.H., Lerach, S., Tang, H., Ma, J., *et al.* (2011). Inactivating mutations of acetyltransferase genes in B-cell lymphoma. Nature *471*, 189-195.

Pattingre, S., and Levine, B. (2006). Bcl-2 inhibition of autophagy: a new route to cancer? Cancer Res *66*, 2885-2888.

Pattingre, S., Tassa, A., Qu, X., Garuti, R., Liang, X.H., Mizushima, N., Packer, M., Schneider, M.D., and Levine, B. (2005). Bcl-2 antiapoptotic proteins inhibit Beclin 1-dependent autophagy. Cell *122*, 927-939.

Pezzella, F., Jones, M., Ralfkiaer, E., Ersboll, J., Gatter, K.C., and Mason, D.Y. (1992). Evaluation of bcl-2 protein expression and 14;18 translocation as prognostic markers in follicular lymphoma. Br J Cancer *65*, 87-89.

Phizicky, E.M., and Fields, S. (1995). Protein-protein interactions: methods for detection and analysis. Microbiol Rev *59*, 94-123.

Pietras, K., and Ostman, A. (2010). Hallmarks of cancer: interactions with the tumor stroma. Exp Cell Res *316*, 1324-1331.

Porter, A.G., and Janicke, R.U. (1999). Emerging roles of caspase-3 in apoptosis. Cell Death Differ *6*, 99-104.

Prakash, S., and Swerdlow, S.H. (2007). Nodal aggressive B-cell lymphomas: a diagnostic approach. J Clin Pathol *60*, 1076-1085.

Puissant, A., Robert, G., Fenouille, N., Luciano, F., Cassuto, J.P., Raynaud, S., and Auberger, P. (2010). Resveratrol promotes autophagic cell death in chronic myelogenous leukemia cells via JNK-mediated p62/SQSTM1 expression and AMPK activation. Cancer Res *70*, 1042-1052.

Puls, A., Schmidt, S., Grawe, F., and Stabel, S. (1997). Interaction of protein kinase C zeta with ZIP, a novel protein kinase C-binding protein. Proc Natl Acad Sci U S A *94*, 6191-6196.

Pyo, J.O., Nah, J., and Jung, Y.K. (2012). Molecules and their functions in autophagy. Experimental & molecular medicine *44*, 73-80.

Qu, X., Yu, J., Bhagat, G., Furuya, N., Hibshoosh, H., Troxel, A., Rosen, J., Eskelinen, E.L., Mizushima, N., Ohsumi, Y., *et al.* (2003). Promotion of tumorigenesis by heterozygous disruption of the beclin 1 autophagy gene. J Clin Invest *112*, 1809-1820.

Ramos-Vara, J.A. (2005). Technical aspects of immunohistochemistry. Vet Pathol *42*, 405-426.
Renna, M., Jimenez-Sanchez, M., Sarkar, S., and Rubinsztein, D.C. (2010). Chemical inducers of autophagy that enhance the clearance of mutant proteins in neurodegenerative diseases. J Biol Chem *285*, 11061-11067.

Rodriguez-Muela, N., Germain, F., Marino, G., Fitze, P.S., and Boya, P. (2012). Autophagy promotes survival of retinal ganglion cells after optic nerve axotomy in mice. Cell Death Differ *19*, 162-169.

Rodriguez, A., Duran, A., Selloum, M., Champy, M.F., Diez-Guerra, F.J., Flores, J.M., Serrano, M., Auwerx, J., Diaz-Meco, M.T., and Moscat, J. (2006). Mature-onset obesity and insulin resistance in mice deficient in the signaling adapter p62. Cell Metab *3*, 211-222.

Rodriguez, D., Rojas-Rivera, D., and Hetz, C. (2011). Integrating stress signals at the endoplasmic reticulum: The BCL-2 protein family rheostat. Biochim Biophys Acta *1813*, 564-574.

Rolland, P., Madjd, Z., Durrant, L., Ellis, I.O., Layfield, R., and Spendlove, I. (2007). The ubiquitin-binding protein p62 is expressed in breast cancers showing features of aggressive disease. Endocr Relat Cancer *14*, 73-80.

Rosenfeldt, M.T., O'Prey, J., Morton, J.P., Nixon, C., MacKay, G., Mrowinska, A., Au, A., Rai, T.S., Zheng, L., Ridgway, R., *et al.* (2013). p53 status determines the role of autophagy in pancreatic tumour development. Nature *504*, 296-300.

Rosenfeldt, M.T., and Ryan, K.M. (2011). The multiple roles of autophagy in cancer. Carcinogenesis *32*, 955-963.

Rosenwald, A., Wright, G., Chan, W.C., Connors, J.M., Campo, E., Fisher, R.I., Gascoyne, R.D., Muller-Hermelink, H.K., Smeland, E.B., Giltnane, J.M., *et al.* (2002). The use of

molecular profiling to predict survival after chemotherapy for diffuse large-B-cell lymphoma. N Engl J Med *346*, 1937-1947.

Rouschop, K.M., van den Beucken, T., Dubois, L., Niessen, H., Bussink, J., Savelkouls, K., Keulers, T., Mujcic, H., Landuyt, W., Voncken, J.W., *et al.* (2010). The unfolded protein response protects human tumor cells during hypoxia through regulation of the autophagy genes MAP1LC3B and ATG5. J Clin Invest *120*, 127-141.

Rubinsztein, D.C., Marino, G., and Kroemer, G. (2011). Autophagy and aging. Cell *146*, 682-695.

Rubinsztein, D.C., Shpilka, T., and Elazar, Z. (2012). Mechanisms of autophagosome biogenesis. Curr Biol *22*, R29-34.

Russell, R.C., Tian, Y., Yuan, H., Park, H.W., Chang, Y.Y., Kim, J., Kim, H., Neufeld, T.P., Dillin, A., and Guan, K.L. (2013). ULK1 induces autophagy by phosphorylating Beclin-1 and activating VPS34 lipid kinase. Nat Cell Biol *15*, 741-750.

Saeki, K., Yuo, A., Okuma, E., Yazaki, Y., Susin, S.A., Kroemer, G., and Takaku, F. (2000). Bcl-2 down-regulation causes autophagy in a caspase-independent manner in human leukemic HL60 cells. Cell Death Differ *7*, 1263-1269.

Sahani, M.H., Itakura, E., and Mizushima, N. (2014). Expression of the autophagy substrate SQSTM1/p62 is restored during prolonged starvation depending on transcriptional upregulation and autophagy-derived amino acids. Autophagy *10*.

Sahni, S., Merlot, A.M., Krishan, S., Jansson, P.J., and Richardson, D.R. (2014). Gene of the month: BECN1. Journal of clinical pathology, jclinpath-2014-202356.

Salaverria, I., and Siebert, R. (2011). Follicular lymphoma grade 3B. Best practice & research Clinical haematology *24*, 111-119.

Salles, G. (2011). Is there a role for bortezomib combinations in the management of patients with follicular lymphoma? J Clin Oncol *29*, 3349-3350.

Salles, G., Seymour, J.F., Offner, F., Lopez-Guillermo, A., Belada, D., Xerri, L., Feugier, P., Bouabdallah, R., Catalano, J.V., Brice, P., *et al.* (2011). Rituximab maintenance for 2 years in patients with high tumour burden follicular lymphoma responding to rituximab plus chemotherapy (PRIMA): a phase 3, randomised controlled trial. Lancet *377*, 42-51.

Sanchez, P., De Carcer, G., Sandoval, I.V., Moscat, J., and Diaz-Meco, M.T. (1998). Localization of atypical protein kinase C isoforms into lysosome-targeted endosomes through interaction with p62. Mol Cell Biol *18*, 3069-3080.

Sarkar, S., Ravikumar, B., Floto, R.A., and Rubinsztein, D.C. (2009). Rapamycin and mTOR-independent autophagy inducers ameliorate toxicity of polyglutamine-expanded huntingtin and related proteinopathies. Cell Death Differ *16*, 46-56.

Sasaki, K., Tsuno, N.H., Sunami, E., Tsurita, G., Kawai, K., Okaji, Y., Nishikawa, T., Shuno, Y., Hongo, K., Hiyoshi, M., *et al.* (2010). Chloroquine potentiates the anti-cancer effect of 5-fluorouracil on colon cancer cells. BMC Cancer *10*, 370.

Sasi, N., Hwang, M., Jaboin, J., Csiki, I., and Lu, B. (2009). Regulated cell death pathways: new twists in modulation of BCL2 family function. Mol Cancer Ther *8*, 1421-1429.

Scaduto, R.C., Jr., and Grotyohann, L.W. (1999). Measurement of mitochondrial membrane potential using fluorescent rhodamine derivatives. Biophys J *76*, 469-477.

Scherz-Shouval, R., and Elazar, Z. (2011). Regulation of autophagy by ROS: physiology and pathology. Trends Biochem Sci *36*, 30-38.

Scherz-Shouval, R., Shvets, E., Fass, E., Shorer, H., Gil, L., and Elazar, Z. (2007). Reactive oxygen species are essential for autophagy and specifically regulate the activity of Atg4. EMBO J *26*, 1749-1760.

Schmid, D., and Munz, C. (2007). Innate and adaptive immunity through autophagy. Immunity *27*, 11-21.

Schmid, S., Tinguely, M., Cione, P., Moch, H., and Bode, B. (2011). Flow cytometry as an accurate tool to complement fine needle aspiration cytology in the diagnosis of low grade malignant lymphomas. Cytopathology *22*, 397-406.

Schroeder, A., Mueller, O., Stocker, S., Salowsky, R., Leiber, M., Gassmann, M., Lightfoot, S., Menzel, W., Granzow, M., and Ragg, T. (2006). The RIN: an RNA integrity number for assigning integrity values to RNA measurements. BMC Mol Biol *7*, 3.

Schweizer, D. (1976). Reverse fluorescent chromosome banding with chromomycin and DAPI. Chromosoma *58*, 307-324.

Seglen, P.O., and Gordon, P.B. (1982). 3-Methyladenine: specific inhibitor of autophagic/lysosomal protein degradation in isolated rat hepatocytes. Proc Natl Acad Sci U S A *79*, 1889-1892.

Sehn, L.H., Berry, B., Chhanabhai, M., Fitzgerald, C., Gill, K., Hoskins, P., Klasa, R., Savage, K.J., Shenkier, T., Sutherland, J., *et al.* (2007). The revised International Prognostic Index (R-IPI) is a better predictor of outcome than the standard IPI for patients with diffuse large B-cell lymphoma treated with R-CHOP. Blood *109*, 1857-1861.

Semenza, G.L. (2010). HIF-1: upstream and downstream of cancer metabolism. Curr Opin Genet Dev *20*, 51-56.

Shaffer, A.L., 3rd, Young, R.M., and Staudt, L.M. (2012). Pathogenesis of human B cell lymphomas. Annu Rev Immunol *30*, 565-610.

Shang, L., Chen, S., Du, F., Li, S., Zhao, L., and Wang, X. (2011). Nutrient starvation elicits an acute autophagic response mediated by Ulk1 dephosphorylation and its subsequent dissociation from AMPK. Proc Natl Acad Sci U S A *108*, 4788-4793.

Shankland, K.R., Armitage, J.O., and Hancock, B.W. (2012). Non-Hodgkin lymphoma. Lancet *380*, 848-857.

Shen, H.M., and Codogno, P. (2011). Autophagic cell death: Loch Ness monster or endangered species? Autophagy *7*, 457-465.

Shi, C.S., and Kehrl, J.H. (2010). TRAF6 and A20 regulate lysine 63-linked ubiquitination of Beclin-1 to control TLR4-induced autophagy. Science signaling *3*, ra42.

Shi, F.D., Zhang, J.Y., Liu, D., Rearden, A., Elliot, M., Nachtsheim, D., Daniels, T., Casiano, C.A., Heeb, M.J., Chan, E.K., *et al.* (2005). Preferential humoral immune response in prostate cancer to cellular proteins p90 and p62 in a panel of tumor-associated antigens. Prostate *63*, 252-258.

Shi, J., Wong, J., Piesik, P., Fung, G., Zhang, J., Jagdeo, J., Li, X., Jan, E., and Luo, H. (2013). Cleavage of sequestosome 1/p62 by an enteroviral protease results in disrupted selective autophagy and impaired NFKB signaling. Autophagy *9*.

Shi, S.R., Cote, R.J., and Taylor, C.R. (2001). Antigen retrieval techniques: current perspectives. J Histochem Cytochem *49*, 931-937.

Shi, S.R., Key, M.E., and Kalra, K.L. (1991). Antigen retrieval in formalin-fixed, paraffin-embedded tissues: an enhancement method for immunohistochemical staining based on microwave oven heating of tissue sections. J Histochem Cytochem *39*, 741-748.

Shibata, M., Yoshimura, K., Furuya, N., Koike, M., Ueno, T., Komatsu, M., Arai, H., Tanaka, K., Kominami, E., and Uchiyama, Y. (2009). The MAP1-LC3 conjugation system is involved in lipid droplet formation. Biochem Biophys Res Commun *382*, 419-423.

Shimizu, S., Kanaseki, T., Mizushima, N., Mizuta, T., Arakawa-Kobayashi, S., Thompson, C.B., and Tsujimoto, Y. (2004). Role of Bcl-2 family proteins in a non-apoptotic programmed cell death dependent on autophagy genes. Nat Cell Biol *6*, 1221-1228.

Simon, R., Mirlacher, M., and Sauter, G. (2004). Tissue microarrays. Biotechniques *36*, 98-105.

Sinclair, A., Latif, A.L., and Holyoake, T.L. (2013). Targeting survival pathways in chronic myeloid leukaemia stem cells. Br J Pharmacol *169*, 1693-1707.

Sivridis, E., Koukourakis, M.I., Mendrinos, S.E., Karpouzis, A., Fiska, A., Kouskoukis, C., and Giatromanolaki, A. (2011). Beclin-1 and LC3A expression in cutaneous malignant melanomas: a biphasic survival pattern for beclin-1. Melanoma Res *21*, 188-195.

Sivridis, E., Koukourakis, M.I., Zois, C.E., Ledaki, I., Ferguson, D.J., Harris, A.L., Gatter, K.C., and Giatromanolaki, A. (2010). LC3A-positive light microscopy detected patterns of autophagy and prognosis in operable breast carcinomas. Am J Pathol *176*, 2477-2489.

Skibola, C.F., Bracci, P.M., Halperin, E., Conde, L., Craig, D.W., Agana, L., Iyadurai, K., Becker, N., Brooks-Wilson, A., Curry, J.D., *et al.* (2009). Genetic variants at 6p21.33 are associated with susceptibility to follicular lymphoma. Nat Genet *41*, 873-875.

Solal-Celigny, P., Roy, P., Colombat, P., White, J., Armitage, J.O., Arranz-Saez, R., Au, W.Y., Bellei, M., Brice, P., Caballero, D., *et al.* (2004). Follicular lymphoma international prognostic index. Blood *104*, 1258-1265.

Song, J.H., and Kraft, A.S. (2012). Pim kinase inhibitors sensitize prostate cancer cells to apoptosis triggered by Bcl-2 family inhibitor ABT-737. Cancer Res *72*, 294-303.

Souers, A.J., Leverson, J.D., Boghaert, E.R., Ackler, S.L., Catron, N.D., Chen, J., Dayton, B.D., Ding, H., Enschede, S.H., Fairbrother, W.J., *et al.* (2013). ABT-199, a potent and selective BCL-2 inhibitor, achieves antitumor activity while sparing platelets. Nat Med *19*, 202-208.

Strappazzon, F., Vietri-Rudan, M., Campello, S., Nazio, F., Florenzano, F., Fimia, G.M., Piacentini, M., Levine, B., and Cecconi, F. (2011). Mitochondrial BCL-2 inhibits AMBRA1-induced autophagy. EMBO J *30*, 1195-1208.

Strosznajder, R.P., Jesko, H., and Zambrzycka, A. (2005). Poly(ADP-ribose) polymerase: the nuclear target in signal transduction and its role in brain ischemia-reperfusion injury. Mol Neurobiol *31*, 149-167.

Takamura, A., Komatsu, M., Hara, T., Sakamoto, A., Kishi, C., Waguri, S., Eishi, Y., Hino, O., Tanaka, K., and Mizushima, N. (2011). Autophagy-deficient mice develop multiple liver tumors. Genes Dev *25*, 795-800.

Tang, D., Kang, R., Livesey, K.M., Cheh, C.W., Farkas, A., Loughran, P., Hoppe, G., Bianchi, M.E., Tracey, K.J., Zeh, H.J., 3rd, *et al.* (2010). Endogenous HMGB1 regulates autophagy. J Cell Biol *190*, 881-892.

Tanida, I., Minematsu-Ikeguchi, N., Ueno, T., and Kominami, E. (2005). Lysosomal turnover, but not a cellular level, of endogenous LC3 is a marker for autophagy. Autophagy *1*, 84-91.

Tomita, N., Takasaki, H., Miyashita, K., Fujisawa, S., Ogusa, E., Matsuura, S., Kishimoto, K., Numata, A., Fujita, A., Ohshima, R., *et al.* (2013). R-CHOP therapy alone in limited stage diffuse large B-cell lymphoma. Br J Haematol *161*, 383-388.

Touzeau, C., Dousset, C., Bodet, L., Gomez-Bougie, P., Bonnaud, S., Moreau, A., Moreau, P., Pellat-Deceunynk, C., Amiot, M., and Le Gouill, S. (2011). ABT-737 induces apoptosis in mantle cell lymphoma cells with a Bcl-2high/Mcl-1low profile and synergizes with other antineoplastic agents. Clin Cancer Res *17*, 5973-5981.

Touzeau, C., Dousset, C., Le Gouill, S., Sampath, D., Leverson, J.D., Souers, A.J., Maiga, S., Bene, M.C., Moreau, P., Pellat-Deceunynck, C., *et al.* (2014). The Bcl-2 specific BH3 mimetic ABT-199: a promising targeted therapy for t(11;14) multiple myeloma. Leukemia *28*, 210-212.

Tse, C., Shoemaker, A.R., Adickes, J., Anderson, M.G., Chen, J., Jin, S., Johnson, E.F., Marsh, K.C., Mitten, M.J., Nimmer, P., *et al.* (2008). ABT-263: a potent and orally bioavailable Bcl-2 family inhibitor. Cancer Res *68*, 3421-3428.

Tsujimoto, Y., Finger, L.R., Yunis, J., Nowell, P.C., and Croce, C.M. (1984). Cloning of the chromosome breakpoint of neoplastic B cells with the t(14;18) chromosome translocation. Science *226*, 1097-1099.

Tsukada, M., and Ohsumi, Y. (1993). Isolation and characterization of autophagy-defective mutants of Saccharomyces cerevisiae. FEBS Lett *333*, 169-174.

van Delft, M.F., Wei, A.H., Mason, K.D., Vandenberg, C.J., Chen, L., Czabotar, P.E., Willis, S.N., Scott, C.L., Day, C.L., Cory, S., *et al.* (2006). The BH3 mimetic ABT-737 targets selective Bcl-2 proteins and efficiently induces apoptosis via Bak/Bax if Mcl-1 is neutralized. Cancer Cell *10*, 389-399.

Vandenberg, C.J., and Cory, S. (2013). ABT-199, a new Bcl-2-specific BH3 mimetic, has in vivo efficacy against aggressive Myc-driven mouse lymphomas without provoking thrombocytopenia. Blood *121*, 2285-2288.

Vandesompele, J., De Preter, K., Pattyn, F., Poppe, B., Van Roy, N., De Paepe, A., and Speleman, F. (2002). Accurate normalization of real-time quantitative RT-PCR data by geometric averaging of multiple internal control genes. Genome Biol *3*, RESEARCH0034.

Vaux, D.L., Cory, S., and Adams, J.M. (1988). Bcl-2 gene promotes haemopoietic cell survival and cooperates with c-myc to immortalize pre-B cells. Nature *335*, 440-442.

Vazquez, P., Arroba, A.I., Cecconi, F., de la Rosa, E.J., Boya, P., and de Pablo, F. (2012). Atg5 and Ambra1 differentially modulate neurogenesis in neural stem cells. Autophagy *8*, 187-199.

Verschooten, L., Barrette, K., Van Kelst, S., Rubio Romero, N., Proby, C., De Vos, R., Agostinis, P., and Garmyn, M. (2012). Autophagy inhibitor chloroquine enhanced the cell death inducing effect of the flavonoid luteolin in metastatic squamous cell carcinoma cells. PLoS One *7*, e48264.

Vidal, L., Gafter-Gvili, A., Salles, G., Dreyling, M.H., Ghielmini, M., Hsu Schmitz, S.F., Pettengell, R., Witzens-Harig, M., and Shpilberg, O. (2011). Rituximab maintenance for the treatment of patients with follicular lymphoma: an updated systematic review and meta-analysis of randomized trials. Journal of the National Cancer Institute *103*, 1799-1806.

Vogler, M., Dinsdale, D., Dyer, M.J., and Cohen, G.M. (2009). Bcl-2 inhibitors: small molecules with a big impact on cancer therapy. Cell Death Differ *16*, 360-367.

Wan, X.B., Fan, X.J., Chen, M.Y., Xiang, J., Huang, P.Y., Guo, L., Wu, X.Y., Xu, J., Long, Z.J., Zhao, Y., *et al.* (2010). Elevated Beclin 1 expression is correlated with HIF-1alpha in predicting poor prognosis of nasopharyngeal carcinoma. Autophagy *6*, 395-404.

Wang, C., Wang, Y., McNutt, M.A., and Zhu, W.G. (2011). Autophagy process is associated with anti-neoplastic function. Acta Biochim Biophys Sin (Shanghai) *43*, 425-432.

Warnke, R., and Levy, R. (1978). Immunopathology of follicular lymphomas. A model of B-lymphocyte homing. N Engl J Med *298*, 481-486.

Wei, Y., Pattingre, S., Sinha, S., Bassik, M., and Levine, B. (2008). JNK1-mediated phosphorylation of Bcl-2 regulates starvation-induced autophagy. Mol Cell *30*, 678-688.

White, E. (2012). Deconvoluting the context-dependent role for autophagy in cancer. Nat Rev Cancer *12*, 401-410.

Wilfinger, W.W., Mackey, K., and Chomczynski, P. (1997). Effect of pH and ionic strength on the spectrophotometric assessment of nucleic acid purity. Biotechniques *22*, 474-476, 478-481.

Wilson, W.H., O'Connor, O.A., Czuczman, M.S., LaCasce, A.S., Gerecitano, J.F., Leonard, J.P., Tulpule, A., Dunleavy, K., Xiong, H., Chiu, Y.L., *et al.* (2010). Navitoclax, a targeted high-affinity inhibitor of BCL-2, in lymphoid malignancies: a phase 1 dose-escalation study of safety, pharmacokinetics, pharmacodynamics, and antitumour activity. The lancet oncology *11*, 1149-1159.

Wooten, M.W., Geetha, T., Babu, J.R., Seibenhener, M.L., Peng, J., Cox, N., Diaz-Meco, M.T., and Moscat, J. (2008). Essential role of sequestosome 1/p62 in regulating accumulation of Lys63-ubiquitinated proteins. J Biol Chem *283*, 6783-6789.

Wright, G., Tan, B., Rosenwald, A., Hurt, E.H., Wiestner, A., and Staudt, L.M. (2003). A gene expression-based method to diagnose clinically distinct subgroups of diffuse large B cell lymphoma. Proc Natl Acad Sci U S A *100*, 9991-9996.

Wu, W.K., Coffelt, S.B., Cho, C.H., Wang, X.J., Lee, C.W., Chan, F.K., Yu, J., and Sung, J.J. (2011). The autophagic paradox in cancer therapy. Oncogene.

Xue, L., Fletcher, G.C., and Tolkovsky, A.M. (2001). Mitochondria are selectively eliminated from eukaryotic cells after blockade of caspases during apoptosis. Curr Biol *11*, 361-365.

Yang, S., Wang, X., Contino, G., Liesa, M., Sahin, E., Ying, H., Bause, A., Li, Y., Stommel, J.M., Dell'antonio, G., *et al.* (2011). Pancreatic cancers require autophagy for tumor growth. Genes Dev *25*, 717-729.

Yang, Z., and Klionsky, D.J. (2010). Mammalian autophagy: core molecular machinery and signaling regulation. Curr Opin Cell Biol *22*, 124-131.

Yang, Z.Z., and Ansell, S.M. (2012). The tumor microenvironment in follicular lymphoma. Clinical advances in hematology & oncology : H&O *10*, 810-818.

Yla-Anttila, P., Vihinen, H., Jokitalo, E., and Eskelinen, E.L. (2009). Monitoring autophagy by electron microscopy in Mammalian cells. Methods in enzymology *452*, 143-164.

Yoon, S., Woo, S.U., Kang, J.H., Kim, K., Kwon, M.H., Park, S., Shin, H.J., Gwak, H.S., and Chwae, Y.J. (2010). STAT3 transcriptional factor activated by reactive oxygen species induces IL6 in starvation-induced autophagy of cancer cells. Autophagy *6*, 1125-1138.

Yorimitsu, T., Nair, U., Yang, Z., and Klionsky, D.J. (2006). Endoplasmic reticulum stress triggers autophagy. J Biol Chem *281*, 30299-30304.

Yu, H., Pardoll, D., and Jove, R. (2009). STATs in cancer inflammation and immunity: a leading role for STAT3. Nat Rev Cancer *9*, 798-809.

Yue, Z., Horton, A., Bravin, M., DeJager, P.L., Selimi, F., and Heintz, N. (2002). A novel protein complex linking the delta 2 glutamate receptor and autophagy: implications for neurodegeneration in lurcher mice. Neuron *35*, 921-933.

Yue, Z., Jin, S., Yang, C., Levine, A.J., and Heintz, N. (2003). Beclin 1, an autophagy gene essential for early embryonic development, is a haploinsufficient tumor suppressor. Proc Natl Acad Sci U S A *100*, 15077-15082.

Yunis, J.J., Mayer, M.G., Arnesen, M.A., Aeppli, D.P., Oken, M.M., and Frizzera, G. (1989). bcl-2 and other genomic alterations in the prognosis of large-cell lymphoma. N Engl J Med *320*, 1047-1054.

Yunis, J.J., Oken, M.M., Kaplan, M.E., Ensrud, K.M., Howe, R.R., and Theologides, A. (1982). Distinctive chromosomal abnormalities in histologic subtypes of non-Hodgkin's lymphoma. N Engl J Med *307*, 1231-1236.

Zalckvar, E., Berissi, H., Eisenstein, M., and Kimchi, A. (2009). Phosphorylation of Beclin 1 by DAP-kinase promotes autophagy by weakening its interactions with Bcl-2 and Bcl-XL. Autophagy *5*, 720-722.

Zhu, W., Pan, X., Li, F., Zhang, Y., and Lu, X. (2012). Expression of Beclin 1 and LC3 in FIGO stage I-II cervical squamous cell carcinoma and relationship to survival. Tumour Biol *33*, 1653-1659.

Appendices

Appendix I

1.0 Cell lines and cell culture

Materials:

- Fetal calf serum (FCS; Gibco Life Technologies - 10500-064)
- Penicillin/Streptomycin (P/S; Sigma – P4333)
- RPMI 1640 (Sigma – R8758)
- HANKS balanced salt solution (HBSS; Gibco – 14025)

1.1 Preparation of culture media

55ml heat inactivated FCS (56°C for 1hr) and 5ml P/S solution (100×) were added to 500ml RPMI 1640 containing stable glutamine and phenol red. Final concentrations are 10% FCS, 2.0 mM L-glutamine, 100U/ml penicillin and 100µg/ml streptomycin. Culture medium is stored at 4°C. Cells were cultured in HBSS to induce autophagy.

1.2 Analysis of cell viability

Cell viability was measured using the automated Beckman Coulter Vi-Cell ™ XR Cell Viability Analyzer which measures cell viability and cell number. This machine differentiates live/dead based on trypan blue staining - live cells with intact membranes exclude trypan blue while dead cells take up the dye due to broken membranes. 0.5-1ml cell suspension was analysed per sample.

2.0 Western blotting

2.1 Preparation of samples for Western blotting

Materials:

- Protease inhibitor cocktail (PIC) (Sigma – P8340)
- CellLytic™ M cell lysis buffer (Sigma – C2978)

2.1.1 Preparation of cell lysates

Cell lysis buffer

10µl PIC was mixed with 1ml CellLytic™ M cell lysis buffer to prevent protein degradation.

2.1.2 Determination of protein concentration

Materials:

- Bio-Rad Protein Assay Dye Reagent Concentrate (Bio-Rad - 500-0006)
- Bovine serum albumin (BSA) (Sigma – A-7906)

Bovine serum albumin (BSA) stock solution:

A 5mg/ml stock solution of BSA was prepared by dissolving 0.013g BSA in 1ml water. Stock solution was stored as 1ml aliquots at -20ºC.

Bovine serum albumin (BSA) working solution:
A 0.5mg/ml working solution of BSA was prepared by mixing 10µl stock solution BSA with 90µl second distilled water.

Bio-Rad reagent
A 1:5 working solution of protein assay dye reagent was prepared by mixing 20ml of concentrated protein assay dye reagent with 80ml second distilled water. Prior to use the working solution was filtered using Whatmann cellulose filter paper to remove any precipitates that may be present. Working solution was stored at 4ºC.

2.2 Buffers for Western blotting

Materials:

- 1× MOPS or MES running buffer (Invitrogen - NP0001; NP0002)
- 1× transfer buffer
- Marvels Original dry semi-skimmed milk
- MagicMark™ XP Western standard (Invitrogen – LC5602)
- Nu-PAGE® LDS sample buffer 4× (Invitrogen – NP0007)
- Pure-Cellulose extra thick 15cm×20cm (Sigma – P7796)
- Nu-PAGE ® 4-12% Bis-Tris gel (Invitrogen – NP0336)
- PVDF membrane (Sigma – P2813)
- Tween-20 (Sigma – P7949)
- ECL Plus Western blot detection system (GE Healthcare – RPN2232)
- Restore PLUS ® Western blot stripping buffer (Thermo Scientific - 46430)
- Polyvinylpyrrolidone (PVP; Sigma - P5288-500g)

2.2.1 MOPS/MES running buffers

100ml of MOPS/MES 20× running buffer was mixed with 900ml second distilled water.

2.2.2 Transfer buffer

10× stock solution of transfer buffer was prepared by dissolving 0.25M Tris BASE and 1.92M Glycine in second distilled water. 1× working solution is prepared by mixing 100ml 10× transfer buffer, 200ml methanol and 700ml second distilled water.

2.2.3 PBS and PBST

1% phosphate buffered saline (PBS) solution was prepared by dissolving 1 PBS tablet (Sigma - P4417) per 200ml of 15 Ω Millipore distilled water. 1× Dulbecco's PBS without calcium and magnesium was also used. 0.1% PBST was prepared by adding 1ml of Tween-20 to 1L of PBS.

2.2.4 10× TBS; 1× TBS; TBST

A 10× Tris-buffered solution (TBS) stock solution was prepared by mixing second distilled water with Tris-HCl and NaCl. 5M NaCl was dissolved in 300ml distilled water and 1M Tris-HCl prepared by dissolving Tris-Base in 500ml distilled water and

adjusted to pH7.4 using HCl. These solutions were mixed together and 200ml of distilled water added giving a final volume of 1L. 1× TBS was prepared by mixing 100ml 10× TBS with 900ml distilled water. 0.1% TBST was prepared by mixing 1ml Tween-20 with 1L 1× TBS.

2.2.5 5% Milk blocking solution

A 5% blocking solution was prepared by dissolving 2.5g dried skimmed Milk was dissolved in 50ml PBST.

2.2.6 PVP blocking solution

A 5% 1L PVP blocking solution was prepared by dissolving 50g PVP in 1000ml 1× TBST.

2.2.7 10% Sodium azide solution

A 10% Sodium azide solution was prepared by dissolving 10g of sodium azide (Sigma – S8032) in 100ml distilled water.

2.2.8 Primary antibody diluent

Primary antibodies were diluted in either 10ml 5% milk blocking solution (2.5) or 7ml PVP blocking solution (2.6) containing 0.35ml FCS and 70µl 10% Azide solution.

2.2.9 Secondary antibody dilutent

Secondary antibodies were diluted in PBST if appendix 2.8 (a) was the primary antibody diluent or in 10ml PVP blocking buffer containing 0.35ml FCS (without sodium azide) if appendix 2.8 (b) was used.

2.2.10 ECL plus

ECL Plus was prepared according to manufacturer's instructions. Solutions A and B were equilibrated to RT 15min prior to use and were mixed in a 1:1 ratio. Membranes were incubated with 1ml mixed solution for 5min in the dark at RT.

2.2.11 Western blotting antibodies

Table A Primary antibodies for Western blotting

Antibody	Species	Company	Clone	Cat. No.	Dilution
Atg4B	Rabbit	Cell Signalling	Polyclonal	5299S	1:1000
Bak	Rabbit	Santa Cruz	G-23	sc-832	1:3000
Bax	Mouse	Santa Cruz	N-20	sc-493	1:500
BCL-2	Mouse	Santa Cruz	100	sc-509	1:1000
BCL-2	Rabbit	Santa Cruz	N-19	sc-492	1:1000
BCL-xL	Rabbit	Santa Cruz	S-10	sc-634	1:1000
Beclin-1	Mouse	Santa Cruz	E-8	sc-48341	1:1000
Bim	Rabbit	Santa Cruz	H-191	sc-11425	1:3000
LC3	Rabbit	Abgent	Polyclonal	APG8	1:1000
MCL-1	Rabbit	Cell Signalling	Polyclonal	4752	1:3000
p62	Mouse	Santa Cruz	D-3	sc-28359	1:1000
p62	Rabbit	Abgent	Polyclonal (C-term)	AP2183B	1:1000
PARP	Rabbit	Santa Cruz	H-250	sc-7150	1:1000
ULK1	Rabbit	Abcam	EPR4885(2)	ab128859	1:1000
β-Actin	Rabbit	Sigma	AC-74	A5316	1:50,000
GAPDH	Rabbit	Cell Signalling	14C10	2118L	1:2000

Table B Secondary antibodies for Western blotting

Antibody	Species	Company	Cat. No.	Dilution
Goat Anti-Rabbit	Rabbit	Santa Cruz	sc-2004	1:3000
Goat Anti-Mouse	Mouse	Santa Cruz	sc-2005	1:3000

3.0 Buffers for immuno-fluorescent microscopy

Materials:

- Superfrost Plus chamber slides (MJ Research Inc - SLS-03111)
- Cytofix/Cytoperm fixation/permeablisation solution (PharMingen/Becton Dickson - 554715)
- Blocking buffer
    - Donkey serum (Sigma - D9663)
    - Goat serum (Sigma – G9023)
    - Saponin (Fluka Biochemika – 47036)
- 4',6-Diamidino-2-Phenylindole, Dihydrochloride (DAPI – Sigma – D9564)
- ProLong® Gold anti-fade mounting reagent (Life Technologies – P36930)

3.1 5% donkey/goat blocking buffer

A 0.1% saponin, 5% donkey/goat serum buffer was prepared by dissolving 0.05g saponin in 2.5mls of donkey or goat serum and brought to a volume of 50mls with 1× TBS. Buffer is stored at -20°C in 10ml aliquots.

3.2 Immunofluorescent microscopy antibodies

Table C Primary antibodies for immunofluorescent microscopy

Antibody	Species	Company	Clone	Cat. No.	Dilution
Bax	Mouse	BD Pharmingen	6A7	556467	1:100
BCL-2	Mouse	Santa Cruz	100	sc-509	1:50
Bip	Rabbit	Cell Signalling	G-584	C50B12	1:25
Beclin-1	Mouse	Santa Cruz	E-8	sc-48341	1:20
Cox IV	Rabbit	Abcam	Polyclonal	ab16056	1:200

Table D Secondary antibodies for immunofluorescent microscopy

Antibody	Species	Clone	Company	Cat. No.	Dilution
Alexa-Flour®488	Mouse	Donkey	Santa Cruz	A21202	1:100
Alexa-Flour®546	Rabbit	Donkey	Santa Cruz	A11035	1:100

3.3 DAPI (4',6-Diamidino-2-Phenylindole, Dihydrochloride)

10µl 50mg/ml DAPI was added to 10mls PBS (1:1000 dilution) to create a 50µg/ml stock solution which was aliquoted and stored at -20°C in darkened eppendorf tubes. The final working solution of DAPI was prepared by mixing 1µl 50µg DAPI with 1ml PBS(T).

4.0 Solutions and buffers for tissue microarrays

Materials:

- Superfrost® Plus slides (VWR– 631-0108)
- 10× Wash buffer (DAKO – S3006)
- Xylene (VWR Chemicals – 28975.325)
- Peroxidase (BDH – 101284N)
- Industrial methylated spirits (IMS; Fisher Chemical – 11482874)
- Unmasking solution (Vector Laboratories – CA94010)
- DPX (Distrene 80, Dibutyl phthalate and Xylene) Mountant (VWR – 360294H)
- SuperSensitive™ Polymer HRP-IHC Detection system (BioGenex – QD430-XAKE)
    - SS Label
    - SuperEnhancer
    - Stable DAB buffer
    - Liquid DAB

4.1 Peroxidase blocking buffer

2% peroxidase in 100% IMS

4.2 Unmasking solution

3L second distilled water was mixed with 30ml DAKO unmasking solution (1:100) and brought to the boil in a pressure cooker.

4.3 Immunohistochemistry antibodies

Table E Antibodies used for immunohistochemistry

Antibody	Species	Company	Cat. No.	Antigen Retrieval	Dilution
p62	Rabbit	Abgent	AP2183B	Pressure Cooker	1:7000
Beclin1	Mouse	Santa Cruz	sc-48381	Pressure Cooker	1:250
LC3B	Rabbit	Sigma	L7543	Pressure Cooker	1:5000
CTSD	Mouse	Sigma	C0715	Pronase Enzyme	1:1000
TGM2	Rabbit	Abcam	ab421	Pressure Cooker	1:750
BCL-2	Mouse	DAKO	M0887	Pressure Cooker	1:200
CD68	Mouse	DAKO	M0814	Pressure Cooker	1:8000

4.4 3.3'-Diaminobenzidine (DAB)

1 drop (~38µl) of DAB chromogen was added to 1ml stable DAB buffer and mixed.

4.5 Acid alcohol

1% hydrochloric acid in 70% IMS

4.6 DPX - Xylene-based permanent mounting agent

TMA slides were mounted with the xylene-based permanent mounting agent DPX, purchased in a ready to use form.

4.7 Wash buffer

50ml DAKO 10× wash buffer was mixed with 450ml second distilled water (1:10)

5.0 Solutions for Caspase-3 activity assay

Materials:

- Dithiothreitol (DTT) (Sigma – D3801)
- Phenylmethylsulfonyl fluoride (PMSF) (Sigma – P7626)
- 7-amino-4-trifluoromethylcoumarin (AFC) (Sigma – A8401)
- Ac-DEVD-AFC (Caspase-3 substrate) (Santa Cruz – sc-311274A)
- 3-[(3-Cholamidopropyl)dimethylammonio]-1propanesulfonate (CHAPS) (Sigma – C9426)
- DMSO (D/4121/PB08)

5.1 Caspase-3 assay lysis buffer

10µl 100mM DTT, 10µl 100mM PMSF and 10µl PIC were added to 1ml caspase-3 reaction buffer.

5.1.1 100mM Dithiothreitol (DTT)

0.015g DTT was dissolved in 1ml DMSO

5.1.2 100mM Phenylmethylsulfonyl fluoride (PMSF)

0.017g PMSF was dissolved in 1ml DMSO

5.2 Caspase-3 assay reaction buffer (pH 7.4; 500ml)

500ml caspase-3 reaction buffer was prepared by mixing the components listed in table H with distilled water and the final pH adjusted to pH7.4.

Table F Caspase-3 reaction buffer components

Reagent	MW (g/L)	Weight (g)/500ml	Final Concentration
HEPES-KOH	238.3	2.383	20mM
KCl	74.56	0.37	10mM
EDTA	372	0.186	1mM
EGTA	380.4	0.192	1mM
CHAPS*	614.9	0.5	0.1%

* 0.1% CHAPS is to be added freshly each time buffer is prepared

5.3 Ac-DEVD-AFC Caspase-3 substrate

5.3.1 10mM Ac-DEVD-AFC (stock solution)

5mg Ac-DEVD-AFC was dissolved in 0.7ml DMSO to create a 10mM stock solution which was stored in 20µl aliquots at -20°C.

5.3.2 400µM Ac-DEVD-AFC (working solution)

6µl 10mM Ac-DEVD-AFC stock solution was mixed with 150µl caspase-3 reaction buffer B (1:25) to create a 400µM working solution. 5µl 400µM working solution was mixed with 100µl caspase-3 reaction buffer B to give a final concentration of 20µM Ac-DEVD-AFC substrate per well.

5.4 7-amino-4-trifluoromethylcoumarin (AFC)

5.4.1 100mM AFC

A 100mM AFC stock solution was prepared by dissolving 0.0229g AFC in 1ml DMSO. Solution was stored in the dark at -20°C.

5.4.2 5µM AFC

1µl 100mM AFC was mixed with 1ml second distilled water (1:1000) to create a 100µM solution. 50µl 100µM AFC was mixed with 1ml second distilled water (1:20) to give a final working solution of 5µM.

6.0 Solutions for flow cytometry

Materials:

- 4', 6'-Diamidino-2-Phenylindole, Dihydrochloride (DAPI) (Sigma – D9564)
- Tetramethylrhodamine, Methyl Ester, Perchlorate (TMRM) (Molecular Probes – T-668)
- DNase (Sigma – D4513)
- Human γ-Globulin (HAG; Sigma – 4386)

6.1 100ng/ml DAPI (4',6-Diamidino-2-Phenylindole, Dihydrochloride) (working solution)

20µl of 50µg/ml DAPI stock solution was diluted to 10ml PBS to create a 100ng/ml working solution.

6.2 Tetramethylrhodamine, Methyl Ester, Perchlorate (TMRM)

6.2.1 2mM TMRM (stock solution)

2mM TMRM stock solution was prepared by dissolving 2mg TMRM in 2ml DMSO. Solution was stored in the dark at -20°C.

6.2.2 TMRM (working solution)

1µl of 2mM TMRM was mixed with 1ml PBS (1:1000) to create a 2µM solution. 400µl 2µM TMRM was mixed with 10ml PBS (1:25) to create a 80nM working solution

6.3 Deoxyribonuclease I from bovine pancreas (DNase)

11g DNase was mixed with 11ml PBS. Prepared DNase was kept at -20°C in 0.5ml aliquots.

6.4 2% Human anti-γ-globulin antibody (HAG)

2% HAG was prepared by dissolving 1g HAG in 50ml sterile PBS for 30min at RT. This solution was then filtered through a Millipore Dualex-Ultra 0.2µm filter and stored in 1ml aliquots at -20ºC. 50µl 2% HAG was used per 1.5×10^6 cells.

6.5 Antibodies used in B cell isolation

Table G Antibodies used to isolate B cells using flow cytometry

Marker	Clone	Isotype	Fluorochrome	Company	Cat. No.	Volume/10^6 Cells
CD3	SK7	Mouse IgG1, κ	FITC	BioLegend	344804	1µl
CD20	2H7	Mouse IgG2b, κ	APC-H7	BD Biosciences	641396	2.5µl
CD19	HIB19	Mouse IgG1, κ	APC-Cy7	BioLegend	302218	2.5µl
CD10	HI10A	Mouse IgG1, κ	PE	BioLegend	312204	2.5µl
Kappa	MHK-49	Mouse IgG1, κ	APC	BioLegend	316510	20µl
Lambda	MHL-38	Mouse IgG2a, κ	PerCp-Cy5.5	BioLegend	316618	5µl

6.6 2% FACS wash

2% FACS wash was prepared by mixing 1ml filtered FCS with 50ml sterile PBS.

6.7 2% FACS wash containing DAPI and 1% DNase

5ml 2% FACS wash with 2.5µl plus 2.5µl 50µg/ml DAPI and 50µl 1mg/ml DNase

6.8 FACs Collection buffer

Cell collection buffer was prepared by mixing 5ml filtered FCS with 50ml sterile PBS (10%)

7.0 Solutions phenol-chloroform based RNA extraction (TRIzol® Reagent)

Materials:

- Trizol (Life Technologies - 15596018)
- Chloroform (Sigma - 366919)
- Isopropanol (Fisher Chemical – P/7500/17)

7.1 75% ethanol

10ml 75% ethanol was prepared by mixing 7.5ml of 100% pure ethanol with 2.5ml of distilled water.

8.0 Solutions for RNA extraction using QIAGEN RNeasy® Mini Kit

Materials:

- RNeasy® Mini Kit (QIAGEN - 74104)
  - Buffer RLT
  - Buffer RW1
  - Buffer RPE
  - RNase-free water
  - RNA-free 2ml collection tubes
  - RNA-free 1.5ml collection tubes
  - QIAshredder spin column
  - RNeasy spin column
- β-mercaptoethanol (BHD Biochemistry – 436022A)
- RNase-free DNase set (QIAGEN - 79254)
  - DNase I, RNase-free (lyophilized)
  - Buffer RDD

8.1 Buffer RLT

Under a fumehood, 10µl β-mercaptoethanol was added to 1ml Buffer RLT and mixed by vortexing for 1min.

8.2 70% ethanol

10ml 70% ethanol was prepared by mixing 7ml of 100% pure ethanol with 3ml of distilled water.

8.3 DNase I

8.3.1 DNase I (stock solution)

550µl of RNase-free water was added to lyophilized DNase and mixed. DNase was stored in 10µl aliquots at -20°C.

8.3.2 DNase I Incubation Mix (working solution)

DNase I incubation mix was prepared by mixing 10µl of DNase with 70µl of Buffer RDD supplied as part of the QIAGEN RNase-free DNase set.

8.4 Buffer RPE

44ml of 100% ethanol was added and mixed to 11ml Buffer RPE.

9.0 Agilent bioanalyser

Materials:

- Agilent 2100 Bioanalyser (Agilent Technologies)
- Agilent RNA 6000 Nano Chips (Agilent Technologies – 5067-1521)
- Agilent RNA 6000 Nano Reagents (Agilent Technologies – 5067-1511)
    - Agilent RNA 6000 Ladder
    - RNA Nano Dye Concentrate
    - Agilent RNA 6000 Nano Gel Matrix

10.0 Quantitative real-time PCR

10.1 cDNA synthesis

Materials:

- RT^2 First strand kit (QIAGEN - 330401)

Table H Genomic DNA elimination mix

Component	Concentration	Volume	Example
RNA	300ng	Maximum 8µl	5µl
Buffer GE	NA	2µl	2µl
RNase-free water	NA	Variable	3µl
Total Volume	NA	10µl	10µl

Table I Reverse-transcription (ReTr) mix

Component	Volume for 1 Reaction	Volume for 8 Reactions
5× Buffer BC3	4µl	32µl
Control P2	1µl	8µl
RE3 Reverse Transcriptase Mix	2µl	16µl
RNase-free Water	3µl	24µl
Total Volume	10µl	80µl

10.2 qRT-PCR reaction

Materials:

- RT^2 SYBR green ROX qPCR Mastermix (QIAGEN - 330521)

Table J qRT-PCR Reagents Mix

Components	384 Array Format E (4 × 96 well)
2 × RT^2 SYBR Green Mastermix	650µl
cDNA Synthesis Reaction	102µl
RNase-free Water	548µl
Total Volume per Sample	1300µl

Table K qRT-PCR Cycling Conditions - Applied Biosystems 7900HT Cycler

Cycles	Temperature	Duration
1	95°C	10 min
40	95°C	15 sec
	60°C	1 min
1	95°C	15 sec
(Dissociation Curve)	60°C	15 sec
	95°C	15 sec

10.3 qRT-PCR validation experiments

Table L qRT-PCR Reagents Mix (Validation Experiments)

Components	384 Array Format E (4 × 96 well)
2 × RT^2 SYBR Green Mastermix	12.5µl
cDNA Synthesis Reaction	1µl
RNase-free Water	10.5µl
Total Volume per Sample	25µl

11.0 Solutions and buffers for Co-Immunoprecipitation

Materials:

- Nuclear Complex Co-IP Kit (Active Motif - 54001)
  - 5× IP Low Buffer
  - 1M DTT (Appendix 5.0)
  - PIC (Appendix 2.1)
- Eluting Solution
  - Nu-PAGE® LDS Sample Buffer 4× (Invitrogen – NP0007)
  - Nu-PAGE® Reducing Agent 10× (Invitrogen – NP0009)
- Dynabeads Protein A (Life Technologies – 10002D)
- Mouse Anti-IgG (Santa Cruz – sc-2025)

11.1 Immunoprecipitation incubation buffer

IP incubation buffer was prepared using Active Motif Nuclear Complex Co-IP Kit and by following the manufacturers' guidelines.

Table M 5× low IP incubation buffer components

5× low IP buffer	100µl
PIC	2.5µl
1M DTT	0.5µl
dH_2O	397µl
Total Volume	500µl

11.2 Immunoprecipitation wash buffer

IP wash buffer was prepared using Active Motif Nuclear Complex Co-IP Kit and by following the manufacturers' guidelines.

Table N 5× low IP wash buffer components

5× low IP buffer	800µl
PIC	8µl
1M DTT	4µl
dH_2O	3188µl
Total Volume	4000µl

11.3 Eluting solution

Eluting solution was prepared by mixing 160µl of Nu-PAGE® 4× LDS Sample Buffer with 16µl of Nu-PAGE® Reducing Agent 10×.

12.0 Drug preparation

12.1 ABT-737

12.1.1 10mM ABT-737 (stock solution)

A 10mM ABT-737 (Selleck – S1002) stock solution was prepared by dissolving 5mg ABT-737 in 615µl DMSO. Stock solution was stored at -80°C in 10µl aliquots.

12.1.2 10µM ABT-737 (working solution)

A 10µM ABT-737 stock solution was prepared by mixing 1µl 10mM ABT-737 with 1ml culture media. Working solution was prepared fresh each time.

12.2 50mM Chloroquine

A 50mM Chloroquine (CQ; Sigma – C6628) stock solution was prepared by dissolving 0.026g CQ in 1ml PBS. Stock solution was stored at -20°C. 1µl 50mM was added per 1ml cell suspension to give a final concentration of 50µM.

12.3 20mM Z-VAD.fmk

A 20mM N-Benzyloxycarbonyl-Val-Ala-Asp(O-Me) fluromethyl ketone (Z-VAD.fmk; Sigma – C2105) stock solution was prepared by dissolving 0.009g Z-VAD.fmk in 1ml DMSO. Stock solution was stored at -20°C. 1µl 20mM Z-VAD.fmk was added per 1ml cell suspension to give a final concentration of 20µM.

Appendix II

1.0 Cell line GEP data

Table O Su-DHL4 and Su-DHL8 RIN

Sample	RIN	260/280	260/230
Su-DHL4 Untreated-1	9.9	2.14	2.2
Su-DHL4 Untreated-2	9.9	2.12	2.22
Su-DHL4 Untreated-3	9.9	2.14	2.18
Su-DHL4 HANKS-1	9.7	2.13	2.16
Su-DHL4 HANKS-2	9.8	2.13	2.14
Su-DHL4 HANKS-3	9.7	2.2	2.19
Su-DHL8 Untreated-1	9.9	2.16	2.21
Su-DHL8 Untreated-2	9.9	2.18	2.11
Su-DHL8 Untreated-3	9.9	2.18	2.23
Su-DHL8 HANKS-1	9.9	2.28	2.21
Su-DHL8 HANKS-2	10	2.17	1.91
Su-DHL8 HANKS-3	10	2.35	1.92

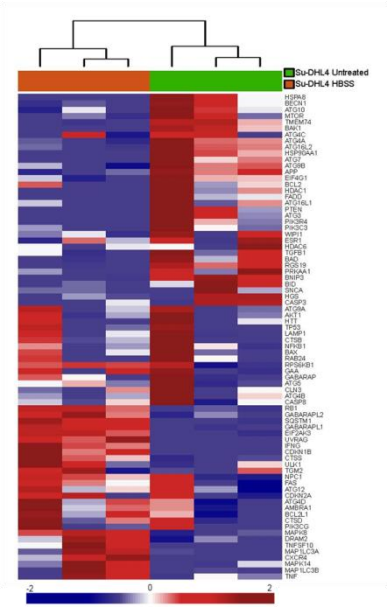

Appendix Figure 1: Unsupervised clustering analysis resolves untreated Su-DHL4 and Su-DHL8 cell lines based on expression of autophagy-related genes

Unsupervised hierarchical clustering using triplicate Su-DHL4 and SU-DHL8 untreated RQ values. Samples were clustered using a Euclidean distance measure and an average agglomeration (JM) where each row represents a gene and each column an RQ value. Gene expression levels are represented on a scale of blue to red colour indicative of low to high expression.

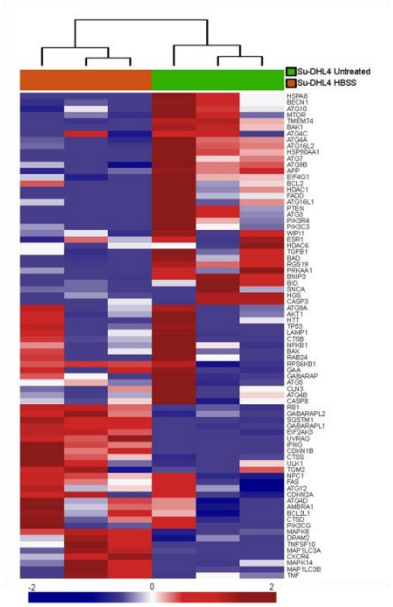

Appendix Figure 2: Unsupervised clustering analysis resolves untreated and starved Su-DHL4 cells based on expression of autophagy-related genes

Unsupervised hierarchical clustering using triplicate untreated and starved (HBSS; 6hrs) Su-DHL4 RQ values. Samples were clustered using a Euclidean distance measure and an average agglomeration (JM) where each row represents a gene and each column an RQ value. Gene expression levels are represented on a scale of blue to red colour indicative of low to high expression

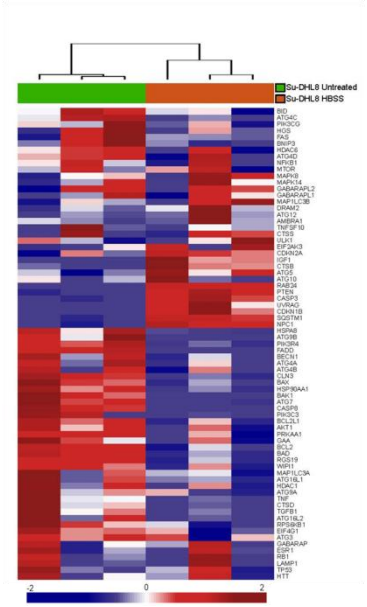

Appendix Figure 3: Unsupervised clustering analysis resolves untreated and starved Su-DHL8 cells based on expression of autophagy-related genes

Unsupervised hierarchical clustering using triplicate untreated and treated Su-DHL4 (HBSS; 6hrs) RQ values. Samples were clustered using a Euclidean distance measure and an average agglomeration (JM) where each row represents a gene and each column an RQ value. Gene expression levels are represented on a scale of blue to red colour indicative of low to high expression

2.0 Patient information

Table P FL patient information for purified and un-purified samples

Pat ID	Gender	Age at Diagnosis	Date of Diagnosis	Date of Transformation	Stage	FLIPI Score	Date of 1st Treatment	Response	Date of Death	Cause of Death
F9835	M	56	20/06/1997	15/04/2008	II	1	15/04/2008	Progression	03/12/2008	NHL
F9220	M	57	01/04/2001	22/01/2008	IV	3	26/04/2001	CR(U) / GPR	N/A	N/A
R8402	F	67	22/08/2005	26/04/2011	II	1	14/05/2010	CR	N/A	N/A
T1979	F	74	01/12/2005	18/05/2009	IV		08/05/2009	Progression	08/07/2009	NHL
T5728	M	29	15/07/2011	13/02/2012	IV	2	02/03/2012	CR	N/A	N/A
R9130	F	25	31/05/2007	N/A	II	1	04/07/2007	CR(U) / GPR	N/A	N/A
T6694	M	48	24/03/2011	N/A	IV	2	21/03/2012	PR	N/A	N/A
R0481	F	54	12/04/2002	N/A	IV	2	11/01/2005	CR(U) / GPR	N/A	N/A
F5997	F	63	01/01/1998	N/A	IV	3	27/08/1998	Relapse	13/01/2005	NHL
F9713	F	89	31/08/2001	N/A	IV	2	14/09/2001	N/A	28/09/2002	N/A
T6713	M	62	07/03/2012	N/A	III	U	N/A	N/A	N/A	N/A
R2856	M	76	06/10/2003	N/A	III	2	N/A	N/A	20/02/2006	Other
T0167	F	74	15/04/2006	N/A	IV	U	N/A	N/A	N/A	N/A

¶ Staging ranges from I to IV with a higher stage indicating more widespread disease. § The Follicular Lymphoma International Prognostic Index (FLIPI) score ranges from 1 to 4 where 1 = low risk (0-1 prognostic factor), 2 = intermediate risk (2 prognostic factors), 3 = high risk (3-5 prognostic factors) and 4 = not assessable; U = unknown. *CR= complete remission; CR(U)= undetermined complete remission; GPR= good partial remission; N/A= not applicable. † NHL= Non-Hodgkin lymphoma; N/A= not applicable.

Table Q DLBCL patient information for purified and un-purified samples

Pat ID	Gender	Age at Diagnosis	Date of Diagnosis	Stage	IPI Score	Date of 1st Treatment	Response	Date of Death	Cause of Death
R1542	F	26	23/12/2002	VI	1	15/01/2003	CR	N/A	N/A
R8374	M	20	29/11/2006	V	1	15/12/2006	CR	N/A	N/A
T1486	M	33	08/01/2009	IV	1	27/01/2009	CR	N/A	N/A
T1485	M	55	13/01/2009	II	0	20/01/2009	CR	N/A	N/A
T2628	M	58	23/07/2009	I	0	20/08/2009	CR	N/A	N/A
T3531	M	60	21/12/2009	III	1	03/02/2010	CR	N/A	N/A
R1723	F	55	28/01/2003	IV	2	28/02/2003	CR	02/01/2006	NHL
R8878	F	79	01/02/2007	IV	4	17/04/2007	Progression	18/03/2008	NHL
R9083	M	33	09/05/2007	III	3	15/05/2007	CR(U) / GPR	15/11/2007	NHL
R9515	M	80	16/08/2007	IV	4	16/08/2007	Stable disease	19/10/2007	Cardiac failure
T0082	F	18	15/01/2008	IV	1	01/02/2008	Progression	N/A	N/A
T0978	M	58	12/08/2008	IV	4	22/08/2008	Progression	N/A	N/A

¶ Staging ranges from I to VI with a higher stage indicating more widespread disease. § The International Prognostic Index (IPI) score ranges from 0 to 5, with 0 indicating absence of all prognostic factors and 5 indicating all prognostic factors are present. *****CR= complete remission; CR(U)= undetermined complete remission; GPR= good partial remission. † NHL= Non-Hodgkin lymphoma.

Table R RIN for purified patient samples

Disease	Pat ID	RIN	260/280	260/230
FL	9430	8.5	1.97	1.62
FL	7260	8.6	2.09	1.85
FL	9093	9.8	2.12	1.61
FL	9183	10	2.11	1.49
FL	7823	9.8	2.11	1.05
DLBCL	8742	7.0	2.10	0.82
DLBCL	8555	9.7	2.78	1.23
Reactive	1234	10	2.13	1.65
Reactive	NML	9.7	2.07	1.65
Reactive	1212	9.8	2.02	2.06

Table S RIN for un-purified patient samples

Disease	Pat ID	RIN	260/280	260/230
FL	R0481	5.9	2.3	1.36
FL	F9713	6.9	1.75	1.79
FL	R9130	6.3	1.82	1.81
FL	F5997	7.6	2.01	1.24
FL	R2856	6.5	2.28	1.73
FL	F9220	6.9	1.84	1.91
FL	R8402	8.3	1.97	1.96
FL	F9835	8.6	2.34	0.73
DLBCL	8209	7.10	2.64	1.58
DLBCL	7851	7.00	1.89	1.58
DLBCL	7676	7.60	2.01	1.39
DLBCL	8105	7.60	2.28	1.19
DLBCL	7889	6.10	2.15	1.33
DLBCL	8365	7.30	2.05	1.57
DLBCL	8265	6.20	2.09	1.30
DLBCL	7535	6.70	2.10	0.55
DLBCL	6411	5.80	2.52	1.33
DLBCL	6488	5.60	2.42	1.54
Reactive	6639	7.30	2.07	1.51
Reactive	19701	6.50	2.00	0.55
Reactive	095286	7.60	2.22	1.49
Reactive	566960	5.90	2.48	0.85
Reactive	2384007	7.50	2.06	1.36
Reactive	6346677	7.00	2.06	1.07
Reactive	961106	8.00	2.07	1.16
Reactive	6639	7.30	2.07	1.51

3.0 Patient information for TMAs

Table T Summary of clinical characteristic of FL patient samples used in IHC/TMA analysis

	No. of patients	Percentage
	117	100
Age, years		
<60	70	59.83
≥60	47	40.17
Gender		
Male	54	46.15
Female	63	53.85
Stage at diagnosis		
I	12	10.26
II	14	11.96
III	16	13.68
IV-VI	75	64.10
FLIPI score		
1 (Low)	35	29.91
2 (Intermediate)	29	24.79
3 (High)	34	29.06
4 (not assessable)	19	16.24
Proceeded to transformation	32	27.35
Time to transformation yr		
0-5	18	56.25*
6-10	8	25.00*
>11	6	18.75*
Cause of death		
Alive	43	36.75
Disease	42	35.90
Unrelated	32	27.35

* indicates % of transformed; patients presented as St. Bartholomew's hospital between 1974 and 2006; median age 56 (Range 26-89).

Table U Summary of clinical characteristic of DLBCL patient samples used in IHC/TMA analysis

	No. of patients	Percentage
	109	100
Age, years		
<60	58	53.21
≥60	51	46.79
Gender		
Male	72	66.06
Female	37	34.94
Stage at diagnosis		
I	12	11.01
II	19	17.43
III	33	30.28
IV-VI	44	40.37
Unknown	1	0.926
B Symptoms		
Yes	31	28.44
No	49	44.95
Unknown	29	26.61
Serum LDH*		
Normal	40	36.70
Elevated	47	43.12
Unknown	22	20.18
IPI score		
0 (Low)	21	19.27
1 (Low)	30	27.52
2 (Intermediate)	27	24.77
3 (High)	25	22.94
4-5 (High)	6	5.5
Cause of death		
Alive	51	46.79
NHL-specific	40	36.70
death	18	16.51
Other diseases		

* LDH values <480 U/L are within the normal range; patients presented as St. Bartholomew's hospital between 1983 and 2009; median age 58 (Range 21-85).

4.0 Statistical analysis of TMA data

Table V Univariate analysis of FLIPI as a continuous variable in FL

Variable	Overall survival		Disease-specific survival		Time to transformation	
	HR (95% CI)	***p***	**HR (95% CI)**	***p***	**HR (95% CI)**	***p***
FLIPI	1.40 (1.15-1.71)	0.001	1.47 (1.12-1.92)	0.005	1.27 (0.95-1.71)	0.113

HR= Hazard ratio; CI= Confidence interval

Table W Univariate analysis of IPI as a continuous variable in DLBCL

Variable	Overall survival		Disease-specific survival		Progression free survival	
	HR (95% CI)	***p***	**HR (95% CI)**	***p***	**HR (95% CI)**	***p***
IPI	1.46 (1.17-1.81)	0.001	1.44 (1.12-1.86)	0.005	1.25 (0.98-1.59)	0.077

HR= Hazard ratio; CI= Confidence interval

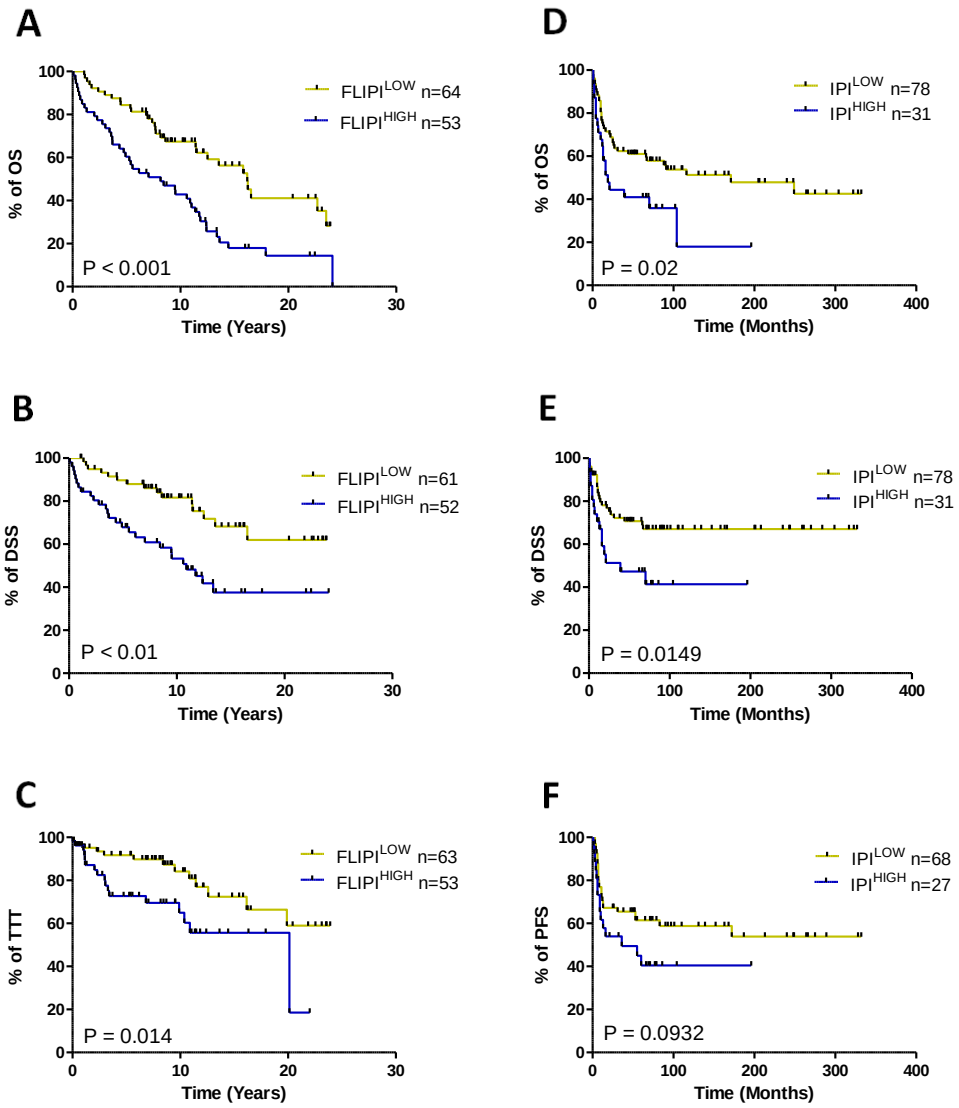

Appendix Figure 4: Higher FLIPI and IPI scores predict a worse outcome in FL and DLBCL respectively

Evaluation of the prognostic significance of FLIPI and IPI scores in FL (A-C) and DLBCL (D-F) respectively. Based on the number of adverse prognostic factors they presented with, 116 FL and 109 DLBCL patients were classified as $FLIPI^{LOW}/IPI^{LOW}$ (0-2) or $FLIPI^{HIGH}/IPI^{HIGH}$ (>3). The prognostic impact of FLIPI scores on OS (A), DSS (B) and TTT (C) in FL and of IPI scores on OS (D), DSS (E) and PFS (F) in DLBCL was visualised using Kaplan-Meier curves. Differences in survival between $FLIPI^{LOW}/IPI^{LOW}$ and $FLIPI^{HIGH}/IPI^{HIGH}$ groups were evaluated using a log-rank (Mantel-Cox) test and GraphPad Prism software. OS= overall survival; DSS= disease specific survival; TTT= time to transformation; PFS= progression free survival; n= number; P = p value, which is classified as significant if <0.05

Table X

(i) X-tile generated cut-points for DLBCL survival analysis

Model variables		Cut point	*p* value
OS	**p62 high vs. p62 low**	8.18	0.0029
DSS	**p62 high vs. p62 low**	8.18	0.0144
PFS	**p62 high vs. p62 low**	8.35	0.0022
OS	**BCL-2 high vs. BCL-2 low**	63.74	0.0605
DSS	**BCL-2 high vs. BCL-2 low**	54.97	0.1514
PFS	**BCL-2 high vs. BCL-2 low**	71.49	0.6391
OS	**LC3 high vs. LC3 low**	18.18	0.1429
DSS	**LC3 high vs. LC3 low**	40.1	0.3457
PFS	**LC3 high vs. LC3 low**	37.17	0.1126
OS	**Beclin-1 high vs. Beclin-1 low**	12.91	0.0154
DSS	**Beclin-1 high vs. Beclin-1 low**	15.01	0.1296
PFS	**Beclin-1 high vs. Beclin-1 low**	12.88	0.0285
OS	**IPI score**	0-2 vs. 3-5	0.0273
DSS	**IPI score**	0-2 vs. 3-5	0.0036
PFS	**IPI score**	0-2 vs. 3-5	0.0932

(ii) X-tile generated cut-points for DLBCL survival analysis

Model variables		Cut Point	*p* value
OS	**p62 high vs. p62 low**	1.54	0.527
DSS	**p62 high vs. p62 low**	2.695	0.479
TT	**p62 high vs. p62 low**	1.54	0.527
OS	**BCL-2 high vs. BCL-2 low**	92.52	0.14
DSS	**BCL-2 high vs. BCL-2 low**	92.14	0.58
TT	**BCL-2 high vs. BCL-2 low**	76.52	0.3
OS	**LC3 high vs. LC3 low**	40.68	0.438
DSS	**LC3 high vs. LC3 low**	36.99	0.9
TT	**LC3 high vs. LC3 low**	26.73	0.75
OS	**Beclin-1 high vs. Beclin-1 low**	5.8	0.2
DSS	**Beclin-1 high vs. Beclin-1 low**	6.12	0.3
TT	**Beclin-1 high vs. Beclin-1 low**	22.84	0.43
OS	**FLIPI score**	0-2 vs. 3-5	<0.001
DSS	**FLIPI score**	0-2 vs. 3-5	<0.01
TT	**FLIPI score**	0-2 vs. 3-5	0.014

Table Y 5 year survival rates for DLBCL patients based on expression levels of autophagy-related proteins

	Protein Expression Level							
% Survival	**p62^{LOW}**	**p62^{HIGH}**	**Beclin-1^{LOW}**	**Beclin-1^{HIGH}**	**BCL-2^{LOW}**	**BCL-2^{HIGH}**	**LC3^{LOW}**	**LC3^{HIGH}**
OS	40	63	34	61	61	48	55	55
DSS	50	71	55	68	68	60	61	67
PFS	34	67	36	62	59	49	41	66

Table Z 5 year survival rates for FL patients based on expression levels of autophagy-related proteins

	Protein Expression Level							
% Survival	**p62^{LOW}**	**p62^{HIGH}**	**Beclin-1^{LOW}**	**Beclin-1^{HIGH}**	**BCL-2^{LOW}**	**BCL-2^{HIGH}**	**LC3^{LOW}**	**LC3^{HIGH}**
OS	73	69	33	73	79	68	68	77
DSS	83	71	52	79	87	70	79	80
TTT	10	21	17	24	14	16	17	19